A classification of large wetlands in Africa's elevated drylands based on their formation, structure, and hydrological functioning using Earth Observation (EO) data and Geographic Information System (GIS)

A thesis submitted

to

Rhodes University

in fulfilment of the requirements for the degree of

Doctor of Philosophy

in

Water Resource Science

by

Zwidofhelangani Lidzhegu

November 2019

ABSTRACT

Due to wetland inaccessibility and limited wetland geomorphological studies, there is limited information on the geomorphological origin and hydrological functioning of different types of wetlands in Africa's elevated drylands. As a result, there is limited information for the development of a comprehensive wetland classification system that classifies wetlands based on long-term geomorphic processes that determine their formation and shape, their structure and hydrological functioning. Therefore, the current study was designed to classify large wetlands in Africa's elevated drylands based on processes that determine their formation, and shape their structure and hydrological functioning using remote sensing and Geographic Information System (GIS) techniques. Although wetlands perform a number of hydrological functions including groundwater recharge and water purification, the current study focuses mainly on their flood attenuation function. Detailed analysis of topographic information was undertaken using Shuttle Radar Topographic Mission (SRTM) elevations measured at the scale of 30 m x 30 m. LandsatLook and Google Earth images, tectonic as well as geological data were used as supplementary data for developing an understanding of the origin, structure and hydrological characteristics of wetlands. The Principal Component Analysis (PCA) of wetland environmental variables was used to identify and explain wetland heterogeneity. The results of the study showed that fluvial processes, tectonic history and the evolution of Africa's landscape played a fundamental role in the formation and evolution of wetlands. This study demonstrates a wide range of processes that contribute to wetland formation, structure and functioning. At one extreme it is clear that tectonic processes may be primarily responsible for the creation of basins that host wetlands. At another extreme, wetlands may be structured primarily by fluvial processes. At a third extreme are wetlands that superficially appear to be structured by fluvial processes, but which have their structures modified by gradual rising of the base level at their distal ends, either through marginal uplift adjacent to rift valleys, or through aggradation of a floodplain that blocks a tributary valley. Overall, the classification of wetlands considered in this study can be summarised into four distinct groupings, with two of these divided further into two groupings each: (1) Tectonic basins with little or no indication of fluvial development (Bahi and Wembere wetlands), (2) Tectonic basins evolving towards a wetland with a structure increasingly shaped by fluvial characteristics (Usangu wetland), (3) Fluvially modified valleys with a local base level at the toe of the wetland such as a resistant lithology or a tectonic control that limits the rate of incision of easily weathered and eroded lithologies, leading to valley widening and

longitudinal slope reduction, which are of two distinct types: (a) With a catchment on Kalahari Group sediment that is transported fluvially as bedload, and therefore with no prominent alluvial ridge or backwater depressions (Upper Zambezi and Barotse wetlands), (b) With a catchment that produces abundant fine sediment that is deposited as overbank sediments, leading to channel migration via meandering and to the construction of an elevated alluvial ridge (Lufira wetland), (4) Fluvially modified basins with evidence of gradual elevation of the base level at the toe of the wetland, which are of two types: (a) Tectonic marginal rift valley uplift such that they behave more as depression wetlands rather than as wetlands shaped by fluvial processes (Kafue and Luapula wetlands), (b) Tributary valley wetlands blocked by aggradation of the trunk valley (Lukanga wetland). In conclusion, although few geomorphological studies have been conducted on southern African wetlands because of their inaccessibility, Africa's surface topography and its historical evolution, as well as aridity, provide an opportunity for illustrating the important role that the long-term tectonic, geological and geomorphological processes play in determining wetland origin, structure and dynamics. GIS methodology and Earth Observation (EO) data on the other hand, provide a practical means for acquiring information on inaccessible and hard to traverse wetland systems. A novel cut-and-fill approach for delineating wetlands from a Digital Elevation Model (DEM) was presented as another way in which GIS methodology and Earth Observation (EO) data can provide practical means for assessing inaccessible and hard to traverse wetland systems.

TABLE OF CONTENTS

LIST OF FIGURES

LIST OF TABLES

LIST OF ABBREVIATIONS

2D	Two Dimensional
3D	Three Dimensional
AI	Aridity Index
amsl	above mean sea level
ASTER	Advanced Spaceborne Thermal Emission and Reflection Radiometer
CGIAR-CSI	Consultative Group for International Agricultural Research Consortium for Spatial Information
DEM	Digital Elevation Model
DEMs	Digital Elevation Models
EARS	East African Rift System
EO	Earth Observation
ESRI	Environmental Systems Research Institute
ETM+	Enhanced Thematic Mapper plus
ETo	Potential Evapotranspiration
FAO	Food and Agriculture Organisation of United Nations
GIS	Geographic Information System
GLWD	Global Lakes and Wetland Database
GPS	Global Positioning System
GTOPO30	Global 30 Arc-Second Elevations
HGM	Hydro-geomorphic
ISC	International Seismological Centre
ITCZ	Inter-Tropical Convergence Zone
Km^2	Square kilometres
KML	Keyhole Markup Language
LiDAR	Light Detection and Ranging
m	metre
Ma	Million years ago
MAE	Mean Annual Potential evapotranspiration
MAP	Mean Annual Precipitation
MBVIs	Multi-band Vegetation Indices

MODIS	Moderate Resolution Imaging Spectroradiometer
NASA	National Aeronautics and Space Administration
NDVI	Normalised Difference Vegetation Index
NDWI	Normalised Difference Water Index
OKZ	Okavango Kalahari Divide
PA	Producers Accuracy
PCA	Principal Component Analysis
PU	Users Accuracy
RS	Remote Sensing
SADC	Southern African Development Community
SMUWC	Sustainable Management of the Usangu Wetland and its Catchment
sq km	Square kilometres
SQL	Structured Query Language
SRTM	Shuttle Radar Topographic Mission
TBVIs	Two Band Vegetation Indices
TCWI	Tasselled Cap Wetness Index
TIN	Triangular Irregular Network
TM	Thematic Mapper
USGS	United States Geological Survey
UTM	Universal Transverse Mercator
WCMC	World Conservation Monitoring Centre
WGS	World Geodetic System
WWF	World Wide Fund for Nature
WWW-TCO	World Wide Fund for Nature Tanzania Country Office
y BP	year before present

ACKNOWLEDGEMENT

I am grateful to the Carnegie-RISE (Regional Initiative in Science and Education) initiative for their financial support during the course of this study.

I would like to direct my deepest gratitude to my supervisors Prof F Ellery and Dr S.K Mantel for their supervision and guidance throughout the study. I would like to thank Prof D.A Hughes for his support and guidance.

I am especially thankful for the significant support that was provided to me by stuff and students within the Institute for Water Research (IWR) during the course of this study. The IWR seminar presentations and contribution from research staff and students greatly provided significant contributions throughout the study. Special thanks go to Mrs Juanita Mclean and Mr David Forsyth for administrative and technical support provided.

I would also like to acknowledge my colleagues and friends, especially F Akamagwuna, E Makungu, O Gwate, D Rugai, C Ndzabandzaba, E Vellemu, T.H Kabanda, and T. Nemalili, thank you so much. Lastly, I would like to thank my family for their encouragement and support throughout the study.

CHAPTER 1: INTRODUCTION

1.1 Understanding wetland geomorphic origin, structure and hydrological functioning from the use of Earth Observation (EO) data

There is limited understanding of the geomorphic origin and hydrological functioning of wetlands in southern Africa (McCarthy and Hancox, 2000). The limited understanding of the geomorphic origin of wetlands in southern Africa may be attributed to the relatively few geomorphological studies that have been conducted on wetlands in Africa's elevated drylands. The limited knowledge of wetland geomorphic processes is a significant gap as it is recognised as essential if management interventions are to be sympathetic with nature and therefore, sustainable (McCarthy and Hancox, 2000; Ellery et al., 2009). In addition, this significant gap has resulted in limited information for developing a comprehensive classification system of wetlands based on geomorphic processes (McCarthy and Hancox, 2000). As a result, most available wetland classification systems are largely descriptive or account for short-term analysis of wetland ecological and hydrological dynamics.

The contribution of the discipline of geomorphology to wetland studies has tended to be limited since geomorphologists have generally neglected wetlands, perhaps because of their complexity (Tooth et al., 2015). However, the high-lying semi-arid interior of southern and eastern Africa presents a number of opportunities to better understand the role of geomorphology in wetland formation, structure and hydrological function. Wetland structure refers to wetland features such as backwater depressions, oxbow lakes and wetland channels, as well as the relation between wetland channels and the adjacent wetland areas. The 3-dimensional structure of wetlands is generally a consequence of the geomorphic processes which determine the origin and long term development of the wetland. Remarkably, in the absence of mountain-building activities, most of Africa's interior is highly elevated as it lies at an elevation above 1 000 m amsl (McCarthy and Hancox, 2000; Flügel, 2014). This means that the region as a whole is in a state of erosion, which means that watercourses are likely to be in a state of long-term incision. In addition, most parts of the continent are characterised by arid and semi-arid climatic conditions where evapotranspiration rates greatly exceed precipitation rates throughout the year (McCarthy, 1993). Yet the continent hosts some of the world's most significant wetlands such as the Okavango Delta and Barotse floodplain (McCarthy, 1993; Schumm, 1993; Tooth et al., 2004; Fraser and Keddy, 2005; Goudie, 2005).

Inland wetlands commonly exist and are most widespread in high rainfall or cooler regions where there is a positive surface water balance and gently sloping terrain (Tooth and McCarthy, 2007). In drylands, the negative surface water balance should limit wetland formation. Given this climate, most large wetlands in drylands are commonly associated with rivers that supply the majority of water and sediment (Mumba and Thompson, 2005; Tooth and McCarthy, 2007). Therefore, dryland wetlands have greater potential to influence basin hydrology relative to their counterparts in high rainfall or cooler regions.

Another factor contributing to the limited understanding of wetland origin and hydrological functioning is the remoteness and difficulty of accessing and working in wetland ecosystems. Wetland geomorphologists tend to rely mostly on field survey methods such as sediment coring, topographic surveying, Global Positioning System (GPS) mapping, and analysis of physical copies of topocadastral maps, in order to understand the morphological characteristics of wetlands (e.g. Longmore, 2001; Tooth and McCarthy, 2007; Grenfell et al., 2010; Joubert and Ellery, 2013). Some wetlands in Africa's elevated drylands, such as the Okavango Delta in Botswana and the Bangweulu swamps in Zambia, cover vast areas spanning thousands of square kilometres, and some of these wetlands are difficult to access using field based methodologies. As a result, information on the characteristics of different large wetlands is scarce and this has resulted in limited scientific studies on their structure and dynamics (Ellery et al., 2009; Tooth et al., 2009; Hughes et al., 2014). However, Earth Observation (EO) data and Geographic Information System (GIS) technologies can provide a means of understanding characteristics of these large wetland systems (Ozesmi and Bauer, 2002; Overton, 2005; Funkenberg et al., 2014; Li et al., 2014; Romshoo and Rashid, 2014) and potentially provide useful information for generating a classification system that groups wetlands based on their geomorphic origin and hydrological functioning.

Although wetlands perform a number of hydrological functions including groundwater recharge (Acharya and Barber, 2000) and water purification (Verhoeven et al., 2006), the current study focuses mainly on their flood attenuation function. This is because through flood attenuation, wetlands can exert an influence on downstream flow regimes. Understanding the nature of their influence on downstream discharge is critical in fully describing basin hydrology (Hughes et al., 2014). The flood attenuation function of wetlands is a function of the dynamic interaction between river channels and wetland areas (Trigg et al., 2013). However, there is limited information on the nature of channel wetland exchanges since the dynamics of the interchange between wetlands and river channels are complex and

vary depending on wetland types (Hughes et al., 2014). The complexity of channel wetland exchanges was highlighted by Hughes et al. (2014), who aimed to incorporate wetland processes into an existing hydrological model in order to reduce model structural uncertainties and improve model simulations in areas where the effects of wetlands or natural lakes on stream flow are evident. The dynamic flow interactions between wetlands and river channels as well as between different areas within the wetland are complex since they are influenced by wetland physiographic structure, which is a function of the geomorphic origin of a wetland (McCarthy and Hancox, 2000; Trigg et al., 2013). Therefore, in order to understand the dynamic interactions between wetlands and river channels it is important to examine the nature of the wetland's hydrological and sedimentological regime. The concept of landscape connectivity, which deals with the extent and rate of transfer of water and sediment between and within landscape units (Fryirs et al., 2007a; Trigg et al., 2013), may provide a useful framework to examine the extent to which different wetlands exert influence on downstream discharge.

With regard to the theory of landscape connectivity, hydrologists focus mainly on hydrological connectivity (e.g. Trigg et al., 2013) while geomorphologists focus mainly on sedimentological connectivity (e.g. Fryirs et al., 2007a). However, hydrological and sedimentological connectivity interact to shape wetland structure and dynamics, which in turn influence wetland hydrological functioning (Tooth and McCarthy, 2007). Therefore, in order to understand dynamic flow interactions between wetlands and river channels it is also vital to determine the geomorphological origin of wetlands. This is because wetlands that form from different geomorphic processes are likely to exhibit different wetland structures (Tooth and McCarthy, 2007) and may influence the hydrological regime differently.

1.2 Scope

This study focuses on large wetlands in elevated arid and semi-arid regions in Africa, thus excluding coastal wetlands. The focus on inland wetlands is mainly because of their potential influence on basin hydrology. The focus on large wetlands is mainly because the flood attenuation function of wetlands is thought to increase with size (Keddy, 2000; Fraser and Keddy, 2005) even though the factors determining the formation of wetlands of all sizes may be similar.

1.3 Aim

The study aims to classify large wetlands in Africa's elevated drylands using remote sensing and GIS techniques based on factors that determine their formation and shape their structure and hydrological functioning.

1.4 Study objectives

- Identify and map large wetlands in southern Africa's elevated drylands using GIS techniques
- Identify the likely geological and geomorphological factors that influence wetland formation
- Relate wetland formation and structure to hydrological functioning
- Classify wetlands based on processes that determine their formation, structure and hydrological functioning

1.5 Thesis structure

General introduction

The current chapter **(Chapter one)** is the background to the study with a brief overview of existing knowledge and challenges towards understanding the geomorphic origin and hydrological functioning of large wetlands in Africa's elevated drylands.

Literature review

In a broader context of the theory of landscape connectivity, the next chapter **(Chapter two)** presents necessary conceptual background on wetland flood attenuation function. The formation and modification of wetland valleys and depressions as a result of the interaction of fluvial systems and the landscape is given. A review of existing wetland formation models and issues with existing GIS and Remote Sensing (RS) approaches which can be used in wetland studies is also given. A review of these approaches helped inform the research methods.

Introduction to the study area

In **Chapter three** a detailed description of the study area is provided, paying attention to the geographic extent of the study area, climatic conditions, hydrology, wetland distribution, socio-economic characteristics and the exploitation of natural resources. Background of the topographic evolution of the study area and the drainage network as a result of tectonic activities is given.

Spatial datasets and methods

Chapter four gives a description of the GIS and EO spatial datasets in terms of their custodians, limitations and merits. The chapter also provides detailed descriptions of GIS and RS approaches used to derive and analyse wetland structure and channel characteristics such as wetland slope, extent, width, length, channel slope, and catchment area.

Results

In **Chapter five**, the results of the criteria for selecting the study sites or mapping the distribution of large wetlands in Africa's elevated drylands are given. The results of the delineation of the boundary of the selected wetlands are also presented, including comparison of the accuracy of the delineated wetland boundaries with other studies. **Chapter six** presents the origin, structure, and hydrological functioning of lithologically controlled floodplain wetlands. **Chapter seven** presents the origin, structure, and hydrological functioning of floodplain wetlands that occur in tectonically controlled graben structures. **Chapter eight** presents the origin, structure, and hydrological functioning of tectonically controlled depression wetlands. **Chapter nine** provides a classification of large African wetlands based on a cluster analysis and principal component analyses of wetland features that influence wetland structure and hydrological functioning.

Discussion and conclusion

Chapter ten discuss the major findings of the thesis in relation to existing knowledge and **Chapter eleven** concludes the major findings of the study and provides suggestions for future research.

CHAPTER 2: THEORETICAL FRAMEWORK

2.1 Wetland flood attenuation

The flood attenuation function of different types of wetlands has received much attention (e.g. Bullock and Acreman, 2003; Williams et al., 2012; Acreman and Holden, 2013; Kadykalo and Findlay, 2016). Although it is acknowledged that there are differences in flood attenuation functioning both within and between different wetland types, floodplain wetlands are perceived to have a great potential to attenuate floods (Acreman and Holden, 2013). The flood attenuation service of a wetland is realised when there is a measurable change in the timing and magnitude of downstream discharge (e.g. McCarthy and Ellery, 1998; Acreman and Holden, 2013). Wetlands can reduce the magnitude of downstream flooding by temporarily storing floodwater within wetland depressions and wetland soils (McCarthy and Ellery, 1998; Williams et al., 2012). Wetlands can also recharge groundwater or lose water through evapotranspiration, while water flowing at a shallow depth through dense stands of vegetation or along shallow and wide channels will be much slower than through a deep and narrow channel. The presence of a valley with a low gradient, which is typical of wetland habitats, also serves to slow and delay the timing of flooding downstream.

The Okavango Delta in Botswana provides a good example of the extent to which wetlands attenuate floods (Figure 2.1). McCarthy and Ellery (1998) documented the flow attenuation function of the Okavango Delta in Botswana. The authors highlighted that rainfall in the Okavango catchment peaks in January such that discharge in the Okavango River rises during this time. However, flooding at the head of the wetland peaks in April such that the water takes about 2 to 3 months to travel from the headwaters in Angola, a distance of about 1700 km. The flood wave takes an additional four months to traverse the 250 km length of the wetland, which is an order of magnitude slower than its travel time from the headwaters to the head of the wetland. The Okavango wetland not only delays the timing of flooding downstream, but it also reduces the amount of water that leaves the wetland, which means that the difference between peak and base flows is low. Much of the water that enters the Okavango Delta is lost through groundwater recharge and evapotranspiration (McCarthy and Ellery, 1998). The authors attributed the physiographic structure of the Okavango Delta to be partly responsible for the flood attenuation function of the wetland as water disperses widely over a vast vegetated wetland area (Figure 2.2) in which large volumes of water are lost to the atmosphere. The undulating topography of the wetland also creates depressions that serve to

temporarily store and retain floodwater until their storage capacity is reached, while the low gradient and dense vegetation serve to impede the passage of the flood wave and reduce the velocity of the flood wave (McCarthy and Ellery, 1998). This example shows how wetland structure, which in this case is related to tectonic and sedimentary processes, greatly influences the flood attenuation function of a wetland.

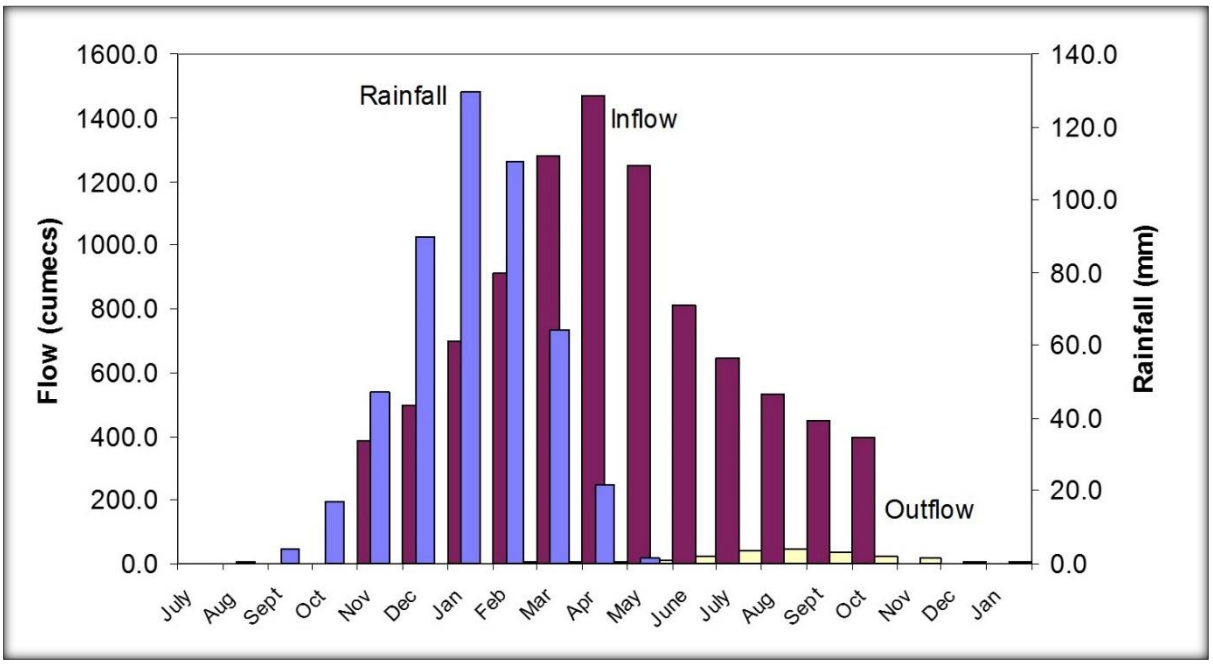

Figure 2.1: The hydrological regime of the Okavango Delta. Source of the data (McCarthy and Ellery, 1998).

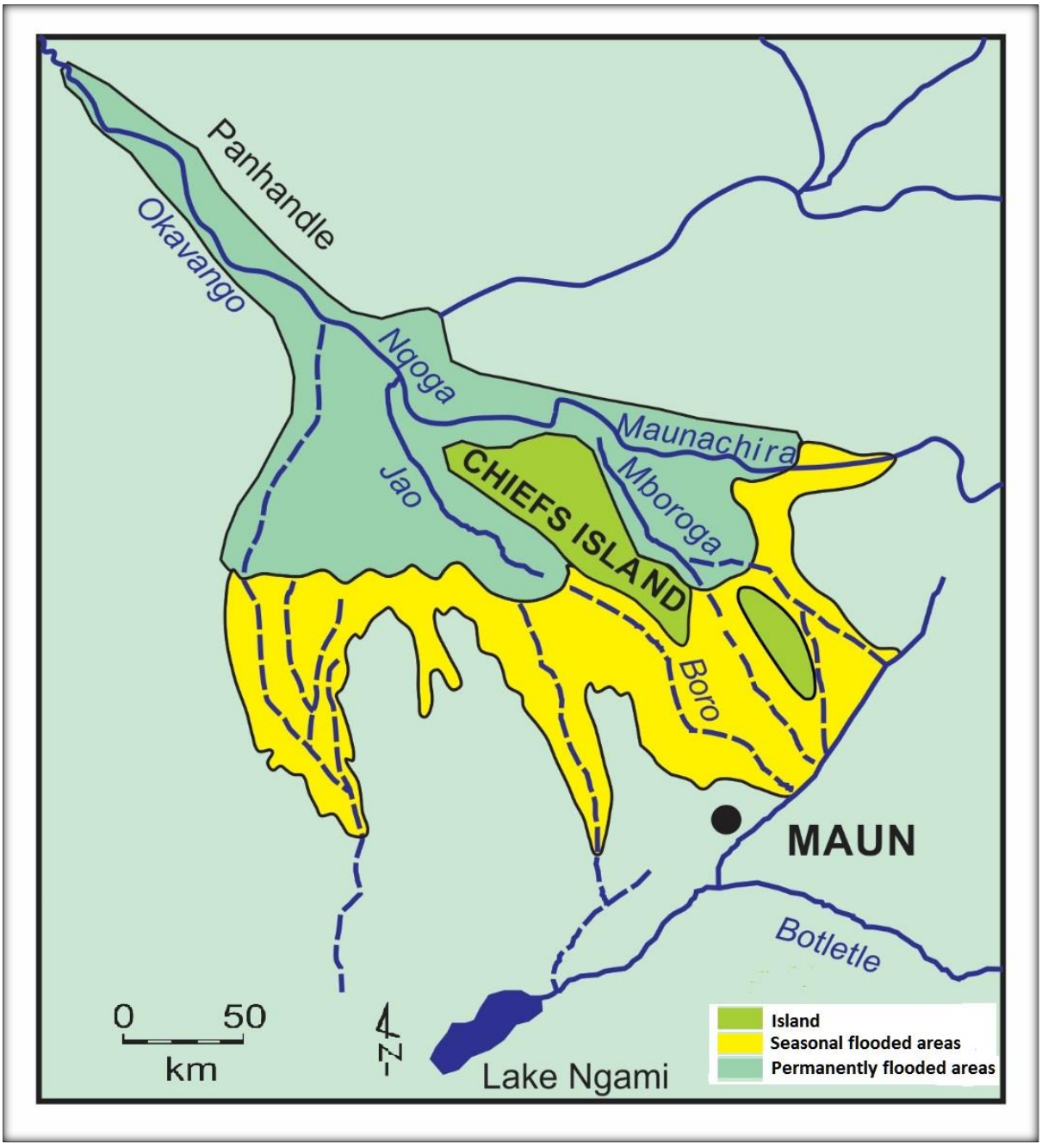

Figure 2.2: The Okavango Delta in northern Botswana.

2.2 Wetland flood attenuation functioning and the concept of connectivity

Connectivity describes the degree to which material and energy can move between or within landscape compartments (Fryirs et al., 2007a; Wohl, 2017). Landscape units have different degrees of connectivity that vary across space and through time. Therefore, the examination of landscape units from a connectivity perspective can provide an understanding of material such as water and sediment transfer within or between landscape units (Fryirs et al., 2007a; Trigg et al., 2013; van der Waal and Rowntree, 2015). The transfer of water and sediment in the context of the current study occurs between river channels and wetland areas, within

different reaches of the wetland, or between the adjacent upland and the wetland. The degree of connectivity between river channels and wetland areas determines the extent of transfer of water and sediment from the channel to the wetland and from the wetland back to the channel. A well connected drainage system allows for the free flow of water and sediment through and across the system. However, various landforms or landform features may impede the exchange of water and sediment, laterally (from the stream to the wetland and vice versa), vertically (from the stream or floodplain to the ground and vice versa), or longitudinally (Fryirs et al., 2007a). Landforms such as alluvial fans and levees can impede the lateral transfer of water and sediment from the wetland or surrounding uplands to the channel and are termed buffers (Brierley et al., 2006; Fryirs et al., 2007b; van der Waal and Rowntree, 2015). Barriers disrupt sediment flux longitudinally through features such as bedrock steps, woody debris or sediment slugs, which impede the downstream or longitudinal transfer of water and sediment within river channels. Blankets disrupt vertical surface-subsurface linkages and include floodplain sediment sheets that smother the floodplain surface and impede vertical transfer of energy and material. Landscape elements or features that impede lateral and longitudinal connectivity may result in flooding, sediment deposition and retention. Brierley et al. (2006) also describe boosters, which are steeply sloping landforms such as gorges, which may enhance the conveyance of sediment and water downstream. Therefore, in order to understand channel-wetland exchanges it is important to identify factors and processes that affect the transfer and retention of sediment and water within a wetland.

With regard to the concept of landscape connectivity, geomorphologists (e.g. Brierley et al., 2006; Fryirs et al., 2007b; van der Waal and Rowntree, 2015) mostly consider the transfer of sediment. Hydrologists (e.g. Trigg et al., 2013) on the other hand, are mostly concerned with the transfer of water between river channels and wetland areas. However, sedimentological connectivity between or within landscape units is mediated by flowing water such that in order to provide an in-depth understanding of the flood attenuation function of wetlands from the theory of landscape connectivity, it is vital to illustrate how hydrological and sedimentological connectivity interact to influence wetland flood attenuation function. This is because this interaction shapes wetland structure through the formation and development of depositional features such as an alluvial ridge, which acts as a buffer and ultimately influences the ability of a wetland to attenuate floods. Other features such as bedrock steps hinder the longitudinal transfer of sediment by acting as a base level, thus slowing down the

rate of vertical incision and enhancing lateral channel migration and sedimentation (Tooth et al., 2002; Brierley et al., 2006; Fryirs et al., 2007b; van der Waal and Rowntree, 2015). Wide and shallow vegetated channels impede the longitudinal transfer of water and sediment, and increase lateral connectivity through increasing the likelihood of overbank flooding. Conversely, through an enlarged channel cross-section, channel incision increases channel capacity and longitudinal connectivity, thus resulting in a decrease in lateral connectivity (van der Waal and Rowntree, 2015). Lateral channel and wetland connectivity varies spatially and temporally, and influences the ability of a wetland to attenuate floods (van der Waal and Rowntree, 2015; Wohl, 2017). This is because the flow magnitude and channel cross-section influence the rate of lateral transfer of water and sediment from river channels to wetland areas (van der Waal and Rowntree, 2015). At low flows and in reaches that are characterised by large channel cross-sections, flow may be insufficient to connect the channel and wetland area. At high flows or during flood peak events, flow may be sufficient to overtop shallow channels and spread over the wetland area. Once the floodwater has spread over the wetland surface during flood peak events, the physical structure of the wetland determines the timing and magnitude of return flows in the waning stages of the flood event.

A comparison of the flood attenuation functioning of an anastomosing (Figure 2.3a) and a meandering (Figure 2.3b) floodplain wetland provides an example of how wetland structure influences channel-wetland exchanges. Anastomosing floodplains are characterised by two or more interconnected channels that are usually associated with avulsions (Makaske, 2001). Avulsions, which are primarily driven by channel bed aggradation as bedload is the primary sediment type transported in these systems, determine the degree of channel-wetland lateral connectivity. Because of the dominance in anastomosing systems of bedload sediment and deposition, aggradation is very locally concentrated and the wetland maintains a relatively flat cross-sectional form (Figure 2.3a). As a result of their relatively uniform topography, anastomosing floodplains may lack features such as backwater depressions and permanently flooded reaches. This is because during peak flood events within a wetland with an anastomosing channel, some of the floodwater that overtops channel banks inundates the wetland surface and may relatively easily return to the river channel during the waning stages of a flood. Although much of the floodwater that gets spread over the wetland area could be lost within the wetland through evapotranspiration or groundwater recharge, anastomosing floodplains show a high degree of channel-wetland connectivity. This suggests that anastomosing floodplain wetlands are likely to have lower potential to attenuate downstream

discharge than equivalent floodplain systems with large-scale meandering streams with alluvial ridges.

Floodplains with meandering streams are characterised by an alluvial ridge with laterally-migrating channels, as well as fluvial features such as oxbow lakes, backwater depressions and backswamps, with abandoned channels (Makaske et al., 2001; Tooth et al., 2002; Ashworth and Lewin, 2012; Lewin and Ashworth, 2014; Larkin et al., 2017a). Within meandering floodplains, channel bed and overbank deposits of fine-grained suspended sediment build an alluvial ridge, elevate the main channel above the adjacent wetland areas, and lead to the formation of backwater depressions along floodplain margins or in distal wetland areas (Figure 2.3a; McCarthy and Ellery, 1998; Makaske, 2001; Tooth et al., 2002; Tooth et al., 2004). Within a meandering floodplain, when floodwater overtops the channel banks during peak flood events, the floodwater can be easily spread from the alluvial ridge to lower-lying backswamp areas. However, the alluvial ridge also serves to impede return flows from backwater depressions to the river channel in the waning stages of the flood event. Although most of the floodwater that spills over from the channel to low-lying wetland areas may be lost through evapotranspiration, some flow returns back to the channel through outflow channels within the lower reaches of the wetland. This is because the alluvial ridge becomes less prominent downstream because of the downstream decrease in overbank sedimentation (McCarthy and Ellery, 1998; Townsend and Walsh, 2001). Given these characteristics, a meandering floodplain shows a high potential to attenuate downstream flooding.

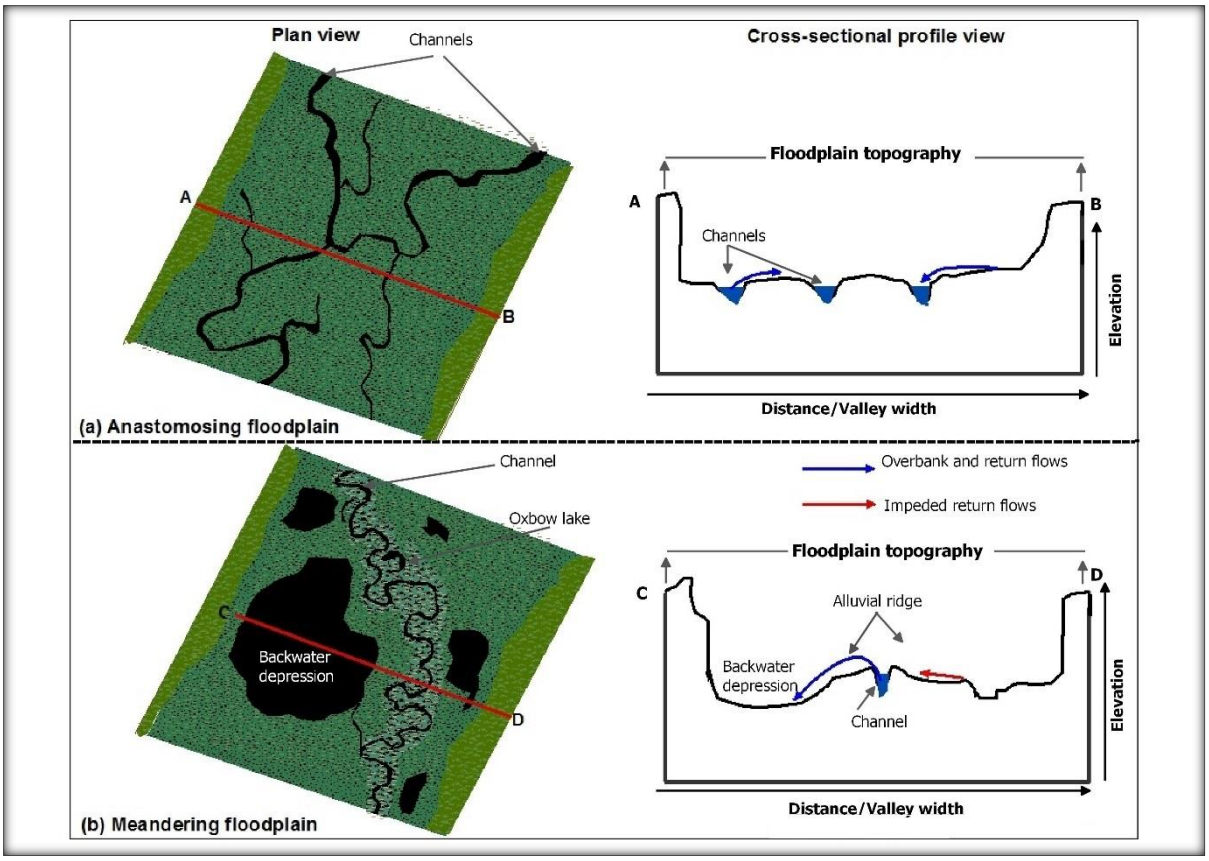

Figure 2.3: Schematic illustration of floodplain structure with respect to floodplain topography.

The comparison between the structure of a meandering and an anastomosing floodplain with respect to channel wetland connectivity and the flood attenuation functioning shows that a classification of wetlands based on sedimentological and hydrological connectivity can provide a deeper understanding of wetland dynamics and hydrological functioning. This is because most available classification systems are largely descriptive in nature or account for short-term analysis of wetland dynamics and do not provide adequate conceptualisation of wetland processes by jointly considering geomorphological and hydrological perspectives (McCarthy and Hancox, 2000). For example, the hydrogeomorphic (HGM) classification system is the most widely used in the United States for wetland functional assessment (Kotze et al., 2007). The HGM classification classifies wetlands based on their location within the landscape, their potential sources and loss of water, and the patterns of water flow through the wetland (Brinson, 1993; Brooks et al., 2013). However, the HGM classification system does not account for the geomorphic processes that influence wetland origin, structure and functionality. For this reason the HGM classification system is viewed as over-generalising the functionality of riverine wetlands, thus ignoring the dynamics and differential functioning of various floodplain wetlands as a result of their origin and associated geomorphic structure.

In addition, some of the wetland types (e.g. mineral soil flats) described within the HGM system do not occur widely in eastern and southern Africa's arid and semi-arid region.

2.3 Wetlands as fluvially integrated features driven by geomorphological processes

Most large wetlands in Africa's elevated drylands are integrated with fluvial networks (Ellery et al., 2009). These wetlands are maintained hydrologically from channel inflows (McCarthy, 1993; Mumba and Thompson, 2005; Ellery et al., 2009) and in turn influence basin hydrology (Hughes et al., 2014). Associated fluvial processes play a vital role in determining wetland formation, shaping their structure, evolution and functioning (McCarthy and Hancox, 2000; Tooth et al., 2002; Grenfell et al., 2008; Edwards, 2009; Grenfell et al., 2010). Therefore, it is vital to illustrate how fluvial geomorphological processes shape wetland dynamics and functioning.

In a drainage basin, streams work to maintain a gradient that is appropriate for a given discharge. Where the discharge is too high for a given slope, the stream erodes its bed and lowers its gradient. Where the discharge is too low for a local slope, the stream aggrades its bed and steepens its gradient. Where the slope is suitable for a given discharge the stream neither aggrades nor erodes its bed (Ellery et al., 2009). Therefore, streams respond to a given discharge through sediment mobilisation (erosion) where the slope is too steep for the discharge, transportation where the slope is appropriate, and deposition where the slope is too gentle. As a result of channel response to a given discharge most streams will achieve a logarithmic longitudinal profile down their length given that discharge typically increases downstream (Figure 2.4).

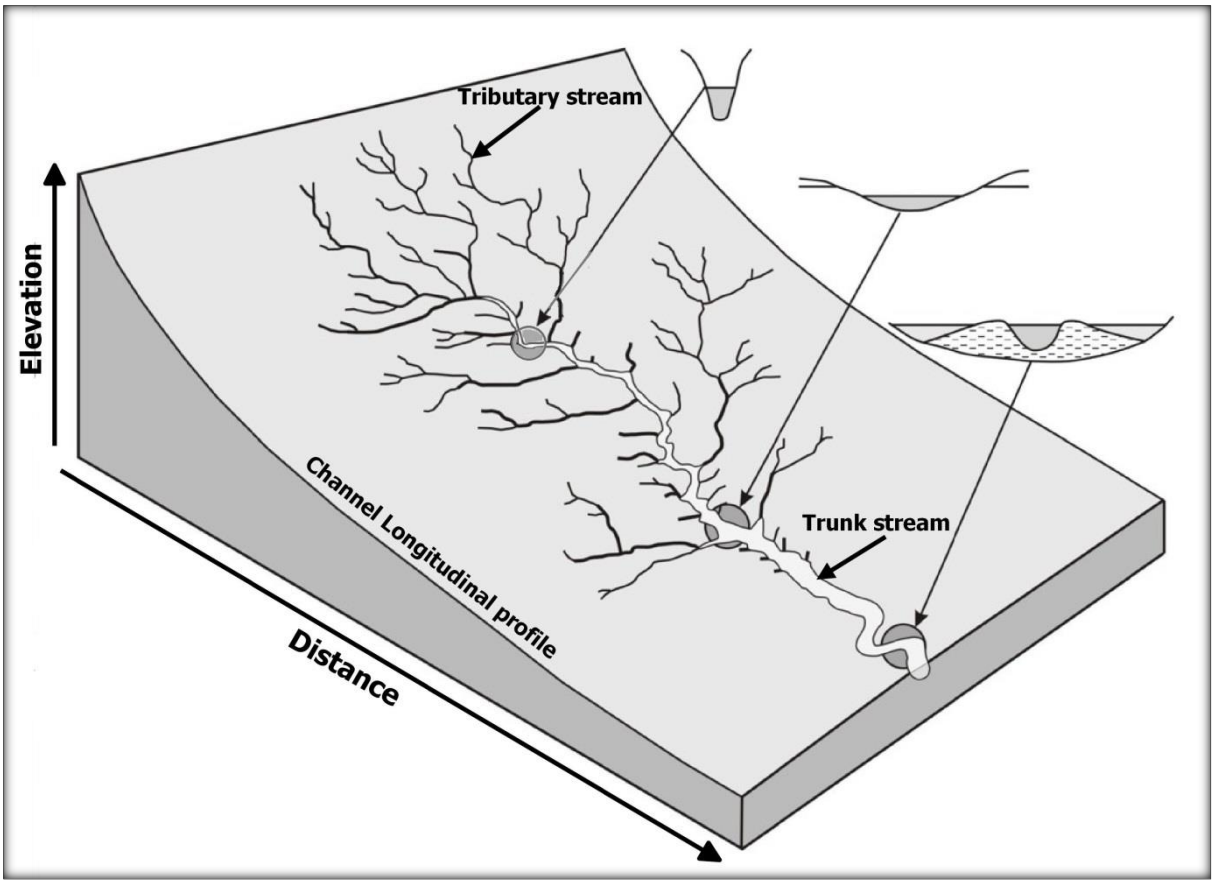

Figure 2.4: Drainage basin and logarithmic channel longitudinal profile as well as valley cross-sectional profiles (modified from Ellery et al., 2009).

Streams will strive to maintain their logarithmic longitudinal profiles given that there are no changes in the base level such that channels maintain constant rates of transfer of water and sediment (i.e. longitudinal connectivity). Sea and lake water level can act as a base level, the trunk stream may act as a base level for tributary streams, while resistant lithologies and fault lines may act as local base levels and influence longitudinal connectivity. Connectivity within a river basin is strongly influenced by channel response to climatological, geological, fluvial and tectonic disturbances (Brierley and Fryirs, 1999; Wohl, 2017). Factors that lower the base level enhance longitudinal connectivity while rising base level impedes longitudinal connectivity. Since river discharge increases downstream, falling sea or lake water levels or continental uplift may lower the base level and result in stream incision. As the bed of the trunk stream incises, tributary streams will respond to their newly established base level by incising their beds, increasing channel connectivity within a drainage network with complex arrangement of connected and disconnected fluvial system, ultimately reducing the basin's sediment and water retention period (Brierley and Fryirs, 1999).

A change from wetter to drier climatic conditions may reduce the rate of sediment mobilisation and therefore enhance stream dis-connectivity (Brierley and Fryirs, 1999). Geological materials such as intrusive bedrocks and fault lines intercepting a river channel may impede longitudinal connectivity upstream by acting as a local base level and reducing the rate of sediment mobilisation. This may result in increased lateral channel migration and decreased lateral connectivity through increased depositional rates, and ultimately transform former sediment source zones into sediment accumulation zones. Such resistant lithologies may form and sustain topographic steps along newly established channel longitudinal profiles (Schumm, 1993; Brierley and Fryirs, 1999; Tooth et al., 2002; Flügel, 2014; van der Waal and Rowntree, 2015). Vertical channel erosion as a result of channel response to enhanced longitudinal connectivity may form deeply incised valleys or lead to desiccation of existing wetland systems, while lateral channel erosion as a channel response to an impeded longitudinal connectivity may lead to upstream valley widening and sedimentation (Tooth and McCarthy, 2007).

2.4 Models of wetland formation and implications for wetland structure

There are several models that consider the role of geomorphic processes in wetland formation that have been developed in southern Africa. These models include: (1) Trunk-tributary interactions in which the longitudinal transfer of water and sediment within a tributary stream are impeded at its confluence with the trunk stream by aggradation along the trunk stream valley, leading to the formation of unchannelled valley-bottom wetlands within the lower tributary valley, often with blocked tributary valley lakes present (e.g. Lake Futululu and Stillerust Vlei; Grenfell et al., 2008; Grenfell et al., 2010). In some instances, deposition of sediment across a trunk stream valley by a tributary stream alluvial fan at the confluence with the trunk stream may impede longitudinal transfer of water and sediment within the trunk stream, resulting in the formation of unchannelled valley-bottom wetlands within the trunk stream (e.g. Wakkerstroom Vlei; Joubert and Ellery, 2013). (2) Lithological controls in which wide valleys which host wetlands on lithologies that are relatively easily eroded are planed laterally upstream of a resistant lithology that acts as a local base level (e.g. Klip River floodplain; Tooth et al., 2002). (3) Within a tectonically controlled landscape, subsidence of the rift valley floor and the creation of rift shoulders adjacent to the subsiding rift valley can impede the longitudinal transfer of water and sediment and result in the formation of wetlands (e.g. the Okavango Delta; Tooth and McCarthy, 2007).

2.4.1 Lithological control on wetland formation

Tooth et al. (2002) reported the formation of a meandering floodplain on the Klip River in the eastern Free State of South Africa. The floodplain was a valley undergoing long-term incision. The river, which overlay sedimentary rocks (sandstones and shales) of the Karoo Supergroup, incised until its bed was positioned over a dolerite dyke (Figure 2.5). Since dolerite weathers and erodes more slowly than sandstone and shale, the dolerite dyke formed a local base level for the river, limiting incision in an upstream direction. Vertical incision of the channel bed upstream of the dolerite dyke could not proceed faster than vertical incision of the dolerite dyke (Tooth et al., 2002). As a response to the base level control imposed by the resistant dolerite lithology, the river increased its sinuosity upstream. With increased sinuosity upstream of the resistant lithology, the channel eroded the valley laterally, widening it and lowering its longitudinal slope. Over time these processes contributed to the formation of a floodplain wetland covering an area of about 30 km^2.

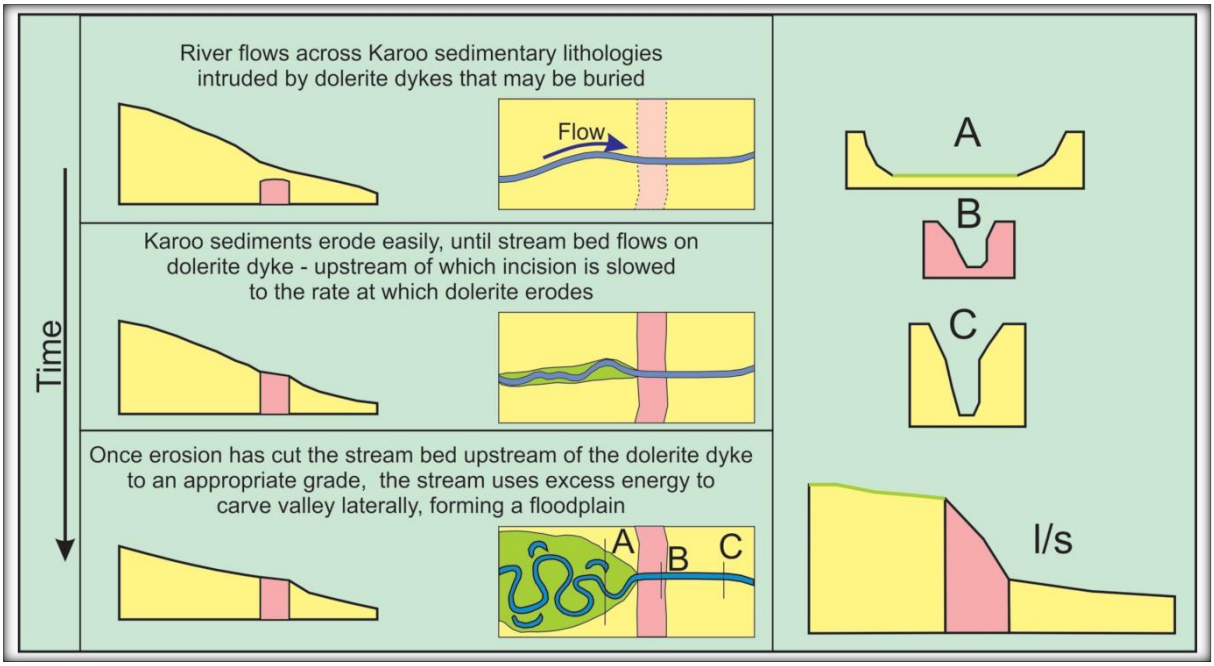

Figure 2.5: Illustration of the processes leading to the formation of channel meander and consequent floodplain wetland (modified from Tooth et al., 2002).

2.4.2 Trunk-tributary stream interactions and wetland formation

Grenfell et al. (2008) documented processes leading to wetland formation within a tributary valley of the Stillerust Vlei in the foothills of the Drakensberg Mountains in KwaZulu-Natal, South Africa. Aggradation along the trunk stream impounded the tributary valley and led to the formation of a wetland in the lower part of the tributary valley. A similar suite of processes was documented along the lower Futululu tributary valley of the Mfolozi River

(Grenfell et al., 2010), where aggradation along the Mfolozi floodplain blocked the tributary valley (Figure 2.6). In both cases continued aggradation and construction of an alluvial ridge on the trunk stream valley, impeded the longitudinal transfer of sediment by raising the base level of the tributary streams. The tributary responded to the elevated base level by aggrading headward and ultimately became disconnected. Within the tributary valley, this resulted in the formation of a wetland characterised by a chain of ponds or by a lake, upstream of which the tributary was characterised by diffuse flow.

It should be noted that tributary streams might also impound trunk streams if tributary streams supply more sediment to the trunk valley than the trunk streams can transport downstream (Grenfell et al., 2010). In such cases, sediments accumulate at the confluence and begin to impede longitudinal connectivity in the trunk channel (Joubert and Ellery, 2013). As a result, the sediment at the confluence acts as a local base level for the trunk stream, upstream of which the trunk stream is characterised by a wetland with diffuse flow.

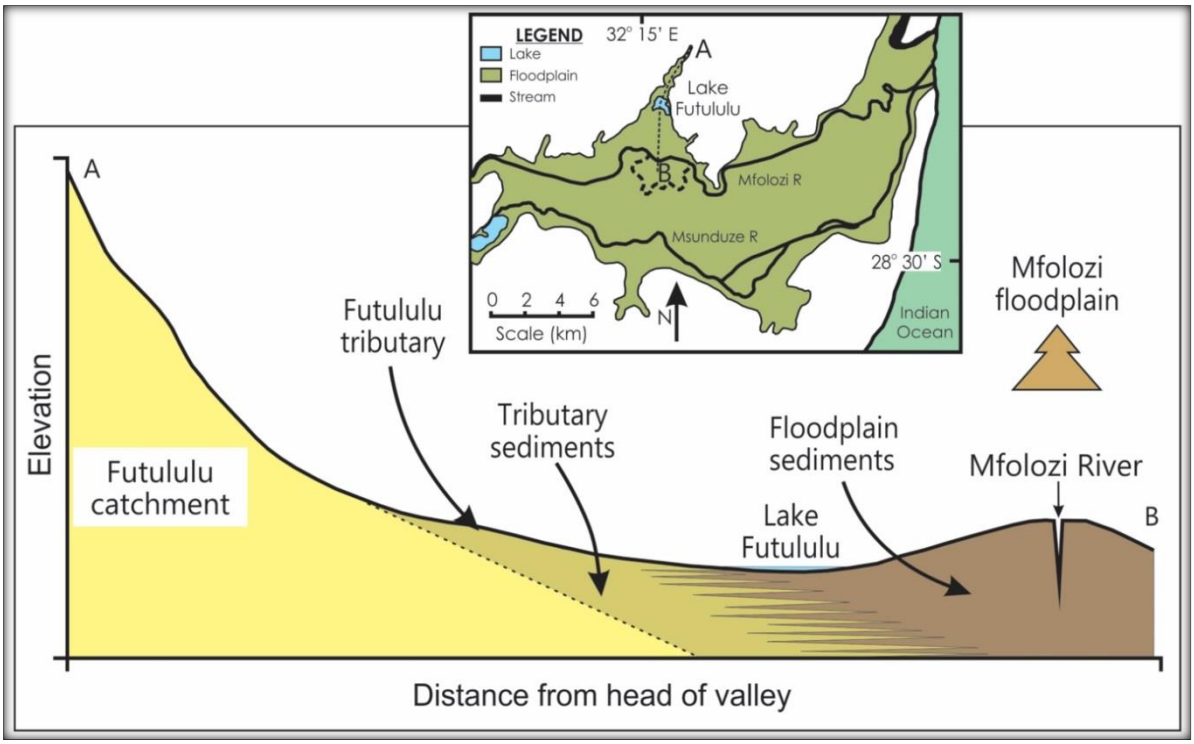

Figure 2.6: Schematic illustration of trunk-tributary relations following a trunk river superimposing upon a resistant lithology and consequent floodplain development (modified from Grenfell et al., 2010).

2.4.3 Tectonic activity and wetland formation

Landscapes that are characterised by faulting and rifting can provide favourable conditions for wetland formation. Rifting is a process that results in the formation of an extended

tectonic depression that is associated with the fracture and movement of the lithosphere due to crustal extension (Olsen and Morgan, 1995). The lithospheric block that becomes lowered as result of tectonic subsidence within the rift valley, which is referred to as a graben, can provide accommodation space for wetland formation. The formation of a graben structure can lower the base level of the influent stream and even divert drainage from the surrounding uplifted blocks into the depression. Over time, flooding and sedimentation within the graben can lead to wetland formation (Kamukala and Crafter, 1993; Ashley et al., 2004; McCarthy et al., 2002). A classic example of a wetland occurring within a graben structure is the Okavango Delta in Botswana (Tooth and McCarthy, 2007). In some cases a tectonic depression may occur between rift shoulders of two or more rift valleys to form a shallow depression wetland or lake, such as Lake Victoria in East Africa (Scholz et al., 1990; Johnson et al., 1996, 2000).

2.5 Use of remote sensing and GIS to understand wetland structure and hydrological functioning

One of the reasons for the limited understanding of wetland processes is that historically, researchers have neglected working in wetlands and primarily focussed on rivers and reservoirs because of their noticeable role in supplying water to sustain human settlements and industry (Malan, 2010; Schael et al., 2015). Historically wetlands were viewed as wastelands and worthless unless they were drained and filled to cater for farms and human settlements as well as industries (McCormick, 1978; Stokes, 1994; Bodini et al., 2000; Yeh, 2009). It is only in the 1950's that the importance of wetlands for waterfowl habitats where realised and soon after that ecologists started identifying knowledge gaps in our understanding of wetland ecology (Cowardin et al., 1977; McCormick, 1978; Stearns, 1978). Over the past 5 decades there has been increasing interest in wetlands from hydrologists, ecologists, geomorphologists and environmental scientists, who recognised the socio-economic benefits of wetlands.

Limited studies on southern African wetlands can be attributed partly to the inaccessibility of some wetland systems (Hughes et al., 2014). The topographic settings of some wetlands such as seep wetlands, and the remoteness of areas where some wetlands are located (e.g. the Okavango wetland; McCarthy et al., 1997), makes them difficult to access. Roads are often in poor conditions, if any exist at all, while soggy grounds and dense stands of emergent

vegetation make it difficult to access some of the wetlands from vehicles. Shallow flooded wetland areas are difficult to traverse by boat.

In areas where wetlands are accessible, conducting field surveys can be dangerous and physically strenuous. Some wetlands such as the Okavango Delta in Botswana and Busanga swamps in Zambia are breeding grounds for insects such as tsetse flies and mosquitoes (Hughes and Hughes, 1992), which may transmit life-threatening diseases such as sleeping sickness and malaria. Wetlands which form part of National Parks (e.g. the Bangweulu and Luangwa valley wetlands; Hughes and Hughes, 1992) are habitats for dangerous wild animals such as elephants, lions, crocodiles, hippopotamus, and leopards. In light of these challenges, wetland scientists deliberately avoid conducting wetland surveys in fear of wild animal attacks, insect bites, and excruciating weather conditions, resulting in limited studies on southern African wetlands.

One of the reasons for the slow pace in generating understanding of wetland geomorphic processes and dynamics is that wetland scientists have in the past relied on costly, time consuming and expertise demanding field survey methodologies. In order to quantify basin hydrology, hydrologists rely on limited numbers of gauging stations and hydrological modelling, which require a large number of inputs that are typically derived from limited existing knowledge and measured data. In order to understand wetland geomorphic processes and improve our limited understanding of these ecosystems, southern African geomorphologists usually use field survey methodologies involving geological, hydrological, topographic and sedimentological characteristics (e.g. Ellery et al., 1993; Smith, 1997; Grenfell et al., 2008). Often, sediment coring is a preferred method for sedimentological analysis (e.g. McCarthy et al., 1993a; Johnson et al., 2001; Humphries et al., 2011; Ellery et al., 2012) and wetland delineation (e.g. Longmore, 2001), while GPS mapping and dumpy level surveying are preferred choices for topographic analysis (e.g. McCarthy et al., 1997; Smith, 1997; Edwards et al., 2016). The analysis of field data is often combined with the analysis of topocodastral maps for topographic analysis and identification of geomorphic features (Tooth et al., 2002; Grenfell et al., 2008; Larkin et al., 2017a). Visual interpretation of aerial photography has been complemented by the analysis of sedimentary sequences to examine the formation of floodplain and lacustrine environments through trunk-tributary interactions (Grenfell et al., 2010). Grenfell et al.'s (2010) study combined the analysis of aerial photography, elevation data from orthophotographs and field survey, and channel and valley longitudinal profiles compiled from GPS data. Longitudinal sedimentary records

determined from a series of sediment cores placed longitudinally down the wetland were used. Valley cross-sections drawn from 1:10 000 orthophotographs with 5 m contour intervals, as well as aerial photographs from different anniversary dates were also used. Other studies have also documented the formation of floodplain wetlands as a result of a lithological control (Tooth et al., 2002; Tooth et al., 2004), again based primarily on field survey techniques complimented by visual image analysis. The construction and analysis of a channel longitudinal profile from 1:50 000 topographic maps to determine variation in channel gradient in response to the effect of lithological variation on channel incision was also used to aid wetland survey methods.

Field survey methods and topocadastral maps have been mostly employed in the study of small wetlands in South Africa such as the Klip River wetland, Stillerust Vlei, Wakkerstroom Vlei and Dartmoor Vlei (McCarthy et al., 1997; Grenfell et al., 2008; Joubert and Ellery, 2013; Edwards et al., 2016) and some parts of the Okavango Delta (Smith, 1997; McCarthy and Ellery, 1998). However, there are some limitations with regard to field based methodologies and the utilisation of topocadastral maps. It is difficult to measure topography in reed beds using basic surveying equipment. Printed maps are static and often represent information at poor and finite spatial resolution. Additionally, because of the inaccessibility of some wetlands and the vast extent of large wetlands such as the Okavango Delta, it may be impractical and time consuming to carry out comprehensive field surveys in such wetlands.

Wetland systems continue to be degraded and lost through anthropogenic activities (Maltby, 1991; Turner, 1991; Finlayson et al., 1999; Gürlük and Rehber, 2006) far more rapidly than knowledge about their structure and functioning is being developed. At the rate at which wetlands continue to be degraded and lost (Davidson, 2014), there is increasing urgency to effectively understand and manage wetlands (Turner, 1991). Therefore, there is a need for carrying out rapid assessments of wetland processes and dynamics in order to inform wetland management.

2.6 Case studies of the use of GIS and remote sensing techniques in wetland studies

Earth Observation (EO) data and GIS technologies are a practical means for carrying out rapid assessments of wetland structure and dynamics. For understanding large and inaccessible wetlands, satellite data and GIS techniques have many advantages (Lyon and McCarthy, 1995). For wetland mapping, satellite data offers repeated coverage that is advantageous for monitoring seasonal, annual, or decadal variability. In addition, these

satellite data are in digital format that make them easy to integrate with GIS (Ozesmi and Bauer, 2002). GIS and Remote Sensing (RS) can be applied in various disciplines including geology (Zervakou and Tsombos, 2010), hydrology (DeVantier and Feildman, 1993), climatology (Tomlinson et al., 2011) and environmental studies (McCarthy et al., 1993b). The application of GIS and RS in various disciplines enables these technologies to offer access to a wide range of archives of spatial datasets such as multispectral images, precipitation and evapotranspiration estimates, geological data and digital elevation models of the Earth's surface. GIS spatial analysis capabilities provide opportunities for overlaying and analysing different spatial datasets (Lyon and McCarthy, 1995).

Earth Observation datasets and GIS techniques have been successfully applied in a wide range of wetland studies including wetland delineation (Li et al., 2014), monitoring wetland change (Haack, 1996) and inundation dynamics (Townsend and Walsh, 1998; Jin et al., 2017). Geomorphological and sedimentological features such as sediment bars, oxbow lakes, abandoned channels, and backwater depressions can be identified from visual analysis of satellite images and aerial photography. Channel longitudinal and valley cross-sectional profiles can be plotted from Digital Elevation Models (DEMs). Wetland inundation and vegetation extent can be mapped using digital image classification techniques. Remote sensing and GIS techniques have been used successfully for wetland mapping but rarely applied in wetland geomorphological studies.

Using satellite data and different techniques for mapping wetlands that cover large geographic areas is less costly and less time consuming than the use of conventional aerial photography (Ozesmi and Bauer, 2002) or field survey techniques. However, few wetland geomorphologists in southern Africa have fully taken advantage of the oportunities that GIS and RS can provide in order to increase our understanding of wetland geomorphic processes and hydrological functioning. The current study sets out to explore and illustrate the potential of EO data as well as GIS techniques in enhancing our understanding of the geomorphic origin and hydrological functioning of large inaccessible wetlands in Africa's elevated drylands.

Li et al. (2014) aimed to develop a hybrid method of extracting spatial patterns of wetland areas that combines month-on-month multispectral classifications of Moderate Resolution Imaging Spectroradiometer (MODIS) data with a single wetland extraction method based on knowledge of the spectral characteristics of satellite data and wetland ecological systems.

Shuttle Radar Topographic Mission (SRTM) DEM and MODIS imagery were used to generate slope maps and to delineate wetlands through supervised and unsupervised approaches. The hybrid classification (i.e. the combination of unsupervised and supervised classification) results showed that the method could extract wetlands automatically to a high degree of accuracy, thus reducing the need for extensive ground knowledge.

Funkenberg et al. (2014) investigated land cover change in an extensive (approximately 40 000 km^2) wetland area of seasonally inundated grasslands in the Mekong Delta, Vietnam, using Landsat images and SRTM DEM. Landsat images of different dates were independently classified through a supervised classification approach using all of the available bands in Landsat Thematic Mapper (TM) as input. The change detection results revealed that large parts of the seasonally inundated grassland in the Ha Tien Plain have been lost because of conversion to agriculture, forestry and aquaculture. A problem with using some of these remote sensing methods (such as image classification) in wetland studies is that there is a high degree of spectral confusion between wetland classes and those of the surrounding uplands (Ozesmi and Bauer, 2002).

To overcome the issue of spectral confusion and to aid interpretation of satellite image, GIS and RS techniques can be integrated. For instance, DEM's can be processed using GIS semi-automated procedures in order to delineate wetland areas (Kulawardhana et al., 2007). These authors evaluated automated and semi-automated methods of mapping wetlands using Landsat Enhanced Thematic Mapper Plus (ETM+) and SRTM 90 m DEM. The automated methods consisted of slope derivation from SRTM, Tasseled Cap Wetness Index (TCWI), Normalised Difference Water Index (NDWI), Multi-band Vegetation Indices (MBVIs), two band vegetation indices (TBVIs), Normalised Difference Vegetation index (NDVI), and data fusion involving ETM+ and SRTM. The results of the study indicated that wetlands were delineated with high accuracy using semi-automated methods.

Another study successfully developed storage-based approaches for incorporating floodplain inundation modelling to a hydrological model for water resource planning and management (Dutta et al., 2013). The study's first approach involved the use of MODIS imagery to produce daily time series imagery to examine the distribution of flooding. The resulting maps were overlaid on 30 m resolution SRTM DEM to provide a daily series of inundation areas and volumes for different river reaches. The second approach entailed the use of available Light Detection and Ranging (LiDAR) data to derive storage characteristics including

disconnected storage volume and hydraulic connectivity between floodplain storage and river reach. The results of the study showed that the second approach successfully simulated inundation depths, duration and wetland extent.

The above brief review indicates that GIS and RS techniques are useful tools in developing an understanding of remote and inaccessible wetland ecosystems. Even though some of the widely utilised RS methods can produce results of poor accuracy, there are ongoing efforts to develop new methods that integrate GIS and RS techniques in order to yield better results. However, for studying the geomorphological origin of complex systems such as large wetlands, these technologies need to be supplemented by an in-depth understanding of the geomorphological, geological, hydrological, climatological, and sedimentological principles pertaining to wetland science.

CHAPTER 3: THE STUDY AREA

3.1 Introduction

The current study focuses on wetlands on the African Superswell which are poorly understood geomorphologically and hydrologically. Large wetlands occurring at an altitude above 600 m amsl and with an aridity index of less than 0.65, in southern African countries, were selected. The aridity index is a climate metric for mapping aridity throughout the world (Girvetz and Zganjar, 2014; section 4.1.3). The climatic and topographic settings in which the selected wetlands occur provide an opportunity to illustrate the important role that geomorphological processes play in shaping the landscape and leading to the formation of wetlands.

The southern and eastern African regions form an elevated landmass called the African Superswell (McNutt, 1998; Zhao et al., 1999; Pik et al., 2006), which is significant on a global scale for a region of the world not experiencing tectonic uplift as a consequence of plate collision. The African Superswell extends from east Africa's Afar depression in Ethiopia to the Cape Fold Mountains in South Africa (Figure 3.1). It is characterised by high plateaus that rise above the surrounding low-lying areas by more than about 1 000 m (McCarthy and Hancox, 2000; Pik et al., 2006). One of the major geological and topographic features within the African Superswell is the East African Rift Systems (EARS). Faulting associated with the EARS extends from the Afar depression in east Africa to the Okavango Delta in northern Botswana (McCarthy and Ellery, 1994; Furman et al., 2016).

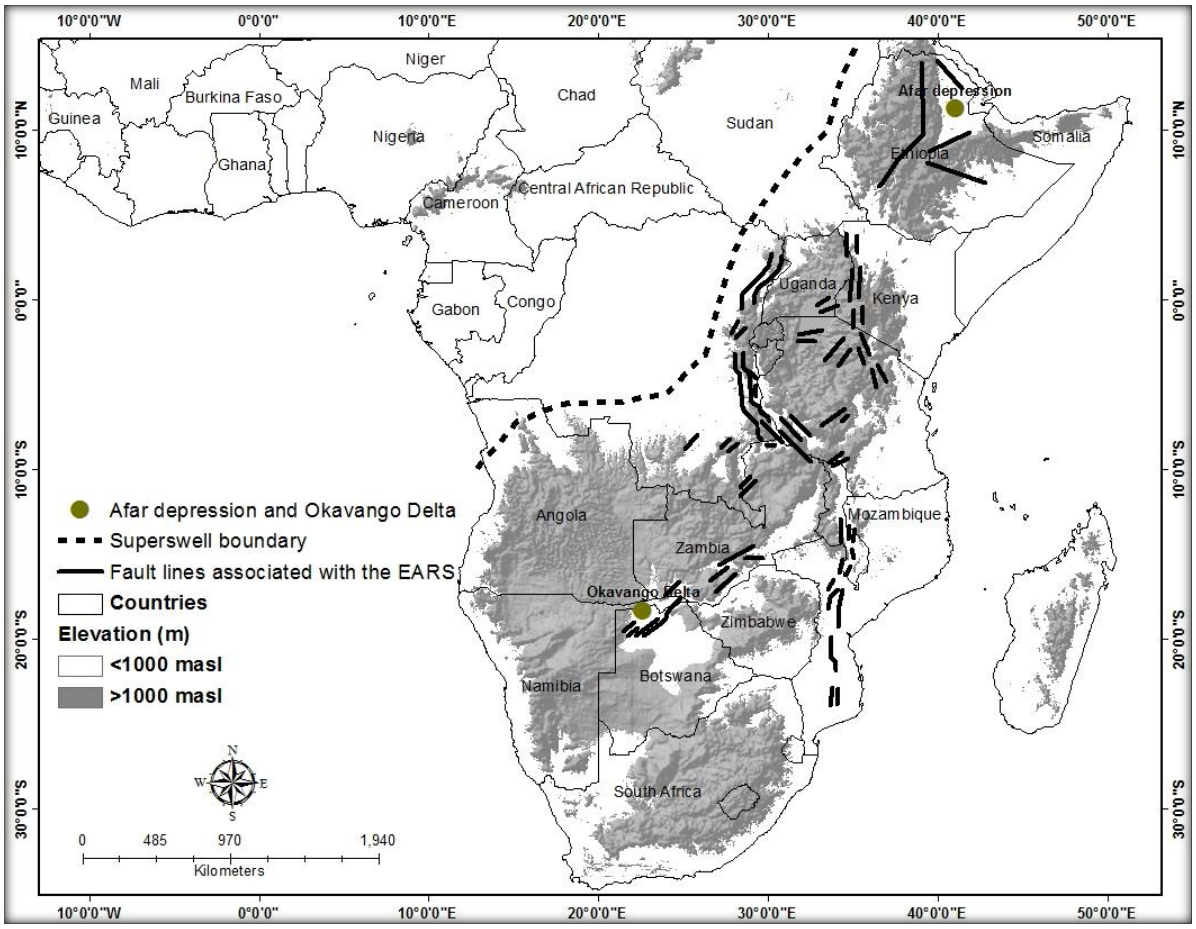

Figure 3.1: The geographic extent, location, topography and major fault lines of study area (Source of fault lines: Pik et al., 2006).

3.2 Climatic conditions of the study area

Although 75% of the study area is classified as arid to semi-arid, climatic conditions vary considerably between different parts of the region with average annual rainfall ranging between 100 and 2 000 mm/year. The northern part of the region has the highest annual rainfall average of about 1 500 mm while the southern part has the lowest annual rainfall average at about 340 mm (Valimba, 2004). Rainfall patterns in the north are largely governed by the position of the Inter-Tropical Convergence Zone (ITCZ). The seasonal movement of the sun from north (June) to south (December) influences the seasonal placement of the ITCZ. The positioning of the ITCZ in the southern summer brings summer rainfall to the region. Average annual potential evapotranspiration ranges from 1 100 mm to over 3 000 mm (McCarthy and Hancox, 2000), and generally greatly exceeds annual rainfall (McCarthy, 1993). The region of the study area is characterised by arid and semi-arid climatic conditions (Figure 3.2), with a single summer rainy season from November to April (WWW-TCO, 2010).

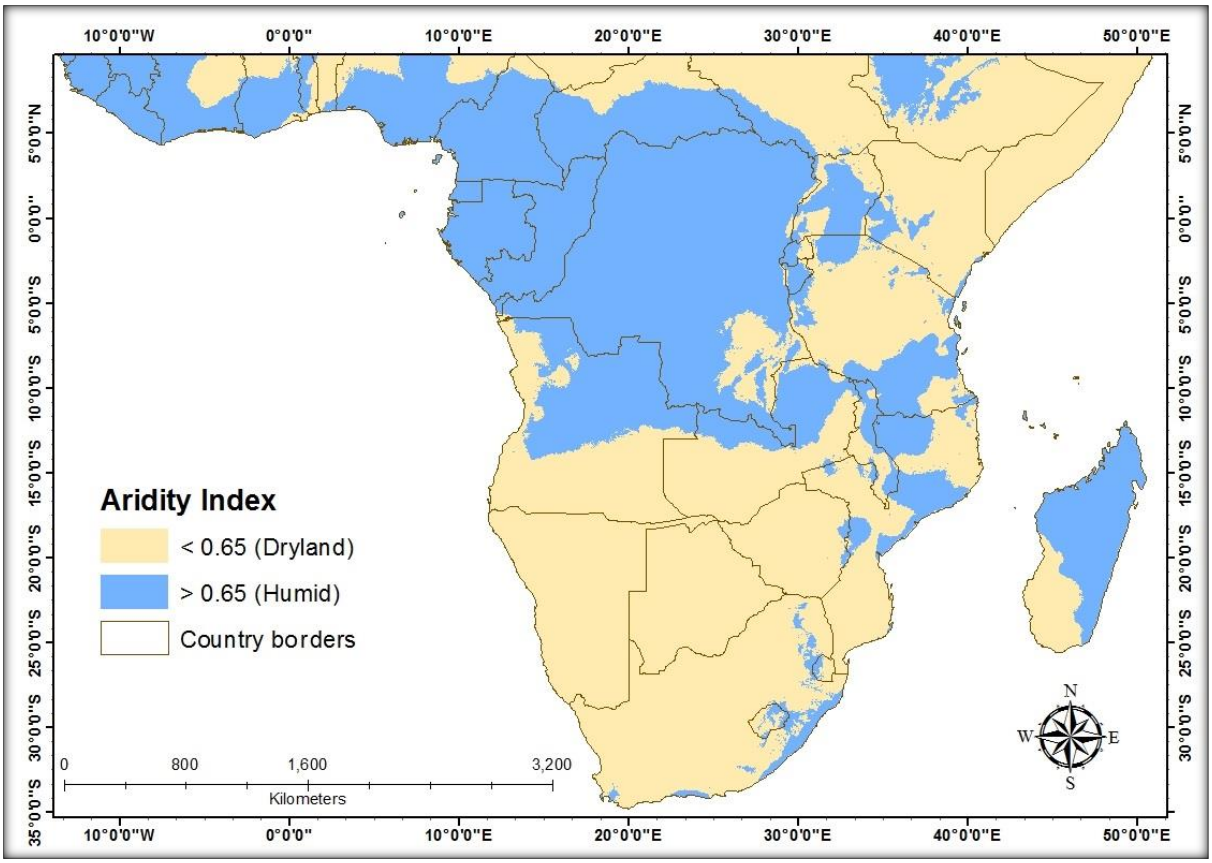

Figure 3.2: Distribution of dryland/semi-arid conditions in the study area (data source: CGIAR-CSI).

3.3 Drainage basins of the study area

There are 21 major drainage basins within the study area (Figure 3.3), of which 15 are shared between two or more countries, while only 6 are confined within the boundaries of individual countries (Figure 3.3). Amongst the shared basins are five of the sub-continents largest basins such as the Congo River basin (2 942 700 km^2), the Zambezi River basin (2 388 200 km^2), the Orange River basin (947 700 km^2), the Okavango River basin (708 600 km^2), and the Limpopo River basin (415 500 km^2). The Congo River, Orange River, Okavango River, and Limpopo River basins are each shared by four countries, while the Zambezi River basin is shared by eight countries. Most of the rivers within the study area originate in highlands and either join large river basins that drain into the Atlantic and Indian oceans, or into inland depressions. There are four inland drainage systems which include the Rift valley and Lake Rukwa basins in Tanzania, Etosha Pan (shared between Angola and Namibia), and the Okavango River basin (shared between Angola, Namibia, Botswana, and Zimbabwe). The Okavango River basin is the largest inland basin of the study area and its tributaries drain into the Okavango Delta and Makgadikgadi Pans in Botswana (McCarthy, 1992).

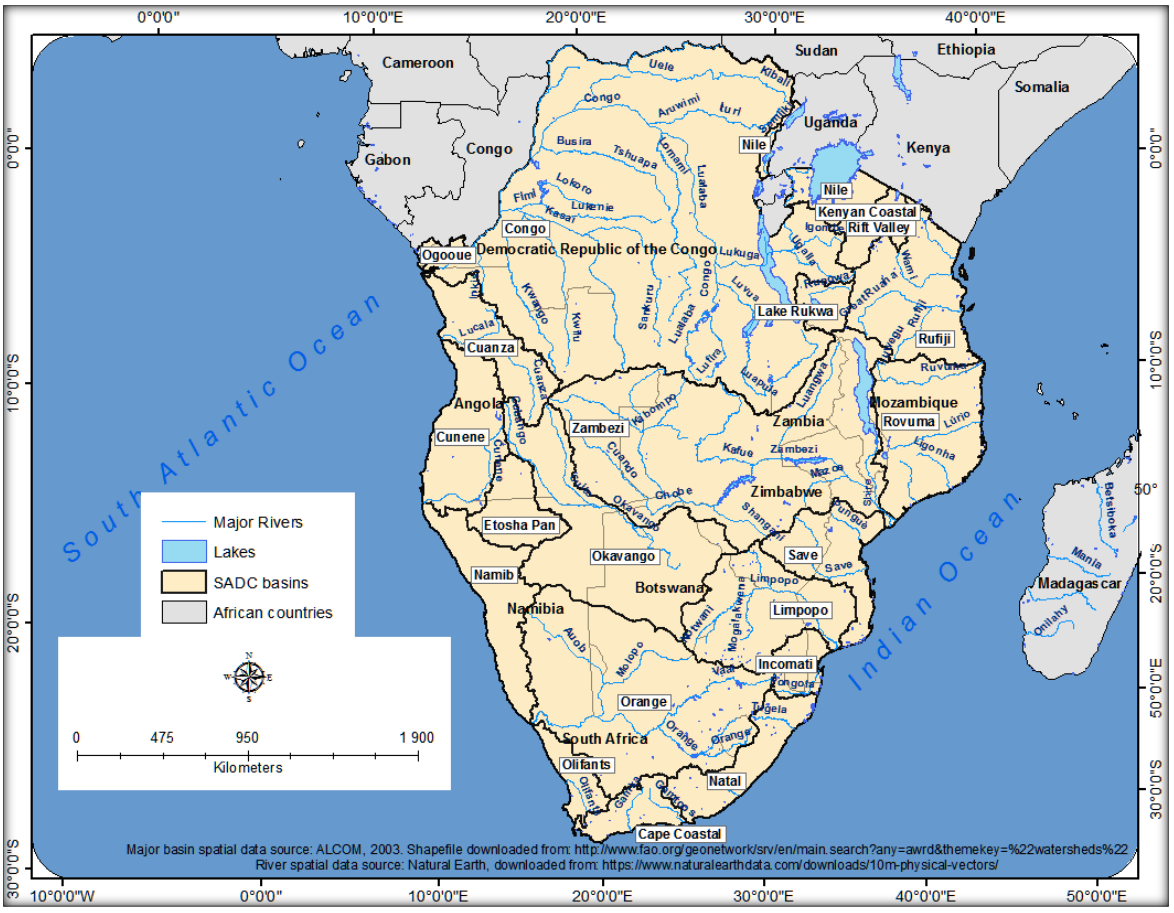

Figure 3.3: Mega-drainage basins of the study area.

3.4 Tectonic history, erosion surfaces, and the evolution of the present-day topographic and hydrological characteristics of the study area

The present-day topographic and drainage characteristics of the continent evolved from the time of the breakup of the Gondwana supercontinent about 180 Ma (Partridge and Maud, 1987). The breaking up of the supercontinent left the southern and eastern African continent with uplifted margins to the east, south and west. The shoulders of the newly formed continental margins were eroded between 180-30 Ma and form the Great Escarpment that extends sub-parallel with the coast all the way round the subcontinent. For a period of about 150 million years, continued erosion reduced the continent to an average elevation of about 500 m above sea level (Guiraud and Bosworth, 1997; Holmes and Meadows, 2012), forming an erosion surface called the African Erosion Surface (Burke and Gunnell, 2008). According to Burke and Gunnell (2008), the African Erosion Surface is the composite erosional surface that dominated Afro-Arabian scenery about 30 Ma as the outcome of up to 150 million years of continental denudation. As such, the African Erosion Surface represents the most extensive

and oldest major erosion surface of the continent (Partridge and Maud, 1987; Burke and Gunnell, 2008).

However, because of two uplift events, occurring about 30 Ma and 5 Ma, the African Erosion Surface has been elevated through isostatic uplift. Following the two uplifts events, the African Erosion Surface has been partially or completely eroded in some parts of the continent (Burke and Gunnell, 2008). Erosion of the African Erosion Surface gave rise to its succeeding erosional surfaces, the Post-African I surface (from 30-5 Ma) and the Post-African II surface (from 5 Ma to present; Partridge and Maud, 1987). The early uplift event (~30 Ma) was associated with uplift between 150-300 m. This uplift event defines the terminal age of the African Erosion Surface and the initial age of the Post African I surface. A second major uplift event that occurred about 5 Ma elevated the continent by an elevation between 150 and 900 m. This uplift event marked the terminal age of the Post-African I surface, the initial age of the Post-African II surface, and gave rise to the modern day expression of the African Superswell (Partridge and Maud, 1987; Burke and Gunnell, 2008).

3.4.1 The distribution of erosion surfaces

The African Erosion Surface has been preserved in many parts of the continent despite erosion initiated by the two uplift events. The African Erosion Surface has been buried to shallow depths in Africa's large internal drainage basins (Kalahari and Chad) and some of the lower-lying smaller basins (Partridge and Maud, 1987; Burke and Gunnell, 2008). The Kalahari Basin, which covers most of the interior of the southern African region including parts of Angola, Zambia, Namibia, Botswana, Zimbabwe, and South Africa, is the extensive depositional basin into which Kalahari Group sediments have been deposited (Haddon, 2005; Haddon and McCarthy, 2005; Figure 3.4a). Some remnants of the African Erosion Surface can be seen covering the Nile-Congo and Chad-Congo divides north of the Congo basin at an elevation of about 500 m above sea level (Figure 3.4b). The Congo and Zambezi divide is also extensively covered by the African Erosion Surface south of the Congo basin at an elevation between 1 200 and 1 400 m above sea level. As seen also from Figure 3.4b, some mountains (Manika Flats and Mount Kundelungu at an elevation of 1 800 m above sea level) which appear to occupy regions flanking the Lake Upemba graben in the Democratic Republic of Congo are also considered to be remnants of the African Erosional Surface (Burke and Gunnell, 2008). According to Burke and Gunnell (2008) the Serengeti Plain in Tanzania and most plateaus in Africa that are at similar elevations to that of the Serengeti Plain (between 1 500 and 1 900 m above sea level) are also considered to be remnants of the

African Erosional Surface. These plateaus (amongst others) include the eastern flank of the Lake Tanganyika Rift, Muchinga Mountains, and the Blue Mountains (Burke and Gunnell, 2008).

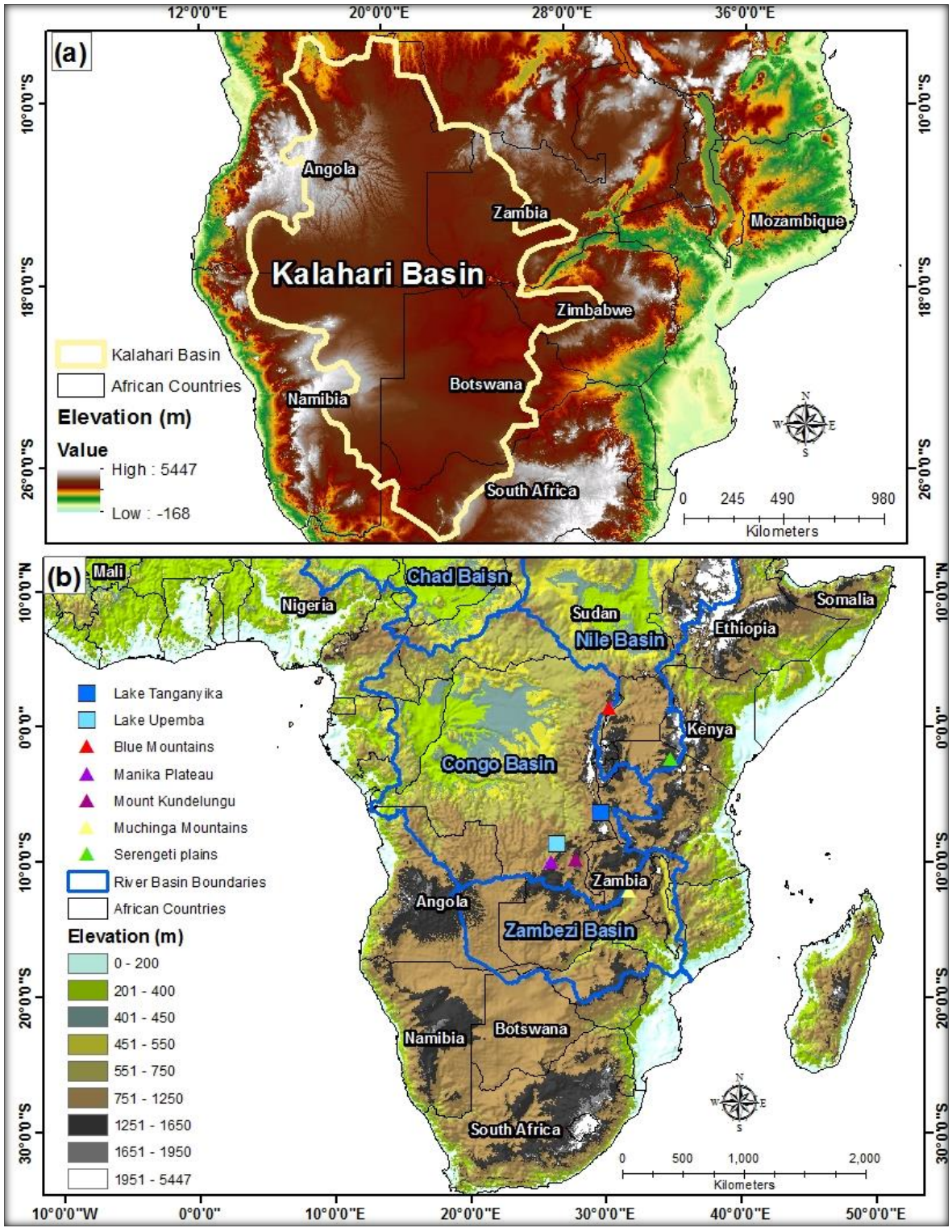

Figure 3.4: The Kalahari Basin (a) and topography of the central and southern African sub-continent, showing the distribution of some remnants of the African Erosion Surface and the large internal drainage basins of Africa (b).

3.4.2 Tectonic history and drainage evolution

The two uplift events not only shaped the African landscape through formation and termination of erosional surfaces, but also initiated the evolution of the continent's drainage systems. The uplift events severed and diverted existing drainage connections, and established new drainage connections through river capture (Thomas and Shaw, 1988; Nugent, 1990; Goudie, 2005; Moore et al., 2007). In addition, most of the large wetlands in Africa's elevated drylands share a complex history of links with major rivers that are today either part of the Zambezi or Congo drainage basins (Cotterill, 2004). Thus, in order to understand the formation of large wetlands in Africa's elevated drylands it is vital to understand the evolution of Africa's drainage systems. However, emphasis on the evolution of the Zambezi, Kafue, Lufira, and Luapula rivers is given here, since most of the selected wetlands in this study occur within these drainage basins.

3.4.2.1 Evolution of the Zambezi River

The present-day course of the Zambezi River is believed to have evolved through drainage capture following major uplift events described above. After the breakup of Gondwana, the Upper Zambezi is thought to have been linked to the Limpopo River system (Figure 3.4) while the Middle Zambezi is believed to have been connected to the Shire River system (Thomas and Shaw, 1988; Stankiewicz and de Wit, 2006). The uplift of the Okavango-Kalahari-Zimbabwe axis (OKZ) about 30 Ma is believed to have severed the link between the Zambezi and Limpopo systems (Stankiewicz and de Wit, 2006). Following the severed link between the Zambezi and Limpopo systems, the upper Zambezi became an endorheic drainage system that supplied sediment to the inland Kalahari Basin (Moore et al., 2007). The endorheic draining Zambezi system is also believed to have been responsible for the formation and maintenance of Lake Palaeo-Makgadikgadi as well as the deposition of sediment within the Upper Zambezi floodplain (Thomas and Shaw, 1988; Goudie, 2005; Stankiewicz and de Wit, 2006; Moore et al., 2007).

According to Nugent (1990), the capture of the Upper Zambezi by the Middle Zambezi is inferred to have resulted from the overtopping of Palaeo-Lake Makgadikgadi as a result of high rainfall in the Late Pleistocene. Moore et al. (2007) on the other hand, attribute the capture of the Upper Zambezi by the Middle Zambezi to headward erosion of the Middle Zambezi (Figure 3.4). According to Moore et al. (2007), the first uplift event (about 30 Ma) could also have been responsible for the rejuvenation of the lower Zambezi, initiating headward erosion and capture of the Luangwa River. Since the capture of the Upper Zambezi

by the Middle Zambezi is believed to have occurred in the Pleistocene (Thomas and Shaw, 1988; Nugent, 1990), the second uplift event (about 5 Ma) could have rejuvenated the Middle Zambezi, initiating a second cycle of headward erosion (Figure 3.4) and ultimately the capture of the Upper Zambezi (Moore et al., 2007).

3.4.2.2 Evolution of the Kafue River

After the breakup of Gondwana, the Kafue River was a south-westward flowing tributary of the Upper Zambezi (Broadley and Cotterill, 2004; Cotterill, 2004; Stankiewicz and de Wit, 2006; Moore et al., 2007; Figure 3.4). It is also believed that at this time, the Chambeshi River formed the upper reaches of the Kafue River (Broadley and Cotterill, 2004; Cotterill, 2004; Moore et al., 2007). It was probably the tectonic activities associated with the first and second uplift events that triggered faulting across the Kafue River. These tectonic activities could have been responsible for the severed connection between the Kafue River and the Zambezi River. Faulting across the Kafue River could also have initiated the formation of the Palaeo-Lake Patrick that covered most of the present-day Kafue wetland during the Early- to Mid-Pleistocene (Simms, 2000). Following the second uplift event, lowering of the base level of the Middle Zambezi could have triggered headward erosion along one of the Zambezi River's tributaries, leading to the formation of the Kafue Gorge and ultimately the capturing of the Kafue River (Moore et al., 2007). Headward erosion following the capture of the Kafue River is believed to have led to the desiccation of Palaeo-Lake Patrick in the Pleistocene (Moore et al., 2007).

3.4.2.3 Evolution of the Luapula River and Lufira River

It is believed that the Chambeshi River formed the headwaters of the Kafue River (Broadley and Cotterill, 2004) and this connection between the Kafue and Chambeshi Rivers could have been established in the Mio-Pliocene. This is because the Palaeo-Chambeshi was thought to have been captured by the Lufira River via the Palaeo-Kafila tributary, contributing to the expansion of Palaeo-Lake Lufura in the Plio-Pleistocene (Broadley and Cotterill, 2004). Faulting and rifting associated with the East African Rift System during the second uplift event could have led to the formation of the graben structures hosting Lakes Upemba and Mweru (Partridge and Maud, 1987; Broadley and Cotterill, 2004). Following the second uplift event and the formation of the Lake Mweru graben, erosion of the Lake Mweru drainage system could have initiated progressive headward erosion of the Luapula River, ultimately leading to the capture of the Palaeo-Chambeshi River by the Luapula River (Partridge and Maud, 1987; Broadley and Cotterill, 2004; Stankiewicz and de Wit, 2006;

Moore et al., 2007; Figure 3.5). Following the second uplift event and the formation of the Lake Upemba graben, erosion was re-activated. The re-activated erosion within the Lake Upemba drainage system could have led to rapid incision within the Lufira River and ultimately the desiccation of Palaeo-Lake Lufira.

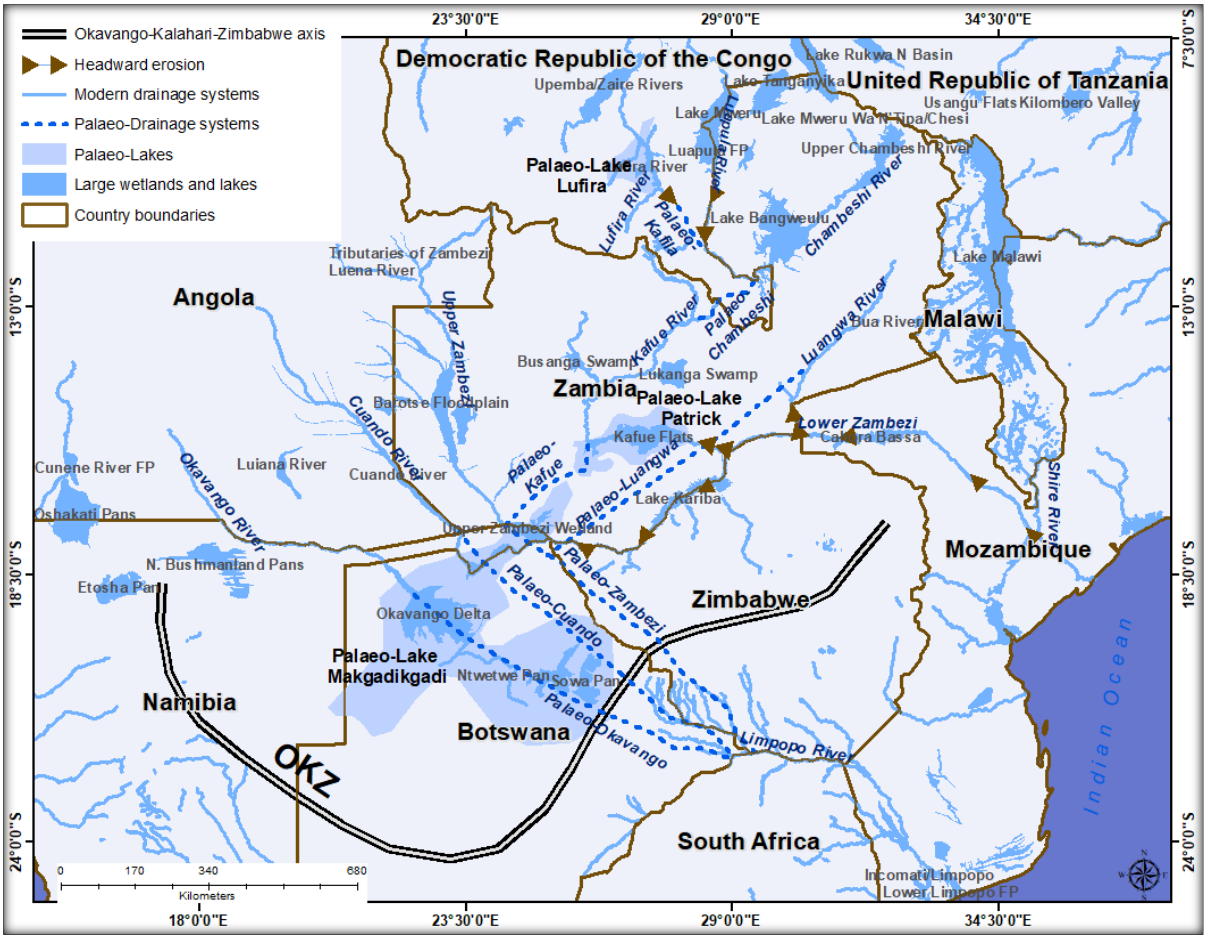

Figure 3.5: The drainage development in central Southern Africa (adapted from Broadley and Cotterill, 2004; Cotterill, 2004; Goudie, 2005; Stankiewicz and de Wit, 2006; Moore et al., 2007).

The evolution of the southern African landscape and its drainage systems show that most large wetlands share a complex history of links with major rivers that were or are today part of the Congo or Zambezi drainage systems (Cotterill, 2004). These major rivers themselves evolved from a process of river capture following two major uplift events. These uplift events and subsequent river capture rejuvenated most drainage systems in the subcontinent and ultimately led to the shrinking and desiccation of Palaeo-Lakes. It is also clear that most rivers in Africa have been rejuvenated and are in a long-term state of incision.

3.5 Distribution of wetlands within the mega river basins of the study area

According to the Global Lakes and Wetlands Database (GLWD) of Lehner and Döll (2004), wetlands (including reservoirs, lakes, and rivers) within the SADC region cover an area of about 572 430 km^2, which equates to 6.1% of the SADC region (excluding island states; Figure 3.6). However, 84% of the area covered by the wetland resources in the region is distributed across the region's five largest basins. More than half (54%) of the wetland coverage within the region lies within the Congo basin, while the Zambezi basin constitutes 19%, followed by the Okavango basin with 7%, while the Limpopo and Orange basins each constitute about 2% of wetland coverage in the region.

The scarcity of wetlands in the region appears to be compensated by the great variety of wetland types (McCarthy and Hancox, 2000). According to the GLWD, other than reservoirs, lakes and rivers, wetlands larger than 0.001 km^2 in the region can be divided into five different types (Table 3.1). These wetland types are 1) freshwater marsh and floodplain, 2) swamp forest and flooded forest, 3) coastal wetland, 4) pan and brackish / saline wetland and 5) intermittent wetland / lake. The most extensive of the GLWD wetland types within the SADC region comprises freshwater marsh and floodplain classes, which constitute about 41% of the regional wetland coverage.

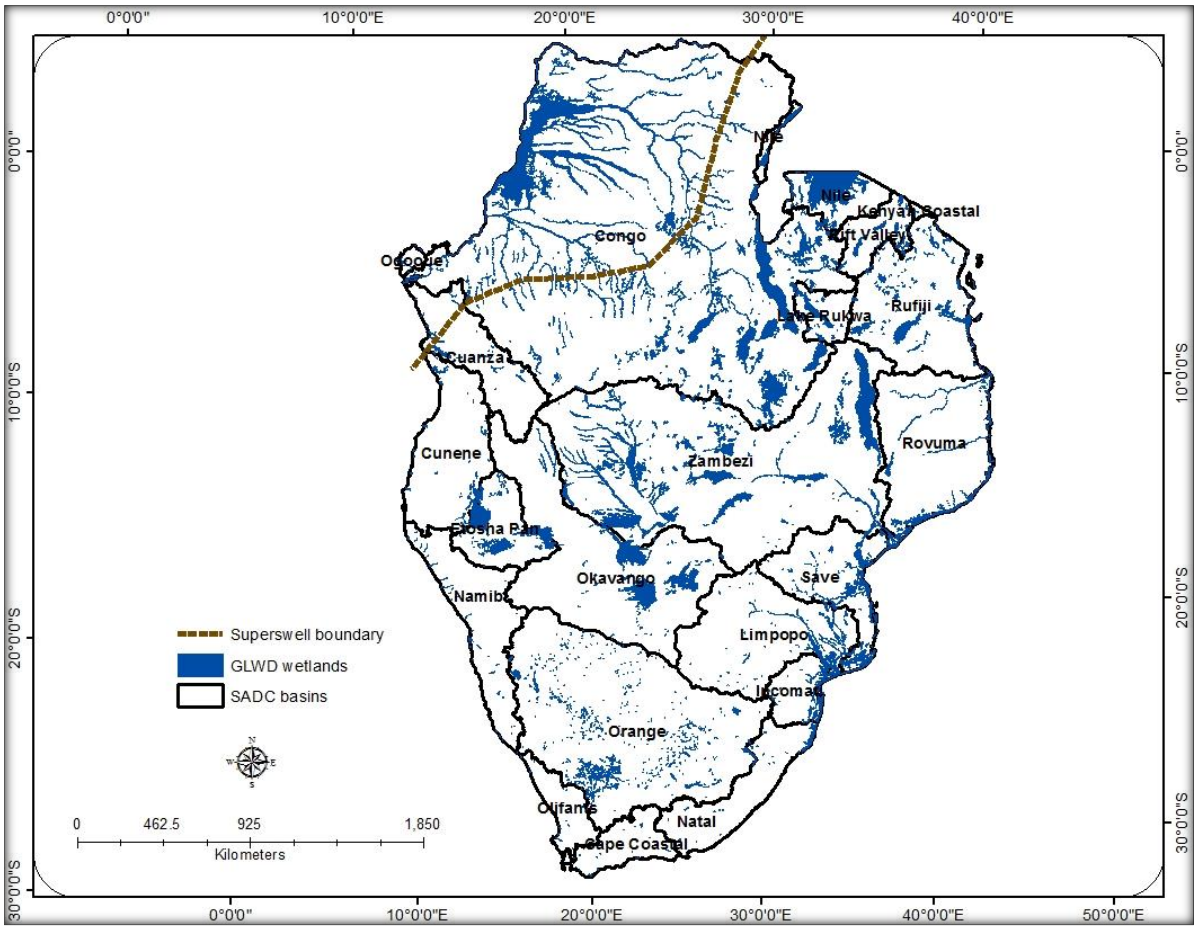

Figure 3.6: The distribution of wetlands across the mega river basins of the SADC region (adapted from GLWD, Lehner and Döll, 2004).

Table 3.1: The classification of wetland types across the SADC region excluding Island States (GLWD; Lehner and Döll, 2004).

GLWD wetland types	*Area (km^2)*
Lake	127 220
Reservoir	14 683
River	20 399
Freshwater marsh, floodplain	235 387
Swamp forest, flooded forest	95 860
Coastal wetland	16 149
Pan, brackish/saline wetland	40 948
Intermittent wetland/Lake	21 781
Total	572 430

3.6 Socio-economic characteristics of the study area

The SADC region (excluding the island states) has a population of about 277 million people (Mabhaudhi et al., 2016) and covers an area of approximately 572 430 km^2. The majority of the population lives in poverty and resides in rural areas. The rural economies and livelihoods are primarily dependent on subsistence farming and are characterised by a lack of access to running water and reticulated energy for basic human needs. As a result, the agricultural productivity is primarily dependant on rainfall, while firewood and charcoal are the preferred source of energy. Political leaders within the region are left with a daunting task of growing national economies and improving the standard of living of poor people (Cai et al., 2012), whose livelihoods are completely reliant on subsistence agriculture and the utilisation of natural resources. According to Mabhaudhi et al. (2016), water and energy security will play a central role in the development of the SADC region.

3.7 The exploitation of wetland resources for sustaining rural livelihoods

Since the livelihoods of most of the people in southern Africa's rural communities are reliant on rain fed agriculture and the utilisation of natural resources, many households rely primarily on the utilisation of wetland resources (Valimba, 2004; Cai et al., 2012). Wetlands offer a wide range of economic and livelihood opportunities centred on farming, fishing, as well as gathering of wild fruits and construction materials (Timberlake, 1998; Turpie et al., 1999; WWW-TCO, 2010). Some of the regions poor rural communities reside within or on the periphery of some of the regions large wetlands, such as the Lukanga wetland, Lufira wetland, Bangweulu swamps, and the Okavango Delta. These include amongst others, the Lozi people of the Barotse floodplain in south-western Zambia and the Hambukushu people of the Okavango Delta. The livelihoods of most of the villages within or on the periphery of

wetlands depend on a mixed livelihood strategy, which combines crop farming, livestock rearing, fishing, and the collection of natural resources such as timber and grass for construction. Most rural households who reside in wetlands construct their houses and courtyard fences from wood, reeds, papyrus and thatching grasses (Turpie et al., 1999).

CHAPTER 4: SPATIAL DATASETS AND METHODS

4.1 Spatial datasets

Since this study relies primarily on GIS and desktop approaches, including the use of Earth Observation (EO) and spatial datasets, it is necessary to provide a description of the datasets used, their custodians, limitations and merits. These spatial datasets include topographic data in the form of digital elevation models (DEMs), climatic data, geological maps and seismic data, and images of the Earth's surface in the form of satellite imagery and web based programmes such as Google Earth (Table 4.1). The spatial datasets were obtained from various custodians and were used to provide information needed to understand the geological, geomorphological and hydrological processes that characterise the origin, structure and hydrological functioning of large wetlands in Africa's elevated drylands.

Table 4.1: A list of the datasets and a description of their resolution, custodians and use in this study.

Dataset	Resolution	Production date	Custodian	Use in the study
GLWD (Section 4.1.1)	1 km	2004	World Wide Fund for Nature (WWF)	Map large wetlands in Africa
GTOPO30 DEM (Section 4.1.2)	1 km	1993	United States Geological Survey (USGS)	Map the African continent's topography
SRTM DEM (Section 4.1.2)	30 m	2000	United States Geological Survey (USGS)	Delineate wetland boundaries, and catchment areas. Generate stream networks and plot channel longitudinal profiles. Plot valley cross-sectional profiles Calculate wetland volume
Global Aridity (Section 4.1.3)	1 km	1950-2000	Consultative Group for International Agricultural Research (CGIAR) Consortium for Spatial Information (CSI)	Classify and map arid and semi-arid zones in Africa
Geological Map (Section 4.1.4)	1:2 500 000	2009	South African Council for Geoscience	Relate wetland formation to lithological controls and faults
Additional Fault Lines (Section 4.1.4)	Not specified by the custodian	No date	Digitised from Foster et al. (1997), Chorowicz (2005), and Macheyeki et al. (2008)	Relate wetland formation and tectonic activities
Seismic Data (Section 4.1.4)	Point data	1904 to present	The Bulletin of the International Seismological Centre (ISC Bulletin)	Map large African wetlands in relation to seismic activities
CLIMWAT (Section 4.1.5)	Point data	1971-2000	Food and Agriculture Organisation of United Nations (FAO)	Analyse wetland's climatic conditions (i.e. evapotranspiration and rainfall)
LandsatLook Images (Section 4.1.6)	30 m	2006-2015	United States Geological Survey (USGS)	Visual analysis of aerial images
Google Earth (Section 4.1.7)	0.4 m to 30 m (data source dependable)	Launched 2005	Google Inc.	Visual analysis of high-resolution aerial images and digitising streams

4.1.1 Wetland distribution as mapped by the Global Lakes and Wetlands Database (GLWD)

The Global Lakes and Wetlands Database (GLWD) was used in this study to identify and support the mapping of large wetlands in Africa. The GLWD map of large lakes and reservoirs, smaller waterbodies, and different types of wetlands, has been compiled from the best available sources for lakes and wetlands on a global scale (Lehner and Döll, 2004). Therefore, the database can be used to estimate wetland extent at global and regional scales. However, the GLWD did not update any of the wetland boundaries that might have undergone alterations because of natural or anthropogenic changes such that the database represents wetlands in their historic rather than current states (Lehner and Döll, 2004). This means that the wetland boundaries may underestimate or overestimate the wetland extents. In addition, the GLWD was generated from a combination of seven global digital map and attribute datasets (Lehner and Döll, 2004). The most comprehensive data source for wetlands was the 1993 Global Wetlands map of the World Conservation Monitoring Centre (WCMC). Since the WCMC Global Wetlands map was also generated from a number of sources (see Global Wetlands 1993 metadata files downloadable at http://www.unep-wcmc.org/resources-and-data/global-wetlands), it is difficult to trace the exact methodology used to generate wetland boundaries. However, it is clear that most wetlands are represented at their extents before 1993 and that the GLWD may have inherited inaccuracies from its data sources (Lehner and Döll 2004). Regardless of this limitation, the database is regarded as a useful basis for establishing the distribution and estimating large wetland resources at global and continental scales (Lehner and Döll, 2004; Rebelo et al., 2010). For instance, Rebelo et al. (2010) used the GLWD to provide an overview of the distribution of wetlands and wetland types across sub-Saharan Africa. This shows that the database is suitable for identifying and mapping wetlands at their correct geographic locations.

4.1.2 Mapping topography using digital elevation models (DEMs)

There are different types of Digital Elevation Models (DEMs) which are (1) Digital Surface Models (DSM) that represent the elevation of the surface of the earth including trees and buildings, and (2) Digital Terrain Model (DTM) that represent the elevation of the barre earth. However, the later are not freely available and as a results only DSM were used in this study. Different sources of digital elevation data have been used to construct DEMs. A DEM is a computerised model representing the elevation of the Earth's surface (Kiamehr and Sjöberg, 2005). These remotely sensed raster datasets have become important sources of

surface elevation data for a range of applications within the earth sciences and environmental disciplines. As is the case for any other model, a DEM is subject to errors (Kiamehr and Sjöberg, 2005). Thus, assessment of the quality of a DEM is crucial to its appropriate use (Carabajal and Harding, 2005). The quality of elevation data is commonly expressed in terms of vertical accuracy, but the accuracy of any DEM is typically not uniform across the extent of the area being examined because most DEMs use a variety of data sources in their construction (Kiamehr and Sjöberg, 2005). Another issue affecting the quality of space-based DEMs is the presence of systematic error patterns such as artificial structures that are higher or lower than the adjacent land surface and therefore not representative of the ground surface. For example, elevations of forested regions or the built environment are often treated as the elevation of the land surface in space-collected DEM data (Hirt et al., 2010). In the past decade, significant advances in public access to global elevation datasets have been made by the release of products such as the GTOPO30 DEM, SRTM and ASTER elevation products.

GTOPO30 DEM was used in this study to map the topography of the African continent (USGS, 1999). The DEM was compiled in 1996 based on data from 8 different sources of elevation information including vector and raster datasets, and is available at 30 arc-second grid spacing (equating to a ground distance of about 1 km at the equator; USGS, 1999). The absolute accuracy of the GTOPO30 DEM varies depending on the source data. The areas derived from raster source data generally have higher accuracy than those derived from vector source data, including Africa.

In some parts of Africa there were areas for which elevations for GTOPO30 were interpolated based on very sparse vector point data, resulting in relatively poor accuracy (USGS, 1999). Even though GTOPO30 is of relatively poor resolution and accuracy as compared to SRTM 1 arc-second and ASTER Global DEM version 2, GTOPO30 is more suitable for mapping at global and continental scales (Miliaresis and Argialas, 1999). This is because DEM data from the Shuttle Radar Topographic Mission (SRTM) and Advanced Spaceborne Thermal Emission and Reflection Radiometer (ASTER) products, which are available at 1 arc second spacing (equating to a ground distance of about 30 m at the equator), generally cover most of the populated regions well but have limited coverage for remote regions (Hirt et al., 2010). Additionally, SRTM and ASTER do not provide global or regional coverage due to voids that are present in datasets for areas where the initial processing did not meet quality specifications. Use of improved interpolation algorithms in conjunction with other sources of elevation data are leading to the release of updates of increasing accuracy.

Despite the data discrepancies, the GTOPO30 DEM is suitable for regional and continental applications since it does not contain voids and it also covers sparsely populated regions (USGS, 1999). However, for applications such as plotting valley cross-sectional profiles, delineating catchment areas and wetland boundaries, and plotting channel longitudinal profiles, which require higher resolution DEM data, the SRTM 1 arc-second global dataset was used in this study.

High resolution SRTM 1 arc-second global DEM data were used in this study as a major source of topographic data at a catchment scale. SRTM DEM was chosen over ASTER GDEM version 2 because ASTER DEM has systematic errors such as step anomaly offsets (Flögel, 2014). The step anomalies are created at image boundaries and they create horizontal offsets of around 10 m between continuous land surfaces (ASTER Validation Team, 2009). The new SRTM 1 Arc-Second Global elevation data offers worldwide coverage of non-void filled and void filled data at a resolution of 1 arc-second (USGS, n.d.). The vertical accuracy of SRTM 1 arc-second elevations varies between 4 m and 6 m in terrain in which variation in elevation is low, but this deteriorates to 11-14 m in rugged terrain (Hirt et al., 2010). However, the overall vertical accuracy of ASTER elevations varies between 10 and 25 m (ASTER Validation Team, 2009).

4.1.3 Mapping aridity in the study area using the Global Aridity Index (AI)

The Aridity Index (AI) is a widely used climate metric for mapping aridity throughout the world (Girvetz and Zganjar, 2014). In this study, the Global Aridity Index dataset from the Consultative Group for International Agricultural Research (CGIAR) Consortium for Spatial Information (CSI) was used for mapping aridity. The Global Aridity Index is modelled using the 30 arc-second WorldClim global geo-database of monthly average climatic data from 1950 to 2000 (see Global Aridity Index metadata document http://www.cgiar-csi.org/data/global-aridity-and-pet-database). An AI is given by the quotient of mean annual precipitation (MAP) and mean annual potential evapotranspiration (MAE). The AI values increase for more humid conditions and decrease with more arid conditions. A value of 0.65 or less is considered to indicate a "dryland" condition (Zomer et al., 2006).

4.1.4 Seismic and geological data

The Bulletin of the International Seismological Centre (ISC Bulletin) is regarded as the definitive record of the Earth's seismicity (International Seismological Centre, 2012). The ISC Bulletin contains global seismic data from 1904 to the present. The ISC Bulletin relies on data contributed by seismological agencies from around the world. Seismic data obtained

from the ISC Bulletin were used in this study to map seismic events and earthquakes on the African continent.

The geology map used in this study was obtained from the South African Council for Geoscience. The Council for Geoscience provided the 2009 Geological Map of the Southern African Development Community (SADC) Countries as georeferenced files at 1:2 500 000 scale.

Fault lines digitised from peer reviewed journal articles and the Geological map of the SADC countries were also used in this study. Fault lines around the Bahi, Wembere, and Usangu wetlands in Tanzania were digitised from Foster et al. (1997), Chorowicz (2005), and Macheyeki et al. (2008), while those around the rest of the wetlands examined in this study were digitised from the Geological Map of the SADC Countries.

4.1.5 Understanding wetland hydrological characteristics using the CLIMWAT climatic database

To understand a wetland's hydrological characteristics, the CLIMWAT 2.0 climatic database, which is used with a computer program CROPWAT 8.0, was used as a source of data for mean annual rainfall and potential evapotranspiration estimates. CLIMWAT is a joint product of the Water Resource, Development and Management Service and the Environment and Natural Resources of the Food and Agriculture Organisation of the United Nations (FAO WATER, 2013). The database and computer programme were downloaded from http://climwat-for-cropwat.software.informer.com/download/. CLIMWAT 2.0 provides direct observations of long-term monthly mean values of seven climatic parameters from over 5 000 stations worldwide for the period 1971-2000 (FAO WATER, 2013). The seven climatic parameters are: (1) mean daily maximum temperature in °C, (2) mean daily minimum temperature in °C, (3) mean relative humidity in %, (4) mean wind speed in km/day, mean sunshine hours per day, (5) mean solar radiation in MJ/m^2/day, (6) monthly rainfall in mm, and (7) monthly effective rainfall in mm. This climate database also provides reference evapotranspiration in mm/day as calculated using the Penman-Monteith method. The advantage of using CLIMWAT is that it enables the analysis of rainfall and evapotranspiration estimates for the same period. The database also provides geographic coordinates and altitude for the location of each weather station (FAO WATER, 2013), which is helpful in mapping and selecting the nearest station for a given area.

4.1.6 Determination of flooding characteristics using LandsatLook images

LandsatLook images acquired for the period corresponding to wetland flood-peak periods, the dry season and the start of the wet (rainy) season, were downloaded from the USGS Earth Explorer website and were used to analyse each wetland's flooding characteristics. The LandsatLook images were used in combination with Google Earth as base maps for analysing a wetland's hydrological characteristics and for assessing the accuracy of the generated datasets. LandsatLook images are derived from Landsat 1-8. Level 1 datasets are available as raster files with a 30 m spatial resolution and are only suitable for visual image interpretation (USGS, 2015). In this study, LandsatLook 'natural colour' images with geographic reference for easy import into a geographic information system were used for visual interpretation purposes.

4.1.7 Use of Google Earth as a wetland base map

Google Earth was used as a base map for analysing hydrological characteristics and for assessing the accuracy of the generated datasets. Google Earth is a computerised geographical information program that combines satellite imagery, aerial photography and vector data to produce a three-dimensional interactive representation of the Earth's surface (Chen et al., 2009). The Google Inc. program can be downloaded from https://www.google.com/earth/download/ge/agree.html. Since its inception in 2005, Google Earth has been widely used for visual geospatial data in a variety of research fields such as archaeology (Kennedy and Bishop, 2011), agriculture (Taylor and Lovell, 2012) and wetland studies (Ramachandra and Kumar, 2008; Gong et al., 2010; Niu et al., 2012). Google Earth's base map images are high-resolution imagery from some of the world's leading providers of high-resolution imagery products such as Airbus Defence and Space, DigitalGlobe, and NASA (Google Inc., n.d: NASA, n.d; Airbus Defence and Space, 2013). Airbus Defence and Space provides images from SPOT 6, SPOT 7, and Pléiades satellites, which offer imagery products at resolution of up to 0.5 m **(**Airbus Defence and Space, 2013**).** DigitalGlobe has been providing high-resolution imagery products from WorldView-3, WorldView-2, WorldView-1, GeoEye-1 and QuickBird satellites, which offer imagery products at a resolution of up to 0.4 m (Google Inc., n.d; Google Earth Blog, 2014). NASA provides images from Landsat satellites that offer imagery products at a resolution of up to 15 m (NASA, n.d).

4.2 Methods

The study relied solely on desktop studies using EO data and GIS techniques supported by available literature. Derivation of a range of different variables from different datasets in order to achieve the objectives of the study is shown in Figure 4.1. The GLWD, GTOPO30 DEM, Global Aridity raster, and seismic datasets were overlaid and analysed in order to select and map large wetlands in Africa's elevated drylands (Objective 1; Section 4.2.1). Once the wetlands were selected, the SRTM DEM was used to delineate wetland boundaries using ArcGIS's cut-and-fill method (Section 4.2.2.1). Wetland catchments were mapped using ArcGIS's ArcHydro tools (Section 4.2.4.1). The GLWD, Google Earth, LandsatLook images and the generated wetland boundaries were overlaid in order to assess the accuracy of the generated wetland boundaries (Section 4.2.2.2).

In order to determine wetland geomorphic origin (Objective 2), Google Earth was used to digitise stream lines (Section 4.2.3). The digitised stream lines were interpolated from the SRTM DEM in ArcGIS in order to plot channel longitudinal profiles (Section 4.2.3.1). The SRTM DEM was also used to plot valley cross sectional profiles. LandsatLook images, wetland boundaries, geological maps, fault lines, valley cross-sectional and channel longitudinal profiles were overlaid and analysed to determine likely wetland geomorphic origin.

To relate wetland formation and structure to hydrological functioning (Objective 3), CLIMWAT's rainfall and potential evaporation data, catchment and wetland sizes, as well as LandsatLook images, were analysed to determine wetland inundation patterns (Section 4.2.4). In order to understand wetland structure, valley cross-sectional profiles and LandsatLook images were used to identify wetland features such as alluvial ridges, backwater depressions, and wetland channels and their characteristics such as channel sinuosity and outflow channels. The potential of a wetland to store floodwater, which is assumed in this study to be primarily a function of wetland geomorphic origin and structure, were evaluated through the analysis of wetted area and volume, which were calculated from the surface difference method in ArcGIS.

To classify wetlands based on their geomorphic origin, structure and hydrological functioning (Objective 4), wetland features such as alluvial ridges and backwater depressions, wetted area and volumes, as well as knowledge of wetland formation, were used to compare different wetlands (Section 4.2.5).

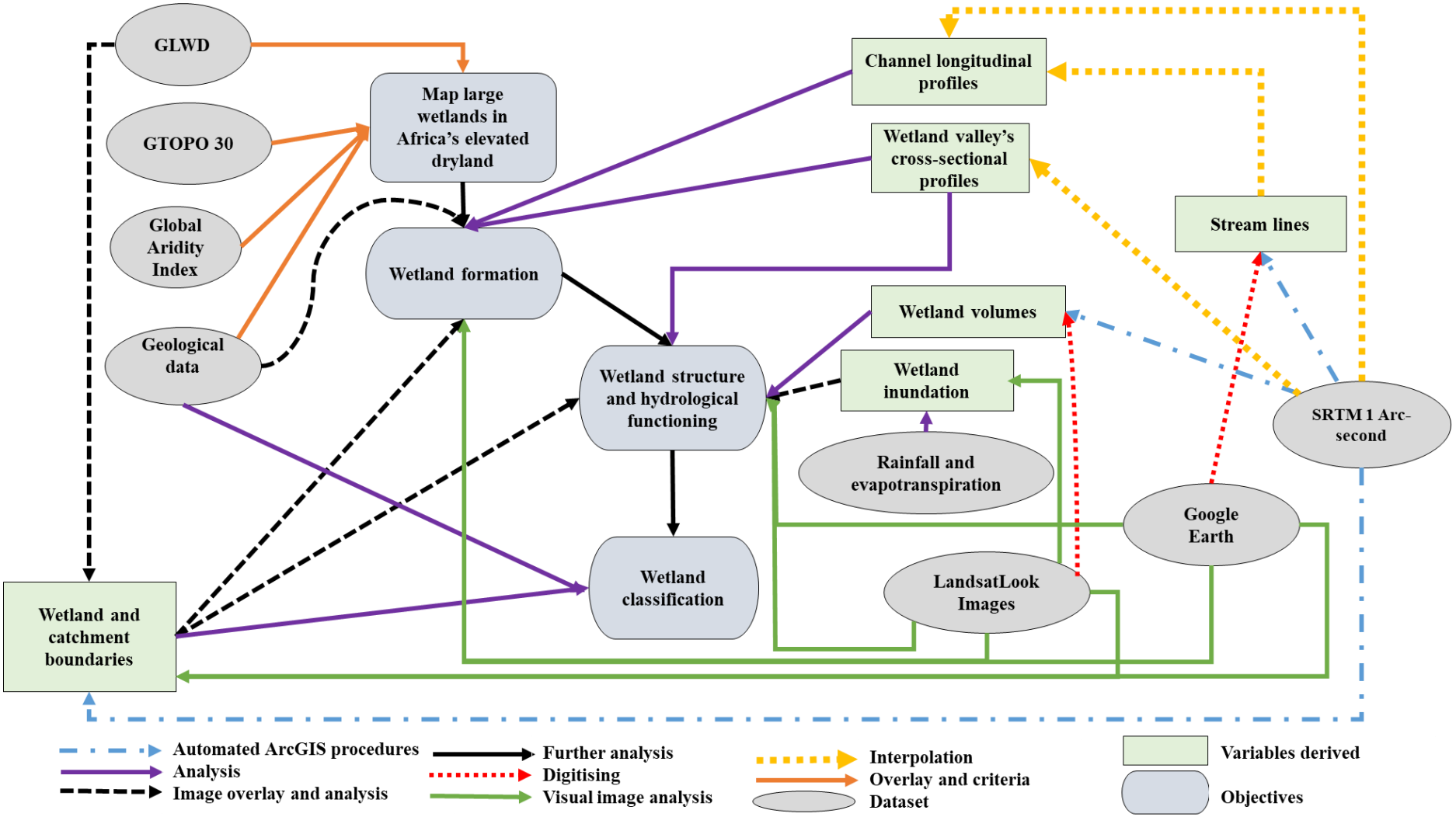

Figure 4.1: A flow chart summarising the objectives of the study, the datasets and methods used to derive variables that were crucial for the realisation of the study objectives.

4.2.1 Identifying and mapping large wetlands in southern Africa's elevated drylands

It was necessary at the outset to define the large wetlands in southern Africa's elevated drylands. The definition of a large wetland based on that of Iriondo (2004) was adopted in this study, namely, a plain area of more than 1 000 km^2 covered by shallow water for a long period (continuously for one month or more). The GLWD spatial dataset was used to select and map all large wetlands in southern and eastern Africa that are equal to or larger than 1 000 km^2. Since the current study focuses on inland wetlands, large wetlands were selected from the freshwater marsh or floodplain wetland class while the other wetland types from the GLWD such as lakes, coastal lagoons, saltpans, mangroves, impoundments, and intermittent wetlands were ignored. In order to include freshwater marsh or floodplain wetlands within dryland climatic regions (i.e. areas with AI < 0.65) and at a high elevation (i.e. above 600 m above sea level), large freshwater marshes or floodplains from the GLWD were overlaid on the GTOPO30 DEM and the Global Aridity Index spatial datasets. These wetlands consisted mainly of freshwater marsh or floodplain wetlands located within the eastern and southern region of the African Superswell.

4.2.2 Determining the extent of wetlands

Most studies use satellite image classification procedures to delineate wetland extent (Overton, 2005; Dutta et al., 2013; Qi et al., 2009; Funkenberg et al., 2014; Romshoo and Rashid, 2014; Gibbs et al., 2016; Dronova et al., 2015). The most commonly used satellites used for this purpose are Landsat and SPOT images, while the most commonly used method is supervised classification (Ozesmi and Bauer, 2002). The use of remote sensing techniques for delineating wetland extents are widely accepted, although there are still many methodological problems that hamper the accuracy of the derived products (Li et al., 2014). This is because wetlands can easily be confused with upland land cover types, which may have overlapping spectral signatures (Ozesmi and Bauer, 2002; Reschke, and Hüttich, 2014; Evans et al., 2014). In order to limit spectral confusion between wetlands and uplands it is preferable to use satellite images taken during wetland flood peak periods. However, images corresponding to flood peak events are often covered with clouds (Ozesmi and Bauer, 2002) and optical sensors cannot penetrate clouds (Qi et al., 2009). This poses a challenge in achieving accurate wetland boundaries from image classification procedures.

Since wetlands occupy topographic basins and occur in relatively gently sloping areas (Li and Chen, 2005) delineation of wetland extents might attempt to delineate topographic depressions from surrounding uplands. This can be achieved using topographic datasets and

methods, whose integrity is not limited by spectral confusion and cloud cover. Given that DEM's have been widely accepted and utilised as sources of topographic data in wetland studies (Kulawadhana et al., 2007; Islam et al., 2008; Li et al., 2014; Qi et al., 2009; Sharma and Tiwari, 2014), these datasets were used in this study to delineate topographic basins from the surrounding uplands. Wetland boundaries were thus generated from DEM datasets using semi-automated procedures that involved (1) interpolating a trend surface from random points of known location and elevation in the wetland, and (2) comparing the interpolated trend surface with the elevation of the land surface using the cut-and-fill algorithm in ArcGIS.

4.2.2.1 The cut-and-fill method

The ArcGIS trend tool uses sample points with known location and elevation values to interpolate a planar surface that represents gradual systematic change in the surface topography over the area of interest (ESRI, 2013). This is the "interpolated planar surface" in the text that follows. The cut-and-fill tool calculates areas and volumes for zones where surface material has been added (net gain) and removed (net loss) within a specific location using two raster surfaces, such as the DEM and an interpolated planar surface (ESRI, 2013). According to ESRI (2013) the tool identifies regions of net loss and net gain as a result of natural processes (such as deposition, erosion, or landslides) or artificial activities (such as excavations and filling). However, the ESRI (2013) explanation of the cut-and-fill method is somewhat tailored to applications in the construction field. With regards to the application of the cut-and-fill method in wetland delineation, areas of "net loss" represent wetland areas where the interpolated planar surface is above the DEM surface, while areas of "net gain" are elevated areas where the interpolated surface is below the DEM surface.

The fundamental principle behind the use of the cut-and-fill method for wetland delineation is that most wetlands form within broad and gently sloping valleys or tectonic depressions surrounded by uplands (Li and Chen 2005; Tooth and McCarthy, 2007; Ellery et al., 2009; Grenfell et al., 2010). Therefore, given an interpolated surface at a slope approximating valley slope and an elevation approximating that of the wetland edges down the length of the valley, the cut-and-fill method should be able to delineate the wetland area as "net loss" zones. The method involves extracting DEM elevation values for some points along the assumed edge of the wetland and to fit a trend surface to these points at an appropriate elevation and slope down the length of the wetland. Using the DEM and the interpolated planar surface as input data, the cut-and-fill method is then able to calculate areas and

volumes where the interpolated planar surface is above the DEM surface (wetland areas) and areas and volumes where the interpolated surface is below the DEM surface (surrounding uplands).

Figure 4.2 illustrates the use of the cut-and-fill method for a wetland with a channel sitting at a lower elevation than the surrounding wetland area. Figure 4.2a shows the wetland area, cross-sectional profiles, marked wetland edges, as well as the planar surface created using the points and their elevation values taken along the wetland edge. The trend surface is expected to be sub-horizontal in a direction orthogonal to the main channel in a downstream direction (evidenced by roughly parallel shading bars). Figure 4.2b shows the results of the cut-and-fill method when the trend surface is set at an elevation approximating the channel water level. In this case, the trend surface is set below most of the surrounding wetland areas and the resultant wetland area is small in extent. Figure 4.2c shows the results of the cut-and-fill when the planar surface is set at an elevation approximating that of the assumed wetland edges which is 24 m above channel water level. The cross-sectional profiles (Figures 4.2d and e) show that the wetland occurs within a confined valley and, more importantly, the elevation differences between the wetland edges and the channel water level can be seen. After changing the elevation of the planar surface, the entire wetland area was below the planar surface while the surrounding uplands remain above the planar surface, thus ensuring total wetland delineation (Figure 4.2c).

Although the differences between the two delineations of wetland extent illustrated in Figure 4.2b and Figure 4.2c are clear, it is rather surprising that an elevation difference of 24 m is required to ensure that the planar surface passes through the identified edge points. However, the wetland in question appears more like a seep wetland upstream with elevation difference between channel water level and the wetland edges increasing in an upstream direction. The resultant cut-and-fill raster ensured delineation of wetland areas. Changing the elevation of the trend surface is thought to be not only useful for total wetland delineation but also for determining the area that is likely to be inundated (and the volume of inundation) under different levels of flooding. The elevation difference between the wetland edges and channel water level in the example used in Figure 4.2 to illustrate the methods also suggests that more thought needs to be given to the approach used to select the wetland edge points that determine the trend surface.

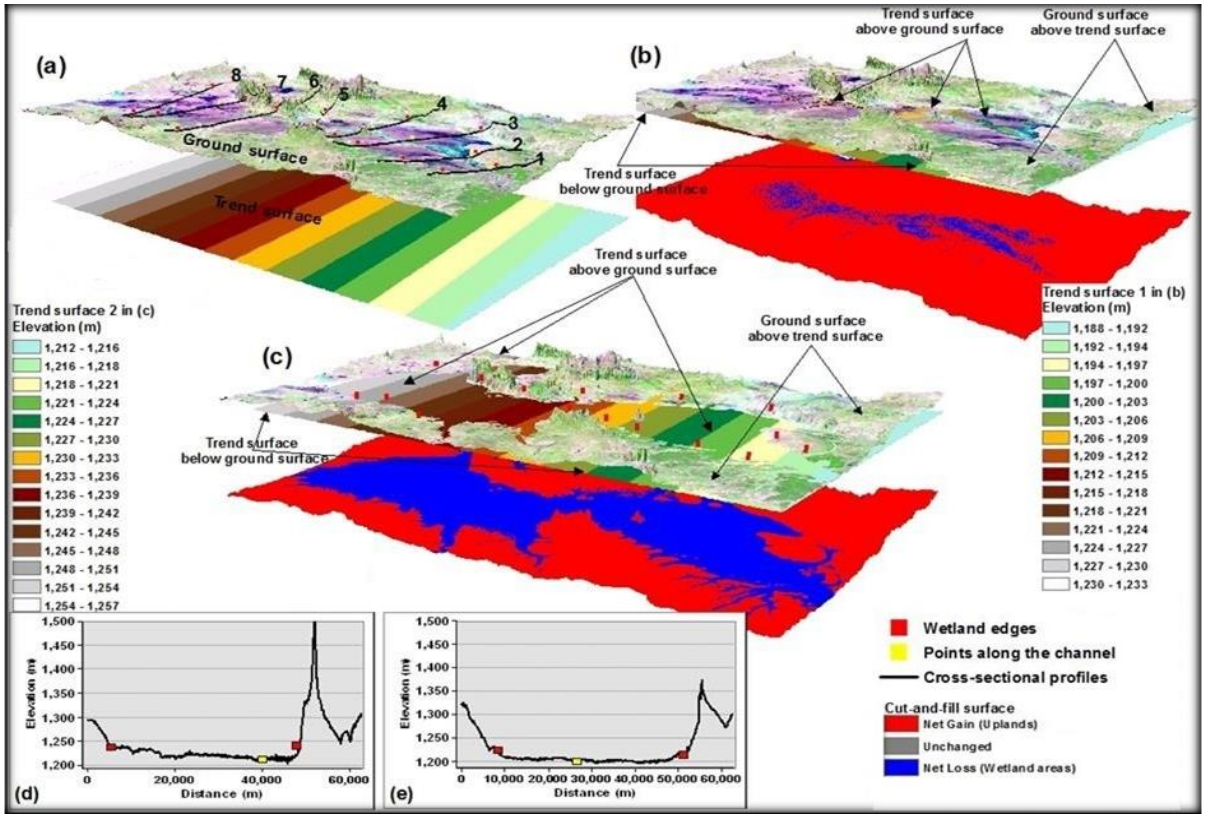

Figure 4.2: Illustration of the determination of the trend surface and use of the cut-and-fill method to delineate wetland boundaries for the Upper Chambeshi wetland in north-eastern Zambia. The raster surface (a) represents the LandsatLook image overlaying the SRTM 1 arc-second DEM, while lines 1 to 8 show the cross-sectional profiles across the wetland. The trend surface is shown below the LandsatLook image in (a). The LandsatLook image overlaying the first and second trend and cut-and-fill surfaces are shown in (b) and (c) respectively. The graphs (d) and (e) represent cross-sectional profiles along lines 1 and 8 in (a), while the attribute table shows the elevation values at channel water level (Z) and modified elevation values that best reveal the wetland boundary (Z1).

An attempt to delineate the Okavango Delta produced results which require further processing in order to delineating wetlands in varying topographic settings. The Okavango Delta comprises an unconfined alluvial fan that occurs within a rifted depression and a linear upper reach (the "Panhandle") that occurs within a confined valley (McCarthy and Ellery, 1994; Figure 4.3). A three-dimensional image of the wetland and the surrounding topography shows the differing topographic settings in which the wetland occurs (Figure 4.3a). While the panhandle occurs within a confined valley (Figure 4.3a1), the alluvial fan is an unconfined depositional feature that occurs within a tectonic depression and is elevated above the surrounding basin floor (Figure 4.3a2). Setting the trend surface to pass through the elevations of the fan surface and the edges of the panhandle successfully delineated the panhandle from the surrounding uplands while the fan was delineated as part of the tectonic

depression (Figure 4.3b). Lowering the trend surface to the edges of the fan successfully separated the fan from the surrounding depression, but in so doing delineated the entire wetland as part of the surrounding upland (Figure 4.3c). The second cut-and-fill results (Figure 4.3c) were inverted and superimposed with figure 4.3(b) to ensure the delineation of the Okavango Delta (Figure 4.4).

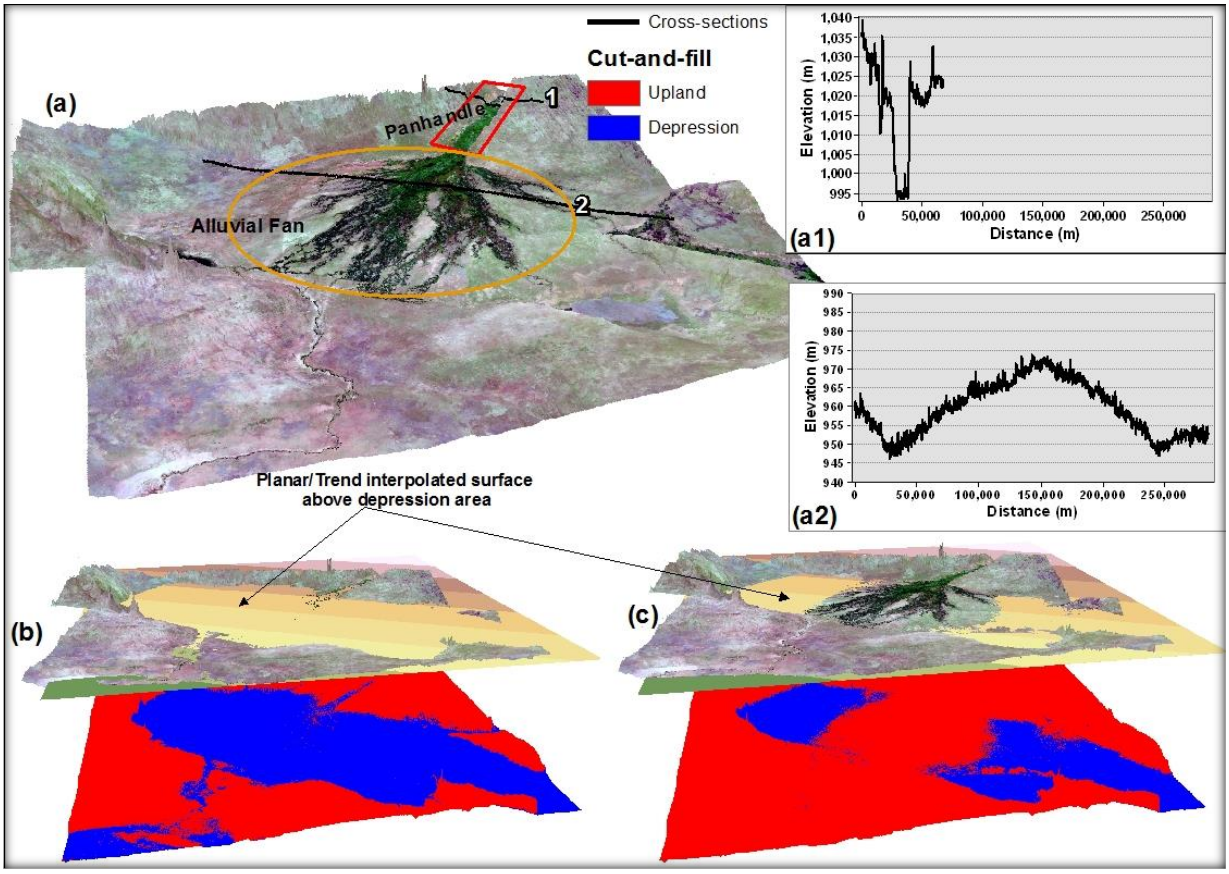

Figure 4.3: Illustration of the trend surface and cut-and-fill method used to delineate the wetland boundary of the Okavango Delta. The LandsatLook image overlaying the SRTM 1 arc-second DEM is shown with cross-sections 1 and 2 (a), with topographic details of these cross-sections shown in (a1) and (a2) respectively. The LandsatLook image overlaying the first and second trend and cut-and-fill surfaces are shown in (b) and (c) respectively.

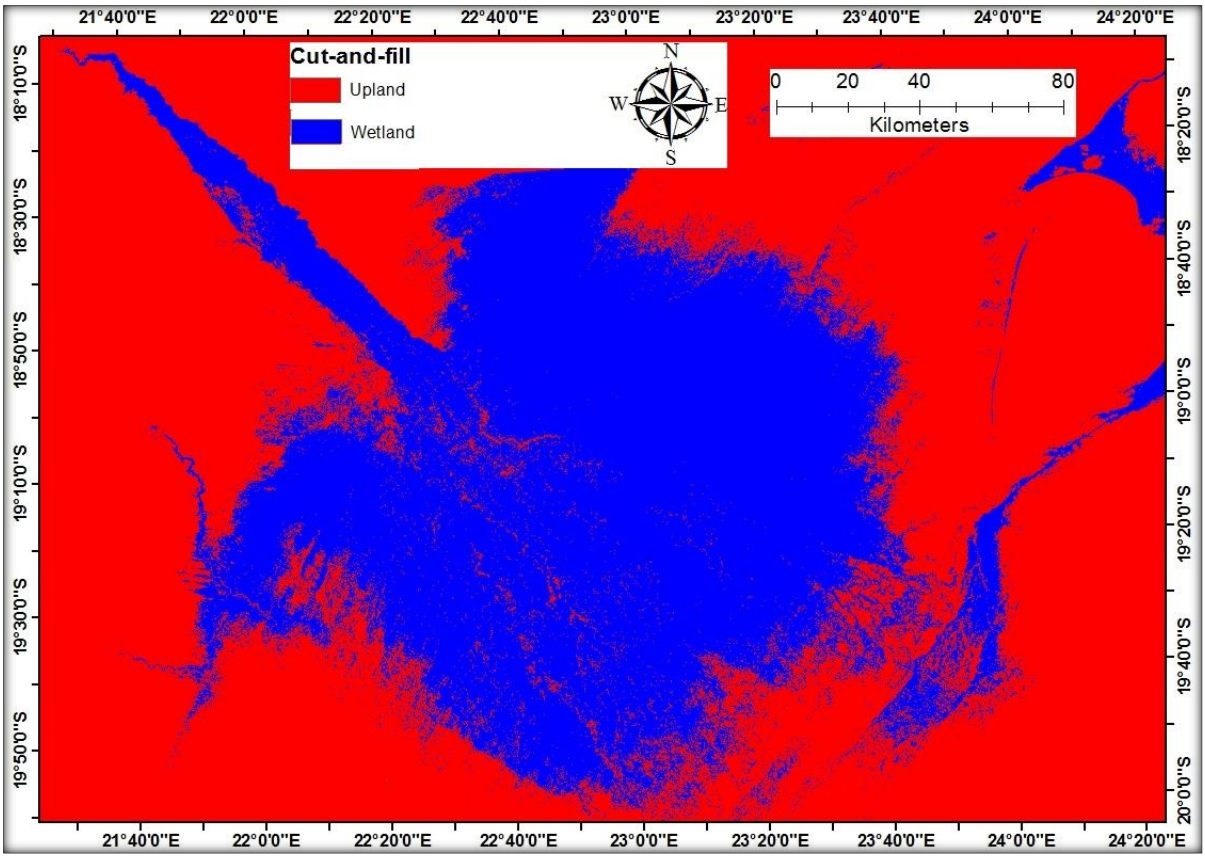

Figure 4.4: Delineation of the Okavango Delta wetland based on an overlay of two cut-and-fill datasets shown in Figure 4.3.

4.2.2.2 Identification of the wetland edge

In support of the approach used in this study, wetland edges can be identified from LandsatLook images by relating key elements for visual image analysis (i.e. colour, tone, pattern, texture, shape, tone/hue, and location/association; Tempfli et al., 2009; Lillesand et al,. 2014) to wetland and geographic features. A good understanding of wetlands, as well as the knowledge of the geographic region under study should make the edge identification process more consistent and reliable. Many wetlands in southern African occur within broad and gentle sloping valleys bound by steep valley walls (Tooth and McCarthy, 2007; Ellery et al., 2009) which separate the wetland basin and the surrounding upland. These steep valleys formed from long-term fluvial and/or tectonic processes and their spatial extent is not influenced by short-term seasonal weather fluctuations. The steep valley sides which confine many of the wetlands are generally less well vegetated, and appear as brighter features in the dry season compared to the green wetland vegetation (Figure 4.5a), or light green vegetation compared to dark open water within the wetland during the wet season (Figure 4.5b).

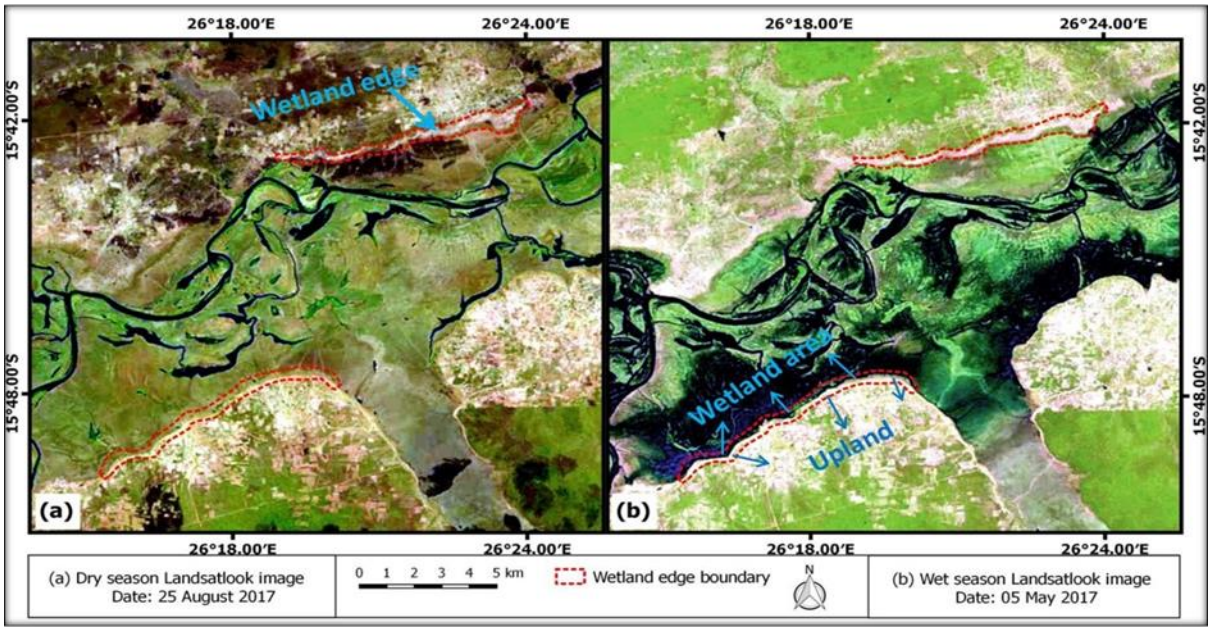

Figure 4.5: LandsatLook images of the Kafue wetland in eastern Zambia showing the wetland area and wetland edges in (a) the dry season and (b) the wet season.

4.2.2.3 Accuracy Assessments

Since the wetland extent delineated from the cut-and-fill procedure will always have some errors, it was vital to gather information on where the errors occur. This was achieved by adopting and populating an error matrix, which is the most commonly used method for assessing image classification accuracy (Lillesand et al., 2004). Accuracy assessment addresses questions related to how well locations of classified land cover types correspond to actual land cover types (Olofsson et al., 2014). Many studies have shown the usefulness of populating error matrix tables in assessing the accuracy of image classification (Cardoso et al., 2014; Chen et al., 2014; Ward et al., 2014; Reschke, and Hüttich, 2014; Dong et al., 2014; Kumar et al., 2014; Furtado et al., 2015; Lane et al., 2014). The error matrix is a simple cross-tabulation of the class labels allocated by the classification of remotely sensed data against the reference data for sample sites (Olofsson et al., 2014). The best assessment of accuracy depends on accessing coincident higher resolution imagery or to ground-truth image data by field-based assessments. Collection of ground reference data is preferred. However, this exercise in most wetland studies is difficult because of their size, remoteness and inaccessibility (Thomas et al., 2015).

In cases where the study area exceeds 500 km^2 in size, it is recommended that at least 75-100 samples per land cover type should be analysed (Banko, 1998). Google Earth has proven to be useful as a source of reference imagery in a number of studies where high-resolution aerial

photographic images were limited (Lidzhegu and Palamuleni, 2012; Van Deventer et al., 2014). In this study, Google Earth were used to randomly collect 200 reference points, of which 100 points represented uplands while the other 100 points were located in the wetland. The randomly selected points were coded as wetland and non-wetland points and the classified pixels were coded as wetland or non-wetland based on the cut-and-fill results. The correctly classified pixels showed matching code values with those from the ground truth points. Frequency and pivot tables, as well as a confusion matrix were computed to summarise and analyse the correctly classified pixels against the incorrectly classified ones.

The most commonly computed parameters for assessing classification accuracy include overall accuracy, producer's accuracy, user's accuracy and the Kappa coefficient to analyse the accuracy of the cut-and-fill generated wetland extent. The overall accuracy gives the percentages of the correctly classified pixels in all categories. Interpreting only the results of the overall accuracy may be misleading since it does not show the accuracies of individual categories (Congalton, 1991). In this case, the producer's accuracy can be computed, which shows how well each category can be classified by showing the percentages of correctly classified pixels for each category. However, it does not show how well the classified land cover classes correspond to actual land cover classes. Therefore, it is appropriate to compute the user's accuracy that measures the reliability of the map (Banko, 1998). The user's accuracy shows how well each category on the map represents what is on the ground. The Kappa coefficient gives an indication of the extent to which the producer's accuracy, the user's accuracy and overall accuracy are due to "true" agreement versus "chance" agreement (Lillesand et al., 2004). The Kappa coefficient is advantageous because, unlike overall accuracy, it considers omission and commission errors, thereby giving a less biased accuracy measure. Omission errors show the percentages of pixels belonging to the class under investigation but that failed to be classified as belonging to the class, while commission error show the percentages of the pixels which belong to another class but have been classified as belonging to the class under investigation. In addition, the Kappa coefficient can be used as a basis for determining the statistical significance of any given matrix (Jensen, 2008). A Kappa coefficient of "1" represents a perfect agreement between the generated results and the ground features, while "0" represents complete randomness (Banko, 1998).

4.2.3 Identifying geomorphological factors that determined wetland origin

According to Ellery et al. (2009), the geomorphic setting of a wetland can be understood to some extent by analysing channel longitudinal profiles. This is because the longitudinal

profiles of most rivers are uniformly logarithmic such that those that are characterised by abrupt changes in slope reflect the influence of geological materials on channel slope (Fryirs and Brierley, 2013). These materials may include a resistant lithology that acts as a local base level along channel beds, leading to topographic steps (Tooth et al., 2004; Fryirs and Brierley, 2013). This indicates that rivers are sensitive to geological materials and are thus likely to provide evidence of tectonic or lithological discontinuities (Schumm et al., 2000). In addition, the analysis of channel longitudinal profiles has proved to be very useful in identifying factors that influence wetland formation (Tooth et al., 2002; Tooth et al., 2004; Grenfell et al., 2010). For example, a sudden increase in channel slope as the stream leaves the wetland would suggest that a resistant lithology may control valley widening and longitudinal slope reduction in an upstream direction (Ellery et al., 2009). However, the absence of an increase in channel slope just below the toe of the wetland may suggest that the wetland may be formed from trunk-tributary interactions (Ellery et al., 2009).

Wetland valley cross-sections may similarly be used to analyse and understand the geomorphological factors that influence the formation of a wetland. A sudden decrease in valley width from the lower reaches of the wetland to areas just below the toe of the wetland suggests a lithological control on the formation of the wetland while a lack of a decrease in valley width may suggest that the wetland could be formed from trunk-tributary interactions (Ellery et al., 2009). Analysis of channel and wetland form is also useful in determining geological and geomorphological controls on wetland formation. A change from meandering to a straight stream across the toe of a wetland suggests a lithological control while the presence of unchannelled valley wetlands or depressions with shallow lakes suggests trunk-tributary interactions.

Analysis of channel longitudinal profiles and valley cross-sections were supplemented by the analysis of the overlay of fault lines, geological maps, and wetland boundaries. This was done in order to identify if the topographic steps from the channel longitudinal profiles or the wetland boundary coincide with a resistant lithology or one or more fault lines. Where a wetland is bounded by fault lines, the wetland may be tectonically controlled within a graben structure.

The analysis of channel longitudinal profiles to identify factors that determine wetland formation can also be aided by relating the continent's geological history with wetland formation. Once correctly identified and mapped, erosional surfaces can be used to correlate wetland formation and the initial or terminal age of erosion surfaces (Partridge and Maud,

1987). This can even be achieved through the analysis of slope profiles since vertical separation of the Post-African I surface from the African Erosion Surface do not exceed 300 m anywhere on the continent (Partridge and Maud, 1987). The Post-African II surface on the other hand, is limited to areas dominated by lithologies that are typically not particularly resistant to weathering or erosion (Partridge and Maud, 1987). In addition, an important outcome of incision of the Post-African II surface was the development of terraces along major rivers (Partridge and Maud, 1987). Since the maximum uplift of the second uplift event was up to 900 m, the vertical separation of the Post-African II surface from the Post-African I surface can be up to 900 m (Burke and Gunnell, 2008).

The analysis of topographic steps controlled by lithological heterogeneity can also be useful in identifying remnants of erosional surfaces that host some of the continent's large wetlands. This is because in Africa, the height of topographic steps that are lithologically controlled but not consistent with different erosion surfaces, is generally 100 m or less and rarely exceeds 200 m (Burke and Gunnell, 2008).

4.2.3.1 Plotting stream courses

In this study DEM's were used to determine stream networks by analysing zones of concentrated flow for each DEM cell using the flow accumulation tool. The results of the flow accumulation process were then used to create a stream network by applying a threshold value to select cells with concentrated flow of greater than 1% of the maximum flow accumulation. This flow accumulation threshold was chosen since it conforms to the ArcHydro default threshold (Ariza-Villaverde et al., 2013). It should be noted that selecting a suitable flow accumulation threshold value as highlighted in Ariza-Villaverde et al. (2013) can only influence the spatial resolution and not the horizontal accuracy of the generated streams. It has been widely observed that generating stream networks from automated DEM procedures may result in spatially dislocated streams (Islam et al., 2008; Flügel, 2014; Bhowmik et al., 2015). According to Soille et al. (2003), the procedure used to fill sinks in a DEM sometimes creates large flat regions that in turn pose challenges for determining accurate flow paths. This is because the flow direction of flat regions cannot be obtained correctly by looking at the value of the 8 nearest neighbours of each cell. As a result, the resultant stream networks on an extensive flat or near-flat land surface may deviate substantially from the observed ones, or it may become disjointed (Soille et al., 2003).

The streamlines generated from the DEM automated procedures were only used to map tributary streams. For plotting channel longitudinal profile, accurate streamlines were

manually digitised from Google Earth. Because of the spatial dislocation of DEM derived streams such as the ones illustrated in Figure 4.6, Flϋgel (2014) resorted to plotting river courses and longitudinal profiles from manually digitised streams. However, Flϋgel's (2014) study used SRTM 3 arc-second DEM and Landsat images as base maps from which manual digitising was undertaken. Given the resolution of these datasets, manual digitising can be achieved at a scale of 1:10 000, but this requires labour-intensive digitising, which may also be inaccurate (Flϋgel, 2014). Erroneous digitising from Flϋgel's (2014) study resulted in considerable editing in order to adjust the DEM digitised streams to the Landsat images, in order to ensure a high degree of horizontal accuracy. Since Landsat images have better spatial resolution than SRTM 3 arc-second DEM imagery, Flϋgel (2014) gave preference to the Landsat digitised streams over the DEM digitised streams. However, the best horizontal accuracy can be achieved through digitising from Google Earth imagery (Figure 4.6) because it can be done at a fine scale of between 1:150 for small rivers like Lufira River and 1:1 500 for large rivers like the Zambezi River.

To appreciate the effect of spatially dislocated streams in identifying topographic steps from the channel longitudinal profiles, a comparison was made between the longitudinal profiles of a stream generated from DEM automated procedures and a stream that had been manually digitised from Google Earth (Figure 4.7). It appears that both longitudinal profiles depict the same general trend as they all identify topographic steps at similar elevation and location. This might be attributed to the low spatial resolution (30 m pixel size) of the DEM used, which can lead to difficulty in detecting changes in surface elevation at a spatial resolution less than that of the DEM's resolution. However, the major deviation between the ways in which the stream course was plotted relates to the total length of the streams as seen in Figure 4.7. The DEM generated stream course is typically shorter than the digitised stream course such that all topographic steps in the automated stream course are at shorter distances than those from the digitised course. This can be attributed to the fact that within large flat areas such as wetlands, the river might meander within the wetland's valley over a greater distance than the valley length (Figure 4.6). On the other hand, within large flat areas the automated DEM procedures usually produce a straight channel and hence reduce the total length of the stream. Therefore, in this study, stream digitising was done using Google Earth to ensure the highest possible stream horizontal accuracy and the most reliable stream length, which are necessary for comparing the total length of the channel within the wetland in relation to the length of the valley.

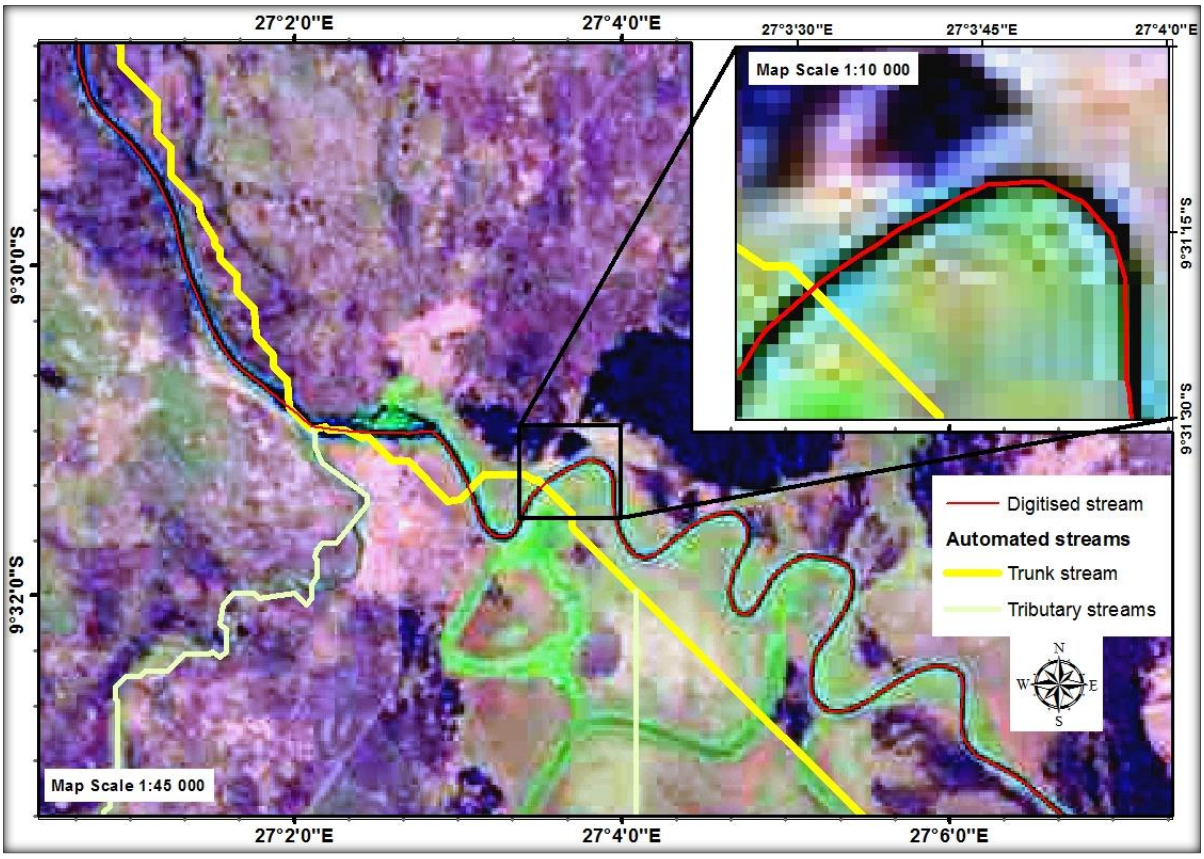

Figure 4.6: Comparison of spatial displacement of the automated DEM stream course (yellow line) and Google Earth digitised stream course (red line) for the Lufira River in the southern Democratic Republic of Congo using the 17 August 2014 LandsatLook image as a base map.

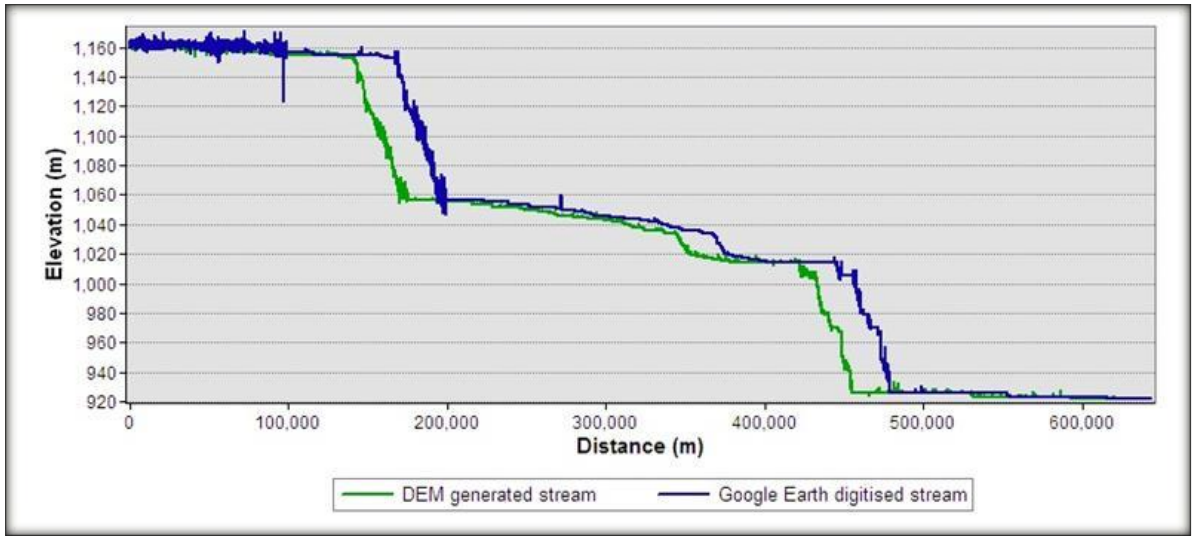

Figure 4.7: Comparison of channel longitudinal profiles plotted from a streamline generated from automated DEM procedures (green line) and a streamline digitised from Google Earth (blue line) for the Luapula River in north-eastern Zambia.

4.2.3.2 Plotting channel longitudinal profile and valley cross-sections

The digitised streamlines from Google Earth and valley cross-sections from LandsatLook images were superimposed on the SRTM 1 arc-second DEM in order to interpolate elevation data to the streamlines and plot channel longitudinal profiles as well as valley cross-sections using the 3D analyst tool. The locations of features such as resistant lithologies, lakes, wetland edges, the head and the toe of the wetland, depressions and river channels, were identified from visual interpretation of LandsatLook images and Google Earth. The locations of these features were plotted on channel longitudinal profiles and valley cross-sections.

4.2.4 Relating wetland origin and structure to hydrological functioning

In order to determine likely factors contributing to the geomorphic origin, structure and hydrological functioning of wetlands, it is necessary to examine wetlands from a catchment scale. This is particularly important in determining the major source of water and sediment characteristics. This was achieved in this study by identifying the major inputs of water for the wetland and analysing wetland features that help store water and sediment. The average depth of flooding for a given stage height in the channel was also evaluated.

4.2.4.1 Catchment delineation

A wetland catchment is the upslope portion of the landscape that generates runoff that contributes flow of water to the wetland (ESRI, 2013; McCauley et al., 2014). The outlet or pour point is the downstream point along the boundary of a watershed from which the water flows from the wetland into a stream in a confined valley (ESRI, 2013). Since floodplain wetlands, particularly in drylands, rely on catchment flows to maintain flooding cycles critical to their ecological integrity (Powell et al., 2008; Dutta et al., 2013), it is vital to determine and compare the wetland's area with its catchment's area. This is because a wetland's catchment size is generally correlated with discharge, as large catchments tend to have greater discharge than small catchments (Ellery et al., 2009). Therefore, the smaller the portion of the catchment area occupied by the wetland, the greater the contribution of catchment runoff to the inundation of the wetland is likely to be. According to Ellery et al. (2009), in drylands where evapotranspiration greatly exceeds precipitation, it is unusual for a wetland to occupy greater than 15% of its catchment area. A wetland occupying greater than this threshold is likely to receive greater input of water from local rainfall.

In this study each wetland's watershed was delineated from the SRTM 1 arc-second DEM using a series of ArcGIS automated procedures. The delineation of watersheds from a DEM is centred on the identification and demarcation of grid cells that contribute concentrated flow

to a common outlet or pour point. To achieve this, the drainage direction for each cell was defined using the flow direction tool. However, owing to the resolution of the DEM or the rounding of elevations to the nearest integer value, some cells or sinks may be lower than their surrounding neighbours resulting in an undefined drainage direction (ESRI, 2013). These cells of undefined flow direction will only receive and retain flow without making any further contribution towards the flow downstream. Therefore, in order to obtain an accurate representation of flow direction it is important to identify and fill these sinks using the sink tool before computing flow direction. After the flow direction of each cell was determined, the flow directions were computed into flow accumulation using the flow accumulation tool. The flow accumulation computes concentrated flow into each cell by accumulating the weight for all cells that flow into each downslope cell. The output cells with a high flow accumulation are areas of concentrated flow. These cells were used to identify the stream channels. Once the flow accumulation raster was generated through the flow accumulation tool, the outlet or pour point was delineated and used in the watershed tool to delineate all cells within a flow direction raster that ultimately drains towards the wetland's outlet.

4.2.4.2 Wetland structure and hydrological functioning

Topographic features such as levees, abandoned channels, and backwater depressions, which characterise floodplain wetlands, play a vital role in controlling the storage and flow of water from the wetland area back to the river (Steinfeld et al., 2013). When floodwater overtops channel banks, features such as depressions serve to store and detain the floodwater, and as such they help to reduce the timing and magnitude of flooding downstream (Acreman and Holden, 2013). It is therefore vital to identify floodplain features that can store water and correlate their existence with wetland formation. In this study, floodplain features were identified from valley cross-sections that were plotted from noise-filtered SRTM 1 arc-second DEM data. Visual analysis of LandsatLook and Google Earth images was also used to identify floodplain topographic features.

Because of high presence of systematic errors in the DEM that are caused by features of minor hydraulic significance such as tall vegetation. Floodplain topography was analysed from a noise filtered SRTM 1 arc-second DEM rather than the original SRTM 1 arc-second DEM. The filter tool (ESRI, 2013) was used to eliminate spurious data from the original SRTM 1 arc-second DEM. The tool removes noise from the DEM by calculating the average value for the "8" nearest neighbours of each cell, thus reducing extreme values in the data. However, since filtering tends to impact on important surface features by lowering hillslopes,

raising valleys, and obliterating important fine details (Gallant, 2011), the filtered DEM was only used in this study to analyse floodplain topography.

The analysis of the average depth of inundation for a given stage height in the channel can be useful in understanding the storage potential, structure or the sedimentation characteristics of a wetland. Wetlands with an elevated alluvial ridge associated with a stream are characterised by the dominance of overbank deposits compared to channel bed aggradation. The presence of an elevated alluvial ridge on a floodplain gives rise to a higher average depth of inundation and storage potential at any given stage height in the channel compared to a wetland without an alluvial ridge.

The average depth of inundation can be analysed by plotting the theoretical volume present in the wetland at various channel water level stages. The current study calculated this volume from the ArcGIS surface difference tool. The surface difference tool uses an input of either Triangular Irregular Network (TIN) or terrain surface (i.e. a generated planar surface) and a reference TIN or terrain surface (i.e. the actual topographic surface of the wetland) to calculate the volume for triangles or areas where the input surface is below, above or at the same elevation as the reference surface (ESRI, n.d; Deshpande, 2013; Figure 4.8). Areas where the input surface is above the reference surface are potential wetted areas. In this study, a DEM was converted to a TIN surface to represent a topographic dataset of the wetland or the reference surface. To enhance the accuracy of the DEM generated TIN, the Z tolerance or the maximum allowable difference between the height of the input raster and the height of the output TIN were kept to 1 m and the maximum number of points added to the TIN were subjectively increased from the default value of 1 500 000 to 150 000 000 points.

The input surface is referred to in this study as the water profile, which is generated from cross-sectional lines plotted down the length of the wetland. At the location of each cross-sectional line, points were taken within the channel in order to extract channel water elevation from the DEM. Elevation values were assigned to the corresponding cross-sectional lines (Figure 4.8a). This was done in order to set the cross-sectional lines at channel water elevations down the length of the wetland. Since optical and radar sensors cannot penetrate water surfaces, channel water elevations can be extracted from a DEM if the width of the channel is greater than the DEM's spatial resolution (i.e. greater than 30 m in this case). Wetlands with no clearly defined channels were ignored for this analysis since the method is heavily reliant on channel water elevation and the average depth of inundation is strongly

influenced by alluvial ridges. Nevertheless, channel water elevation values assigned to the cross-sectional lines were subjected to decrements and increments in order to lower and lift the channel water level to represent different stage heights in the channel. The cross-sectional lines were converted to TIN surfaces to represent water profiles at channel water level and different stage heights above and below channel water level (Figure 4.8b). The resultant wetland volume (km^3) at a given stage height in the channel were divided by the wetland size (km^2) in order to determine the average depth of inundation for each wetland. The average depths of inundation for all wetlands were plotted against various channel stage heights relative to the bankfull stage height, which was assigned a value of 0. Where the channel water level was below bankfull, negative values were used, but where the channel water level was above the bankfull channel water level it was assigned a positive value. Depression wetlands with no clearly defined channels were ignored for this analysis since the method is heavily reliant on channel water elevation and the average depth of inundation is strongly influenced by the presence and relative elevation of alluvial ridges.

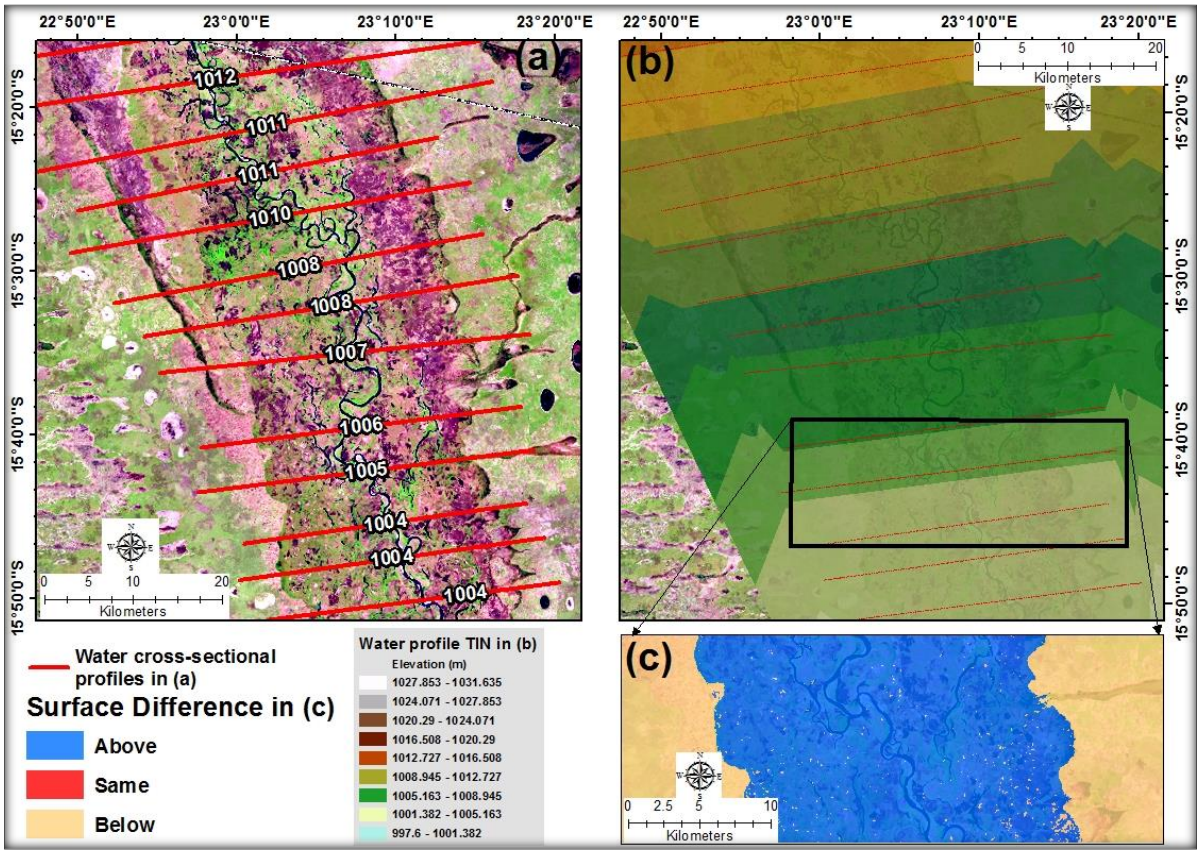

Figure 4.8: Illustration of the use of the Surface Difference method to calculate wetland volume and wetted area.

The surface difference method was used in this study to differentiate wetlands based on their structures and to quantify the wetland's storage potential rather than quantifying the actual wetland inundation characteristics. This is because the method assumes that the channel from which the water profiles were generated is the only source of inundation and it ignores the contribution of other sources such as tributaries. The method also ignores the effect of downstream loss of floodwater from the wetland area through drainage channels and the wetland outlet. The effects of conduits (such as breached levees, drainage channels and outlets) and conduit barriers (such as channel banks, levees, alluvial ridges and sediment bars) in wetland inundation are also ignored. This is because simple topographic analyses are used to estimate the possible inundated areas by restricting wetted area and volume calculations to a series of discrete water cross-sectional profiles from which wetland areas adjusted to each profile are either of the same or higher elevation (areas not inundated) or lower elevation (areas inundated). Estimation of wetland inundation characteristics can be achieved using two-dimensional (2D) hydraulic models (McMillan and Brasington, 2007). Even though the scope of this study does not extend to hydraulic models, it is important to note that such models derive potential flooded areas by using a water balance approach based on a wetland's topographic characteristics and hydraulic connectivity at a given discharge (Gibbs et al., 2016). A concurrent hydrological modelling study titled "Hydrological Modelling of Channel Wetland Exchanges in Different Landscape Settings in Africa" at the Institute for Water Research, Rhodes University, seeks to estimate the impacts of different wetlands on downstream flows using a 2D hydraulic model. The results of the hydraulic modelling study conducted by Ms Eunice Makungu under the supervision of Prof Denis Hughes, will be used to substantiate the findings of the current study. With hydraulic modelling, the potential for any area to flood, retain and release floodwater, depends on the elevation difference between that area and the nearest hydrological link such as the main channel, levee breach, tributary stream, oxbow lake, drainage channel and wetland outlet (Junk et al., 1989; Townsend and Walsh, 1998).

The water storage potential for different wetland types varies significantly based on their structure and topographic characteristics as a function of natural geomorphic processes that led to the formation of the wetland (Figure 4.9). Wetlands with sinuous and anastomosing streams with limited alluvial ridges are likely to have lower average depths of flooding and water storage volumes per unit wetland area (Figure 4.9a) than wetlands with meandering streams with elevated alluvial ridges and low-lying backwater depressions (Figure 4.9b).

While flooding of wetlands does not behave as suggested by the model, wetlands with a large volume below the water level are likely to have greater potential to spread floodwater to the backwater depressions and other low-lying areas, and as such a higher water storage potential than those wetlands without alluvial ridges present. However, the potential storage capacity or average depth of inundation for backwater depressions that are inundated throughout the year, may be higher than estimated since optical sensors cannot penetrate below the water surface.

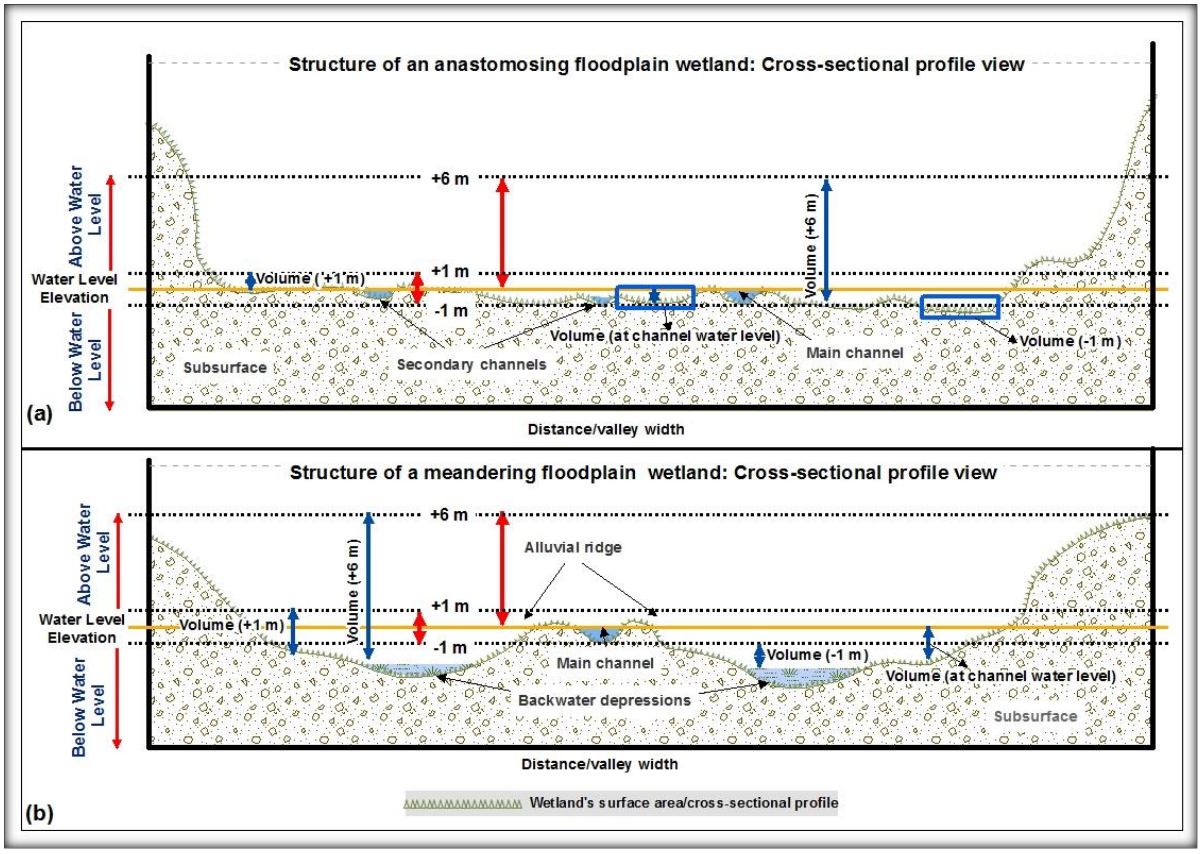

Figure 4.9: Floodplain wetland structures and wetland water storage capacity for an anastomosing (a) and meandering (b) floodplain. The yellow lines show the water cross-sectional profiles set at channel bankfull stage (relative water level elevation = 0). The dashed black lines show the water cross-sectional profiles set at specific depths above and below channel water level. The red arrows show water profile depths that were derived by raising and lowering the water level profile in order to represent the depth of flooding for a given stage height in the channel. Blue arrows show the average water depth at a specific channel flood stage as represented by the different water cross-sectional profile depths.

4.2.5 Classification of wetlands based on processes that determine their formation and their associated structure and hydrological functioning

Wetland features and characteristics were identified and compared in order to discriminate between different wetland types. Wetland characteristics that were considered for classification are wetland and catchment sizes, catchment geological characteristics, processes determining wetland origin, weakly versus strongly channelled wetlands, wetland connectivity to the drainage network downstream, presence of alluvial ridges, backwater depressions, channel and valley slopes, as well as sinuosity ratio.

Both nominal and quantitative variables for wetland features and characteristics were standardised and analysed using Principal Component Analysis (PCA) in order to clarify the main axes of variation underpinning wetland heterogeneity. The data were standardised by converting the means of all the variables to 0 and the standard deviation to 1 while nominal data were binarily coded. Since the data had both nominal and quantitative variables, PCA was computed in Statistica and the cluster analysis was computed using the FactoMineR package in R Studio version 3.4.1. FactoMineR was designed mainly to take into consideration different types of variables such as quantitative and nominal data (Lê et al., 2008). From the standardised wetland variables, a cluster analysis was performed in order to group wetlands based on similarity in wetland features. More details on wetland classification have been provided in Chapter 9.

CHAPTER 5: THE DISTRIBUTION OF LARGE WETLANDS IN AFRICA'S ELEVATED DRYLANDS

5.1 Site selection in relation to climatic and topographic anomalies

Overlay and analysis of the distribution of Africa's large wetlands in relation to the Global Aridity Index and elevation reveal that Africa has many large wetlands (Figure 5.1a). The largest wetland system is in the Congo River basin on the equator at a longitude of approximately 15^{o} E. Also evident from this map is that about 75% of Africa can be considered to be dryland (Table 5.1).

Examination of the distribution of large wetlands in relation to Africa's drylands reveals a belt of large wetlands on the periphery of the humid Congo River basin (Figure 5.1b). Very large wetlands are situated on lowlands in the interior to the north of humid areas, including the Inland Niger Delta in Mali (approximately 15^{o} N and 10^{o} W), Lake Chad and the Plaines d'inondation des Bahr Aouk et Salamat in Chad (approximately 10^{o} N and 10^{o} E respectively), and the Sudd in southern Sudan (approximately 8^{o} N and 30^{o} E). Most of the remaining large wetlands in Africa based on the GLWD are situated on elevated land at an elevation of greater than 600 amsl (Figure 5.1c). Based on this analysis twenty-two wetlands in elevated (non-coastal) and dryland settings were selected as candidates for further investigation (Table 5.2).

Because of the inaccuracy of the GLWD (Section 4.1.1) and the impracticality of considering all twenty-two wetlands, nine wetlands were selected. The inaccuracies in the GLWD dataset are highlighted for the Bua River floodplain by overlaying the wetland boundary as shown in the GLWD on Google Earth (Figure 5.2). The GLWD considerably overestimates the size of this wetland. Based on similar evidence, the size of those wetlands in Table 5.2 that are presented as shaded rows appear to be significantly exaggerated in the GLWD database. As such, further investigation of individual wetlands was based on wetlands in the unshaded rows in Table 5.2. The Okavango was not considered for further investigation in the current study because it has been studied in considerable detail (McCarthy and Ellery, 1998) and the Cuando floodplain was not considered because of time constraints and its similarities in structure to the Upper Zambezi and Barotse wetlands.

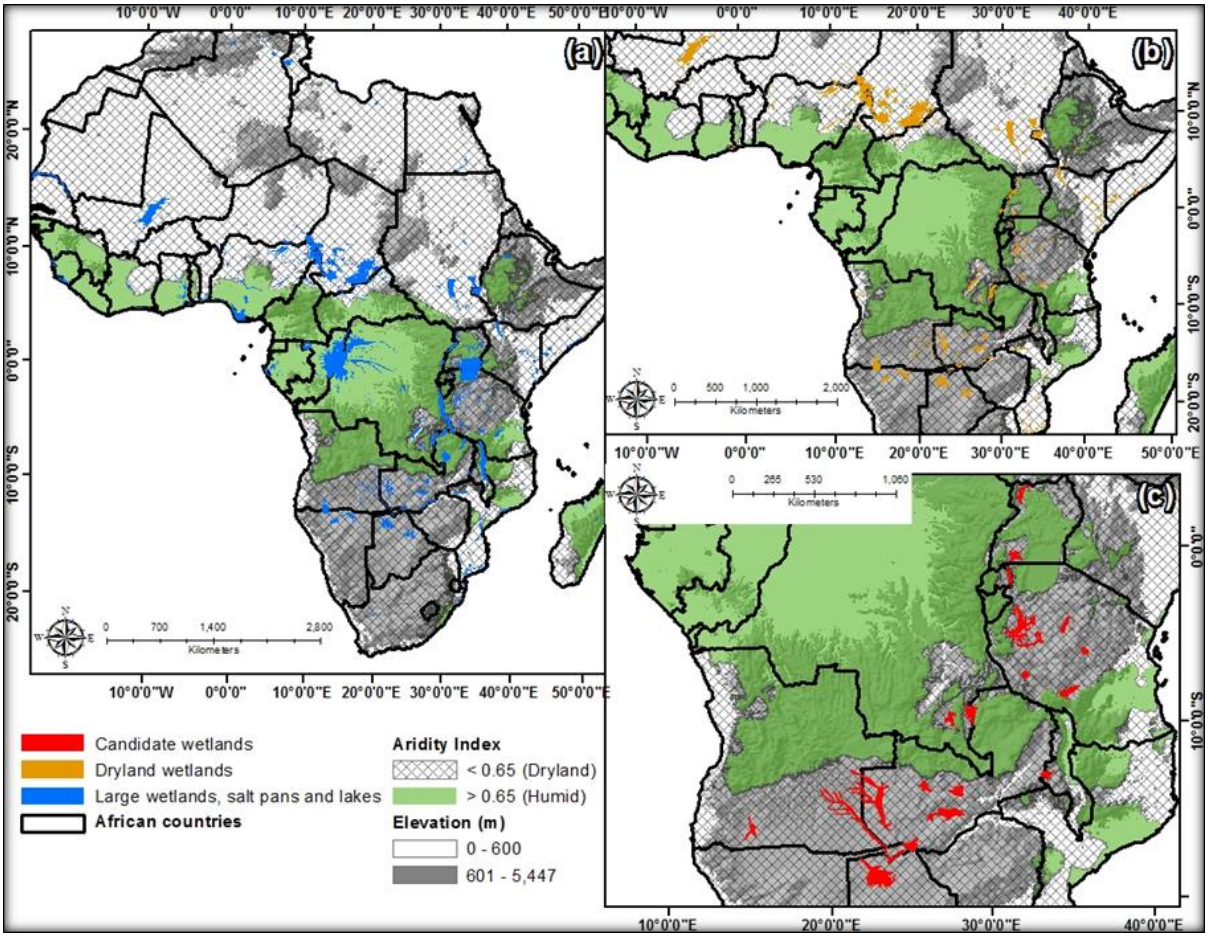

Figure 5.1: The distribution of large African wetlands (a) in relation to the continent's aridity (b) and on the topographic anomaly referred to as the African Superswell (c).

Table 5.1: Area statistics of African climatic zones based on the Aridity Index from the CGIAR-CSI.

Climatic zones	AI	Surface area	Surface area (%)
Humid	> 0.65	7 450 461 km^2	24.9%
Arid and semi-arid	< 0.65	22 428 114 km^2	75.1%

Table 5.2: A list of large African wetlands that occur in elevated arid and semi-arid zones of southern and eastern Africa. The non-shaded rows indicate candidates wetlands for more detailed study (see text for details).

	Wetland name	Country	Area (km^2)
1.	Okavango Delta	Botswana	14 351
2.	Barotse Floodplain	Zambia	10 898
3.	Kafue Flats	Zambia	7 234
4.	Cuando Floodplain	Namibia and Botswana	7 229
5.	Myowosi and Mkombo Rivers Floodplain	Tanzania	7 085
6.	Luapula Floodplain	DR Congo and Zambia	3 875
7.	Lukanga Swamp	Zambia	3 291
8.	Zambezi River Floodplain	Zambia and Namibia	2 986
9.	Usangu Flats	Tanzania	2 768
10.	Lufira River Floodplain	DR Congo	2 063
11.	Cunene River Floodplain	Angola	1 796
12.	Lakes Kijanebaloa and Kachira Wetland System	Uganda	1 717
13.	Zivwe River Floodplain	Tanzania	1 689
14.	Wembere Wetland	Tanzania	1 660
15.	Lake Bisina/Opeta Okere Wetland System	Uganda	1 646
16.	Busanga Swamp	Zambia	1 497
17.	Ugalla/Wala River Floodplain	Tanzania	1 462
18.	Albert Nile Floodplain	Uganda	1 337
19.	Bua River Floodplain	Zambia and Malawi	1 249
20.	Kagera River Floodplain	Tanzania	1 204
21.	Rukwa Floodplain	Tanzania	1 075
22.	Bahi Swamp	Tanzania	1 064

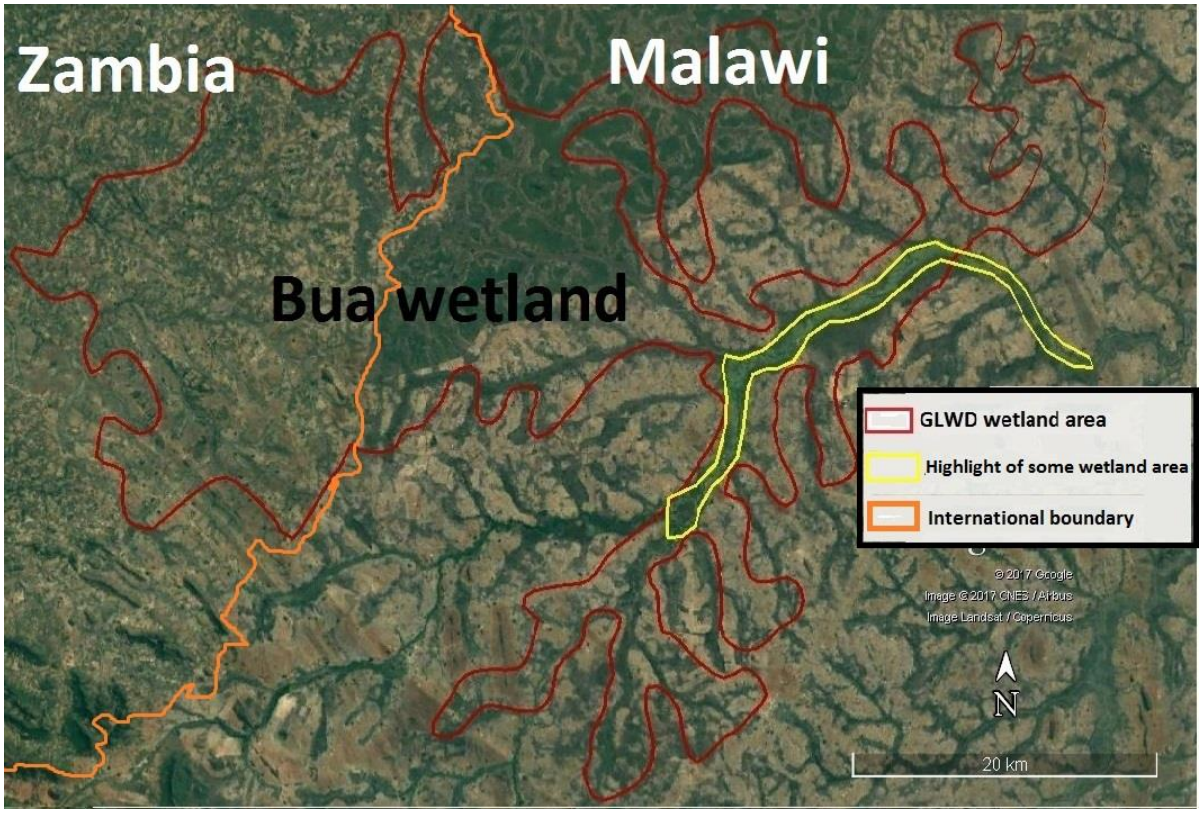

Figure 5.2: The GLWD wetland boundary (red line) and the highlight of some of the actual wetland areas (the digitised yellow line) of the Bua wetland in Zambia and Malawi. The image is a Google Earth image with image data from Google, CNES/Airbus and Landsat/Copernicus.

5.2 The distribution of large African wetlands in relation to rifting

The distribution of large wetlands in southern Africa, as identified using the GWLD, appears to show some relationship with seismic activity associated with rifting mapped according to the International Seismological Centre (ISC; Figure 5.3). The epicentres of earthquakes stretch from Ethiopia to Botswana and Mozambique in alignment with the East African Rift Valley. The East African Rift Valley is an elevated topographic feature that is associated with uplift, such that depressions are formed in areas marginal to the rift valley. This is extremely well illustrated in East Africa where a massive basin that hosts Lake Victoria is a consequence of a shallow basin having been formed between the eastern and western branches of the East African Rift Valley. Lake Victoria and the wetlands surrounding it are therefore a consequence of regional landforms created as a consequence of rifting (Figure 5.3a). Many of the vast papyrus dominated wetlands in Uganda owe their origin to the formation of similar depressions between the eastern and western branches of the East African Rift Valley. Further southwards, wetlands are situated in gentle depressions that abut the limited variation in relief associated with uplift that has taken place in association with

early development of the rift valley in this region, including wetlands to the west of the rift valley in the south-eastern DRC, and to the north of the rift valley in western Zambia and eastern Angola (Figure 5.3b). The Okavango Delta in northern Botswana is situated in a half-graben that is directly linked to the extension of the East African Rift Valley in southern Africa, while Bangweulu Lake and its associated wetlands are likely to owe their origin to a depression created between the arm of the Rift Valley in southern Zambia and one further north that hosts Lake Mweru.

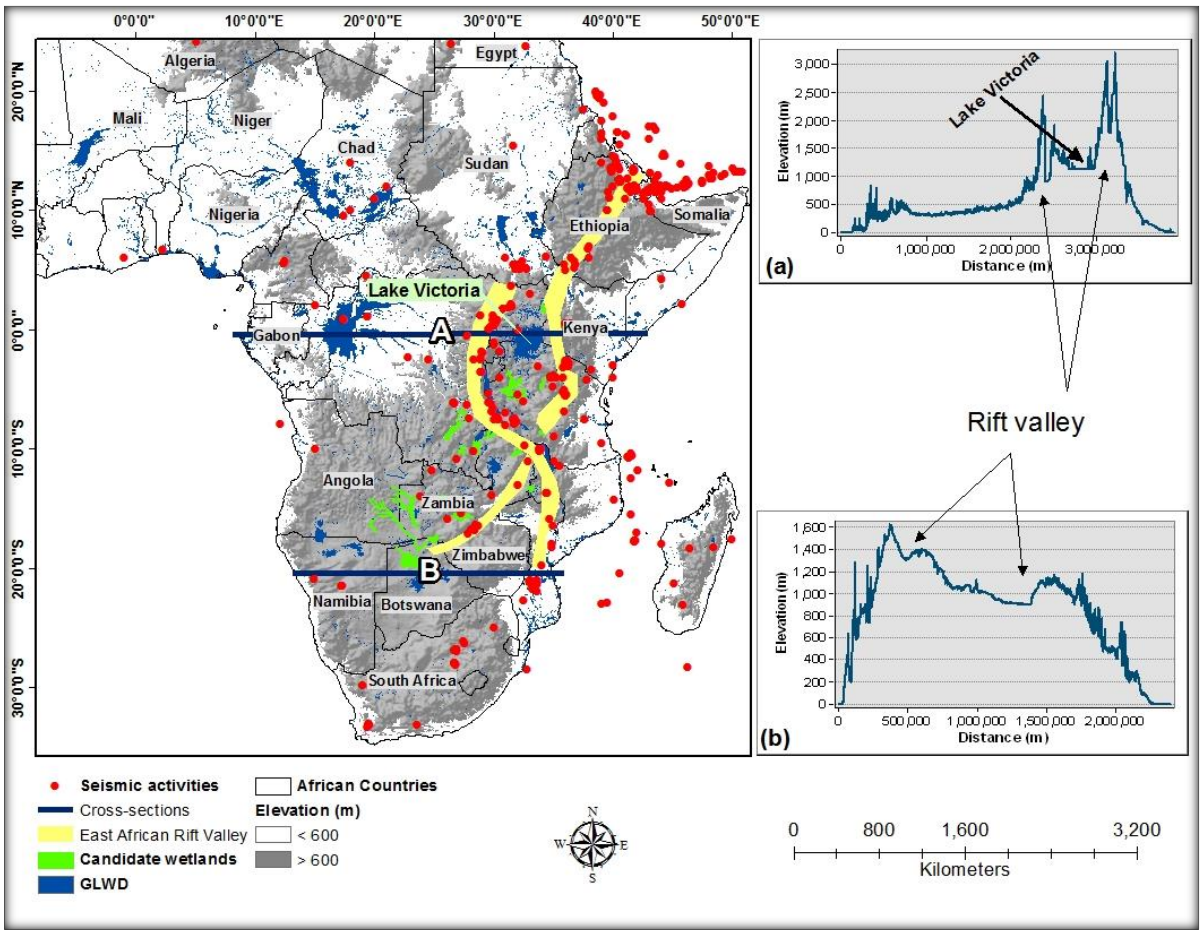

Figure 5.3: The distribution of candidate wetlands in relation to seismicity within the African continent. Graphs (a) and (b) show the elevation profile of transect A and B.

5.3 Wetland extent and accuracy assessment

The cut-and-fill results based on the method developed in this study were used to produce wetland boundaries, which were compared with the boundaries of wetlands mapped for the GLWD (Figure 5.4 to 5.7 and Table 5.3). Comparison of the results of the cut-and-fill method with the GLWD wetland boundaries shows that the two boundaries are markedly dissimilar for some wetlands. The results also show that the GLWD wetland boundaries were smaller than estimated in this study for the Lukanga wetland (Figure 5.4), Luapula wetland,

and Wembere wetland (Table 5.3). The wetland boundaries as mapped for the GLWD were larger than the current study's estimations for some wetlands such as the Lufira (Figure 5.5), Usangu (Figure 5.6), Kafue and Barotse wetlands (Table 5.3). For the Bahi wetland (Table 5.3), the GLWD and the cut-and-fill method showed a similar extent of wetland boundaries. However, from Figure 5.6, it appears that the cut-and-fill method had excluded some parts of the Usangu wetland, especially towards the north-eastern part of the wetland. For the Lufira (Figure 5.5) and Upper Zambezi wetlands (Figure 5.7), the GLWD wetland boundary extended to include small tributary valley bottom wetlands. For the purposes of this study the impinging tributary valley wetlands were excluded from the trunk wetland as the focus here is on understanding the origin, structure and hydrological functioning of the trunk stream wetlands.

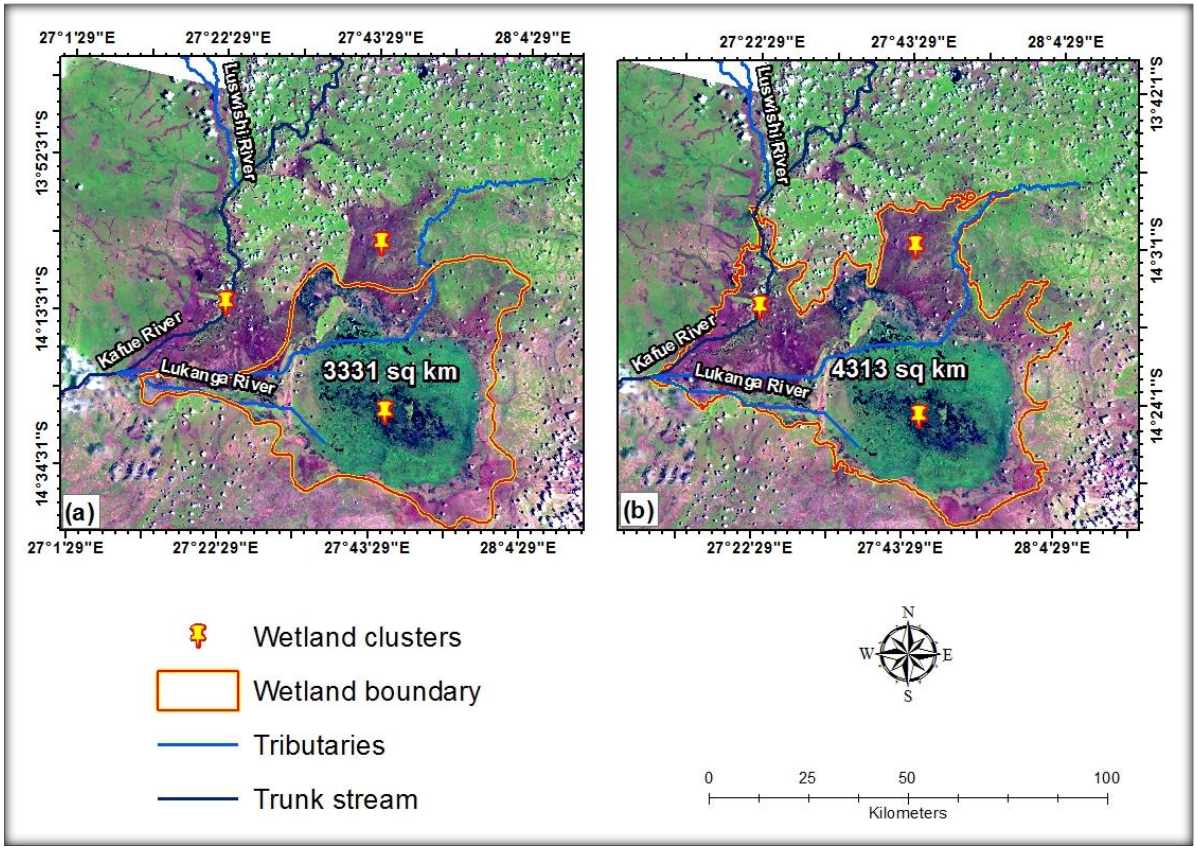

Figure 5.4: Comparison of the Lukanga wetland boundary based on the GLWD (a) and the cut-and-fill method used in this study (b), overlaid on a 27 November 2013 LandsatLook Image.

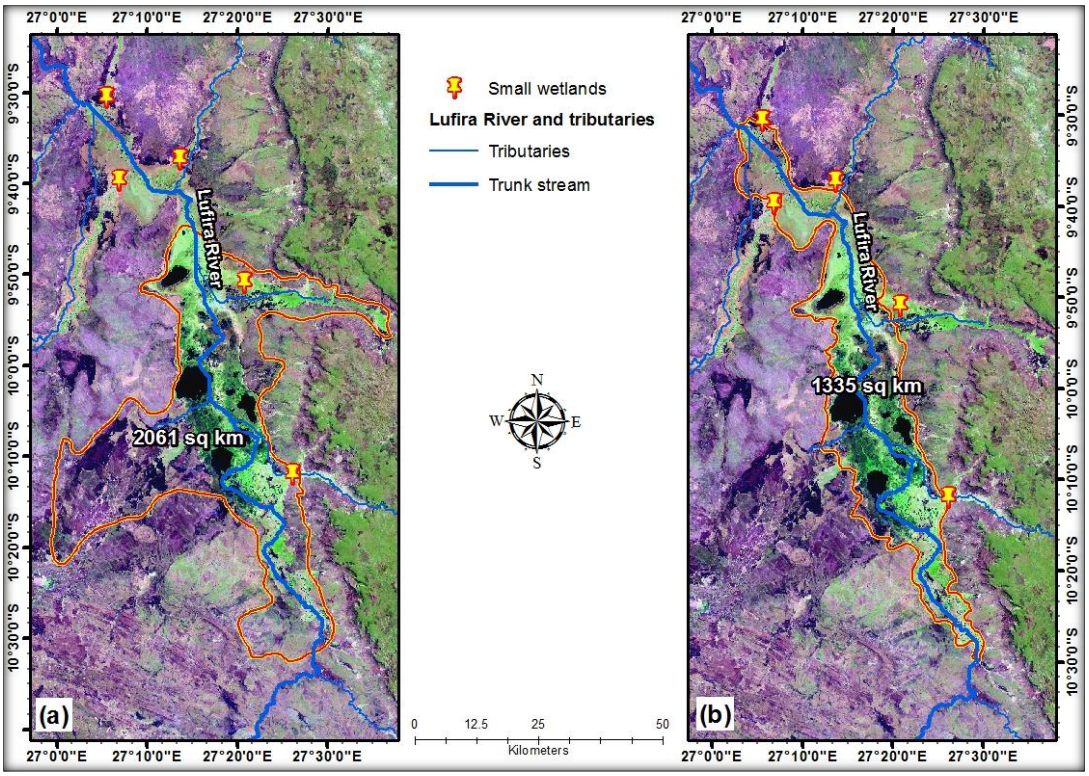

Figure 5.5: Comparison of the boundary of the Lufira wetland boundary based on the GLWD (a) and the cut-and-fill method used in this study (b), overlaid on a mosaic of 10 and 17 June 2015 LandsatLook images.

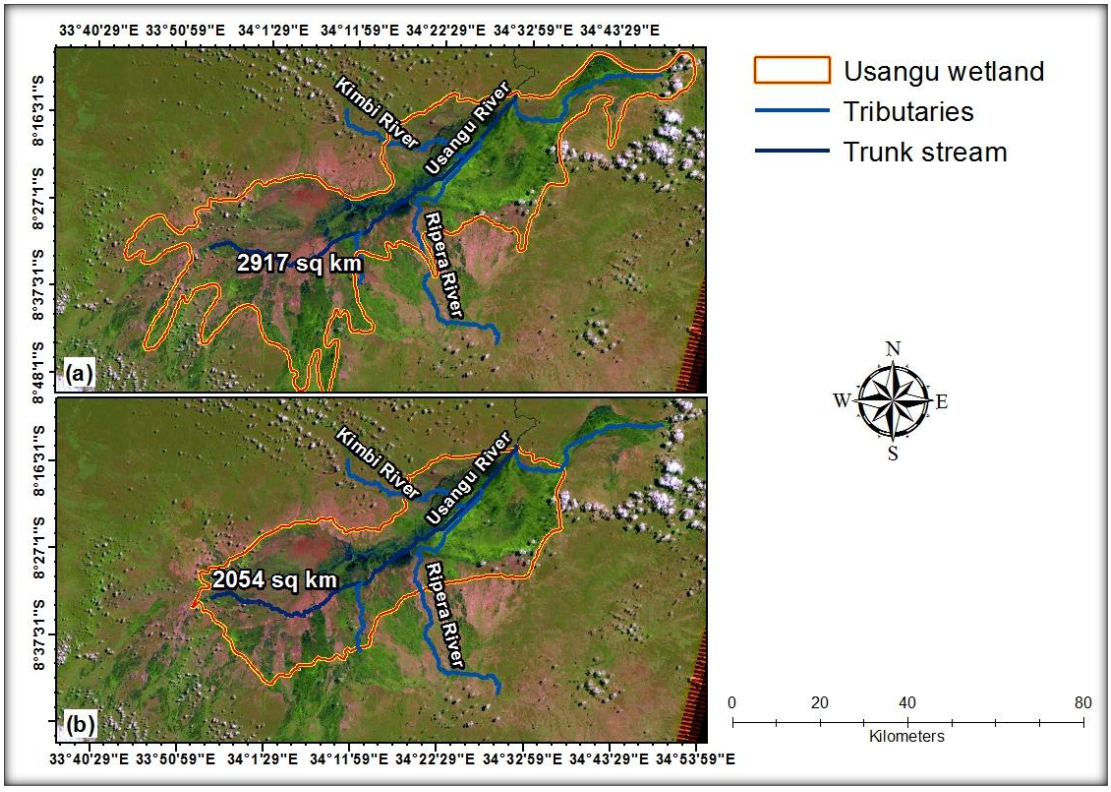

Figure 5.6: Comparison of the boundary of the Usangu wetland boundary based on the GLWD (a) and the cut-and-fill method used in this study (b), overlaid on a 08 October 2014 LandsatLook image.

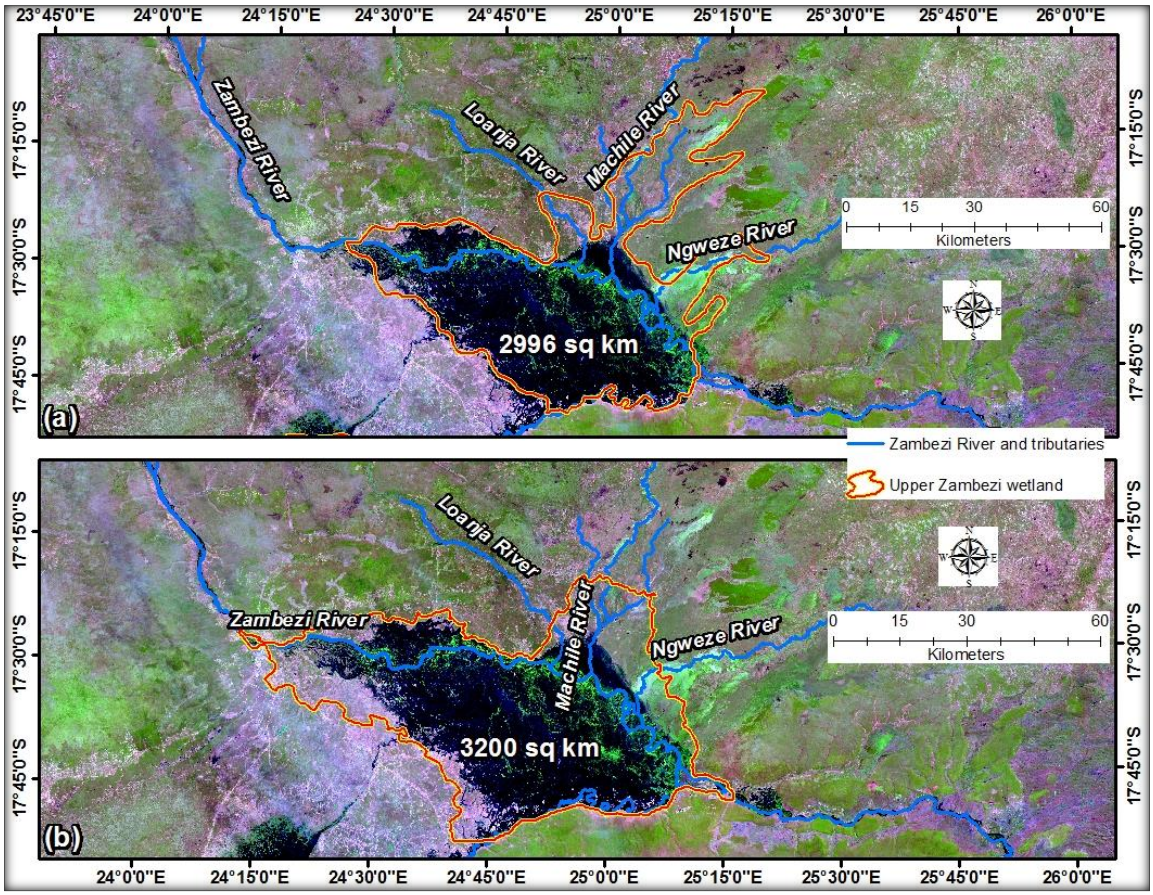

Figure 5.7: Comparison of the boundary of the Upper Zambezi wetland based on the GLWD (a) and the cut-and-fill method used in this study (b), overlaid on a 17 April 2009 LandsatLook image.

Table 5.3: Comparison of wetland extent based on the GLWD and the cut-and-fill method used in this study.

Wetland name	GLWD area (km^2)	Cut-and-fill area (km^2)
Luapula wetland	3 937	5 302
Wembere wetland	1 746	2 714
Barotse wetland	10 899	8 368
Kafue wetland	7 306	7 926
Bahi wetland	1 130	1 086
Lukanga wetland	3 331	4 313

The reliability of the results generated from the cut-and-fill method was assessed in terms of the compatibility of the produced maps with ground features. The accuracy of the cut-and-fill generated maps as summarised in Table 5.4 shows high producer's and user's accuracies for all wetlands. The producer's accuracies for the wetland class in all maps ranged from 68 to 100%, while the user's accuracies (the overall class accuracy) for the wetland class were

above 81% in all wetlands. In addition, high overall accuracies (ranging from 76 to 96%) were achieved for all wetlands. Most importantly, the results of the Kappa coefficients (ranging from 0.61 to 0.92) indicate that there is agreement between delineated wetland boundaries and features on the ground.

Table 5.4: A summary of the accuracy of wetland boundary delineated from the cut-and-fill procedure.

Topographic Feature	**Large African wetlands**															
	Barotse wetland		Kafue wetland		Luapula wetland		Lukanga wetland		Upper Zambezi wetland		Usangu wetland		Lufira wetland		Wembere Wetland		Bahi wetland	
	PA	**UA**	**PA**	**UA**	**PA**	**UA**	**PA**	**UA**	**PA**	**UA**	**PA**	**UA**	**PA**	**UA**	**PA**	**UA**	**PA**	**UA**
Upland	98	83	92	100	83	100	99	93	92	90	91	79	96	97	100	78	97	94
Wetland	80	98	100	93	100	85	92	99	86	90	76	89	97	96	71	100	94	97
Overall Accuracy (%)	**89**		**96**		**92**		**96**		**90**		**84**		**97**		**86**		**96**	
Kappa Coefficient	**0.78**		**0.92**		**0.83**		**0.91**		**0.79**		**0.67**		**0.94**		**0.72**		**0.91**	

PA = Producer's Accuracy (%), and UA = User's Accuracy (%)

5.4 Discussion

Inconsistencies between the cut-and-fill generated wetland boundaries and the GLWD wetland boundaries were clearly evident in this study. This illustrates a widespread problem since different authors use different methods for delineating wetland areas. For example, according to McCartney et al. (2011) the Lukanga wetland covers an area of 1 800 km^2 but according to the IMCG (2004) it covers an area of 2 500 km^2. In this study it is mapped as occupying an area of 4 313 km^2. With regard to the Lukanga wetland, most studies only delineate the boundary of the shallow flooded depression and exclude the other HGM units (e.g. McCartney et al., 2011; IMCG, 2004). The Barotse and Kafue wetlands are believed to cover 9 000 km^2 and 6 500 km^2 respectively (van Steenbergen et al., 2015) while according to IMCG (2004) the Kafue wetland covers an area of 6 000 km^2 and according to Chomba (2014) the Barotse wetland has an area coverage of 10 750 km^2. These inconsistencies can be attributed to the lack of a common and reliable wetland database, the use of different methods to delineate wetland areas, and the purpose of wetland delineation.

From the GLWD, some wetlands are mapped as a cluster of a single large wetland within the trunk stream valley and a number of small wetlands occurring within tributary valleys (e.g. the Lufira and Barotse wetlands). The delineation of wetlands as clusters is common for spectrally-based image classification techniques. In most cases, the large wetland occupies the low-lying trunk stream valley while the associated small wetlands occur within slightly elevated tributary valleys. Satellite image classification methods based on spectral reflectance may fail to separate the main wetland from small wetland clusters because of the spectral reflectance similarities of wetland vegetation, soil or water. In contrast, the topographically-based method for delineating wetlands, such as the cut-and-fill method used in this study, typically excludes the small wetland clusters from the large wetland (e.g. small wetland clusters were excluded from the Lufira and Barotse wetlands). However, using the cut-and-fill method, the tributary wetlands could be added to the trunk by analysing each tributary separately, such that the entire wetland complex of trunk and tributary wetlands can be mapped using this technique. An advantage of this is that each hydrogeomorphic unit in a wetland complex would be mapped separately.

The main wetland that occurs within the trunk stream usually forms from different geological and geomorphological processes compared to tributary valleys impinging on the trunk valley, and the trunk valley in turn influences the formation of the small wetland clusters occurring

within tributary valleys. In order to determine the geomorphic origin, structure and hydrological functioning of large wetlands it was considered important to distinguish the main wetland from smaller tributary wetland clusters. The exclusion of small wetland clusters from the main wetland also considered the hydrological relations of the wetlands under investigation in order to determine the hydrological functioning of large wetlands.

Since Lehner and Döll (2004) do not provide details on how data from various databases were used to compile the GLWD, it is difficult to evaluate the techniques used to delineate wetland areas for the GLWD. One could assume that the GLWD datasets were compiled from wetland areas delineated from image classification procedures. This is because spectral image classification procedures are the most widely used procedures for delineating wetland areas. However, the most common errors for spectral based image classification procedures are spectral confusion between wetland and surrounding areas (Ozesmi and Bauer, 2002). Similarly, the use of spectral analysis based methods to delineate the boundary of wetland complexes may be inaccurate. This is because the spectral signature of an annually flooded wetland may vary significantly during the year. This can explain the exclusion of the other HGM units from the Lukanga wetland complex (e.g. McCartney et al., 2011; IMCG, 2004).

The assessment of the accuracy of the wetland boundaries delineated from the cut-and-fill method showed high accuracies across all wetlands. The higher-class accuracies achieved by the cut-and-fill method can be attributed to the success of the method in distinguishing lowlands from uplands. The cut-and-fill method eliminated the effect of cloud cover and spectral confusion that characterise spectrally-based methods.

CHAPTER 6: THE ORIGIN AND HYDROLOGICAL FUNCTIONING OF LITHOLOGICALLY CONTROLLED FLOODPLAIN WETLANDS

6.1 Introduction

Wetlands presented in this chapter are floodplain wetlands that occur in broad and gently sloping valleys characterised by meandering streams and that terminate as the valley crosses a resistant lithology. However, the sedimentological processes, geological characteristics, geomorphic features, and hydrological functioning of these wetlands differ from each other. Differences include channel and floodplain features such as backwater depressions and alluvial ridges, which are influenced by the sedimentation regime, and in turn influence the average depth of inundation as well as the flood attenuation potential of the wetland. These wetlands include the Lufira wetland that is part of the Congo River catchment and the Barotse wetland that is part of the Zambezi River catchment.

6.2 Lufira wetland

The Lufira wetland is located about 110 km north-west of the city of Lubumbashi in the Democratic Republic of Congo (Figure 6.2.1). The wetland is located between latitude 09º 31'S and 10º 30'S and longitude 27º 02'E and 27º 30' E. The Lufira River rises from what appears to be a remnant of the high-lying African Erosion Surface (Katanga plateau). From the Katanga plateau, the Lufira River flows in a north-eastern direction and descends from Lake Tshangalele to the head of the Lufira Depression (Cotterill, 2004). The Depression is bounded by Mount Kundelungu to the east and the Manika Flats to the west. Within the Lufira Depression, the river flows in a north-north-west direction towards Kiubo Falls, after which the river flows into Lake Upemba, which is situated in a north-east trending graben.

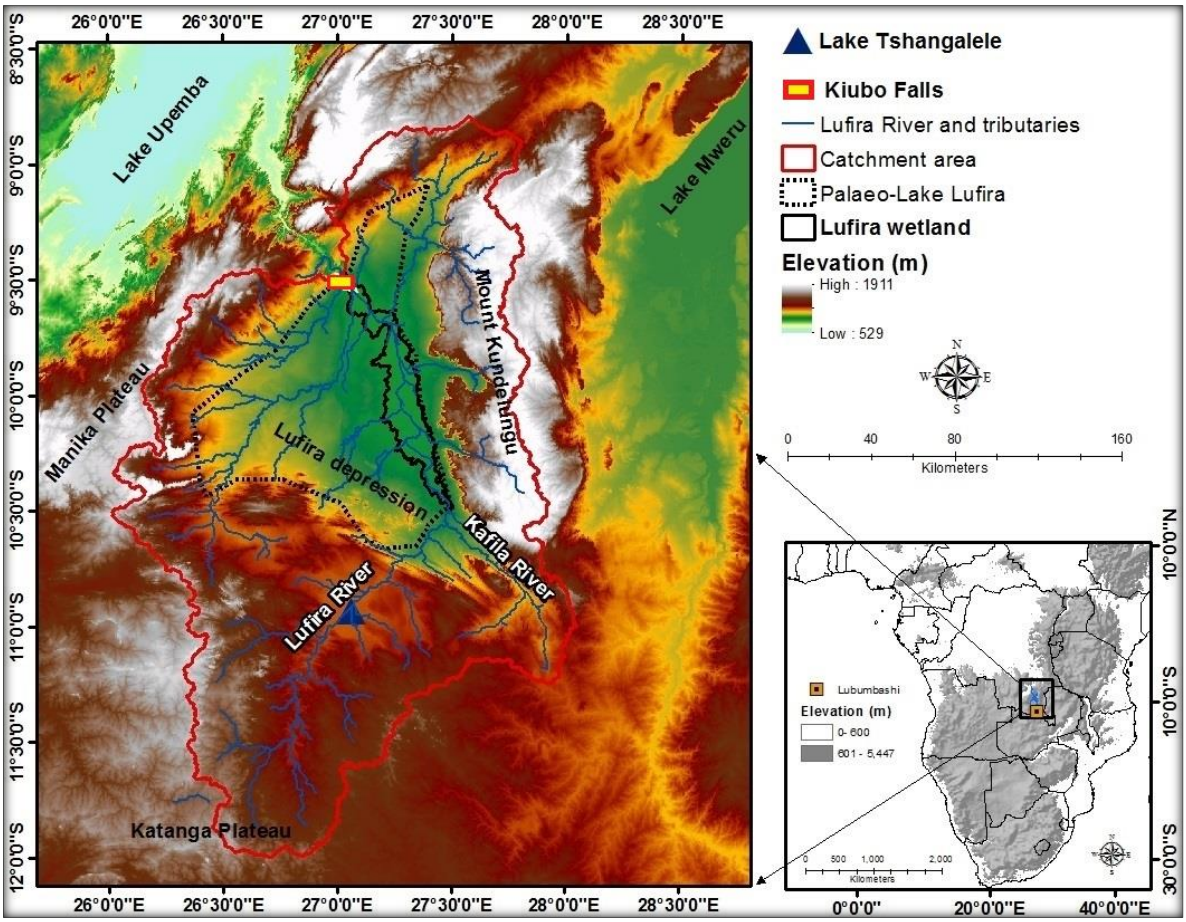

Figure 6.2.1: The location of the Lufira wetland in relation to the topographic settings of the wetland catchment and major rivers.

6.2.1 Hydrological conditions of Lufira wetland

The wetland and catchment boundaries show that the 1 286 km^2 wetland occupies 2.8% of its 45 688 km^2 catchment. The topographic characteristics of the Lufira wetland's catchment area (Figure 6.2.2) shows that the valleys upstream (cross-sectional profile g) and downstream (cross-sectional profile b) of the wetland are v-shaped and do not support any wetland habitats. However, between these two confined valley cross-sections the valley is broad and supports the wetland (cross-sectional profiles c to f). The channel is generally elevated above the wetland area (cross-sectional profiles c to f).

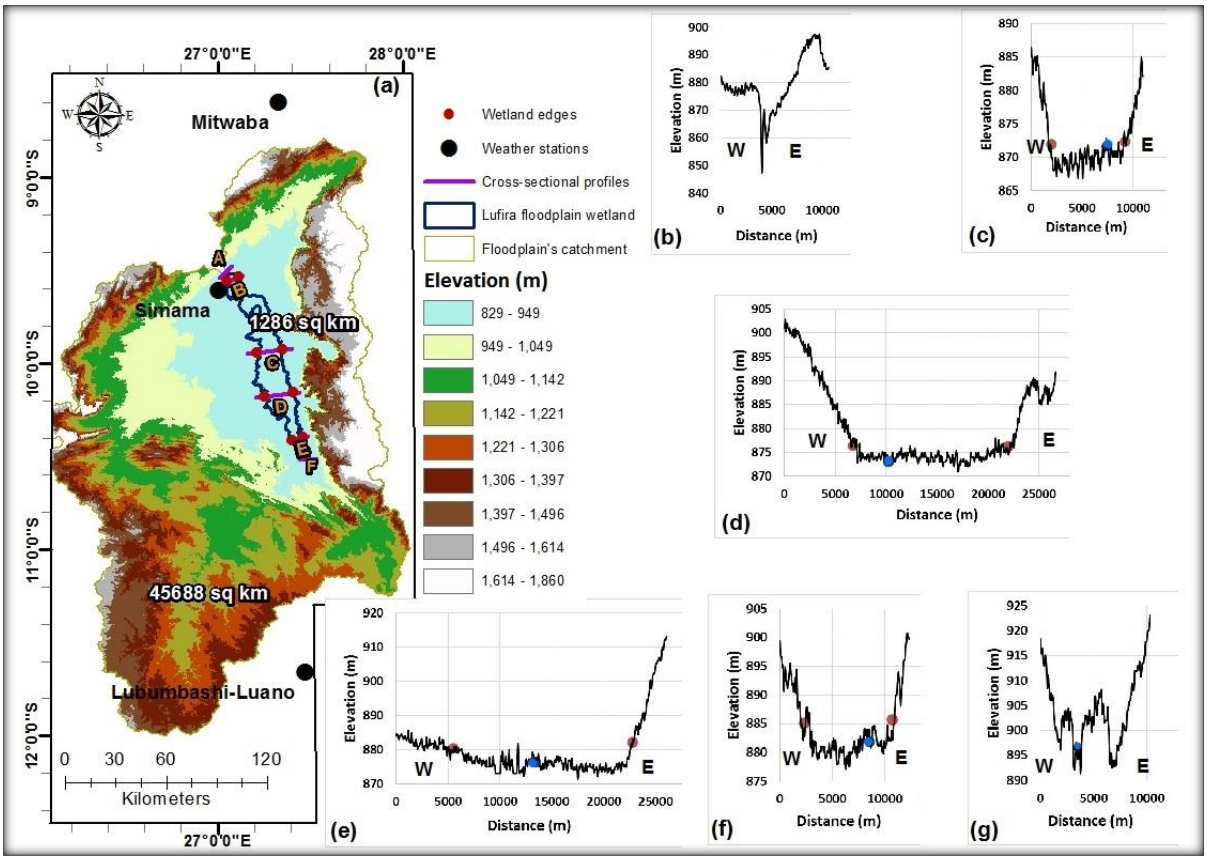

Figure 6.2.2: The topographic characteristics of the Lufira valley and catchment area, and the location of weather stations (a). Cross-sectional profiles at locations A-F in the map are shown in (b) to (g). The blue markers on the graphs indicate the position of the trunk stream. W and E in the graphs indicate their West to East orientation.

From the analysis of climatic data from three local weather stations, it appears that annual evapotranspiration rates within the catchment greatly exceed precipitation rates for at least 7 months of the year (Figure 6.2.3). The climatic parameters observed from Mitwaba weather station show that rainfall starts in September, intensifies around November and December, peaks in March, subsides in April and decreases further in May. These climatic parameters correlate with those of Simama and Lubumbashi-Luano weather stations. Therefore, within the catchment, rainfall can be characterised as generally commencing around October, peaking from December to February, and subsiding from March.

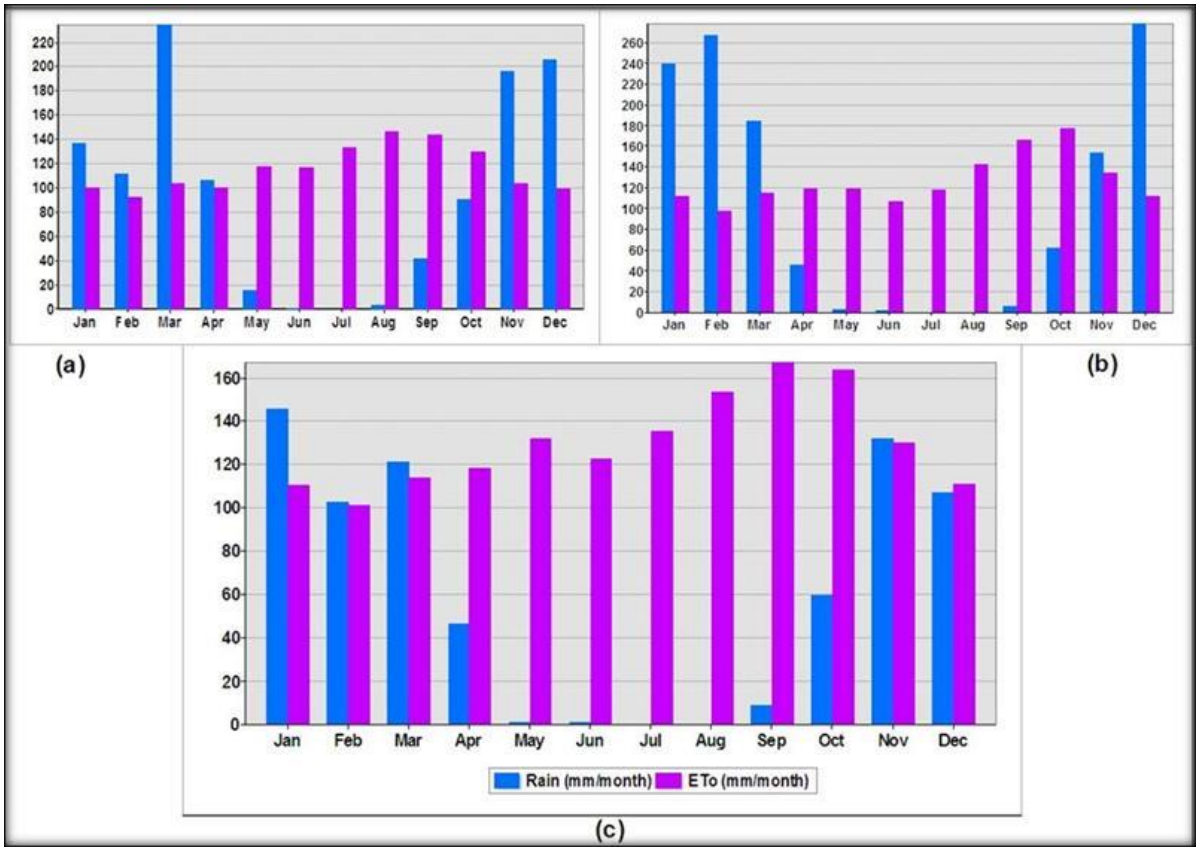

Figure 6.2.3: Monthly average rainfall and potential evapotranspiration for Mitwaba (a), Simama (b), and Lubumbashi-Luano (c) weather stations within the Lufira wetland catchment and in close proximity to the wetland.

Visual interpretations of the LandsatLook images in Figure 6.2.4 show that the wetland is dry in November while inundation peaks around April (Figure 6.2.4a and b respectively). However, the comparison of November (Figure 6.2.4c) and April (Figure 6.2.4d) images revealed that flooding of some depressions within the floodplain occur around November (Figure 6.2.4c) and these areas are driest in April (Figure 6.2.4d). This suggests that precipitation and run-off from the adjacent uplands play a crucial role in inundating some areas of the floodplain.

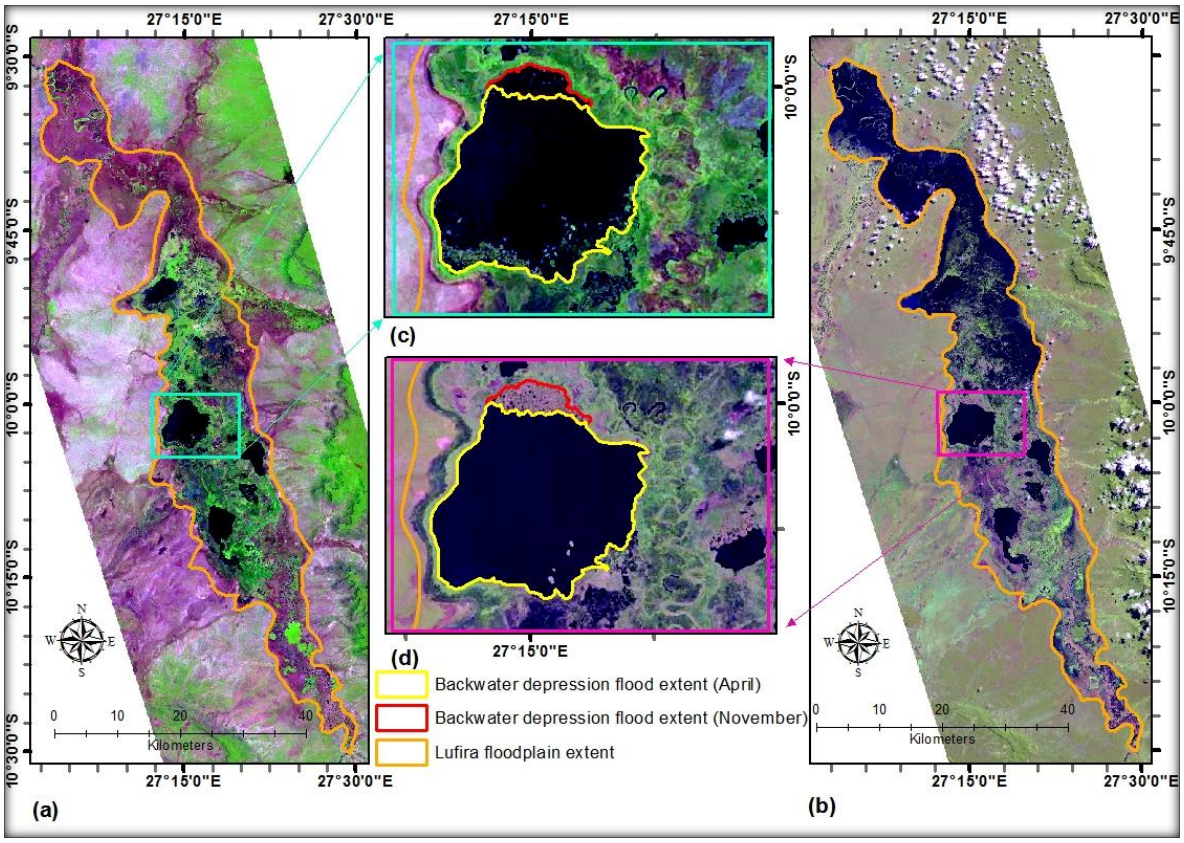

Figure 6.2.4: LandsatLook images depicting the saturation condition of Lufira wetland on 05 November 2014 (a), 17 April 2014 (b). The wetness of one of the wetland's depressions is shown on 05 November 2014 (c) and 17 April 2014 (d).

6.2.2 Geomorphology of the Lufira wetland

The assessment of the LandsatLook image showing the toe of the Lufira wetland shows that the toe of the wetland coincides with Kiubo Falls (Figure 6.2.5a). The channel is sinuous and appears to have a meandering planform within the wetland area upstream of the waterfall and appears to straighten below the toe of the wetland. The cross-sectional profiles in Figure 6.2.5b to f show that valley width increases systematically upstream of the Kiubo Falls.

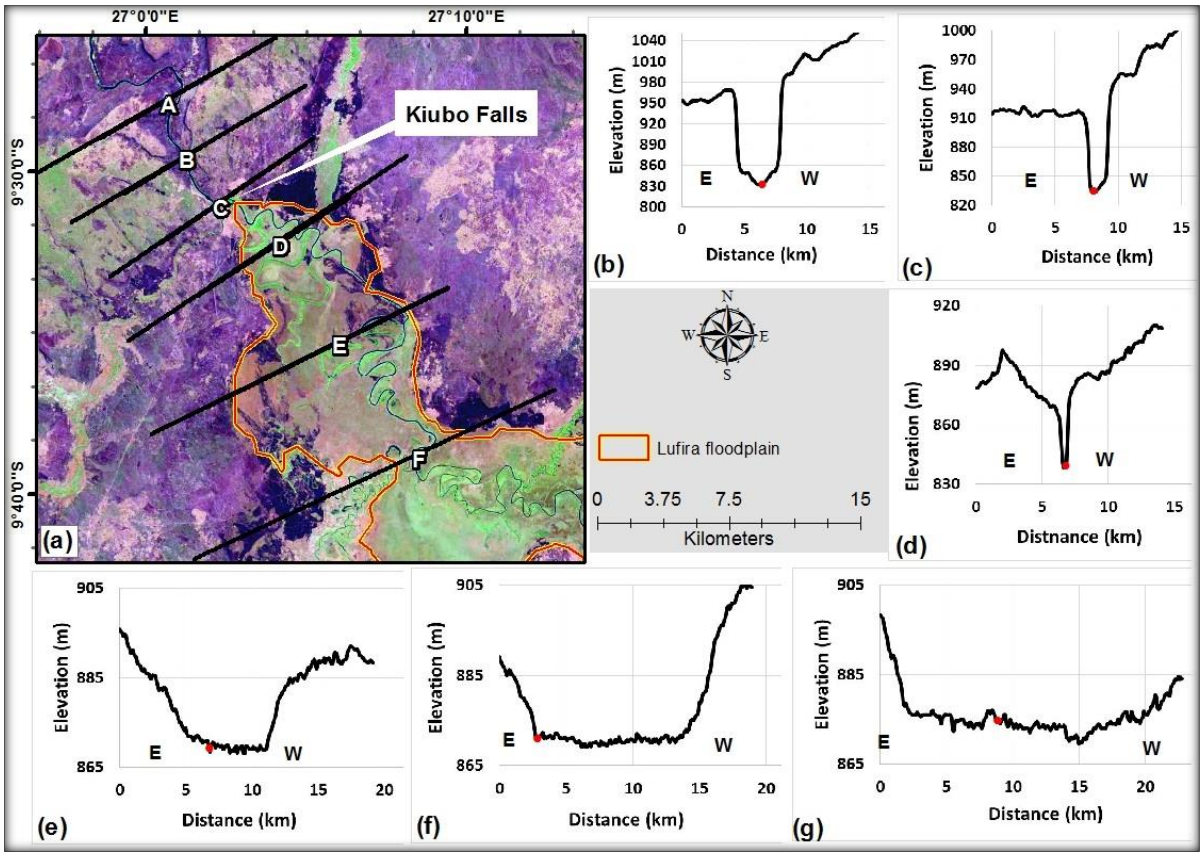

Figure 6.2.5: November 2014 LandsatLook image showing an increase in channel sinuosity upstream of the Kiubo Falls (a). Figures (b)-(g) represent the cross-sectional profiles of lines A-F on the map respectively. The red markers on the graphs show the position of the main stream.

The river is characterised by two major topographic steps (Figure 6.2.6a). One is located downstream of Lake Tshangalele and the other at Kiubo Falls. The overlay of points depicting locations of the toe and head of the wetland over the longitudinal profile shows that the toe of the wetland is located at the Kiubo Falls. The Google Earth image at the Kiubo Falls shows an exposed lithology as seen in Figure 6.2.6b, which suggests that the 35 m high Kiubo Falls (Figure 6.2.6c) is co-incident with a lithology that is resistant to channel incision. From Figure 6.2.6a it appears that a 233 m high topographic step separates the wetland from the surface upstream, which likely coincides with the elevation difference between the Post Africa I and the African Erosion Surfaces respectively.

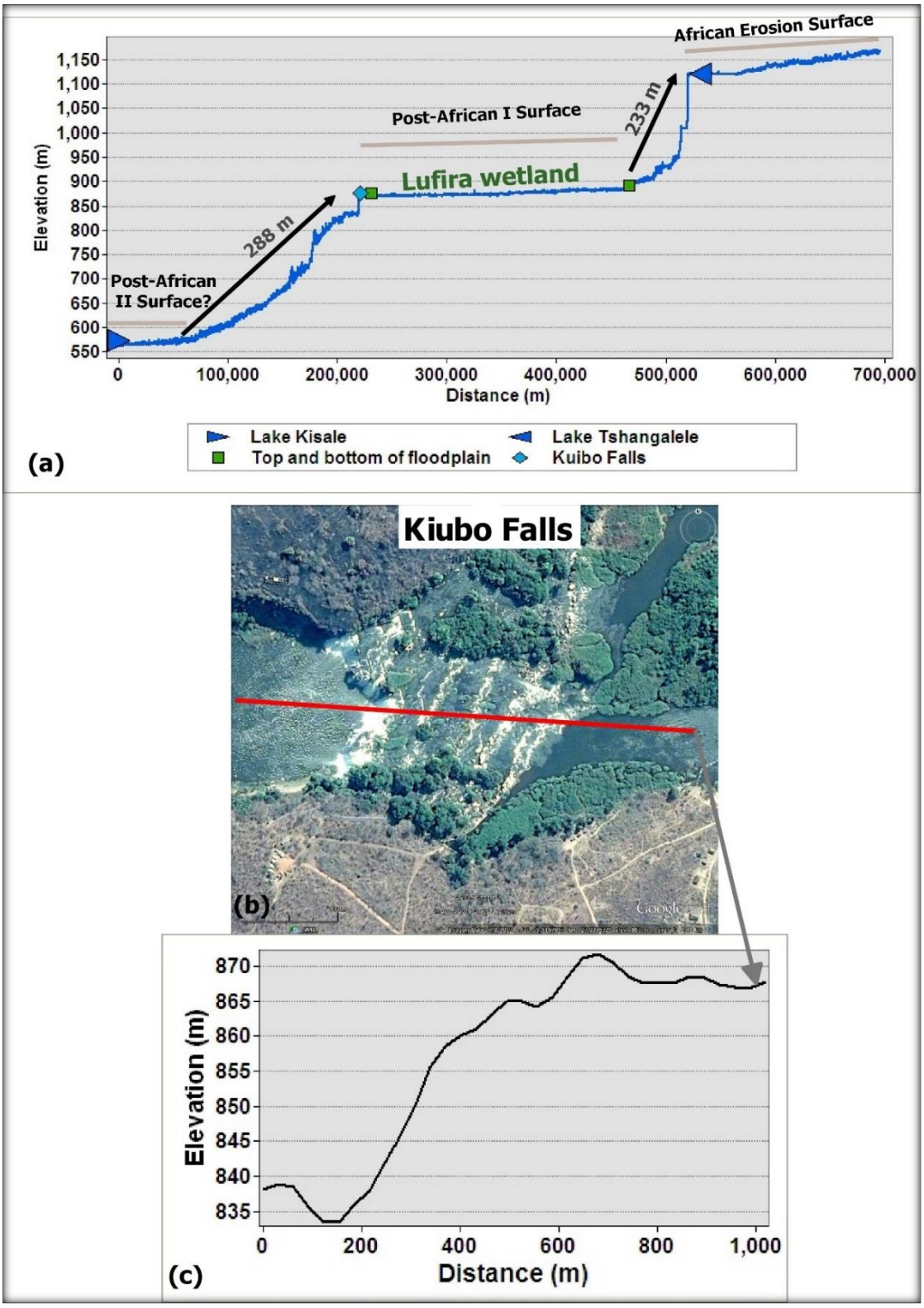

Figure 6.2.6: The longitudinal profile of Lufira River including the Lufira wetland, lakes and a water fall within the longitudinal profile, as well as the different erosional surfaces across which the river flows (a), a Google Earth image showing the exposed bedrock at the Kiubo Falls (b), and the longitudinal profile of the Kiubo Falls (c) along the red line indicated in (b).

The overlay of the wetland boundary over a Geological Map of the Southern African Development Community (Figure 6.2.7a) shows that the Lufira River drains a catchment that is mainly characterised by rocks such the Kundelungu Group (P_3Kku) and Monwezi Subgroup (P_3Kkl), before entering the Lufira wetland. The Kundelungu Group sediments comprise a combination of metamorphic rocks (quartz schist) and consolidated sedimentary rocks such as feldspathic sandstone, while the Monwezi Subgroup is a combination of consolidated sedimentary rocks such as shale and carbonate. The geology of the Lufira Depression is characterised by Kalahari Group sediments (Nvu) of unconsolidated alluvium and colluvium, while that of the wetland area is Quaternary sediment (Qa) associated with floodplain deposits, including alluvium and calcrete. The area around and below the Kiubo Falls is Kundelungu Group sediments (Figure 6.2.7b), which are resistant to weathering and erosion as the strata are lithified quartzitic metamorphic rocks.

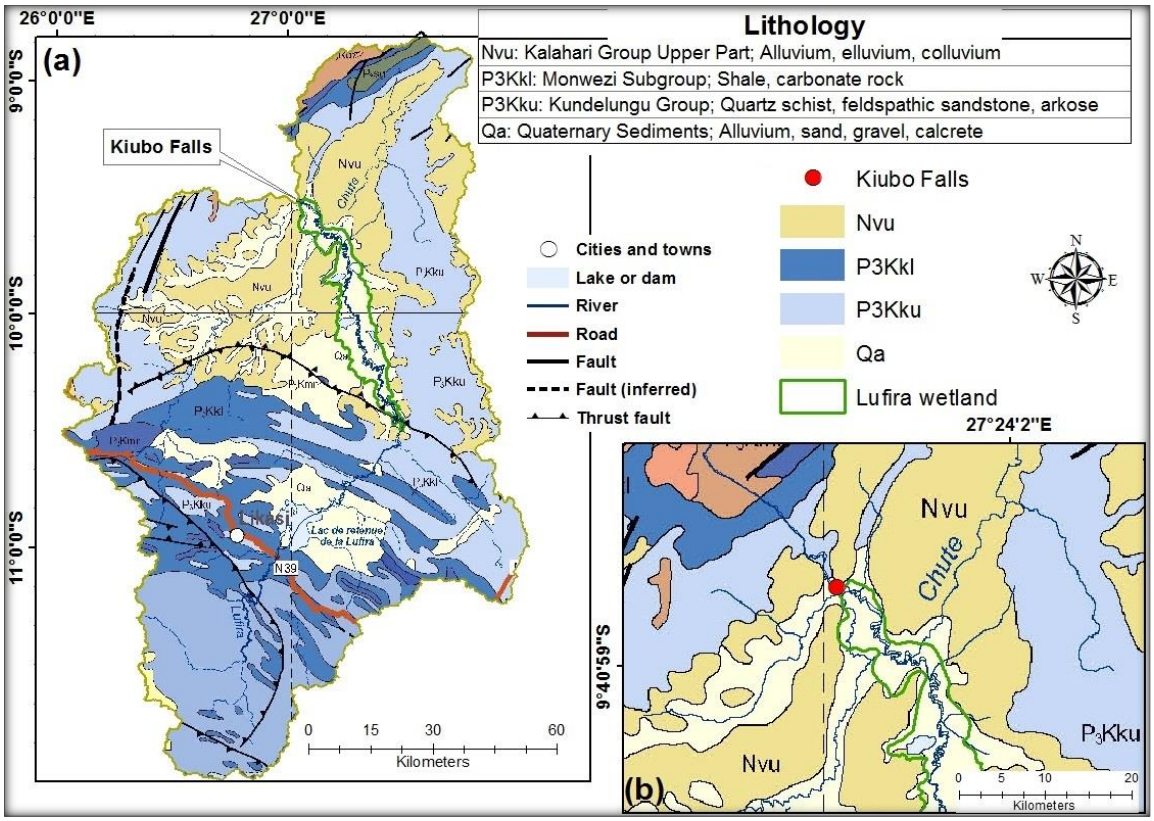

Figure 6.2.7: The geology of Lufira Depression (a) and the areas below the toe of the wetland (b).

6.2.3 Lufira wetland's structure and hydrological functioning

Visual interpretation of the August 2014 LandsatLook image and the analysis of wetland cross-sectional profile (Figure 6.2.8a and b) show that the channel is elevated above the surrounding wetland area. The wetland is characterised by floodplain features such as an alluvial ridge and backwater depressions. The alluvial ridge appears to be raised at an

elevation of about 3 m above the water level in the surrounding backwater depressions, which means that during flood events water is likely to overtop the banks and inundate the floodplain surface. However, the return flow of water from the floodplain back into the stream is likely to be limited.

The analysis of the Lufira River's channel characteristics within the wetland shows that the river length (307 km) is more than twice the wetland length (124 km) (Figure 6.2.9a), with a sinuosity ratio of 2.47. The river drops 16 m in elevation from 886 m to 870 m from the head to the toe of the wetland, translating to a longitudinal slope of 0.005% (Figure 6.2.9b). There appears to be a systematic decline in the longitudinal slope of the stream along its course within the wetland.

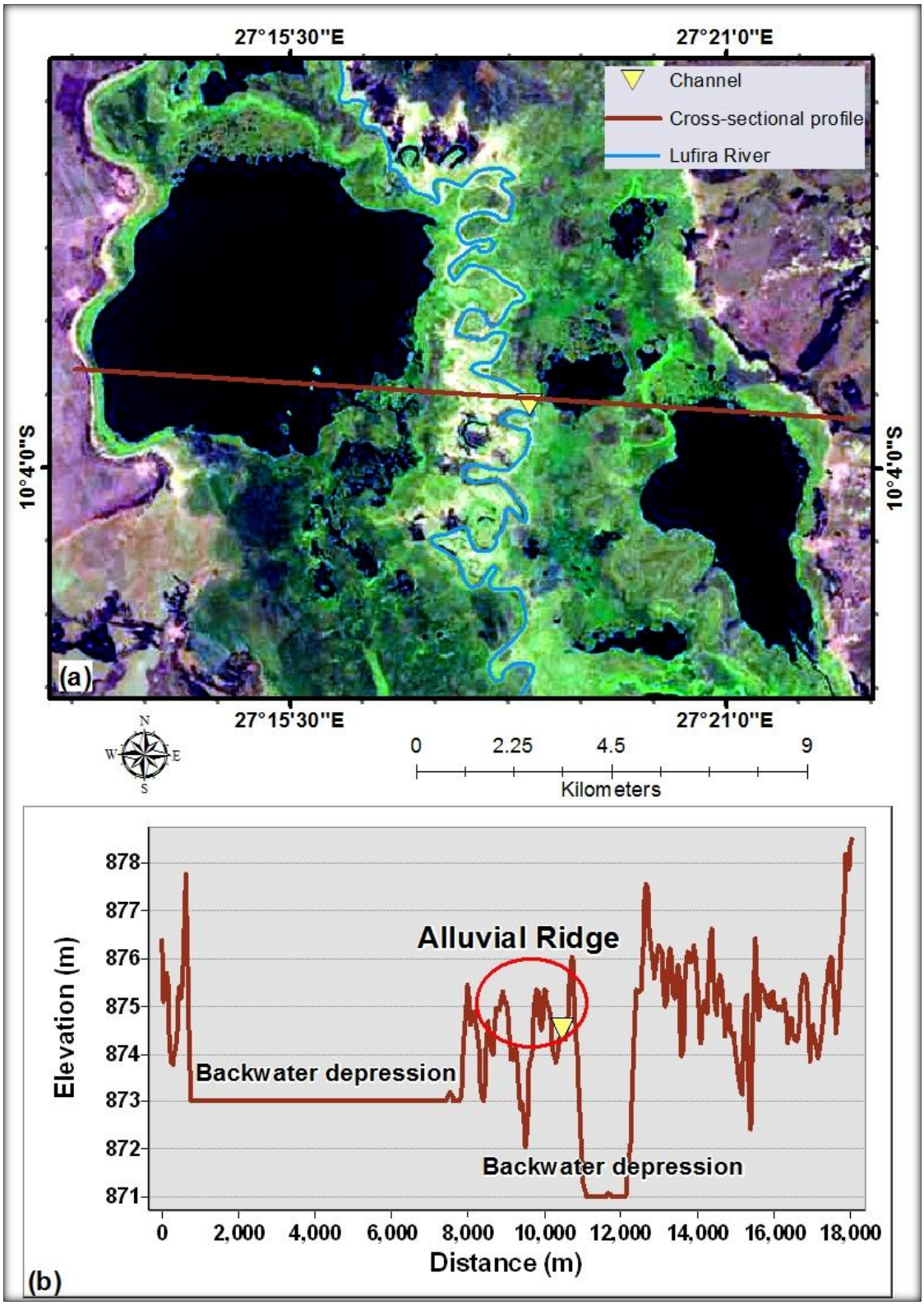

Figure 6.2.8: Floodplain features within the Lufira wetland, with (a) showing the plan view of a selected section in the middle reaches of the wetland and (b) showing the cross-section along the red line in (a). The image in (a) is a November 2014 LandsatLook image.

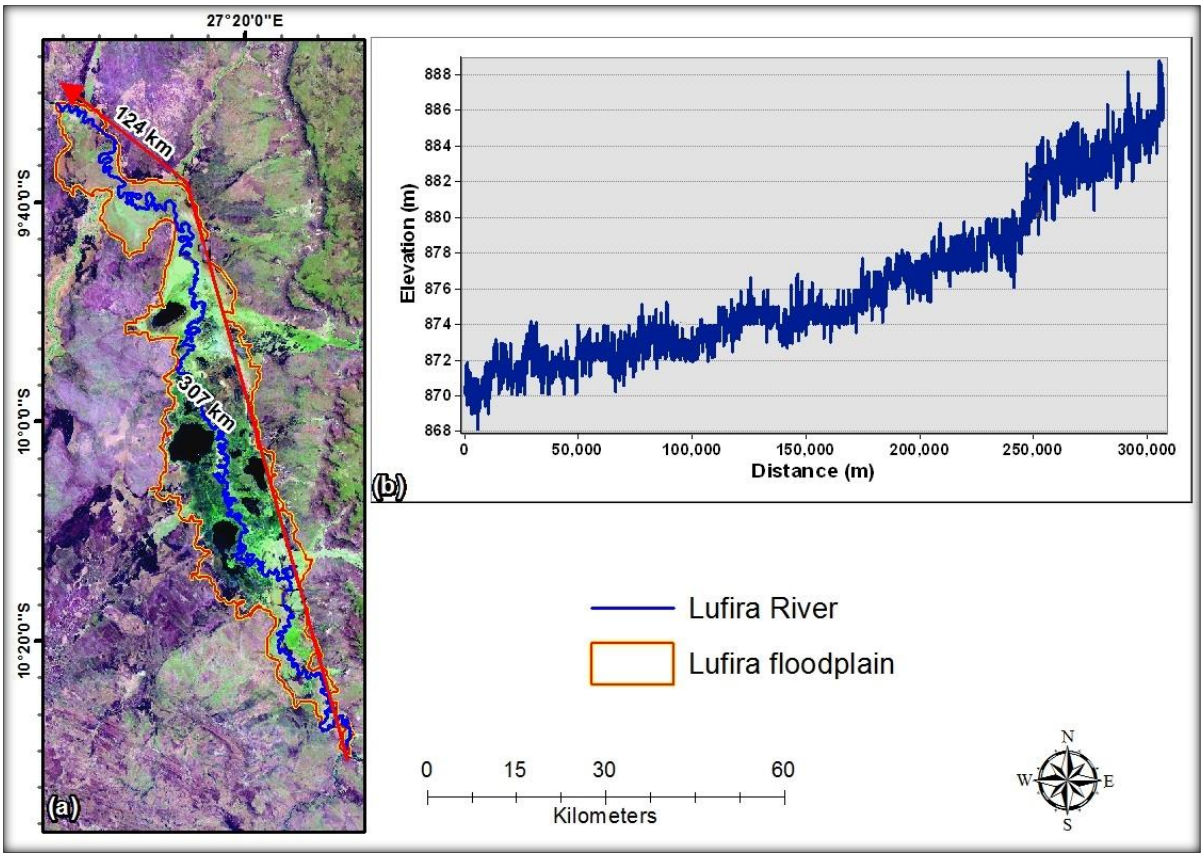

Figure 6.2.9: Characteristics of the Lufira wetland including the total length of the wetland (red line), the total length of the river within the wetland (blue line; (a)) and the longitudinal slope of the river within the wetland area (b). The main image is the November 2014 LandsatLook image.

A comparison of the average depth of flooding of the wetland for a given stage height in the channel between distinct reaches of the Lufira wetland shows that there is a high average depth of inundation for all reaches when the channel stage height is greater than zero. The upper reach has a higher average depth of inundation, followed by the middle reach, with the lower reach having the lowest average depth of inundation for a given stage height (Figure 6.2.10).

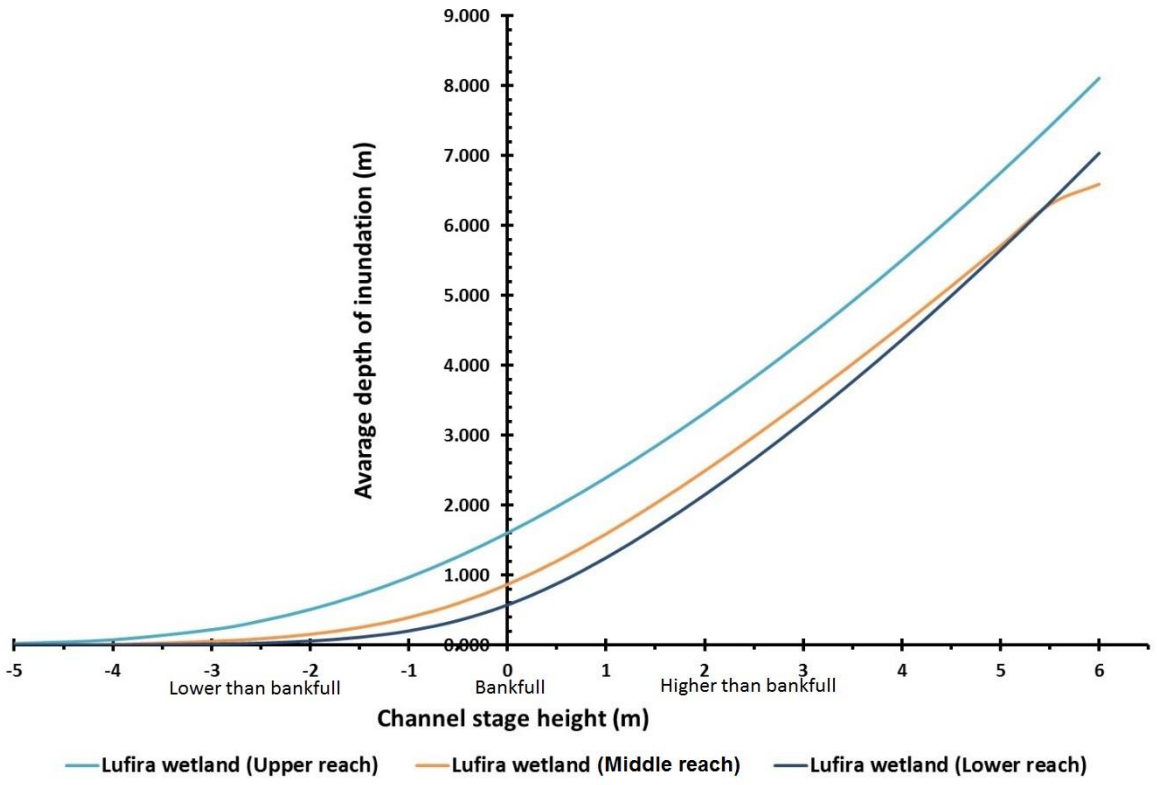

Figure 6.2.10: Comparison of the average depth of inundation within three distinct reaches of the wetland. The "0" depth represents channel water level while the positive and negative depths represent channel inundation height above and below channel water level respectively.

6.3 Barotse wetland

The Barotse wetland is situated in western Zambia between latitudes 16°39'S and 14°16'S and longitudes 23°08'E and 23°34'E, near the town of Mongu (Figure 6.3.1). The north-south trending wetland stretches from the Zambezi's confluence with Lungwebungu and Kabompo Rivers in the north to the Ngonye Falls in the south. The wetland is connected with a number of streams that drain the catchment. To the north is the Zambezi River that flows within the wetland and to the west and east are perennial tributaries of the Zambezi River. However, the wetland lies within the upper reaches of the Zambezi River. The Zambezi River originates from the north of the Barotse wetland in Angola and flows southwards. The river enters the Barotse wetland at an elevation of about 1 034 m amsl and leaves the wetland at the Ngonye Falls at an elevation of about 969 m amsl.

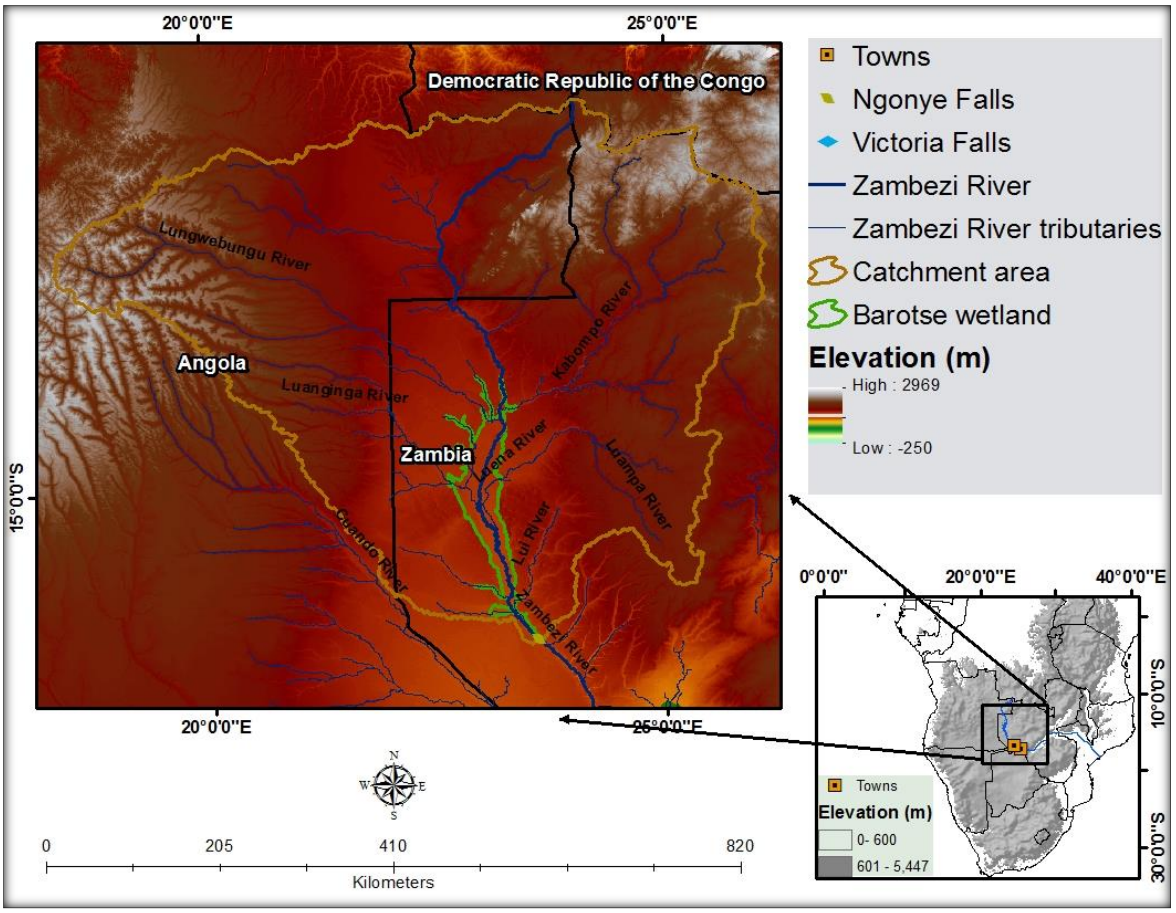

Figure 6.3.1: The location of Barotse wetland in western Zambia, the topographic settings of the wetland catchment, and major rivers.

6.3.1 Hydrological conditions of Barotse wetland

The analysis of the Barotse wetland's catchment characteristics shows that the 8 368 km^2 wetland covers only 2.62% of its 318 888 km^2 catchment (Figure 6.3.2a). The cross-sectional profiles illustrate that the river appears to be the lowest elevated feature within the wetland (Figure 6.3.2d to f). In addition, the wetland occurs within a broad valley (Figure 6.3.2d to f) while upstream (Figure 6.3.2c) and downstream (Figure 6.3.2g) of the wetland the valleys are confined and do not support wetlands.

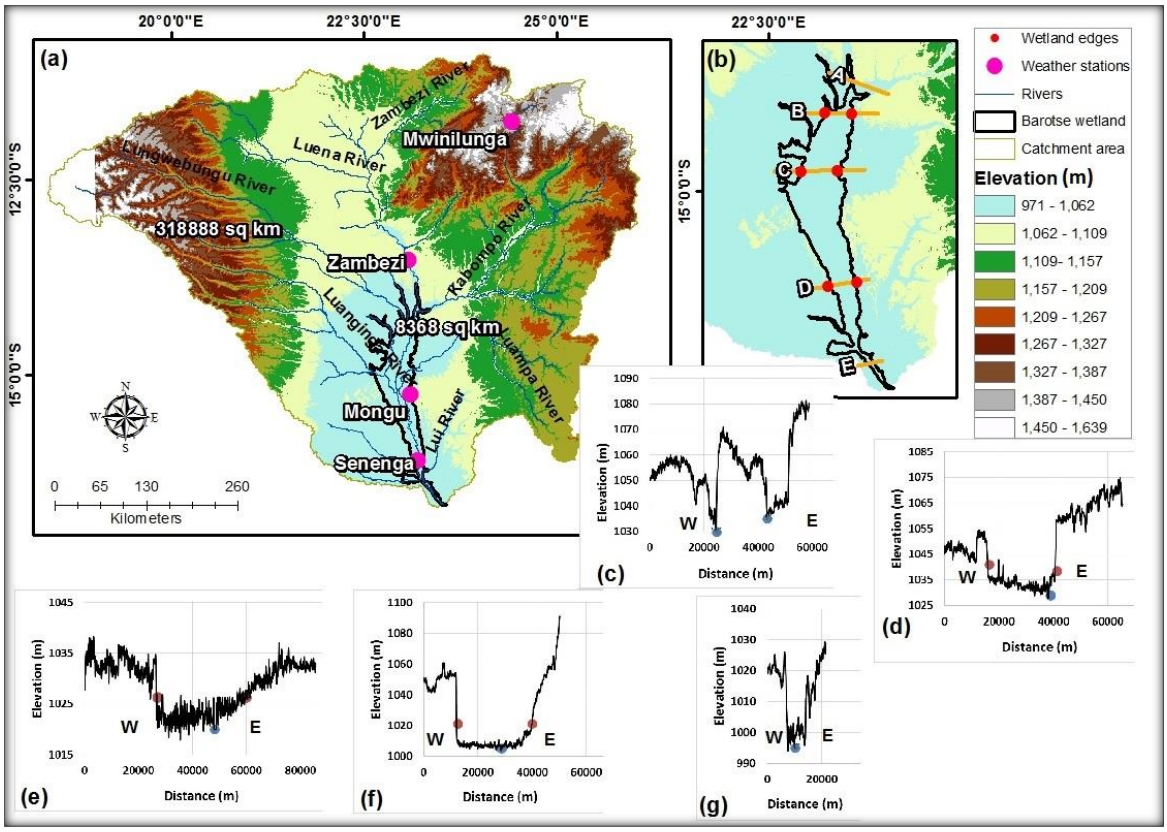

Figure 6.3.2: The topographic characteristics of the Barotse wetland valley, its catchment area, and the location of weather stations (a). Graphs (c)-(g) show cross-sectional profiles at location A-E respectively shown in (b). W and E in the graphs indicate the West to East orientation of graphs and the blue markers indicate channel location.

The analysis of climatic data for the four weather stations shows that annual potential evapotranspiration greatly exceeds precipitation for 7 to 9 months of the year (Figure 6.3.3), suggesting a negative surface water balance within the catchment. The climatic data show that rainfall within the area starts in September and October, peaks in December to February, and ends in April and May.

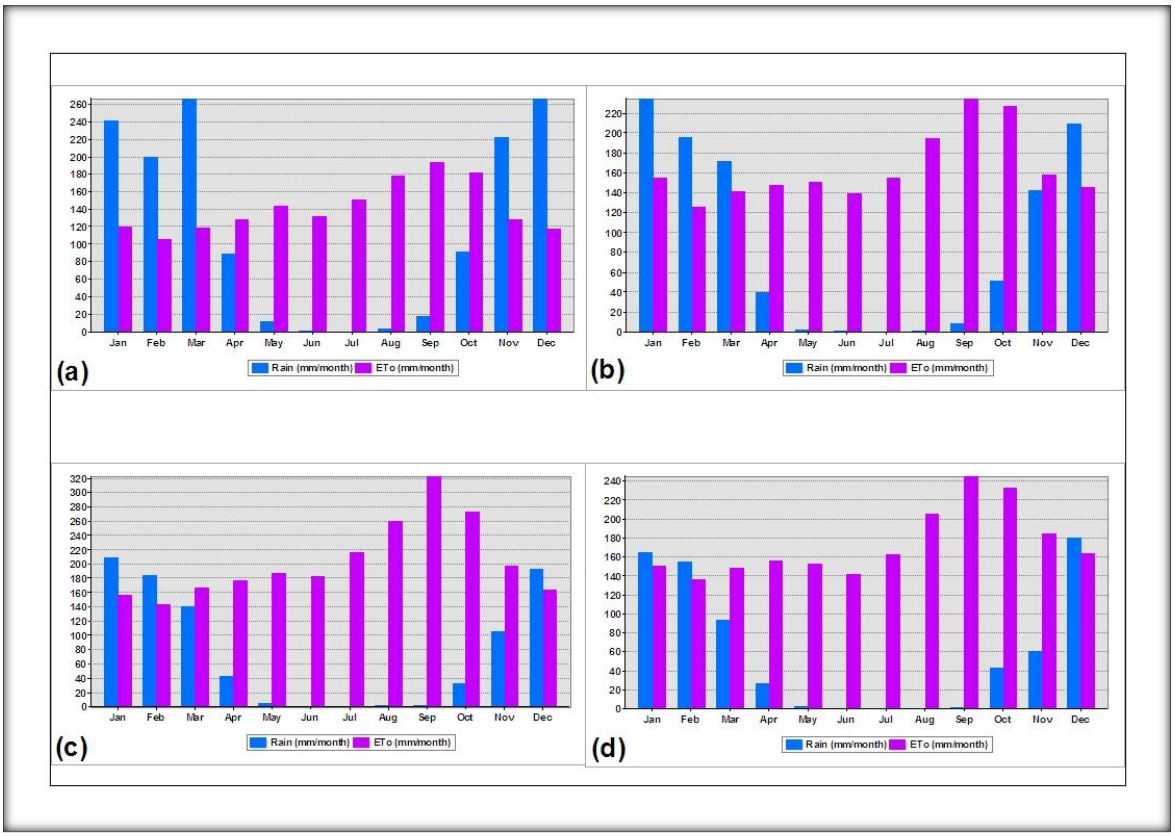

Figure 6.3.3: The monthly rainfall and potential evapotranspiration rates for Mwinilunga (a), Zambezi (b), Mongu (c), and Senenga (d) weather stations within the Barotse wetland catchment.

The analysis of the flooding characteristics of the Barotse wetland shows that the wetland is dry around October at the beginning of the rainy season (Figure 6.3.4a) and wet towards the waning stages of the rainy season in April (Figure 6.3.4b). However, some areas within the wetland do not appear to be inundated (Figure 6.3.4b). These areas include the upper reaches of the wetland just above the Zambezi River's confluence with the Luanginga and the Luena Rivers, as well as the lower reaches of the wetland just below the confluence between the Zambezi River and the Lui River, and just above the Ngonye Falls. Flooding can also be observed within the tributary streams down the length of the wetland (Figure 6.3.4b).

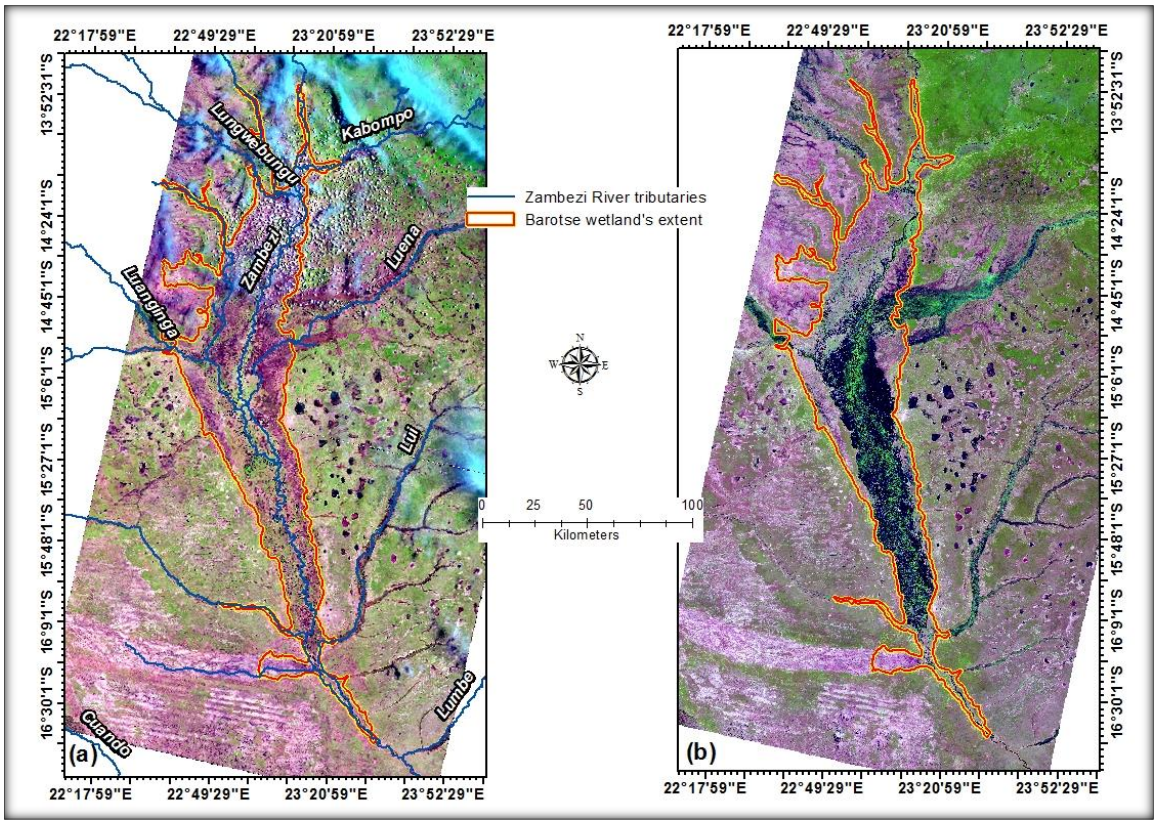

Figure 6.3.4: LandsatLook images depicting the saturation condition of Barotse wetland on 18 October 2014 (a), and showing the wetlands saturation conditions on 28 April 2015 (b).

6.3.2 Geomorphology of Barotse wetland

From the analysis of the Zambezi River's longitudinal profile, it appears that the Zambezi River is characterised by a number of topographic steps (Figure 6.3.5a). The most apparent natural topographic step coincides with the Victoria Falls. The Barotse wetland occurs upstream of the Upper Zambezi wetland. Given the scale of the Zambezi River's longitudinal profile (i.e. showing the entire river), the topographic step at the toe of the Barotse wetland cannot be clearly identified. However, the overlay of points depicting locations of Ngonye Falls and the bottom and top of the wetland over the longitudinal profile (Figure 6.3.5a) and the visual analysis of Google Earth images (Figure 6.3.5b and c) show that the toe of the Barotse wetland coincides with the Ngonye Falls. The images suggest that the Ngonye Falls coincides with a resistant lithology.

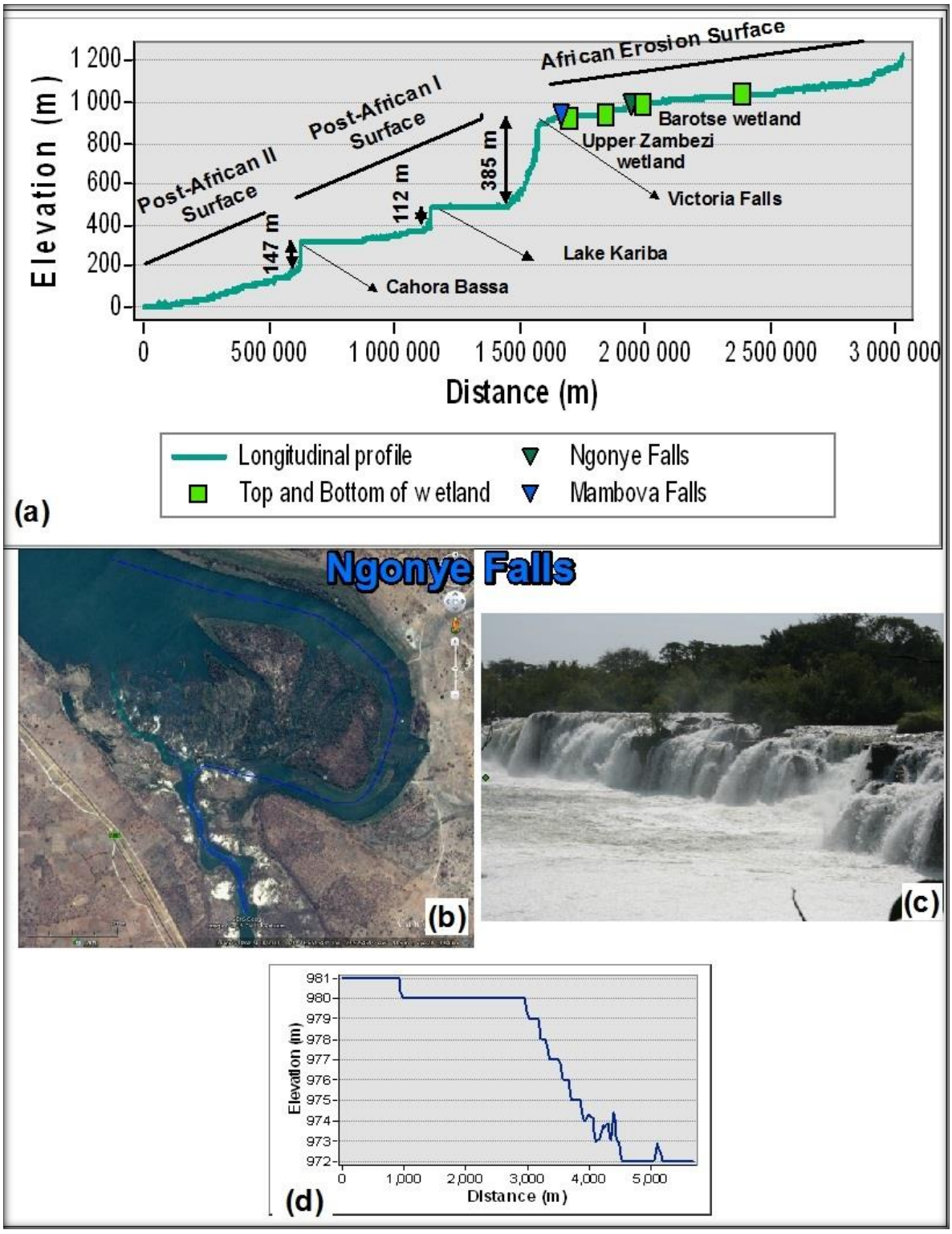

Figure 6.3.5: The longitudinal profile of the Zambezi River showing the locations of the Barotse wetland, waterfalls, lakes, topographic steps and the likely erosional surfaces drained by the Zambezi River (a) as well as an aerial (b) and a pictorial (c) view of the Ngonye Falls (Source: Google Earth with image data from DigitalGlobe and CNES/Airbus). Graph (d) show the longitudinal profiles of the Zambezi River channels (i.e. the blue line) at the Ngonye Falls as seen in (b).

The valley widths within the lower reaches of the Barotse wetland and areas just below the toe of the wetland (Figure 6.3.6a) show that there is a decrease in valley width from the lower reaches of the wetland to areas below the toe of the wetland (Figure 6.3.6c to h).

The geology of the catchment upstream of the wetland is mainly Kalahari Group material (Nk) of a combination of unconsolidated aeolian sand and consolidated sedimentary rocks such as sandstone and limestone, and Quaternary sediments (Qa) of unconsolidated sedimentary material such as alluvium, sand and gravel (Figure 6.3.7a). The toe of the Barotse wetland coincides with a change in the geology from Quaternary sediments (Qa) to the Kalahari Group (Nk; Figure 6.3.7b). Although the Kalahari Group may be more resistant to channel incision than the Quaternary sediments, both the Quaternary sediments and the Kalahari Group are prone to channel incision. Therefore, Kalahari Group is unlikely to support the topographic step at the Ngonye Falls. However, it is likely that there is a resistant lithology at the Ngonye Falls.

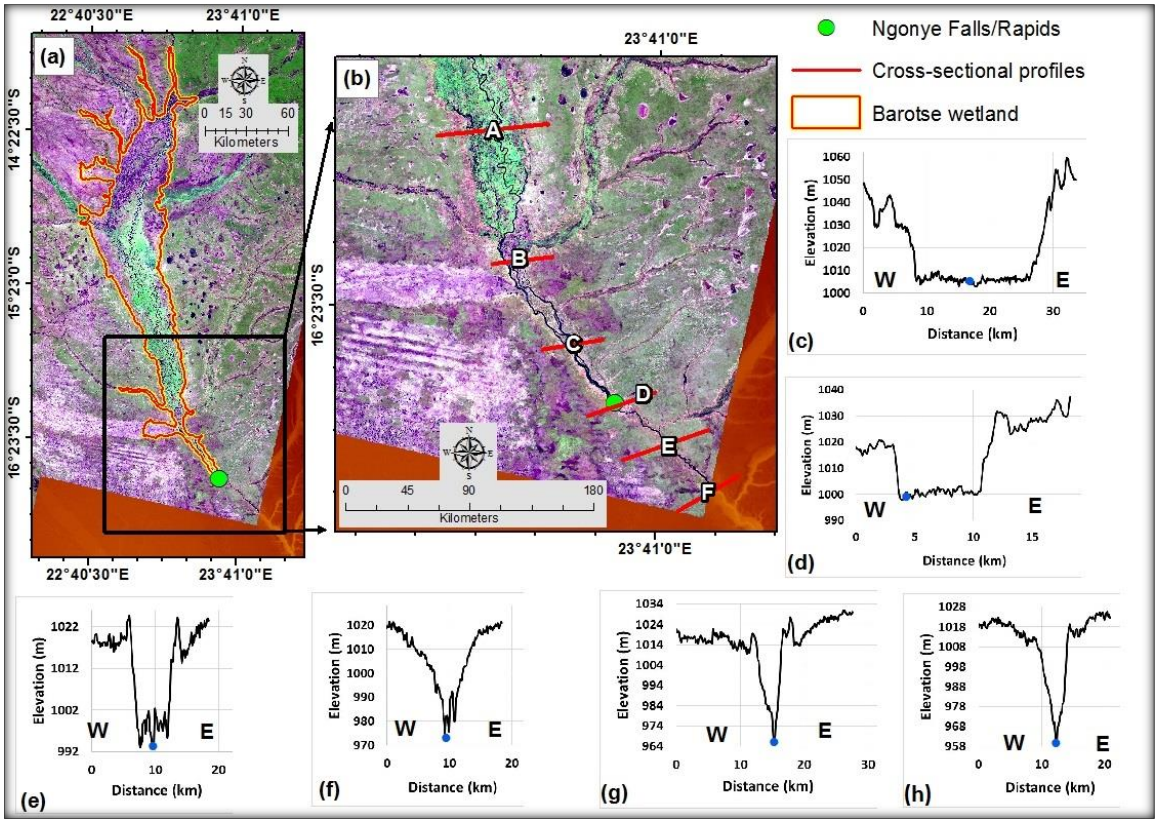

Figure 6.3.6: The valley characteristics within the lower reaches of the Barotse wetland (a) and in the vicinity of the toe of the wetland (b). Graphs (c)-(h) represent the cross-sectional profiles of lines A-G respectively shown in (b). LandsatLook imagery of 28 April 2015 was used as a basemap. The blue markers on the cross-sections show the location of the Zambezi channel.

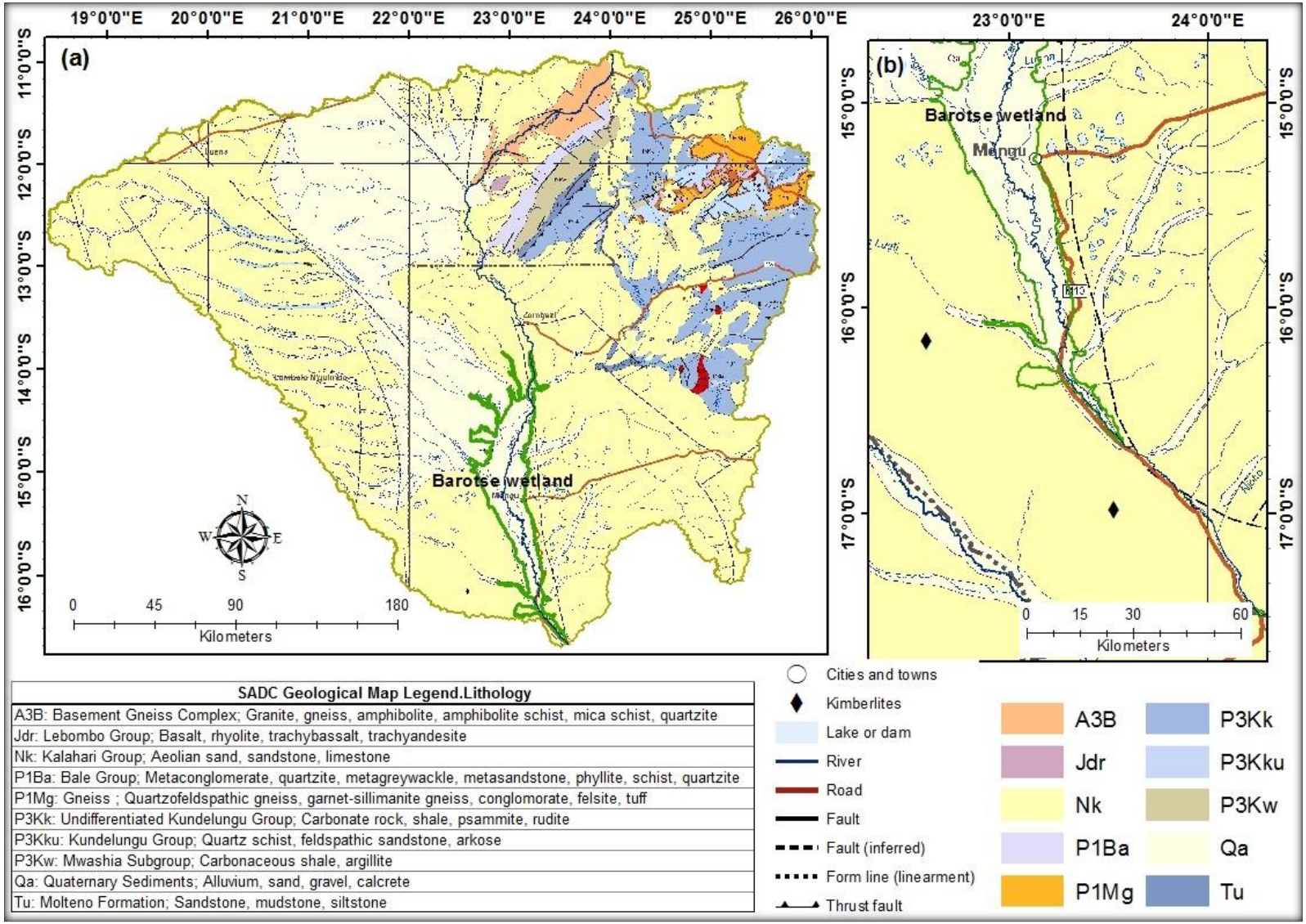

SADC Geological Map Legend.Lithology
A3B: Basement Gneiss Complex; Granite, gneiss, amphibolite, amphibolite schist, mica schist, quartzite
Jdr: Lebombo Group; Basalt, rhyolite, trachybassalt, trachyandesite
Nk: Kalahari Group; Aeolian sand, sandstone, limestone
P1Ba: Bale Group; Metaconglomerate, quartzite, metagreywackle, metasandstone, phyllite, schist, quartzite
P1Mg: Gneiss ; Quartzofeldspathic gneiss, garnet-sillimanite gneiss, conglomorate, felsite, tuff
P3Kk: Undifferentiated Kundelungu Group; Carbonate rock, shale, psammite, rudite
P3Kku: Kundelungu Group; Quartz schist, feldspathic sandstone, arkose
P3Kw: Mwashia Subgroup; Carbonaceous shale, argillite
Qa: Quaternary Sediments; Alluvium, sand, gravel, calcrete
Tu: Molteno Formation; Sandstone, mudstone, siltstone

Figure 6.3.7: The geology of the Barotse wetland, its catchment (a) and the area below the toe of the wetland (b).

6.3.3 The structure and hydrological functioning of the Barotse wetland

Visual analysis of the LandsatLook image shows that the Barotse wetland lacks floodplain features such as backwater depressions while the river appears to exhibit characteristics typical of a meandering stream (Figure 6.3.8a). The cross-sectional profiles show that the wetland is near-horizontal in cross-section (Figure 6.3.8a2 and b2) while the channel is at a similar or lower elevation than the surrounding wetland areas. The cross-sectional profiles of lines A and B show that the wetland is characterised by an elevated island to the west of the channel about 10 m above the channel water level (Figure 6.3.8a2) and elevated wetland areas towards the wetland edges elevated at about 5 m above the channel (Figure 6.3.8b2). This means that the Zambezi channel needs to be flooded to a depth of approximately 6 m in order to flood the rest of the wetland area.

The channel characteristics within the Barotse wetland shows that the 416 km long river flows within the 292 km wetland valley, translating to a sinuosity ratio of 1.4 (Figure 6.3.9a). The area upstream of the Ngonye Falls is characterised by islands that divide the channel into narrow channels, but the channel is not strikingly sinuous (Figure 6.3.9a1). However, parts of the wetland area are characterised by meander scars (Figure 6.3.9a2). From the channel length (Figure 6.3.9a) and the elevations from the longitudinal profile (Figure 6.3.9b) it appears that the wetland has a slope of 0.012%. The longitudinal profile also shows that the slope steepens towards the lower reaches of the wetland near the Ngonye Falls, which suggests that a resistant lithology could be preventing the river from lowering its bed in an upstream direction.

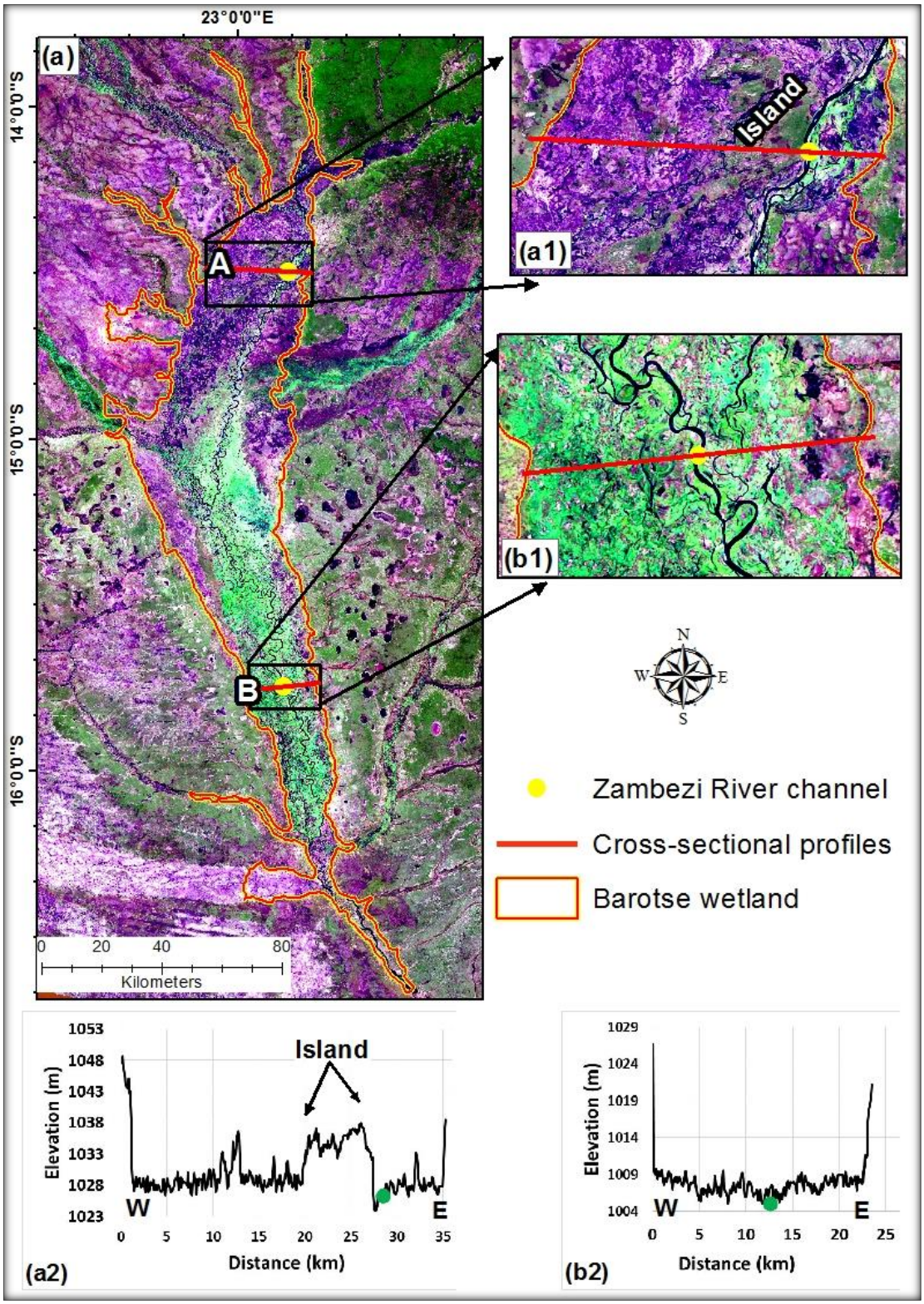

Figure 6.3.8: Floodplain features within the Barotse wetland. Detail of the upper (a1) and lower (b1) regions of the wetland are coincident with cross-sections A and B respectively. The cross-sectional graphs (a2) and (b2) shows the cross-sectional profiles of lines A and B respectively and the green markers indicate the location of the trunk channel. The image is a mosaic of 01 July 2015 LandsatLook images.

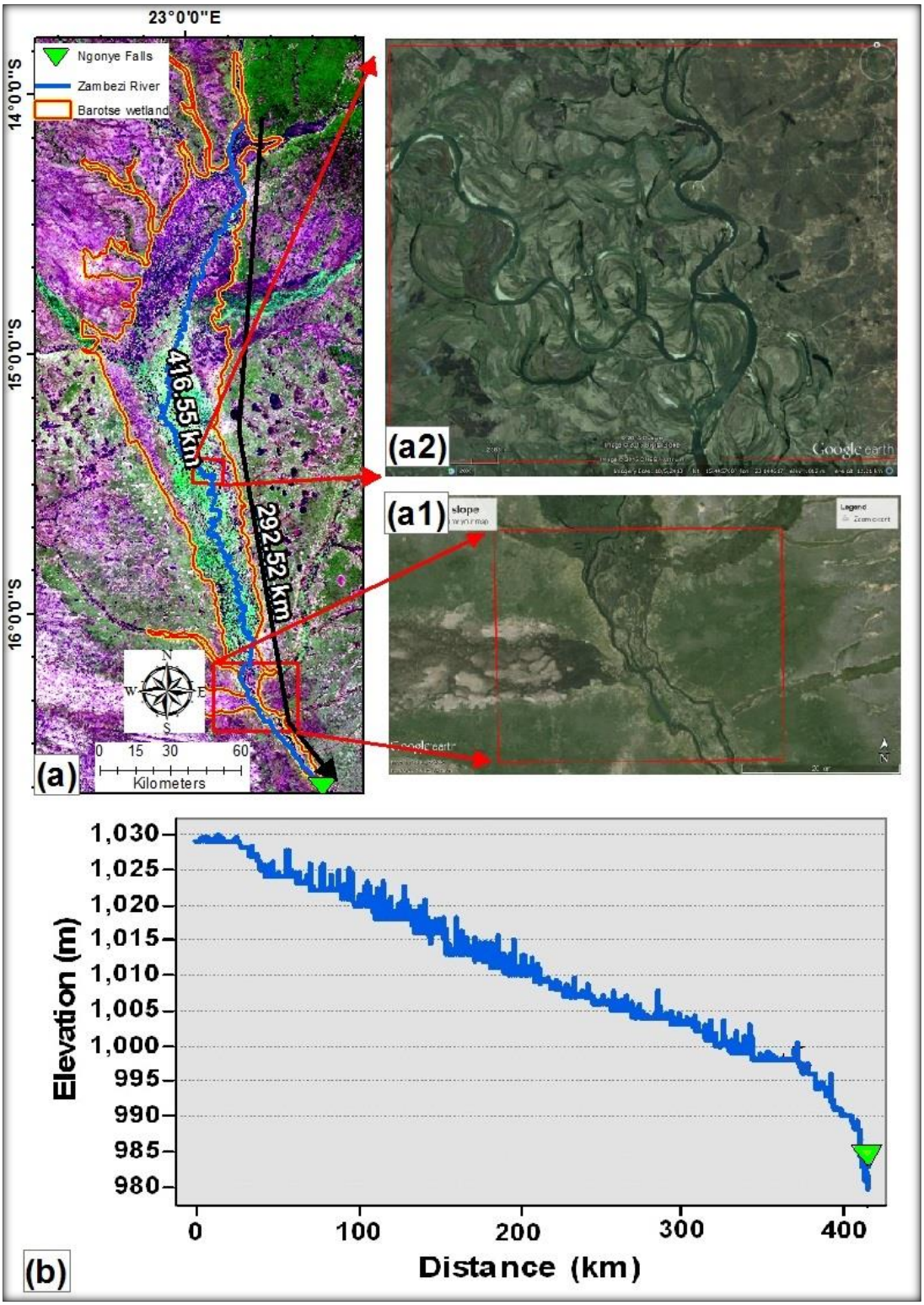

Figure 6.3.9: Characteristics of the Zambezi River within the Barotse wetland (a) and the longitudinal slope of the river within the wetland (b). The black line shows the total length of the wetland while the blue line shows the total length of the river within the wetland. The basemaps are a 01 July 2015 LandsatLook image (a) and Google Earth images with image data from DigitalGlobe and CNES/Airbus (a1) and (a2).

The analysis of the average depth of inundation shows that for both the upper and lower reaches of the wetland, the depth of inundation is much lower than the channel stage height (Figure 6.3.10). Although the lower reach shows higher average depth of inundation than the upper reach at stage heights greater than zero, both the upper and lower reaches show zero average depth of inundation below the zero channel stage height.

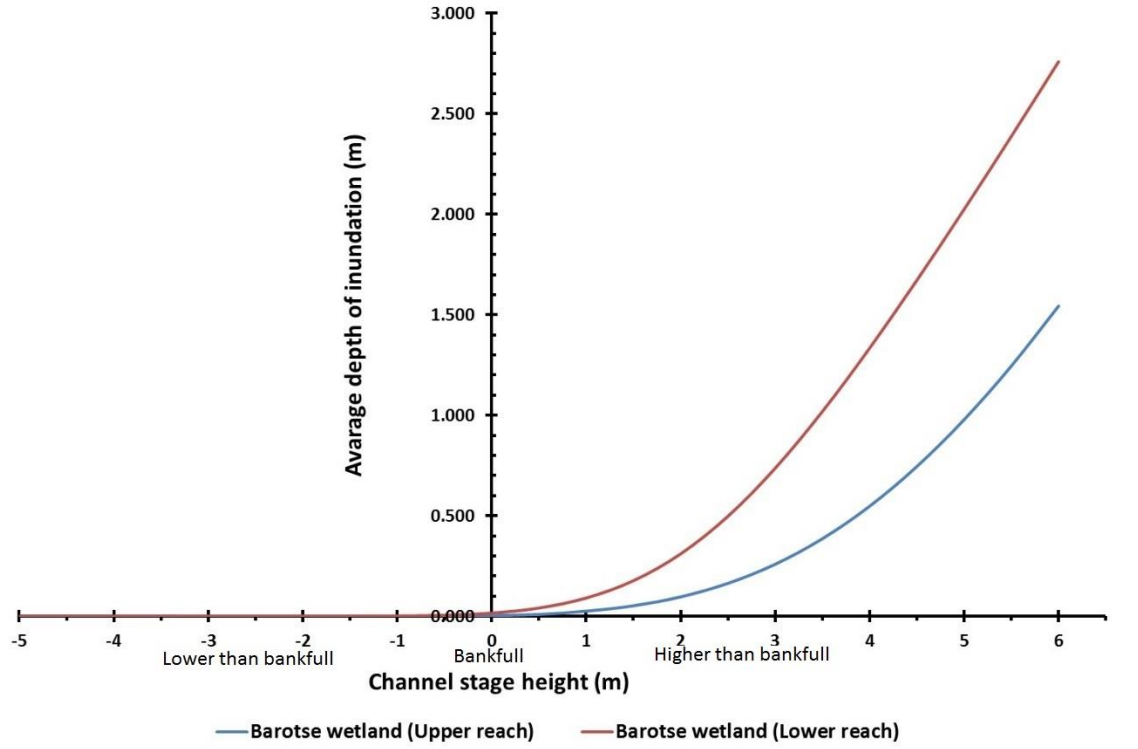

Figure 6.3.10: Comparison of the average depth of inundation within two distinct reaches of the Barotse wetland. The "0" depth represents channel water level at bankfull stage height while the positive and negative depths represent channel inundation height above and below bankfull water level respectively.

6.4 Discussion

Both the Lufira and Barotse wetlands occupy less than 3% of their catchment areas and are characterised by a negative surface water balance for over 7 months of the year. The two wetlands show a two months lag between peak wetland flooding and peak local rainfall. This suggests that water from the catchment is a factor influencing the hydrology of these wetlands.

Both the Lufira and Barotse wetlands are likely to be a lithologically controlled. The processes following the formation of these wetlands appear to be similar to processes described by Tooth et al. (2002) involving channel incision until its bed overlays a resistant lithology at the toe of the wetland. The resistant lithology acts as a base level and limits

incision in an upstream direction. The channel responds to the base level effect by increasing sinuosity upstream, widening the valley, ultimately lowering valley slope and creating conditions suitable for wetland formation (Tooth et al., 2002). With regard to the formation of the Lufira wetland, faulting within Lake Upemba (Cotterill, 2004) could have lowered the base level of the Lufira River and initiated headward erosion, leading to the capture and desiccation of Palaeo-Lake Lufira. Subsequently, the Lufira River could have incised into Palaeo-Lake Lufira until its channel bed overlay the metamorphic Kundelungu Group at the Kiubo Falls. The Kundelungu Group appears to have acted as a base level of the Lufira River upstream of the Kiubo Falls.

With regard to the Barotse wetland, the observed topographic step at the toe of the wetland and meandering scars within the wetland suggest that it is likely to be lithologically controlled. The lack of fault lines around the wetland suggests that the wetland is not tectonically controlled, and the coincidence of the toe of the wetland with the Ngonye Falls suggests that the wetland is lithologically controlled. According to Nugent (1990) and Moore et al. (2007), the base level of the Zambezi River was significantly lowered in association with the uplift events of the last 30 Ma, which initiated channel incision. Erosion lowered the bed of the upper Zambezi River to a point where, at the Ngonye Falls, the channel bed overlay Karoo basalt (Wellington, 1949; Shaw 1988; Thomas et al., 2000). Subsequently there must have been longitudinal slope reduction and valley widening as described by the Tooth et al.'s (2002) lithological control model. This is supported by the observed meander scars and increased valley width upstream of the Ngonye Falls, and the extensive catchment that is underlain by easily weathered and eroded rocks.

The catchment of the Lufira wetland is mainly dominated by consolidated metamorphic and sedimentary rocks such that weathering produces sediment that includes a large proportion of fine material. Deposition of sediment during floods therefore leads to aggradation of the channel margin and the formation of an active meandering channel. Channel migration is associated with the formation of an alluvial ridge such that the wetland shows a high average depth of inundation in relation to channel stage height. Although the alluvial ridge persists throughout the wetland, the upper reach shows higher average depth of inundation compared to middle and lower reaches. This suggests that the alluvial ridge is better developed in upper reaches than the lower reaches of the wetland. The predominance of this alluvial ridge in the upper reaches of the wetland suggests that most of the sediment supplied to the system is deposited within the upper reaches.

With regards to the Barotse wetland, the channel is the lowest elevated feature across the wetland such that the wetland valley is near-horizontal with no alluvial ridge present down its length. This means that the average depth of inundation was lower than the channel stage heights throughout the wetland. Given that the catchment of the Barotse wetland is composed mainly of unconsolidated Kalahari sediments made of Kalahari sand, sediment is transported mainly as bedload (McCarthy and Ellery, 1998). This means that deposition of sediment is confined to the channel bed and overbank deposition is therefore limited (McCarthy and Ellery, 1998). The geology of the catchment therefore contributes to a near-horizontal floodplain form and an inundation regime that does not promote storage of large volumes of water in backwater depressions.

CHAPTER 7: THE ORIGIN AND HYDROLOGICAL FUNCTIONING OF TECTONICALLY CONTROLLED FLOODPLAIN WETLANDS

7.1 Introduction

Floodplain wetlands that occur in broad and gentle depressions that are bounded by fault lines are investigated in this chapter. Some of these wetlands occupy reaches that overlay less resistant lithologies upstream of a resistant lithology. However, the variation in lithological composition does not appear to have a major influence in the origin of these wetlands since these wetlands appear to have replaced tectonically controlled palaeo-lakes. These wetlands include the Kafue wetland and the Upper Zambezi wetland, which are part of the Zambezi River catchment. The Luapula wetland that is part of the Congo River catchment is located upstream of Lake Mweru.

7.2 The Luapula wetland

The Luapula wetland lies on the border between Zambia and the Democratic Republic of Congo (Figure 7.2.1). The wetland is located between latitude 09°26'S and 10°32'S and longitude 28°32'E and 28°39'E, with most of the wetland located in the Democratic Republic of Congo. At an elevation between 932-921 m amsl, the N-S orientated floodplain is confined by a narrow valley that broadens northwards towards Lake Mweru, which bounds the wetland to the north. The major source of water for the Luapula wetland and its fringe lake is the Luapula River, whose headwaters are located within the Bangweulu catchment.

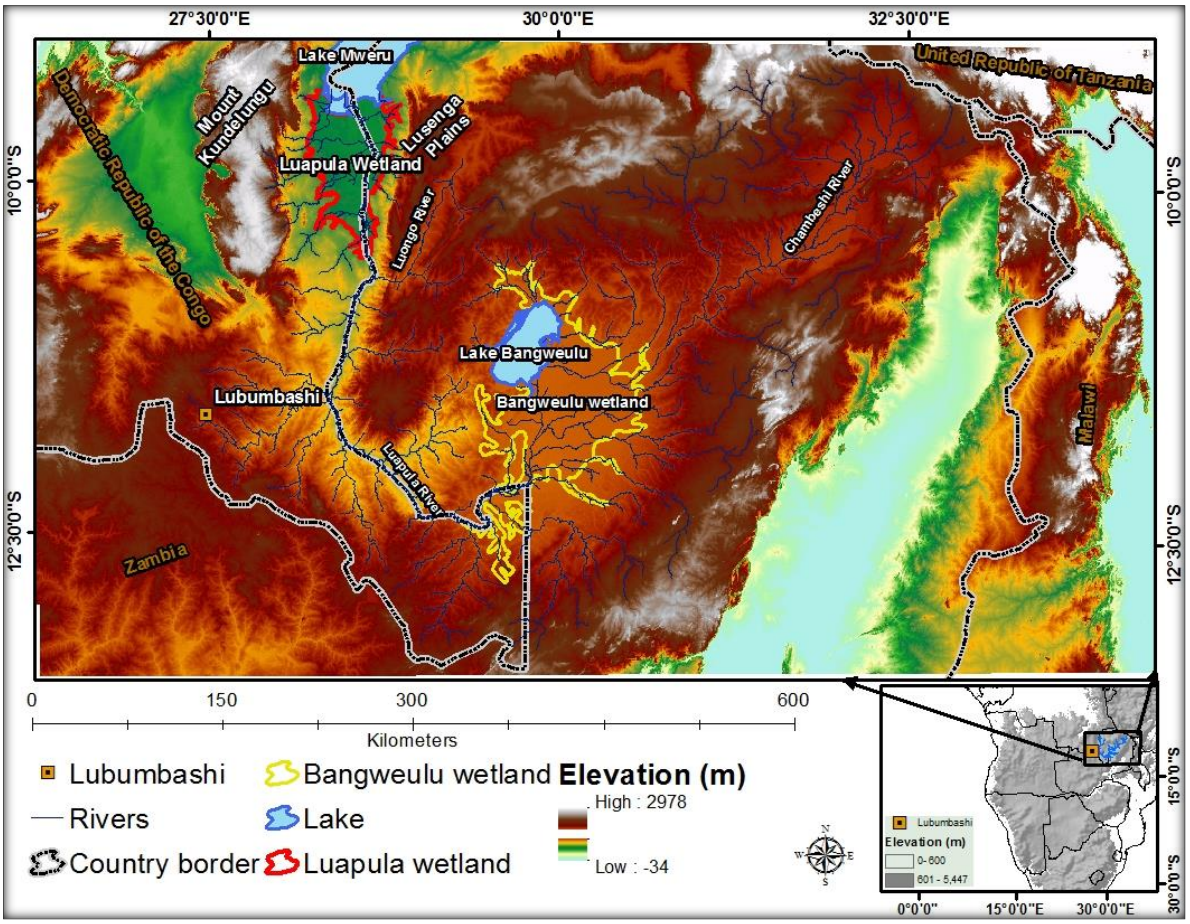

Figure 7.2.1: The location of Luapula wetland within the borders of the Democratic Republic of Congo and Zambia, the topographic setting of the wetland catchment, and major rivers.

7.2.1 Hydrological conditions of Luapula wetland

The Luapula wetland of 5 302 km^2 occupies 3.03% of its 174 135 km^2 catchment (Figure 7.2.2a). The analysis of topographic characteristics (Figure 7.2.2b) of the wetland show that upstream of the wetland the valley is narrow and confined while it gets wider and near-horizontal downstream, with the channel at a slightly lower elevation than the surrounding wetland (Figure 7.2.2c to g).

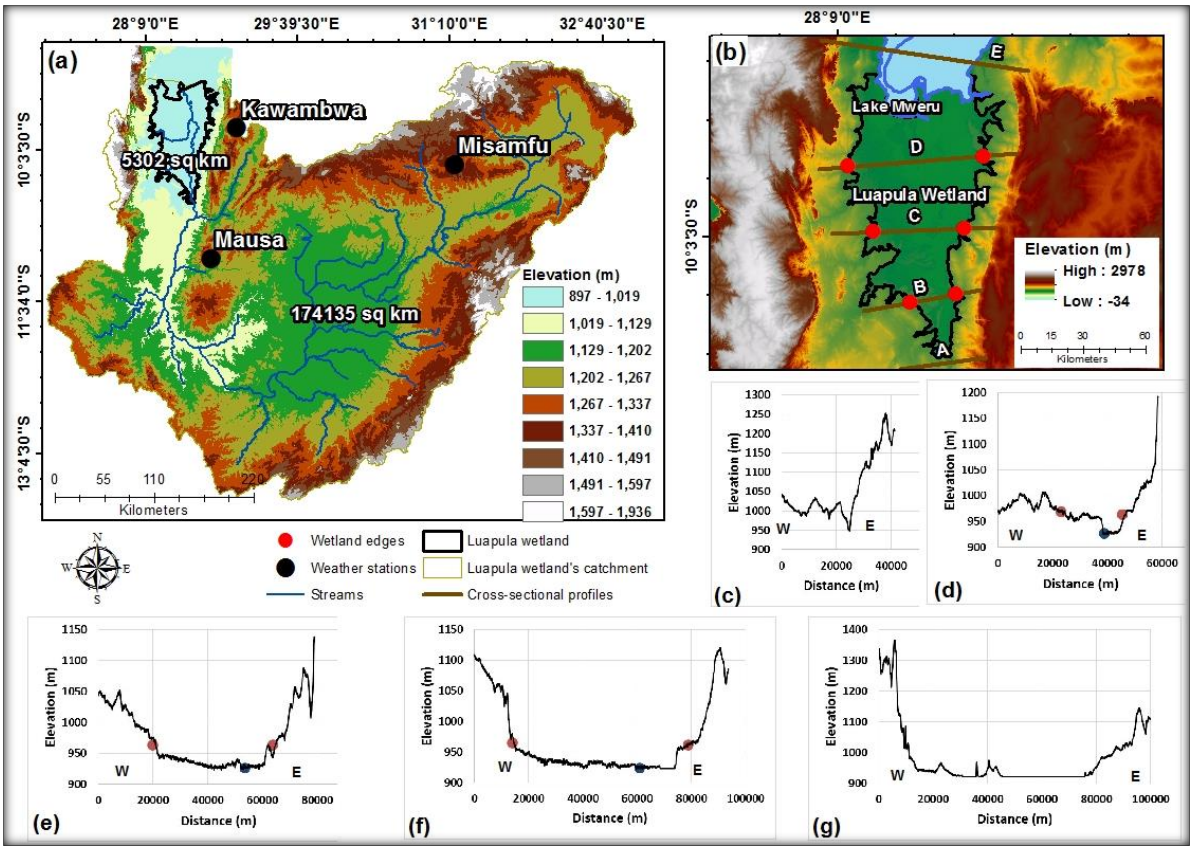

Figure 7.2.2: The location of weather stations, topographic characteristics of the Luapula wetland catchment area (a) and wetland valley (b). Graphs (c)-(g) show cross-sectional profiles at location A-E in the map. W and E in the graphs indicate their West to East orientation.

The climatic data of the three weather stations in the catchment show that potential evapotranspiration exceeds precipitation for 7 to 8 months (Figure 7.2.2a to c). This shows that there is a negative surface water balance within the catchment and the wetland. Rainfall within the catchment starts around September and October, peaks from December to March and subsides in April to May.

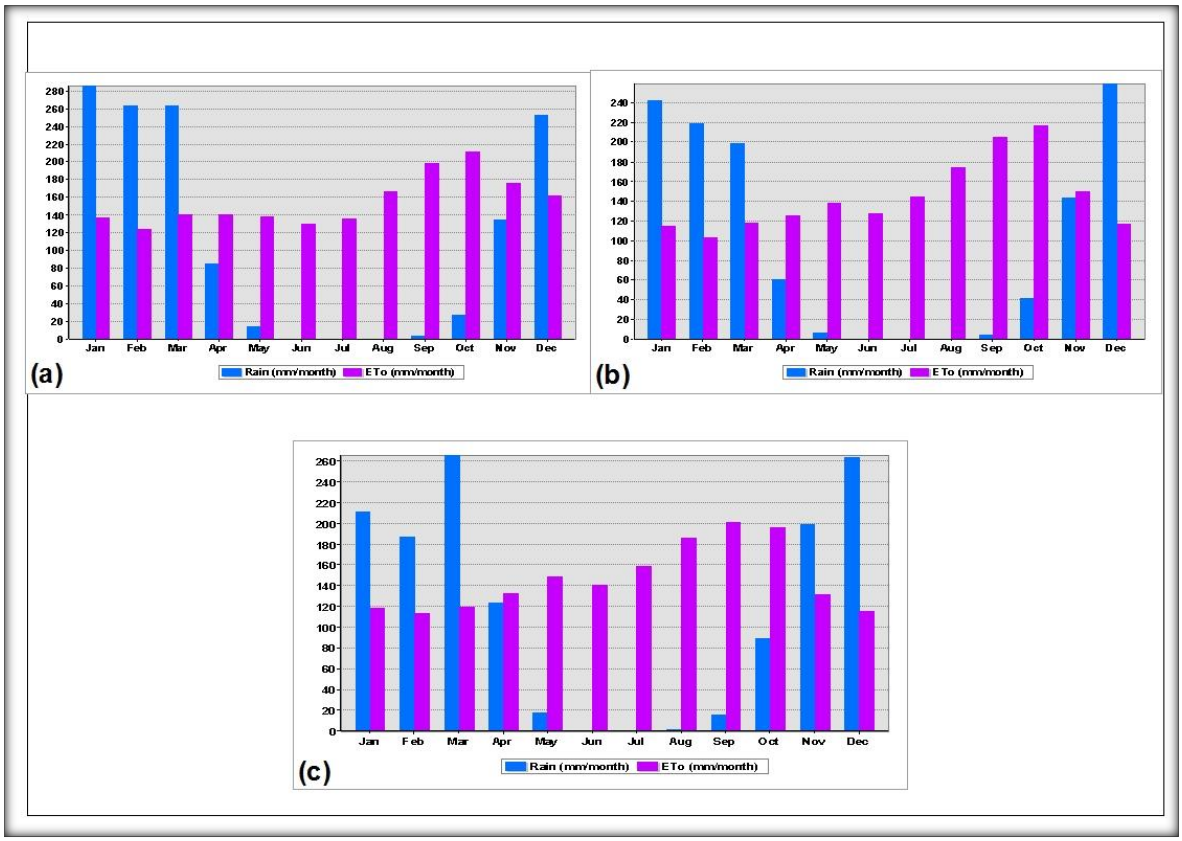

Figure 7.2.3: Monthly average rainfall and potential evapotranspiration for Misamfu (a), Mausa (b), and Kawambwa (c) weather station within the Luapula wetland catchment.

The analysis of the LandsatLook images showing the saturation condition of the wetland (Figure 7.2.4) shows that wetland inundation in October at the onset of the rainy season is limited (Figure 7.2.4a), while peak inundation is around late March to early April (Figure 7.2.4b). The wetland dries from May at the end of the rainy season (Figure 7.2.4c).

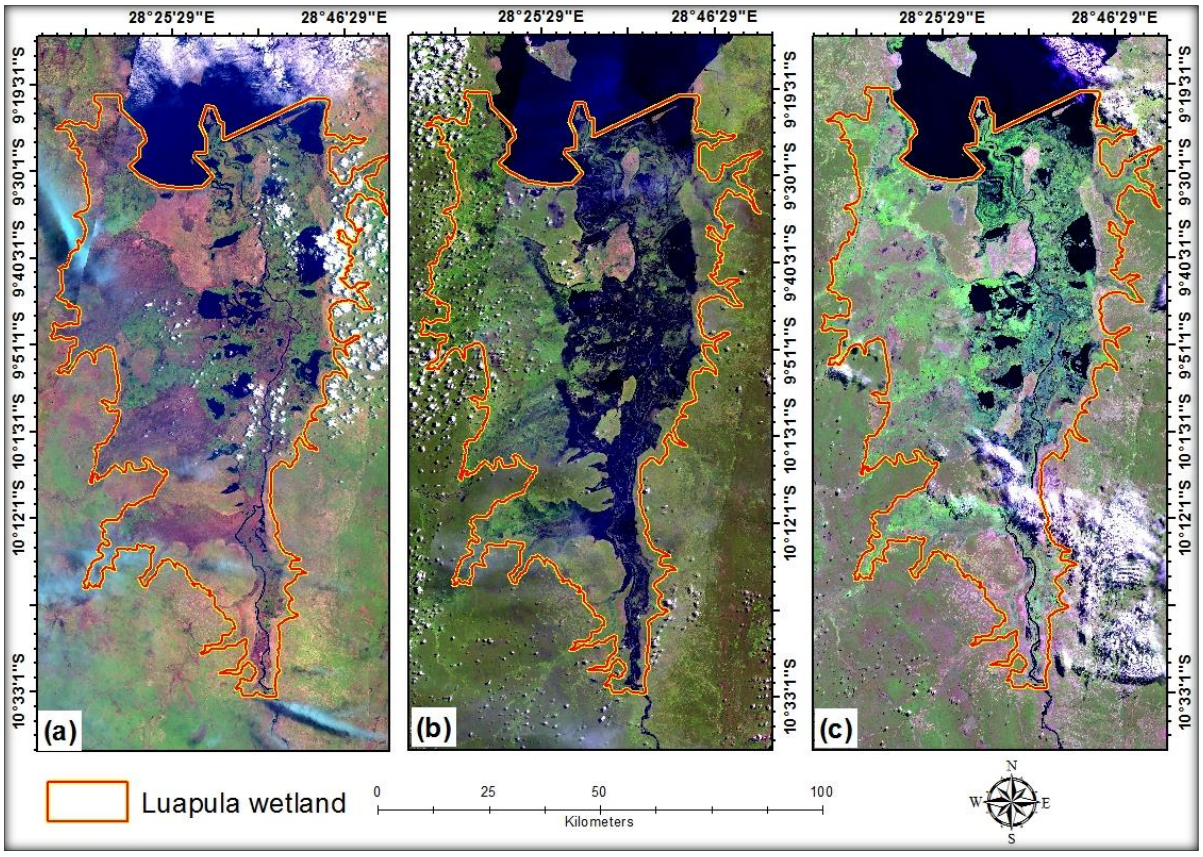

Figure 7.2.4: Mosaicked LandsatLook images depicting the saturation condition of Luapula wetland on 18 and 25 October 2016 (a), 31 March and 09 April 2010 (b), and 18 and 27 May 2010 (c).

7.2.2 Geomorphology of Luapula wetland

From the analysis of the Luapula River's longitudinal profile, it appears that the Luapula River is characterised by two topographic steps, each of which is almost 100 m high (Figure 7.2.5). The overlay of the locations corresponding to the top and bottom of the Luapula wetland over the longitudinal profile shows that the toe of the wetland is at the mouth of the Luapula River where it enters Lake Mweru. Given the presence of a lake there are no lithological controls affecting the formation of the wetland.

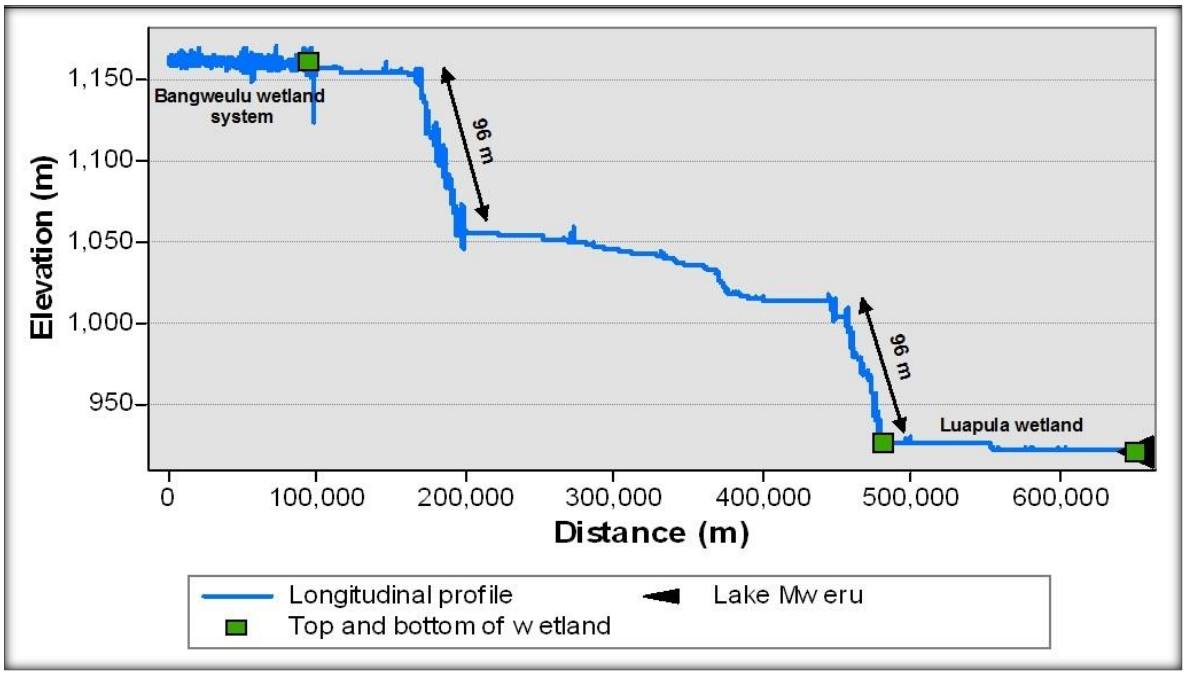

Figure 7.2.5: The longitudinal profile of Luapula River including the Bangweulu wetland system, Luapula wetland, and Lake Mweru.

The cross-sectional profiles show that valley width increases systematically from the head of the wetland to Lake Mweru (Figure 7.2.6a and graphs (b) to (h)). The wetland cross-sectional profiles become progressively near-horizontal downstream towards Lake Mweru. The wetland is also characterised by elevated islands west of the Luapula River channel.

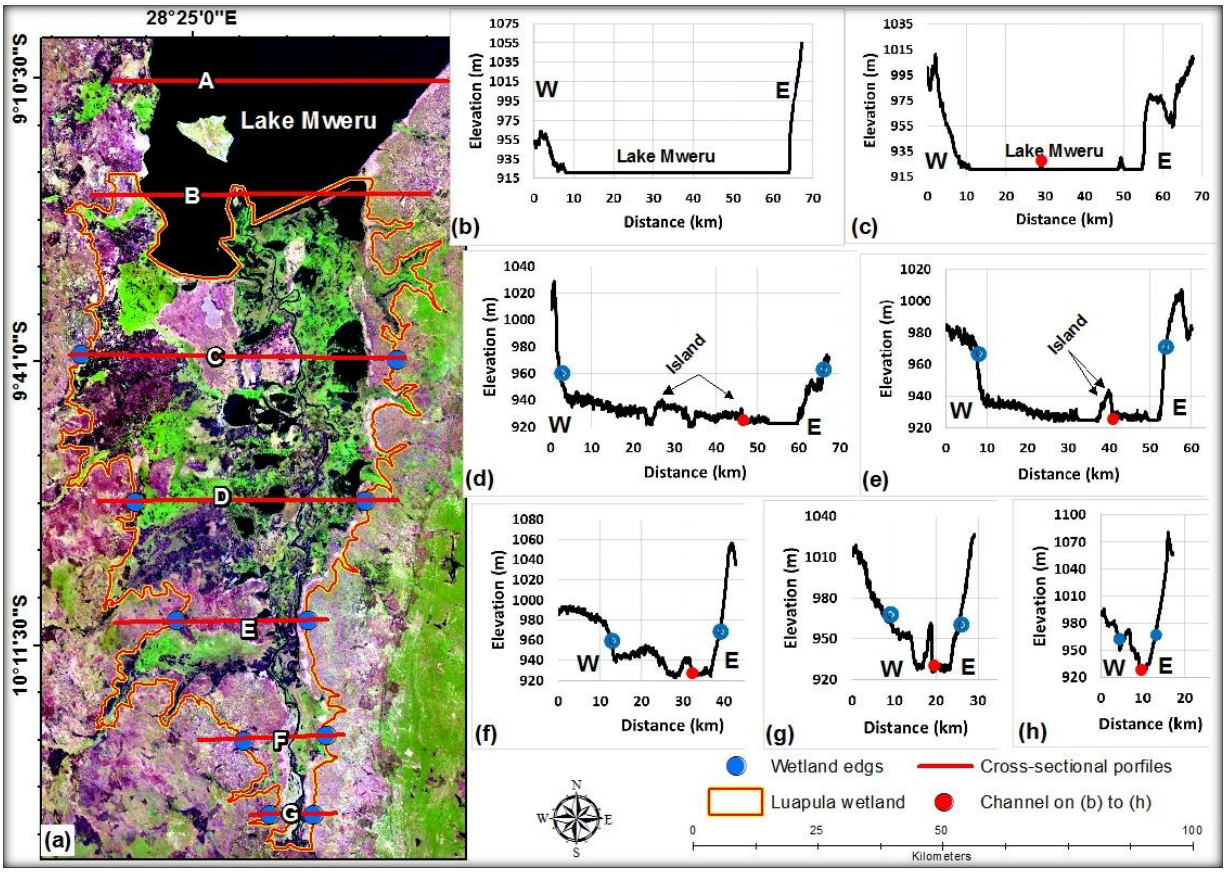

Figure 7.2.6: Mosaic of 13 and 20 August 2015 LandsatLook images (a) and graphs (b)-(h) showing the cross-sectional profiles of lines A-G. The red markers on the graphs show the position of the trunk stream.

7.2.3 Luapula wetland's structure and hydrological functioning

From the cross-sectional profiles in location 1 and 2 (Figure 7.2.7a), it appears that the wetland is characterised by backwater depressions but lacks a prominent alluvial ridge since the channel is the lowest-lying feature within the wetland (Figure 7.2.7b and c). The lack of alluvial ridges within the wetland suggests that floodwater from the wetland can recharge stream channels during the waning stages of a flood event. However, the presence of backwater depressions suggests that the wetland can store surface water for long periods.

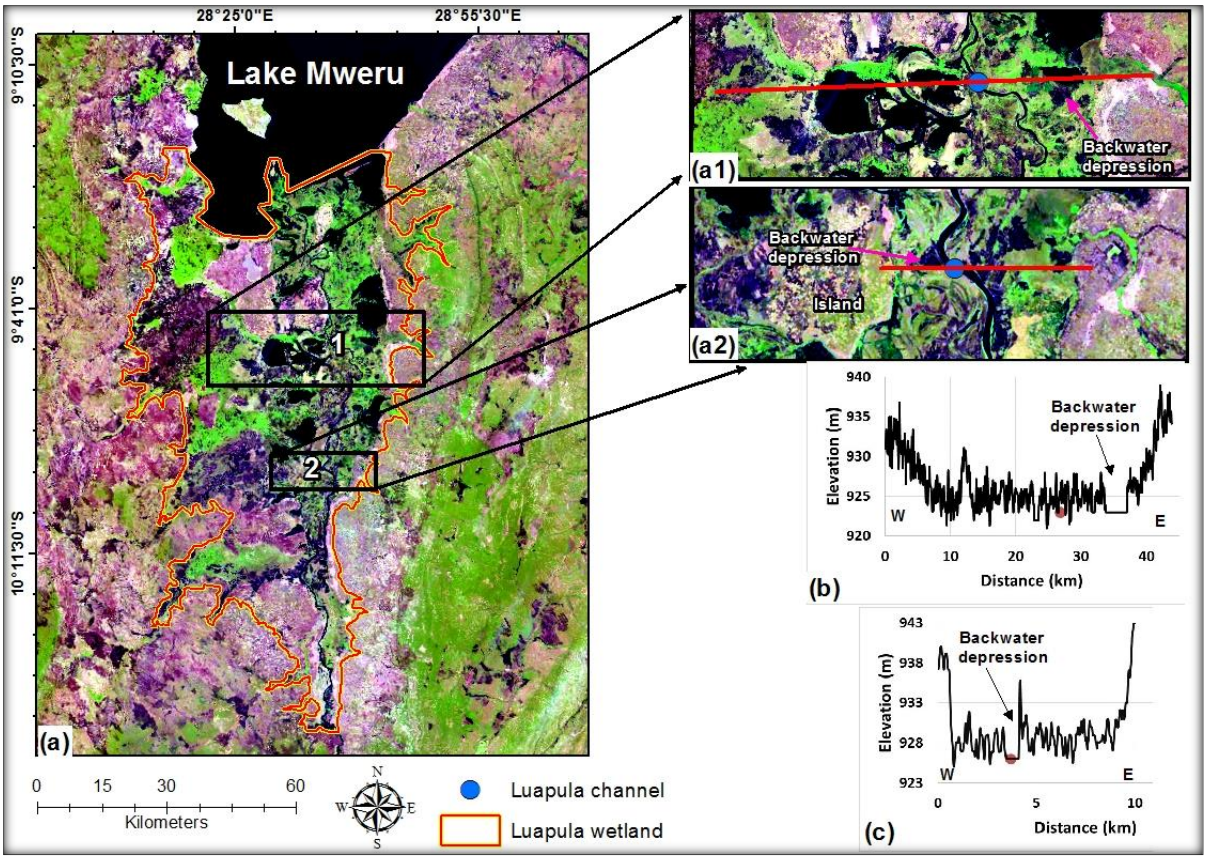

Figure 7.2.7: Mosaic of 13 and 20 August 2015 LandsatLook images showing floodplain features within the Luapula wetland (a) with (a1) and (b1) showing an enlargement of two selected sections in the middle reaches of the wetland while (b) and (c) show the cross-sectional profiles of the cross-sections in (a1) and (a2) respectively.

From the analysis of the Luapula River's channel characteristics within the wetland it appears that the 171 km long river flows within the 160 km long wetland with a low sinuosity ratio that equates to 1.07. This shows that the river is relatively straight within the wetland, and explains the absence of depositional features such as alluvial ridges. From the length of the river (Figure 7.2.8a) and the elevation values from the longitudinal profile (Figure 7.2.8b) the wetland has a slope of 0.003%.

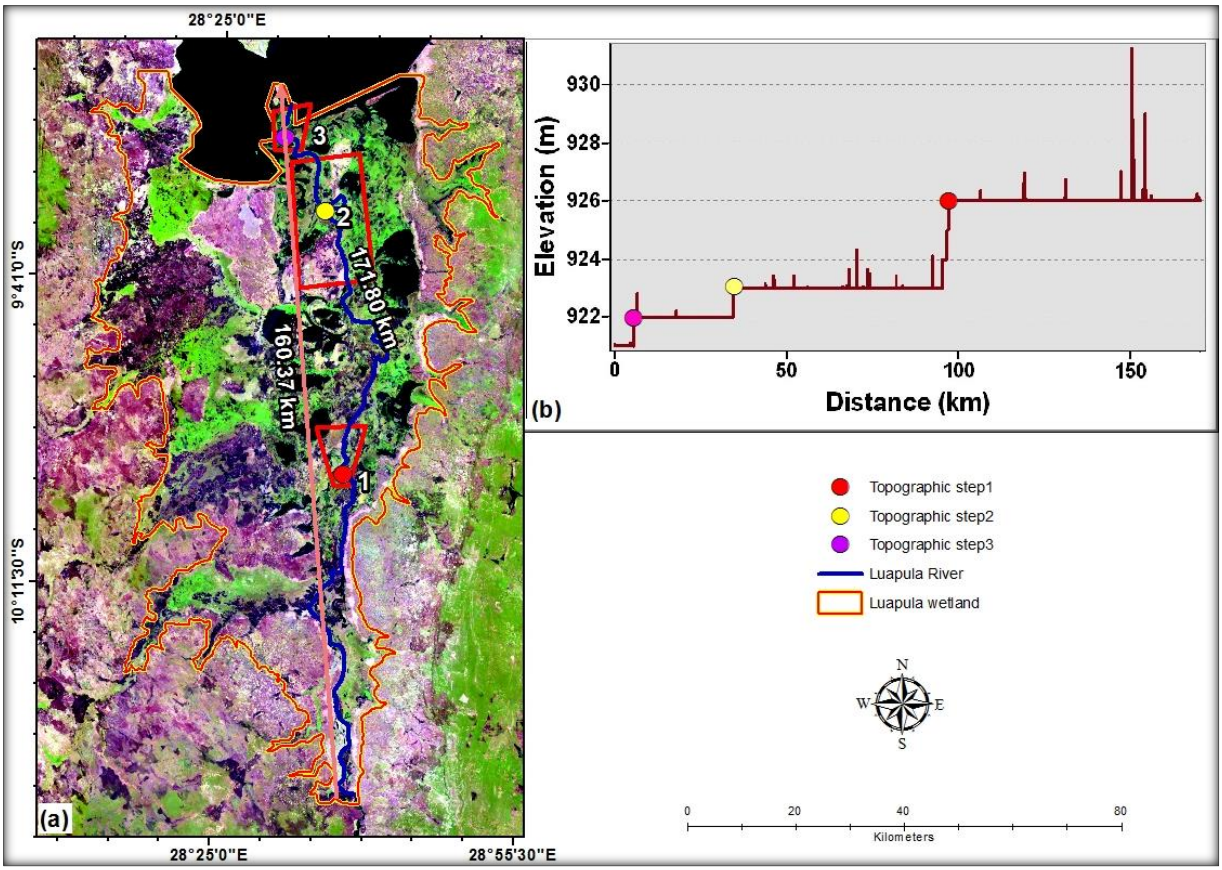

Figure 7.2.8: Mosaic of 13 and 20 August 2015 LandsatLook images showing characteristics of the Luapula wetland including the total length of the wetland (the pink line), the total length of the river within the wetland (blue line; (a)), and the longitudinal slope of the river within the wetland (b). The red boxes 1-3 represent areas that were examined from the analysis of Google Earth imagery.

Although the longitudinal profile shows a number of very minor topographic steps along the course of the stream in the wetland, analysis of Google Earth imagery (DigitalGlobe, CNES/Astrium and CNES/Spot; boxes 1-3 in Figure 7.2.8) shows no evidence of topographic irregularities in the vicinity of the positions of these steps on the topographic profile. The steps are therefore likely to be an artefact of the poor vertical accuracy of the Digital Elevation Model (DEM) at the scale of the topographic profile.

The geology of the wetland catchment (Figure 7.2.9a) shows that streams drain the area that is mainly characterised by Undifferentiated Kundelungu Group (P_3Kk) sediments (metamorphosed sandstone, shale and carbonates), Gneiss (A_4Sgr), and Muva Group (P3M) metamorphosed sediments. The wetland occurs downstream of two large wetland systems (i.e. the Bangweulu wetland and Upper Chambeshi wetland) which may retain sediment and therefore limit sediment flux downstream. Given this, the area that is likely to be the major source of sediment to the wetland lies between the Luapula wetland and Bangweulu wetland

and the area is mainly characterised by Undifferentiated Kundelugu Group (P_3Kk) sediments. The geology around the wetland area (Figure 7.2.9b) shows that the lake and wetland are surrounded by significant fault lines in the west and east.

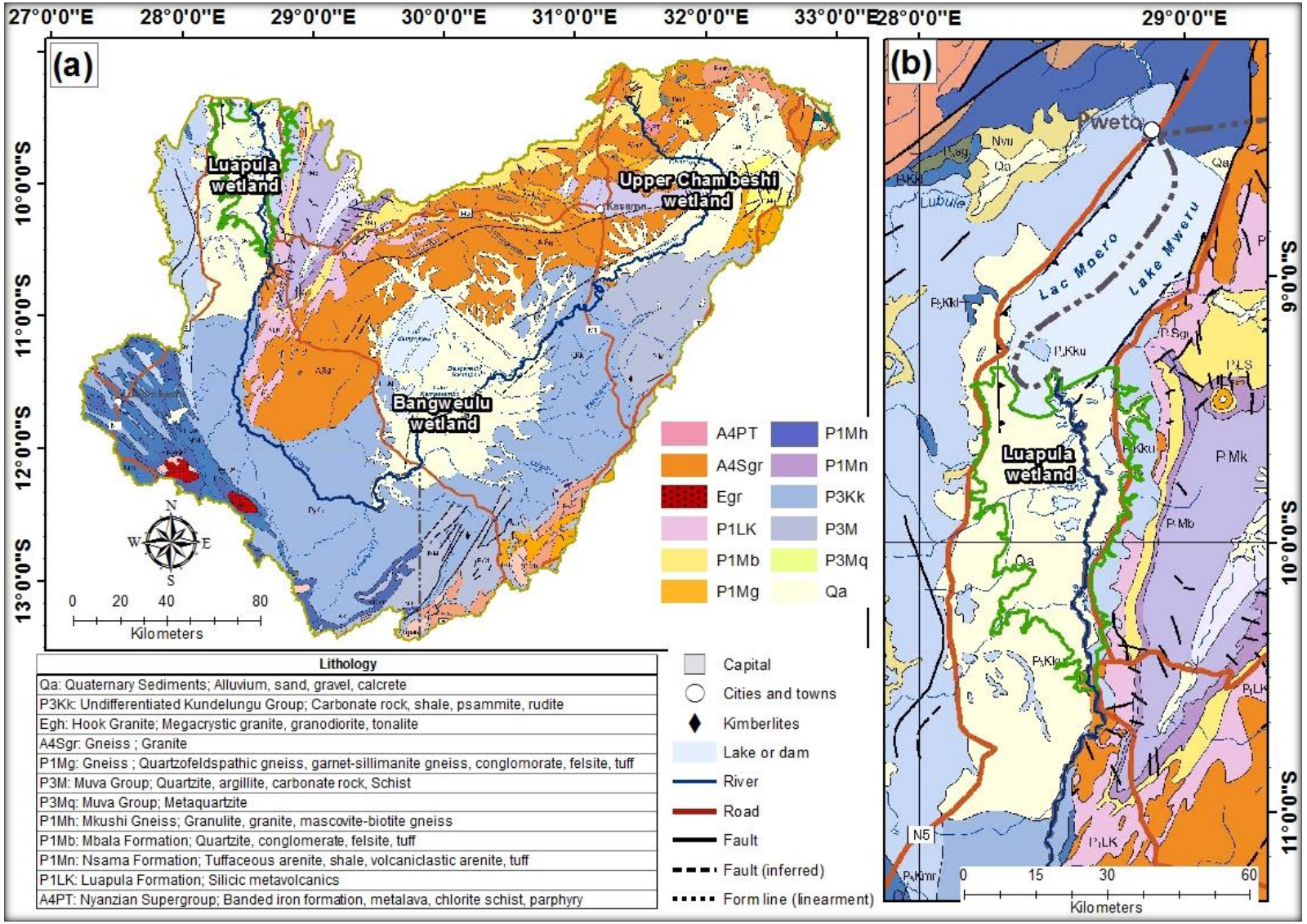

Figure 7.2.9: The geology of Luapula wetland catchment (a) and the area immediately surrounding the wetland and Lake Mweru (b).

Although the Luapula wetland does have backwater depressions, the wetland lacks an alluvial ridge as indicated by the observed low average depth of inundation in relation to the channel stage heights throughout the wetland (Figure 7.2.10). The lower reach shows slightly higher average depth of inundation compared to the upper reach.

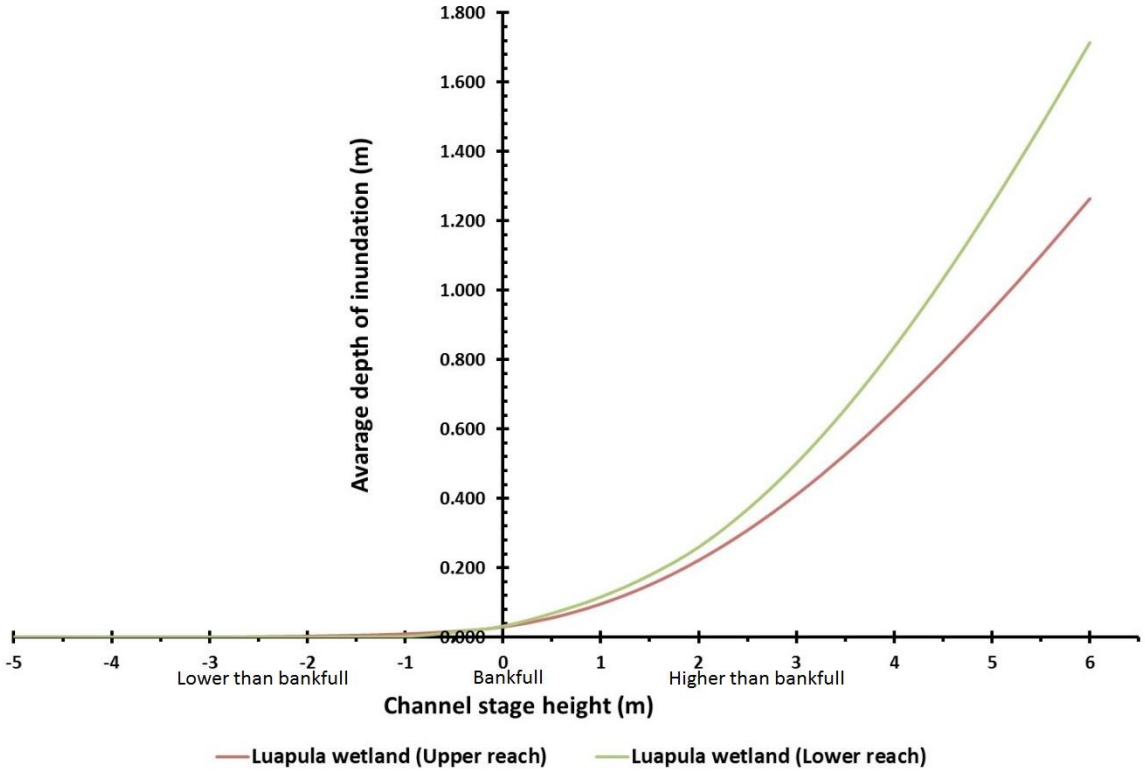

Figure 7.2.10: Comparison of the average depth of inundation within the upper and lower reaches of the wetland. The "0" depth represents channel water level while the positive and negative depths represent channel inundation height above and below bankfull channel stage height.

7.3 The Kafue wetland

The Kafue wetland is located between latitude 15°45'S and 16°45'S and longitude 26°01'E and 28°05'E in the central part of Zambia about 50 km south-west of the city of Lusaka (Figure 7.3.1). The wetland occurs within the Kafue River valley. The Kafue River originates in the north-western part of Zambia and from its headwaters the river maintains a south-westward course but changes to a southward course as far as the Itezhi-tezhi Dam. As the Kafue River leaves the Itezhi-tezhi Dam it suddenly flows eastward as it enters the wetland and upon leaving the wetland until it joins the Zambezi River.

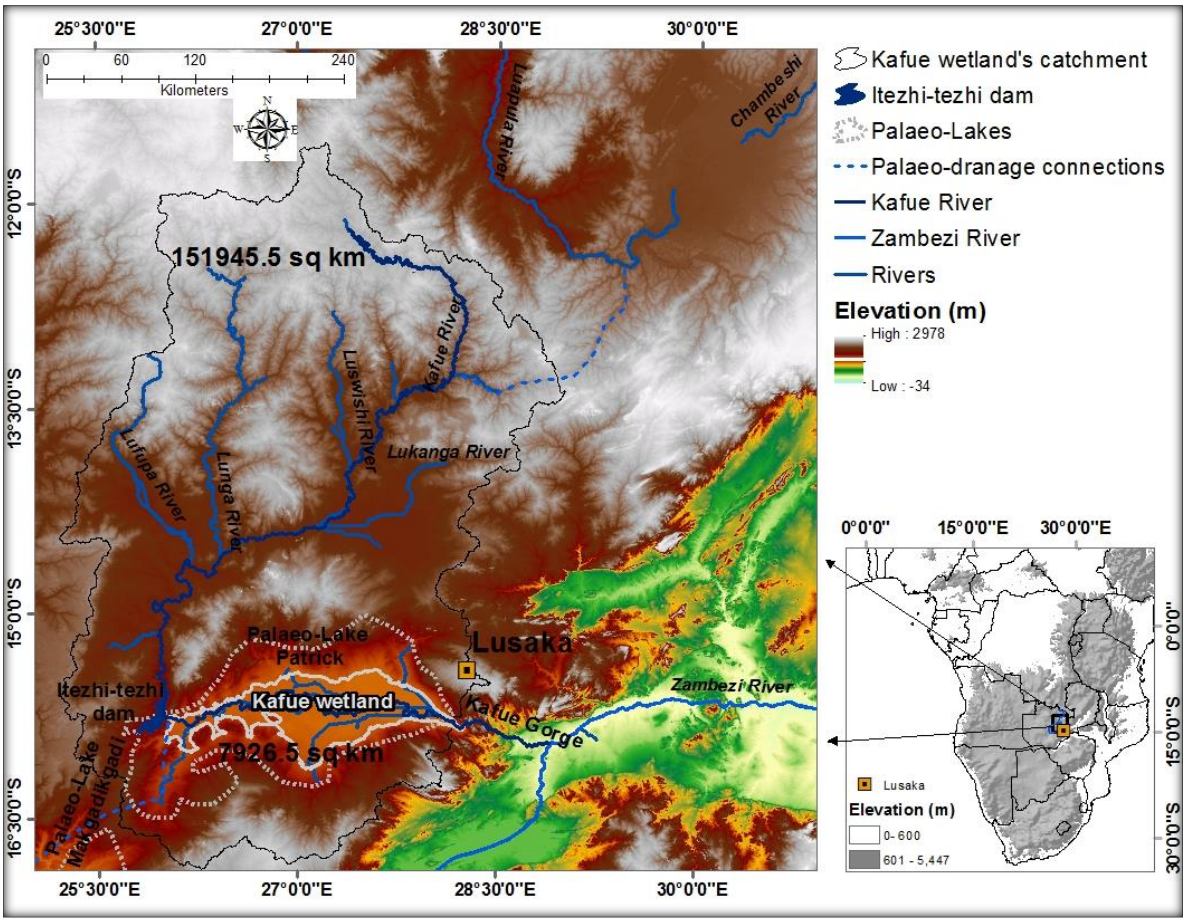

Figure 7.3.1: The Kafue River course and location of the Kafue wetland in central Zambia.

7.3.1 Hydrological conditions of the Kafue wetland

The analysis of the characteristics of the Kafue wetland's catchment revealed that the 7 926 km^2 wetland occupies 2.18% of its 362 972 km^2 catchment (Figure 7.3.2a). Figure 7.3.2 b to g show that the wetland occurs within a broad valley that is widest in the middle reaches of the wetland. It also appears that the Kafue River's channel within the wetland is at a lower elevation than the surrounding wetland areas within the upper and lower reaches of the wetland (Figure 7.3.2c and f). However, the channel appears to be at the same elevation as the surrounding wetland areas within the middle reaches of the wetland (Figure 7.3.2d and e).

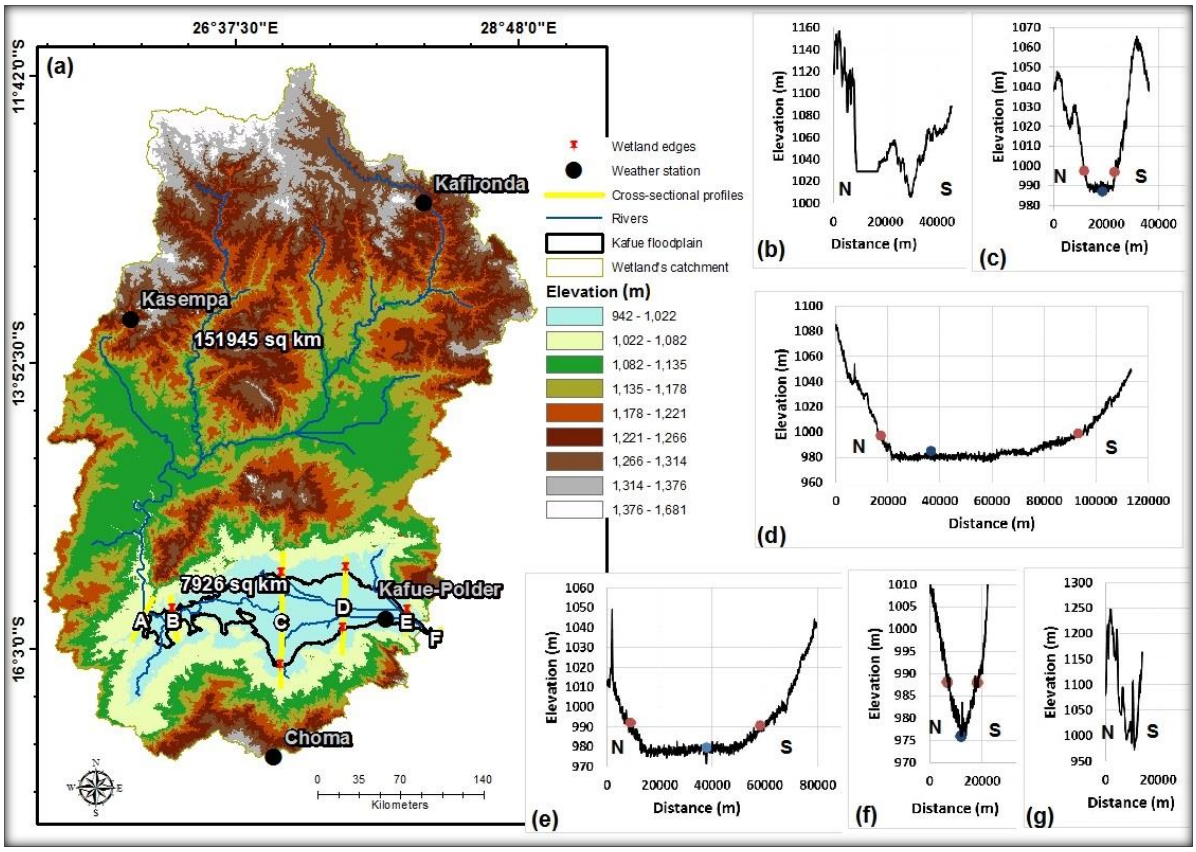

Figure 7.3.2: The topographic characteristics of the Kafue wetland, its catchment area, and the location of weather stations (a). Graphs (b)-(g) showing the cross-sectional profiles of transects A to F down the length of the wetland. The blue markers on the graphs show the location of the main channel.

The analysis of potential evapotranspiration and rainfall for the four weather stations within the catchment shows that evapotranspiration greatly exceeds rainfall for 7 to 9 months of the year (Figure 7.3.3). The observed climatic parameters from the four weather stations show a negative surface water balance. The climatic data from the four weather stations also shows that the rainfall season starts around October, peaks from December to February, and ends around March to April.

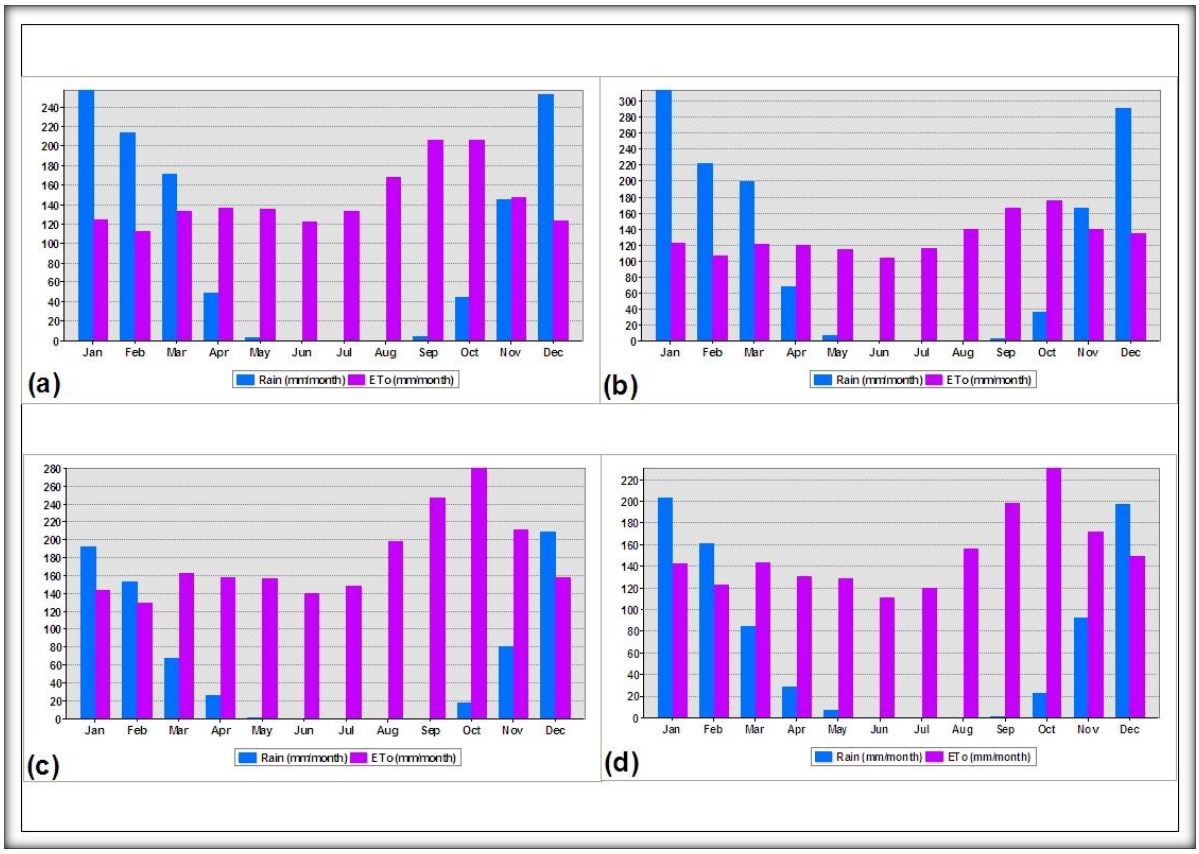

Figure 7.3.3: Monthly rainfall and potential evapotranspiration rates for Karifonda (a), Kasempa (b), Choma (c), and Kafue-Polder (d) weather stations within the Kafue wetland catchment and in close proximity to the wetland.

Visual interpretation of the LandsatLook images showing saturation conditions within the wetland shows that the wetland is relatively dry in November (Figure 7.3.4a) and wettest around April (Figure 7.3.4b).

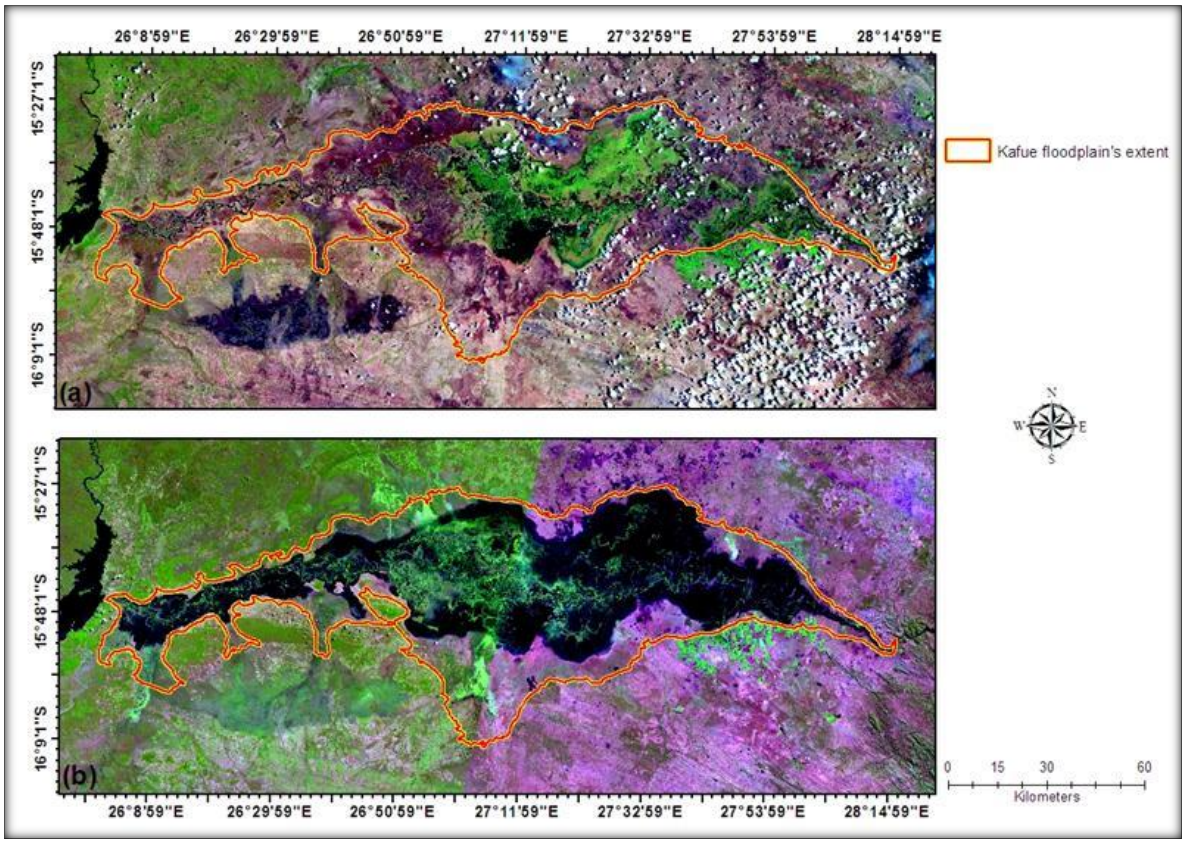

Figure 7.3.4: Mosaics of LandsatLook images showing the saturation condition of Kafue wetland on 14 and 21 November 2014 (a), and 03 and 19 April 2011 (b).

7.3.2 Geomorphology of the Kafue wetland

The longitudinal profile of the Kafue River shows that the river is characterised by three topographic steps (Figure 7.3.5). The first two topographic steps that occur within the upper and middle reaches of the river have a height of less than 200 m each. The overlay of points depicting the locations of the head and toe of the wetland over the longitudinal profile shows the last topographic step occurs just below the toe of the Kafue wetland and extends over a height of about 600 m. This topographic step coincides with the Kafue Gorge and is likely to have formed following the second uplift event and suggests that the Zambezi River in the vicinity of the Kafue Wetland occupies the Post-Africa I Surface.

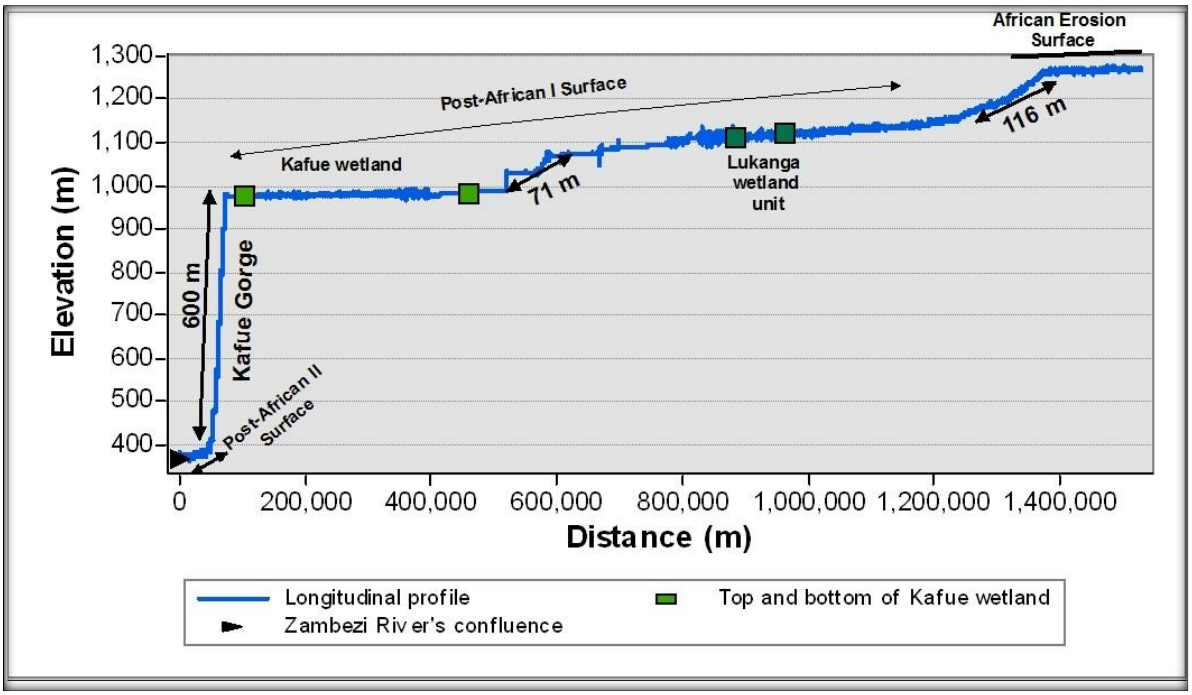

Figure 7.3.5: The longitudinal profile of the Kafue River showing the location of Kafue floodplain wetland and the Lukanga wetland, as well as the likely erosion surfaces drained by the Kafue River.

Visual analysis of the LandsatLook images showing the lower reaches of the Kafue wetland (Figure 7.3.6a and b) show that there is no increase in channel sinuosity upstream from the toe of the wetland. The cross-sectional profiles within the lower reaches of the wetland and below the toe of the wetland show that there is a systematic downstream decrease in valley width (Figure 7.3.6c to j).

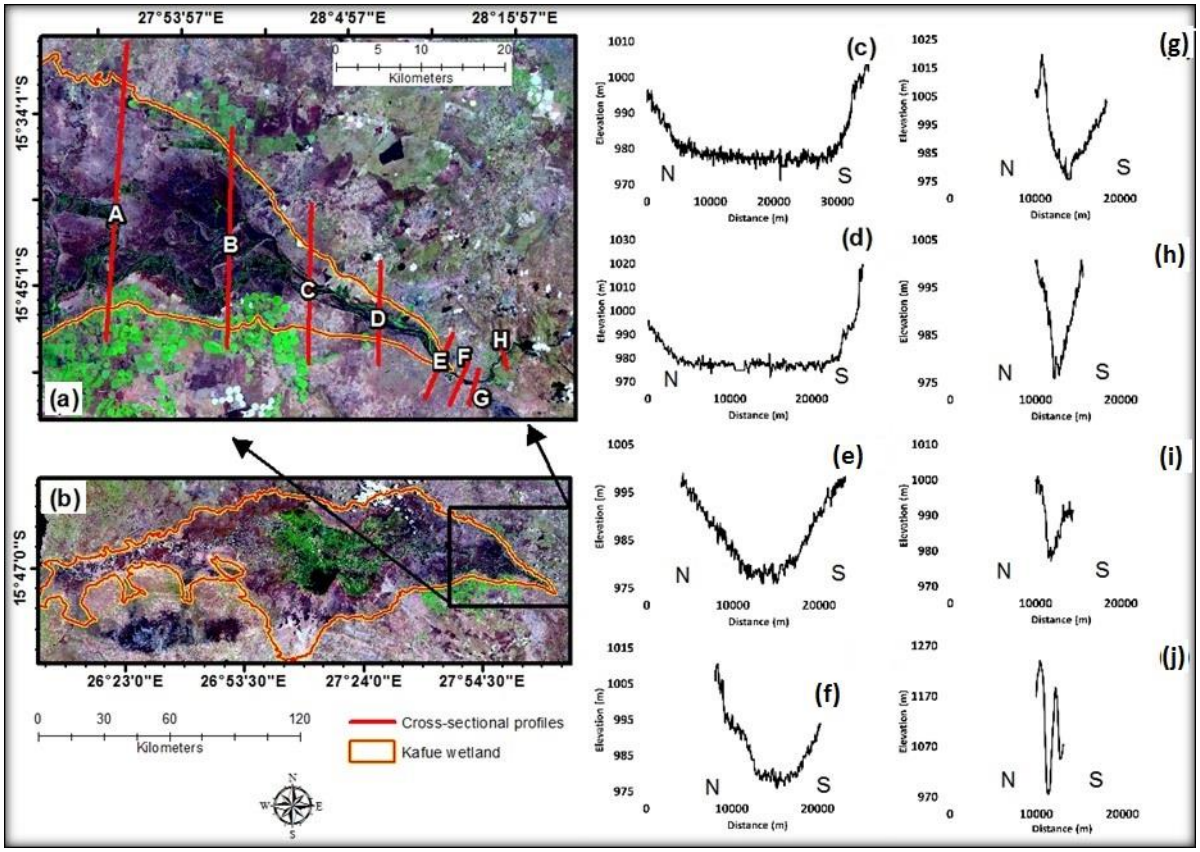

Figure 7.3.6: Valley width characteristics within the lower reaches of the Kafue wetland and below the toe of the wetland (a) and (b). Graphs (c)-(j) show the cross-sectional profiles of transects A-H respectively. The images are a mosaic of 14 and 21 November 2014 LandsatLook images.

The geological map of the Kafue wetland catchment shows that streams drain an area underlain mainly by the Hook Granite (Egh) and consolidated sedimentary rocks such as the Undifferentiated Kundelungu Group (P_3Kk), Monwezi Subgroup (P_3Krl), and Molteno Formation (Tu), as well as the Lower Roan Group (P_3Kkl) metamorphic rock (Figure 7.3.7a). The area between the Kafue wetland and the Lukanga wetland is mainly characterised by the Hook Granite and is likely to be the major source of sediment for the wetland since the Lukanga wetland may trap sediment and reduce sediment flux. The overlay of the wetland boundary over a geological map shows a number of east-west trending fault lines to the north and east of the wetland (Figure 7.3.7b). The toe of the wetland and the areas below the toe of the wetland are underlain by the Muva Group (P_3Mc) metavolcanic rock that is relatively resistant to erosion. The toe of the wetland coincides with a change in lithology from unconsolidated Quaternary sediments (Qa) to Muva Group metavolcanic rocks (P_3Mc).

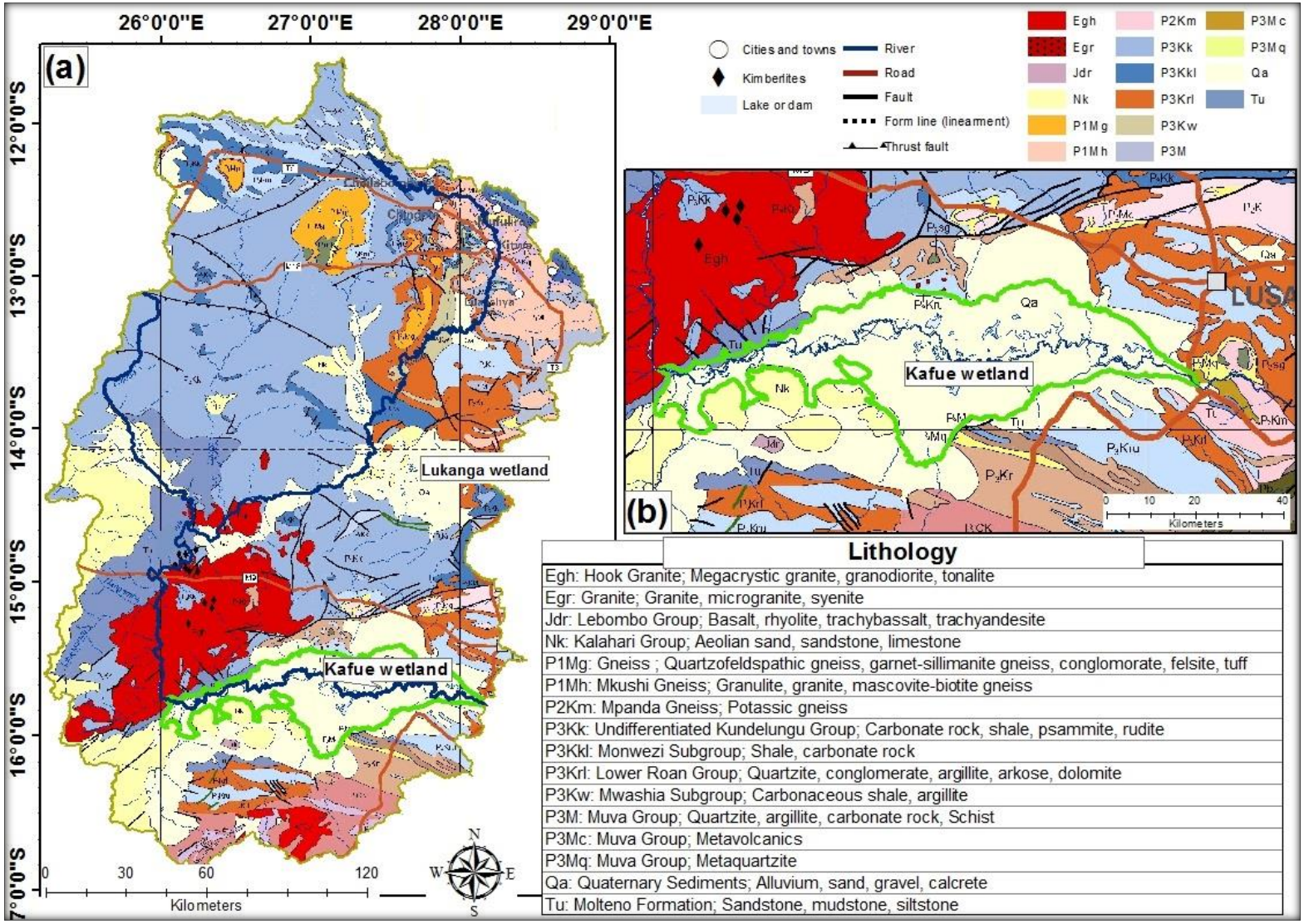

Figure 7.3.7: The geology of the Kafue wetland catchment (a) and the area in the vicinity of the toe of the wetland (b).

7.3.3 The structure and hydrological functioning of the Kafue wetland

The LandsatLook images show that the Kafue wetland is characterised by meandering features such as active cut banks and meander scars within the upper reach (Figure 7.3.8a-b). Although there is no clear evidence of floodplain features such as meander scars and active cut banks within the middle reach, the reach is characterised by backwater depressions (Figure 7.3.8c-d and b1-c1). Within the lower reach, there is no clear evidence of floodplain features or backwater depressions (Figure 7.3.8e and d1). The observed floodplain features suggest that the channel is meandering within the upper reach and that the middle and lower reaches could be characterised by palaeo-meandering features as the current stream is very much smaller than the meander features preserved on the wetland surface. Furthermore, Figure 7.3.8b1 shows that channel banks have been raised to an elevation of about 4 m above the water level of the surrounding backwater depression, suggesting that the wetland can flood to a depth of about 4 m.

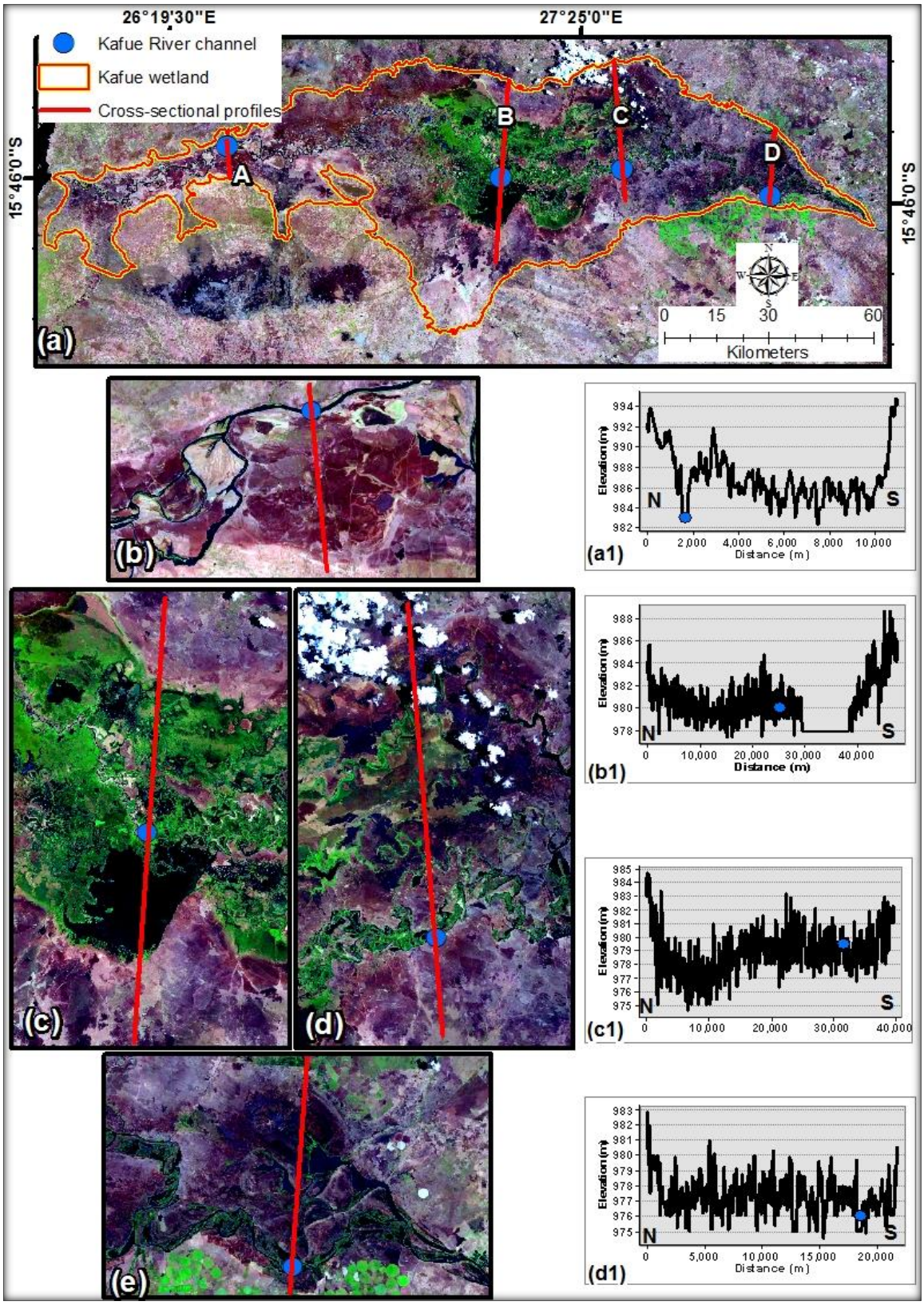

Figure 7.3.8: A mosaic of 14 and 21 November 2014 LandsatLook images of the Kafue wetland (a). Images (b) to (e) show an enlargement of the area around cross-sectional profiles A-D respectively. Graphs (a1)-(d1) show the cross-sectional profiles of lines A-D respectively. The blue markers on the graphs show the location of the main stream.

The analysis of the Kafue River within the Kafue wetland shows that the 412 km distance covered by the river almost doubles the 227 km wetland's valley length giving a sinuosity ratio of about 1.8 (Figure 7.3.9a). Furthermore, the river length and the elevation data from the longitudinal profile of the section of the Kafue River within the wetland show that the wetland has an average slope of 0.003% (Figure 7.3.9b). The longitudinal profile shows that the middle reaches of the wetland (the areas between points 2 and 3 in Figure 7.3.9b) are characterised by an extremely low slope (0.0008%), while the upper reaches (between points 1 and 2) are characterised by a slope that is steeper by an order of magnitude.

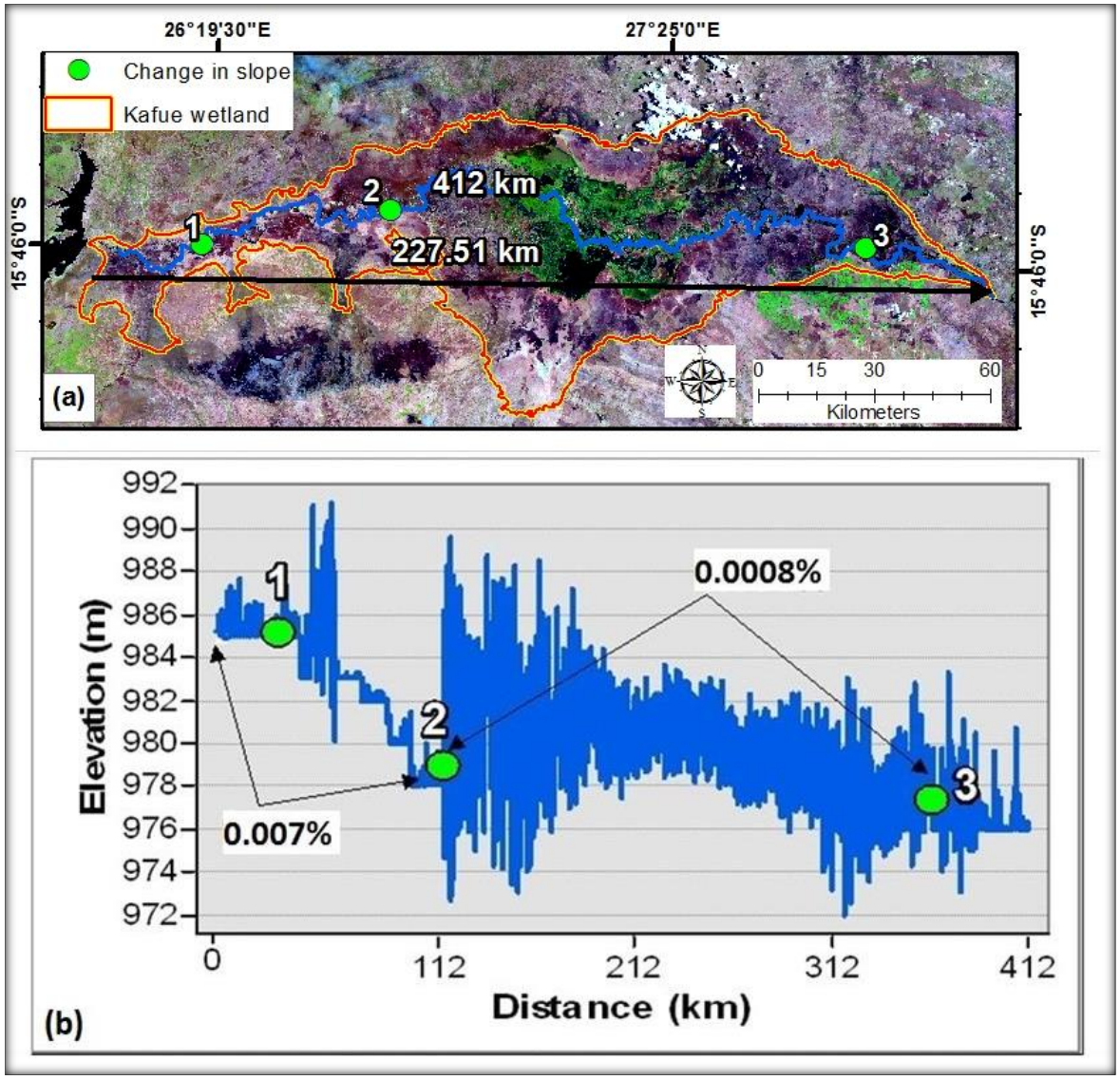

Figure 7.3.9: Characteristics of the Kafue River within the Kafue wetland (a) and the longitudinal profile of the river (b). The black line shows the total length of the wetland while the blue line shows the total length of the river within the wetland. Points 1, 2 and 3 show sections with a relatively uniform longitudinal slope. The images in the map are a mosaic of 14 and 21 November 2014 LandsatLook images.

The average depth of inundation within the upper and lower reaches of the wetland shows that the average depth of inundation is lower within the upper reach of the wetland compared to the lower reach (Figure 7.3.10). For both the upper and lower reaches, the mean depth of flooding is lower than the channel stage heights, which suggests that an alluvial ridge associated with the current channel is absent throughout the wetland.

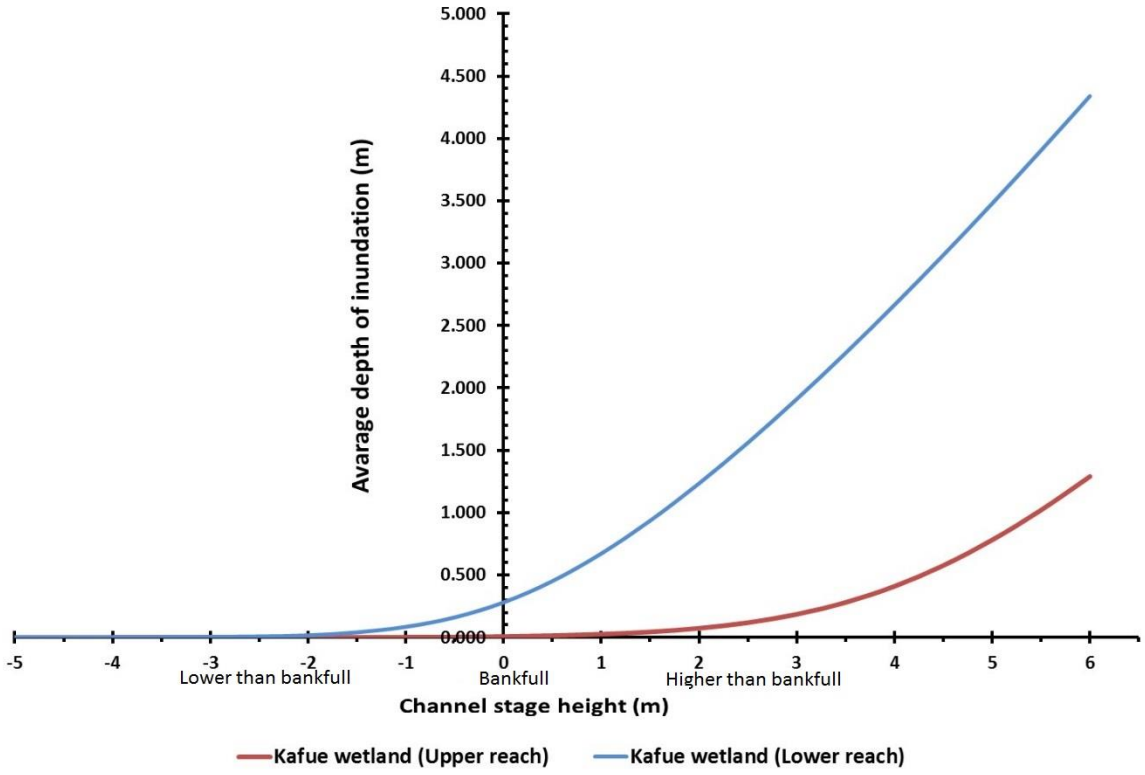

Figure 7.3.10: Comparison of the average depth of inundation within two distinct reaches of the Kafue wetland. The "0" depth represents channel water level while the positive and negative depths represent channel inundation height above and below channel water level respectively.

7.4 The Upper Zambezi wetland

The SE-NW trending Upper Zambezi wetland is located downstream of the Barotse wetland, between the towns of Sesheke in Zambia and Kasane in Botswana (Figure 7.4.1). The wetland is situated mainly in Namibia between latitude 17°29'S and 17°47'S and longitude 24°17'E and 25°15'E. The floodplain is located at the confluence of the Zambezi and Cuando Rivers. Several tributaries of the Zambezi River, including the Cuando River to the west and the Machile River to the north, drain into the Upper Zambezi wetland.

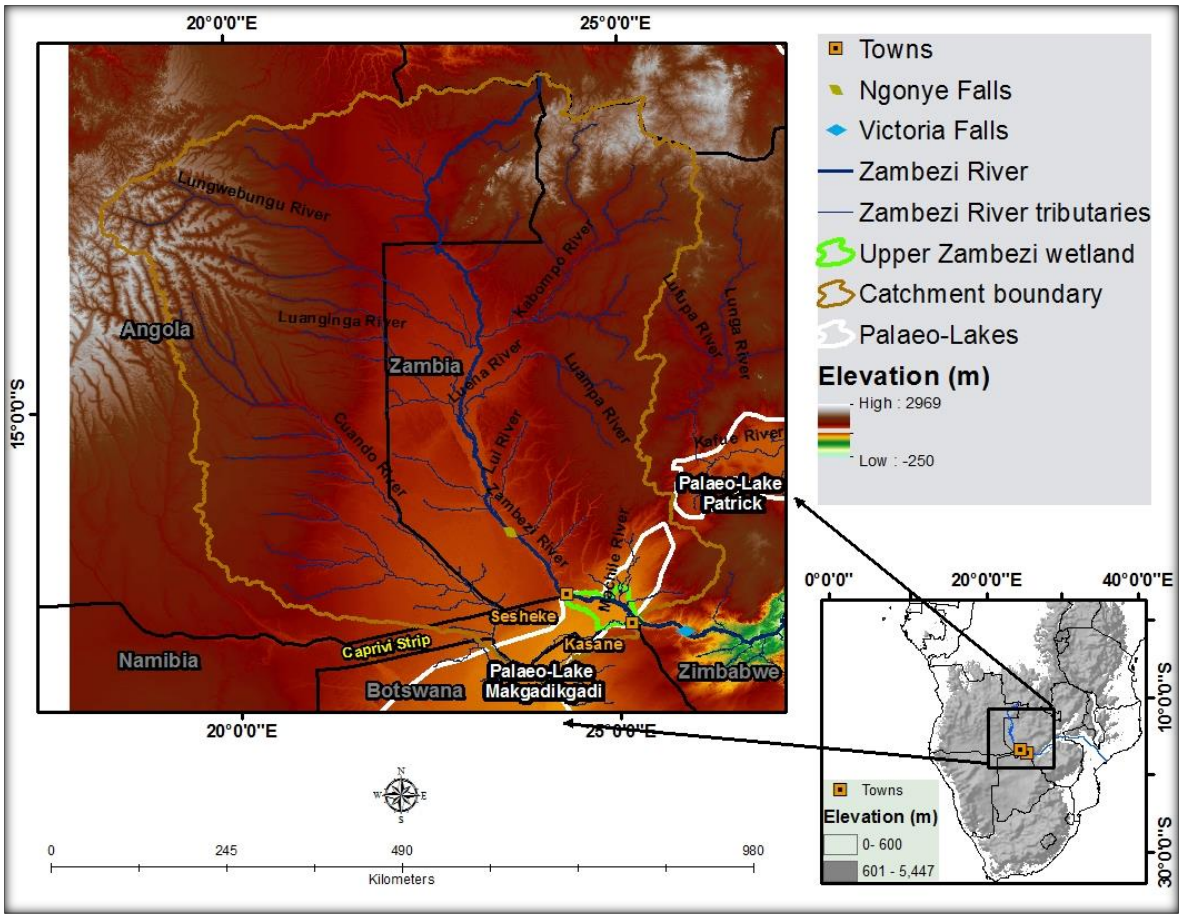

Figure 7.4.1: The location of Upper Zambezi wetland in Namibia and Zambia, the topographic setting of the wetland catchment, and major rivers.

7.4.1 Hydrological conditions of Upper Zambezi wetland

The analysis of the topographic characteristics of the Upper Zambezi wetland shows that upstream (Figure 7.4.2c) and downstream (Figure 7.4.2g) of the wetland the valley is narrow and steep sided, while the wetland occupies a broad valley (Figure 7.4.2d to f). For a given distance down the valley the elevation of the Zambezi River's channel within the wetland occupies the lowest elevation across the wetland. It can also be noted that within the upper reaches of the wetland, the northern side of the wetland abuts a steep valley side, while the southern side is relatively poorly confined (Figure 7.4.2d and e). However, the lower reaches of the wetland show that the southern side is confined by a steep margin (Figure 7.4.2d). The 3 200 km^2 wetland occupies 0.6% of its 499 816 km^2 catchment area.

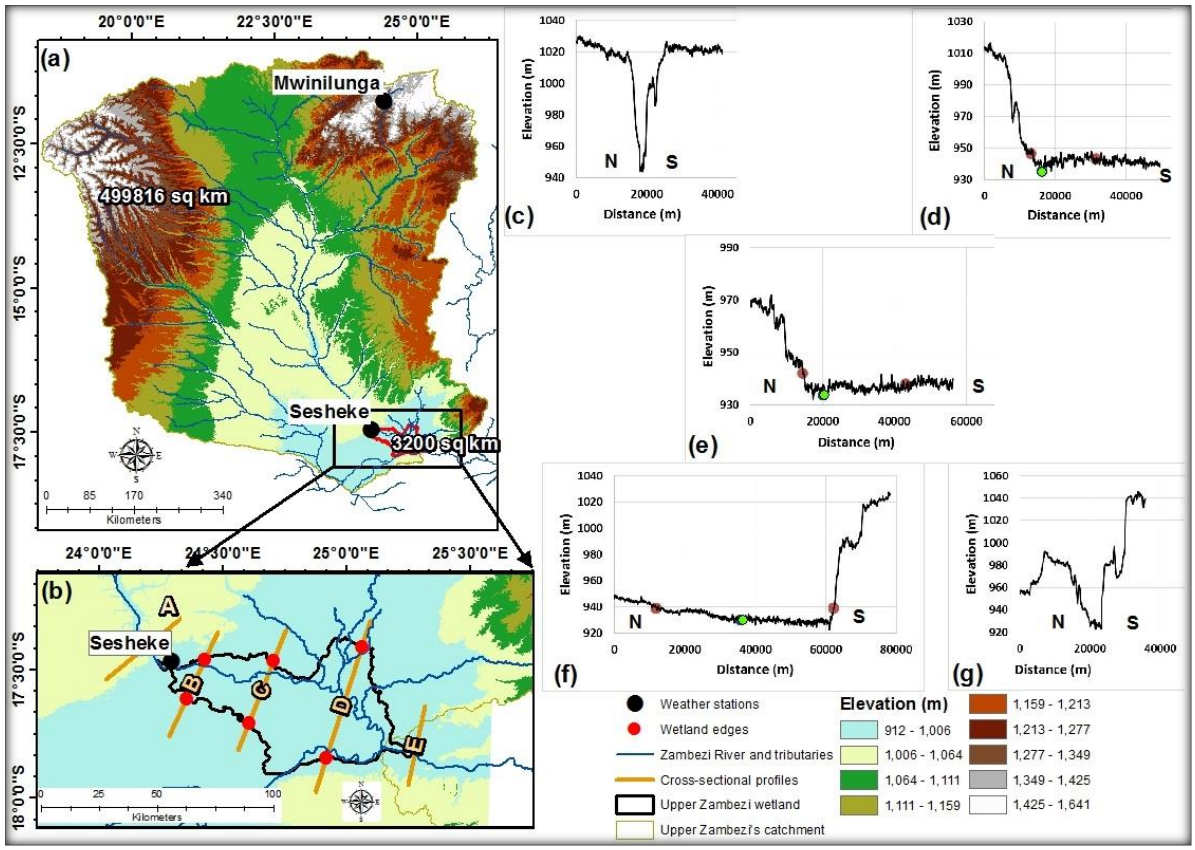

Figure 7.4.2: The topographic characteristics of the Upper Zambezi wetland, its catchment area, and the location of weather stations ((a) and (b)). Graphs (c) to (g) show cross-sectional profiles of lines A-E respectively.

The analysis of potential evapotranspiration and rainfall for the two nearby weather stations within the catchment shows that the catchment is characterised by high annual evapotranspiration and low annual rainfall for between 7 and 9 months of the year (Figure 7.4.3a and b). Furthermore, the analysis of the climatic parameters from the two weather stations show that rainfall within the catchment and the wetland area commences around September, peaks around January to March, and ends around May.

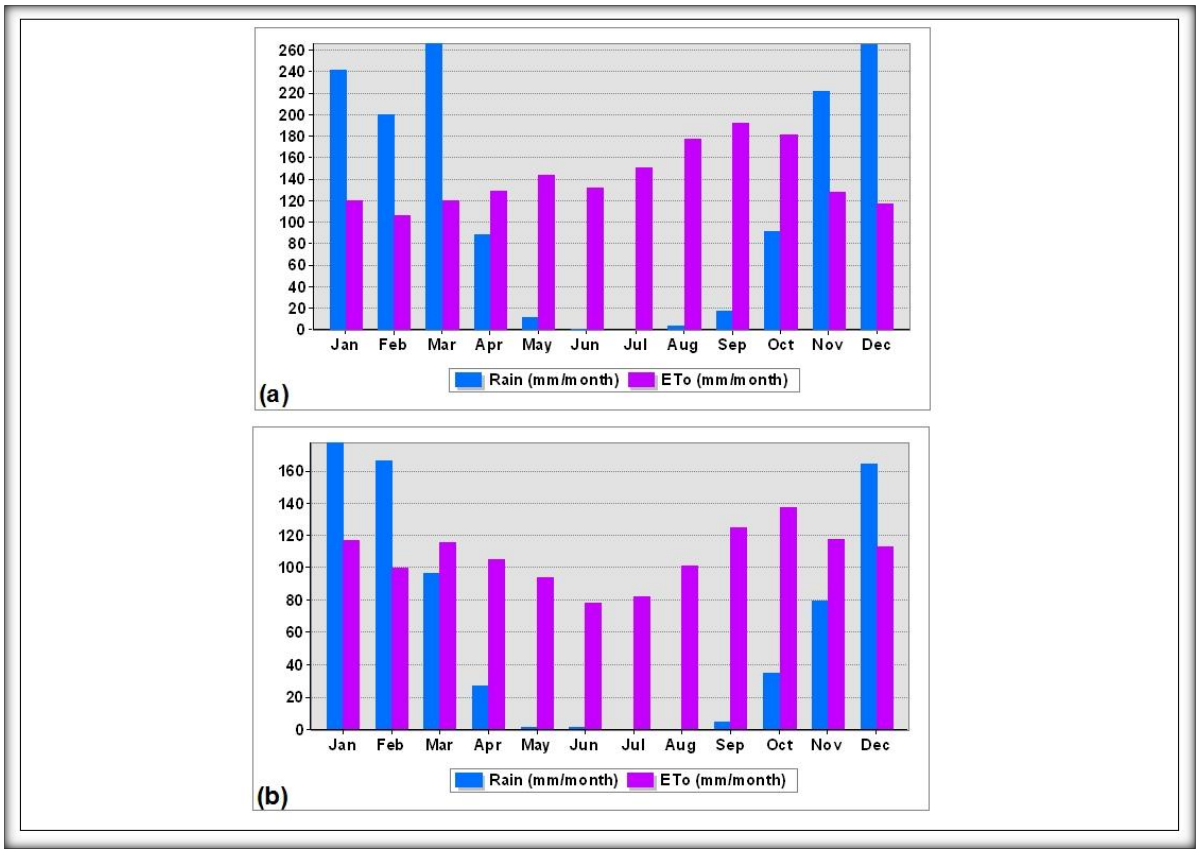

Figure 7.4.3: Monthly rainfall and potential evapotranspiration rates for Mwinilunga (a) and Sesheke (b) weather within the Upper Zambezi wetland catchment.

The LandsatLook images of the saturation characteristics of the wetland show that the Upper Zambezi wetland is dry in October at the start of the rainy season and flood extent peaks around May towards the end of the rainy season (Figure 7.4.4a and b). The lag between peak rainfall and peak wetland inundation may also be influenced by the attenuating effect of the Barotse wetland that is located upstream along the Zambezi River and the Linyanti wetland that is located along the Cuando River, which is the major eastward-flowing tributary of the Zambezi River in Namibia.

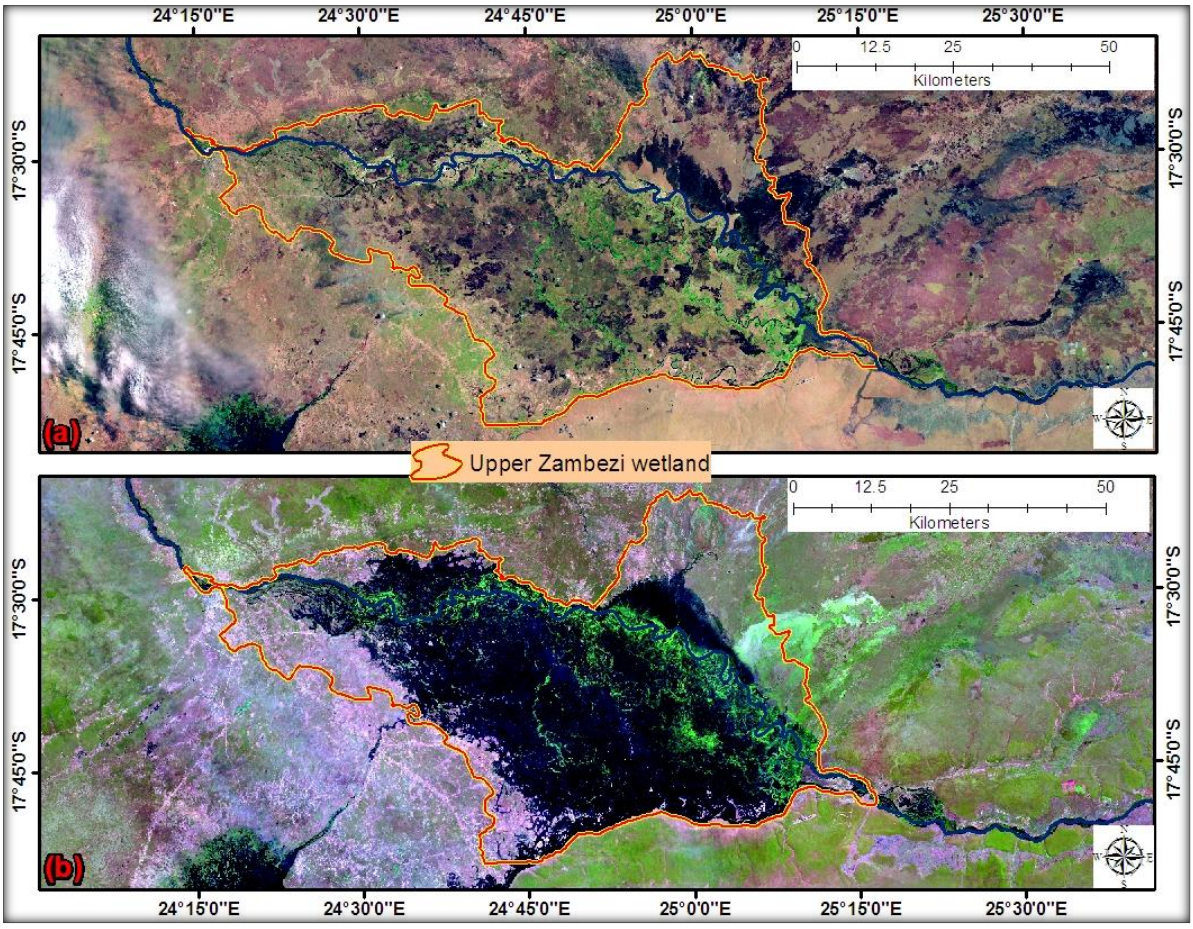

Figure 7.4.4: The mosaics of LandsatLook images depicting the saturation condition of Upper Zambezi wetland. The wetlands saturation conditions on 17 and 24 October 2013 (a), and 13 and 20 May 2014(b).

7.4.2 Geomorphology of the Upper Zambezi wetland

As highlighted previously from the Zambezi River's longitudinal profile (Figure 6.3.5 in section 6.3.2), the Upper Zambezi wetland occurs downstream of the Barotse wetland along the Zambezi River. The toe of the Upper Zambezi wetland coincides with what appears to be a small topographic step that coincides with the Mambova Rapids.

The analysis of valley cross-sectional profiles within the lower reaches of the wetland and the areas below the toe of the wetland shows that valley widths are broad and unconfined within the wetland while they are narrow and confined below the wetland (Figure 7.4.5a and a1 to a5). Within the wetland the river appears to be anastomosing and straightens below the wetland (Figure 7.4.5a). Topographic profiles (b1) and (b3) show that the wetland is confined by steep escarpments to the north-west and south-east while (b2) shows that the Zambezi River has incised the south-eastern escarpment at the outlet.

Before the Zambezi River enters the wetland, the Zambezi River and its tributaries drain a large area overlain mainly by the Kalahari Group (Nk) of a combination of unconsolidated aeolian sand and consolidated sedimentary rocks such as sandstone and limestone. There are also extensive Quaternary sediments (Qa) of unconsolidated sedimentary material such as gravel and sand (Figure 7.4.6a). The upper reach of the wetland is underlain by the Kalahari Group while the lower reach overlies Quaternary sediments, which is unconsolidated recent sediment. There is a change in lithology at the toe of the wetland from unconsolidated sedimentary material (Qa) such as alluvium, sand, and gravel to the Lebombo Group (Jdr) of volcanic rocks such as basalt and rhyolite. The toe of the wetland also coincides with a NE-SW trending fault line, which suggests a degree of tectonic control that has exposed resistant Lebombo Group volcanics.

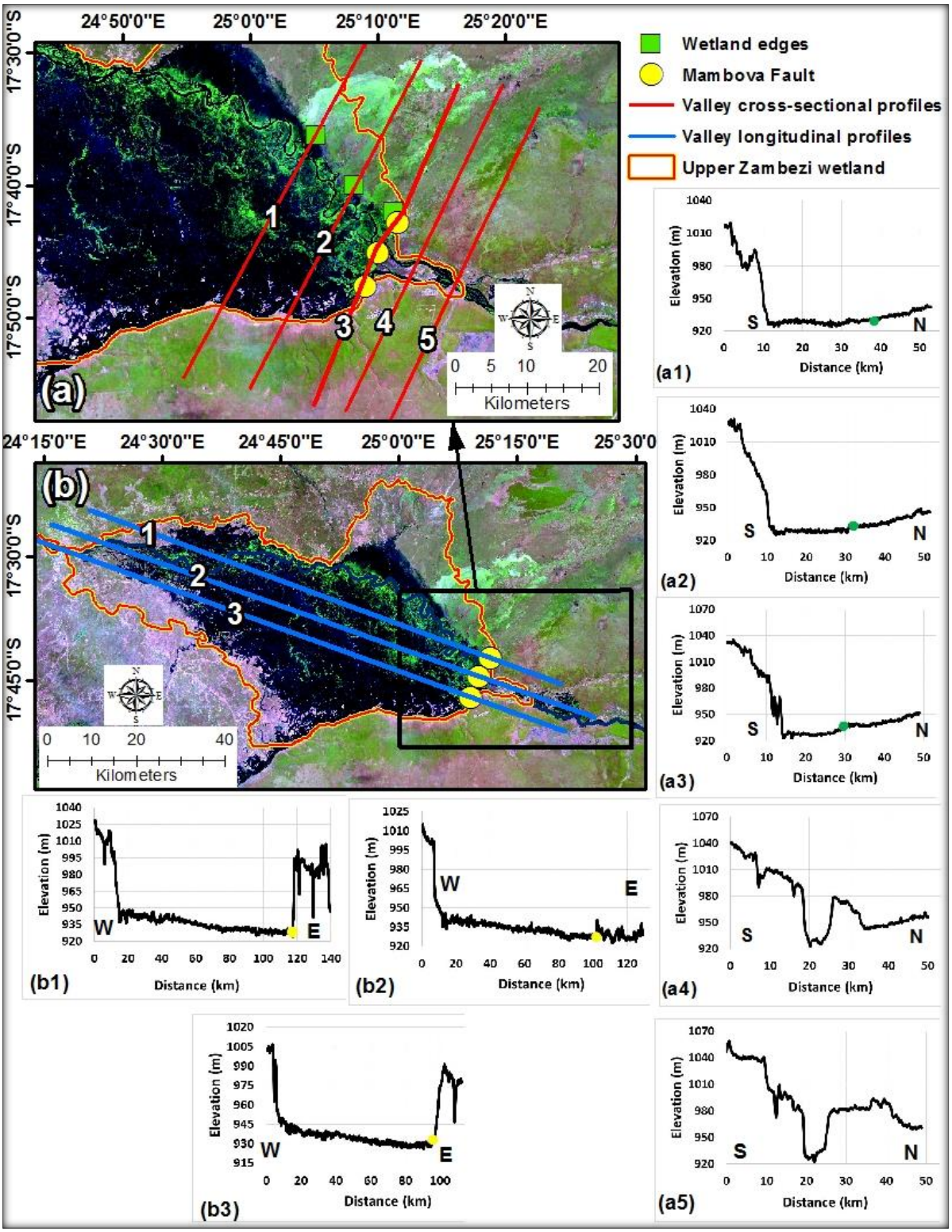

Figure 7.4.5: May 2014 LandsatLook images showing the valley cross-sectional characteristics within the lower reach (a) and cross-sectional profiles (a1)-(a5), and the valley longitudinal characteristic (b) and longitudinal profiles (b1)-(b3).

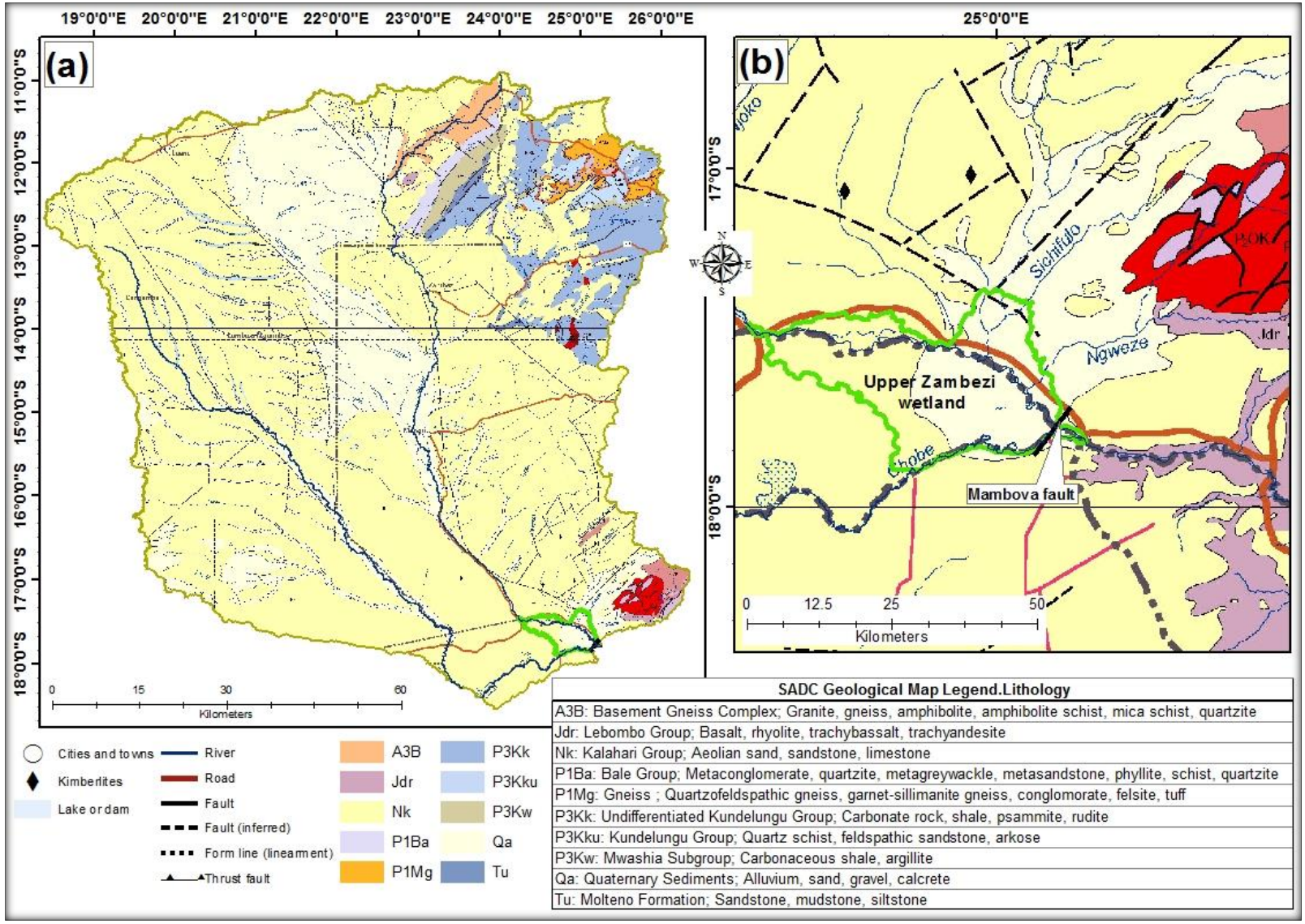

SADC Geological Map Legend.Lithology
A3B: Basement Gneiss Complex; Granite, gneiss, amphibolite, amphibolite schist, mica schist, quartzite
Jdr: Lebombo Group; Basalt, rhyolite, trachybassalt, trachyandesite
Nk: Kalahari Group; Aeolian sand, sandstone, limestone
P1Ba: Bale Group; Metaconglomerate, quartzite, metagreywackle, metasandstone, phyllite, schist, quartzite
P1Mg: Gneiss ; Quartzofeldspathic gneiss, garnet-sillimanite gneiss, conglomorate, felsite, tuff
P3Kk: Undifferentiated Kundelungu Group; Carbonate rock, shale, psammite, rudite
P3Kku: Kundelungu Group; Quartz schist, feldspathic sandstone, arkose
P3Kw: Mwashia Subgroup; Carbonaceous shale, argillite
Qa: Quaternary Sediments; Alluvium, sand, gravel, calcrete
Tu: Molteno Formation; Sandstone, mudstone, siltstone

Figure 7.4.6: The geological of the Upper Zambezi wetland catchment (a) and the area below the toe of the wetland (b).

7.4.3 The structure and hydrological functioning of the Upper Zambezi wetland

The analysis of the LandsatLook image (Figure 7.4.7a) and the valley cross-sectional profiles (Figure 7.4.7b to d) show that there are no floodplain features such as backwater depressions or alluvial ridges within the Upper Zambezi wetland. This is because the cross-sectional profiles within the upper, middle, and lower reaches of the Upper Zambezi wetland show that both the Zambezi and Cuando channels appear to be lower or at similar elevations to the surrounding wetland areas. The absence of alluvial ridges and backwater depressions suggests that floodwaters from the wetland can be easily lost to the river during the waning stages of the flood.

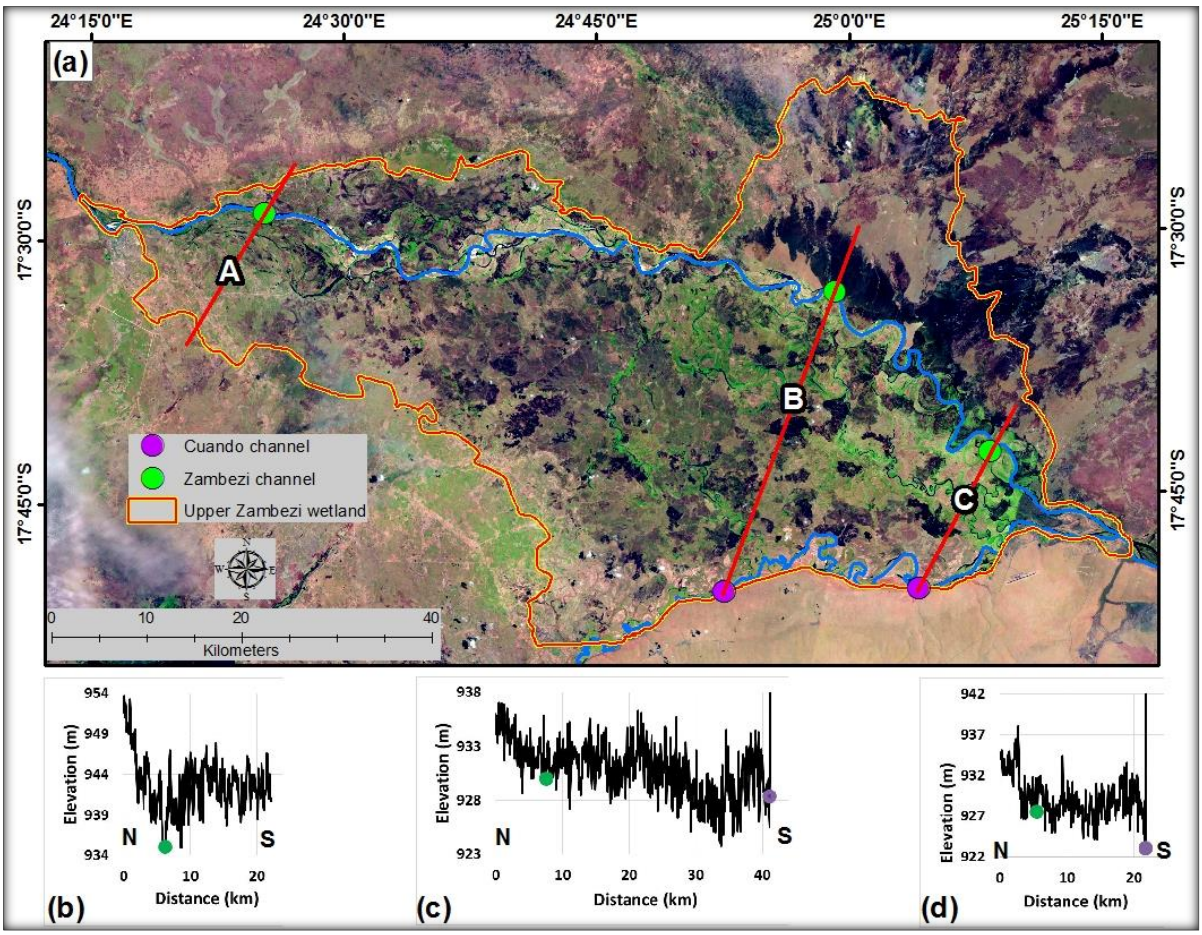

Figure 7.4.7: October 2013 LandsatLook image showing the valley cross-sectional characteristics of the wetland (a). Graphs (b) to (d) show cross-sectional profiles of transects A to C.

The elevations from the longitudinal profile (Figure 7.4.8a) and the channel length (Figure 7.4.8b) show that the wetland has a slope of 0.009%. Further analysis of characteristics of the Zambezi River's channel within the Upper Zambezi wetland revealed that the 150 km river flows within the 106 km long wetland valley with a sinuosity ratio of

1.4. The sinuosity ratio suggests that the river is not meandering, which is supported by the absence of depositional features such as alluvial ridges and backwater depressions (Figure 7.4.8b). The Google Earth image suggests that the Zambezi River within the Upper Zambezi wetland is characterised by deposition, and the channel does appear to divide and re-join, suggesting that it is anastomosing (Figure 7.4.8c).

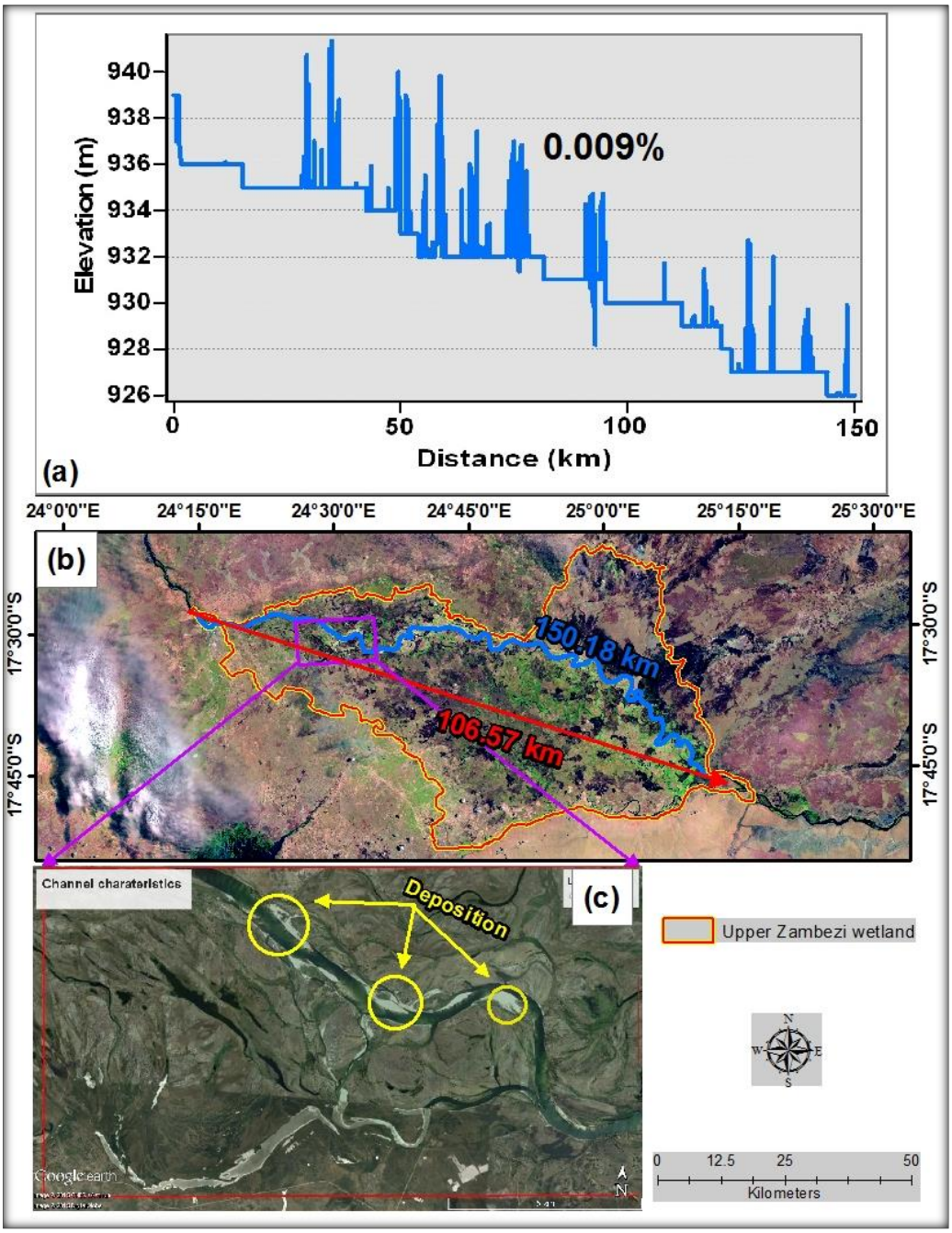

Figure 7.4.8: Characteristics of the Upper Zambezi wetland including the longitudinal slope of the river within the wetland (a), the total length of the wetland (red line), the total length of the river within the wetland (blue line; (b)), and Google Earth image showing deposition in the upper section of the wetland (c). The main image is a mosaic of 17 and 24 October 2013 LandsatLook images.

The analysis of wetland average depth of inundation for the upper and lower reaches of the wetland shows that the average depth of inundation is higher within the lower reach compared to the upper reach (Figure 7.4.9). For both reaches the average depth of inundation is generally lower than the channel stage heights, which suggests an absence of levees and alluvial ridges down the length of the wetland.

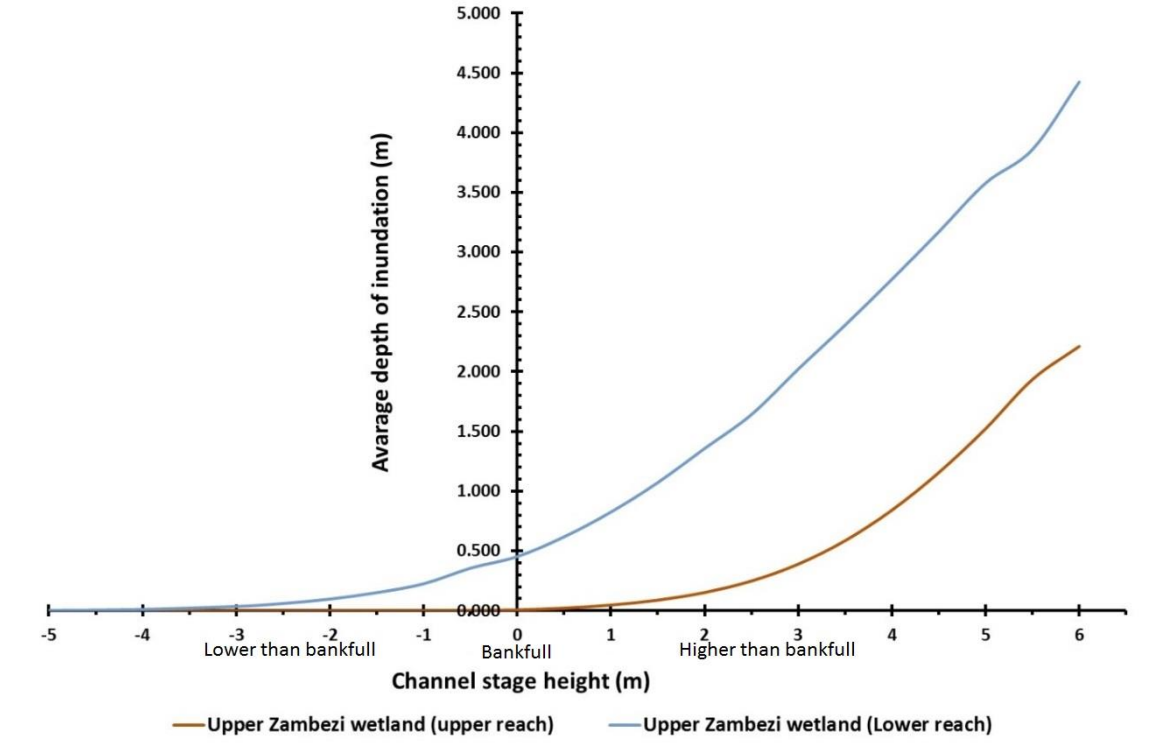

Figure 7.4.9: Comparison of the average depth of inundation within two distinct reaches of the wetland. The "0" depth represents channel water level while the positive and negative depths represent channel inundation height above and below channel bankfull stage respectively.

7.5 Discussion

The three wetlands (i.e. the Luapula, Kafue and Upper Zambezi wetlands) occur within catchments characterised by a negative surface water balance and occupy between 0.6 to 3.03% of their catchment areas. The small percentages of the catchment occupied by the wetland, the negative surface water balance and the observed 1 to 3 months lag between peak local rainfall and peak wetland inundation suggest that streams that drain the catchment area are likely to be responsible for maintaining these wetlands hydrologically.

The Luapula wetland occurs upstream of Lake Mweru and its formation appears to be associated with formation and evolution of Lake Mweru that formed as a result of local warping in the late-Tertiary (Dixey, 1944). The observed arrangement of fault lines to the east and west of Lake Mweru substantiate its tectonic origin. Subsequent to its formation,

Lake Mweru is believed to have been larger than it is today with its coverage extending southward to the area that is the Luapula wetland. In the early Pleistocene, tectonic activities associated with the second uplift event could have lowered the base level of the Luvua River downstream of Lake Mweru (Dixey, 1944; Cotterill, 2004). Over time, the Luvua River eroded headward capturing and draining the palaeo-lake to its present-day water level. The partial drainage of the palaeo-lake lowered the base level of its southern tributary stream (i.e. the Luapula River) such that the tributary incised into the palaeo-lake bed to the south (Dixey, 1944). Incision into the palaeo-lake bed as a result of falling lake water level can be substantiated by the observed islands within the Luapula wetland. Headward erosion of the Luapula River progressed until the river captured the Chambeshi River severing the connection between the Chambeshi and Kafila Rivers (Dixey, 1944; Cotterill, 2004). The capture of the Chammbeshi River by the Luapula River could have increased the amount of sediment supplied to the previously incised valley and lake downstream (Hughes and Hughes, 1992; Cotterill, 2004). Increased sedimentation within the southern parts of the lake could have resulted in gradual elevation of the base level of the Luapula River and ultimately led to the formation of Luapula wetland.

The Upper Zambezi wetland also known as Sesheke Maramba floodplain (Hughes and Hughes, 1992) has a fault line at the toe of the wetland that is coincident with a small but marked ridge downstream of the wetland, suggesting that the wetland could be tectonically controlled. The wetland appears to be a remnant of Lake Palaeo-Makgadikgadi (Nugent, 1990) that formed from faulting subsequent to the first (~30 Ma) uplift event (Stankiewicz and de Wit, 2006; Moore et al., 2007). Headward erosion of the Zambezi River is believed to have breached the Mambova Fault and led to the desiccation of Lake Palaeo-Makgadikgadi (Moore et al., 2007). The desiccated Lake Palaeo-Makgadikgadi was replaced by the Upper Zambezi wetland. The geological map shows that the toe of the wetland is characterised by a change in lithology from Kalahari Group sediments to Lebombo Group volcanic rocks. The resistant lithology at the toe of the wetland was also observed by Thomas and Shaw (1991) who reported that the Mambova fault coincides with Karoo basalt. Basalt is more resistant to weathering and erosion than the Kalahari sediments, such that erosion of the valley is limited in an upstream direction. Therefore the Tooth et al. (2002) model may explain the origin of the wetland, except that the absence of meandering streams in the Upper Zambezi wetland suggests that the model will need to be modified given that lateral planing of the valley floor in this case is not due to the lateral migration of a meandering stream.

Geological factors similar to those responsible for the formation of the Upper Zambezi wetland can best describe the formation of the Kafue wetland. Downstream of the Kafue wetland, a resistant lithology in the form of the Muva Group metavolcanic rocks dominates the narrow Kafue Gorge that is characterised by straight channels. Upstream of the gorge and underlying the Kafue wetland with a low channel gradient of 0.0008% is the more easily eroded Kalahari Group sediments. The low channel slope of the Kafue wetland suggests that the resistant lithology acts to prevent headward erosion of the Kafue River into the wetland, but it seems to play little role in structuring the wetland through base-level induced upstream slope adjustment and valley widening, as described in the Tooth et al. (2002) model. This is because streams strive to maintain a longitudinal slope appropriate for the available discharge. If the slope is too low for a given discharge a stream increases its slope through deposition, but if the slope is too high for the discharge a stream lowers the slope through erosion such that the longitudinal slope is appropriate for the discharge down the length of the valley (Leopold and Maddock, 1953; Ellery et al., 2009). Therefore, the 0.0008% channel gradient observed within the middle and lower Kafue wetland is unexpectedly low for a wetland of this size, raising the question as to whether the slope is a consequence of fluvial processes.

The analysis of the topographic settings around the Kafue and Upper Zambezi wetlands in relation to the south-westward extending arm of the East Africa Rift System shows that rifting could have significantly influenced local slopes and ultimately shaped the formation of the two wetlands (Figure 7.4.10). The topographic profiles of the section that is oriented sub-parallel with the wetland to the north of the Kafue (Figure 7.4.10b and c) and Upper Zambezi wetlands (Figure 7.4.10b and d) show that the wetlands occupy depressions to the east of the uplifted shoulders of the rift valleys. The observed fault lines that intercept the topographic profile to the north of the Kafue wetland (Figure 7.410b and c) suggest a tectonic influence on the topographic characteristics around the wetland. Therefore, coupled with faulting, the uplifted margin of the Luangwa-Kariba rift valley could have played a role in reducing local slopes to the west of the uplifted rift margin and thus led to the formation of the basins that now host the Kafue and Upper Zambezi wetlands.

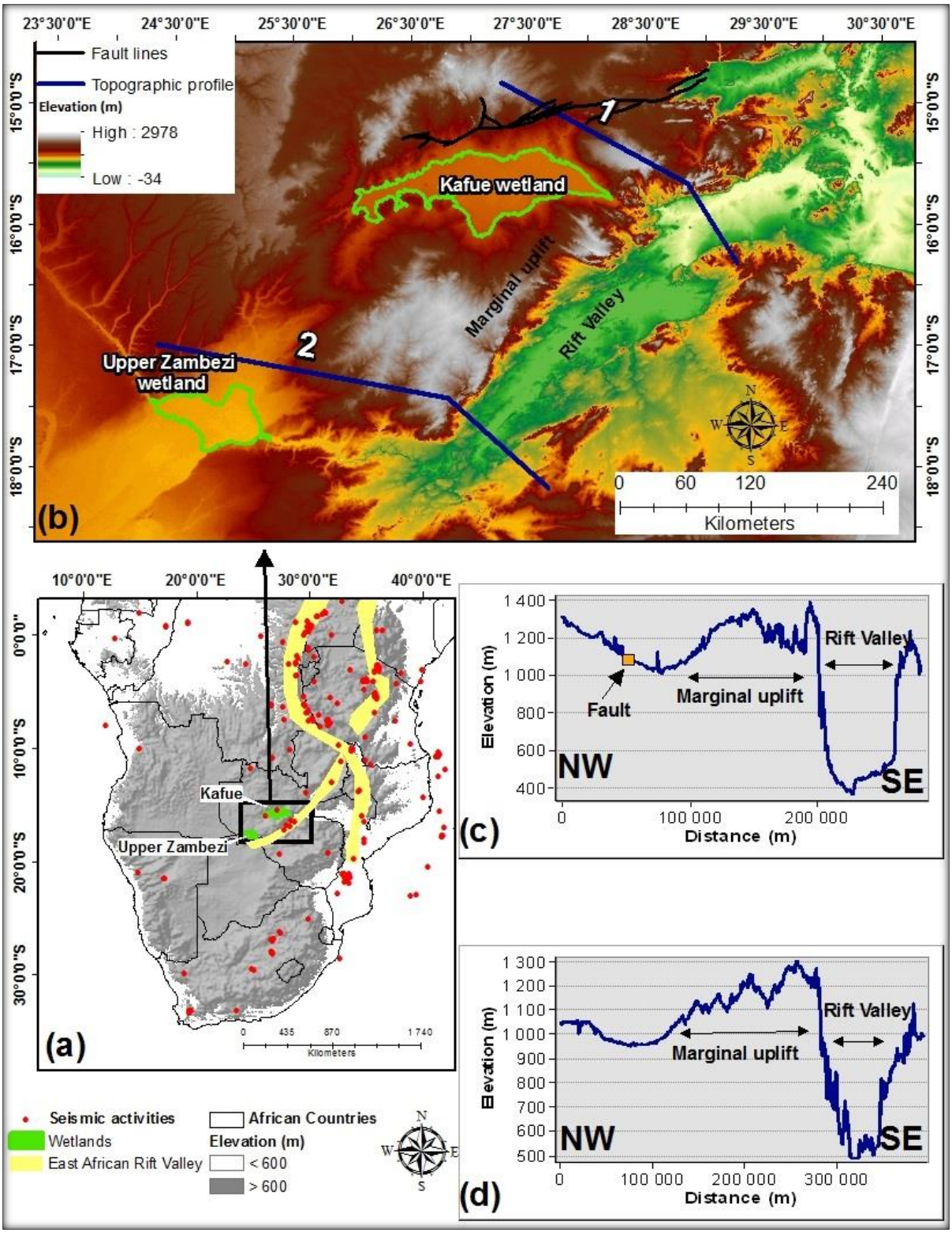

Figure 7.4.10: The location of the Kafue and Upper Zambezi wetlands in relations to the East African Rift System (a), the topographic characteristics around the Kafue and Upper Zambezi wetlands (b), and topographic profile graphs (c) and (d) for lines 1 and 2 in (b) respectively.

CHAPTER 8: THE ORIGIN AND HYDROLOGICAL FUNCTIONING OF TECTONICALLY CONTROLLED DEPRESSION WETLANDS

8.1 Introduction

The wetlands presented in this chapter are depression wetlands with no clearly defined trunk stream running through the wetland, therefore ruling out the possibility of their origin being related to the role of fluvial systems in shaping the landscape. These include the Wembere, Bahi, and Usangu wetlands. These wetlands can be further discriminated based on the level of basin modification through fluvial processes as these wetlands vary from channelled to unchannelled wetlands. For unchannelled wetlands such as the Bahi and Wembere wetlands, the average depth of inundation for a given channel stage height was not computed. With the exception of the Lukanga wetland that is part of the Zambezi basin, these wetlands occur within graben structures that are bounded by fault lines. The Bahi and Wembere wetlands form part of endorheic basins and have no influence on downstream discharges. The Usangu is part of the Rufiji River catchment.

8.2 The Wembere wetland

The Wembere wetland is located about 100 km west of the town of Singida in Tanzania and lies between latitudes 04°01’S and 05°15’S and longitudes 34°00’E and 34°02’E (Figure 8.2.1). The Wembere wetland is bounded by the Iramba plateau to the east and an escarpment to the west. The Wembere River drains the NE-SW trending wetland from the south-west to the north-east before discharging into the endorheic Lake Eyasi to the north-east of the wetland. The wetland is connected to a number of streams that emanate from the surrounding uplands. To the north, the eastward flowing Manonga River and southward flowing Sanga River feed into the wetland while other short and seasonal streams enter the wetland from the surrounding uplands.

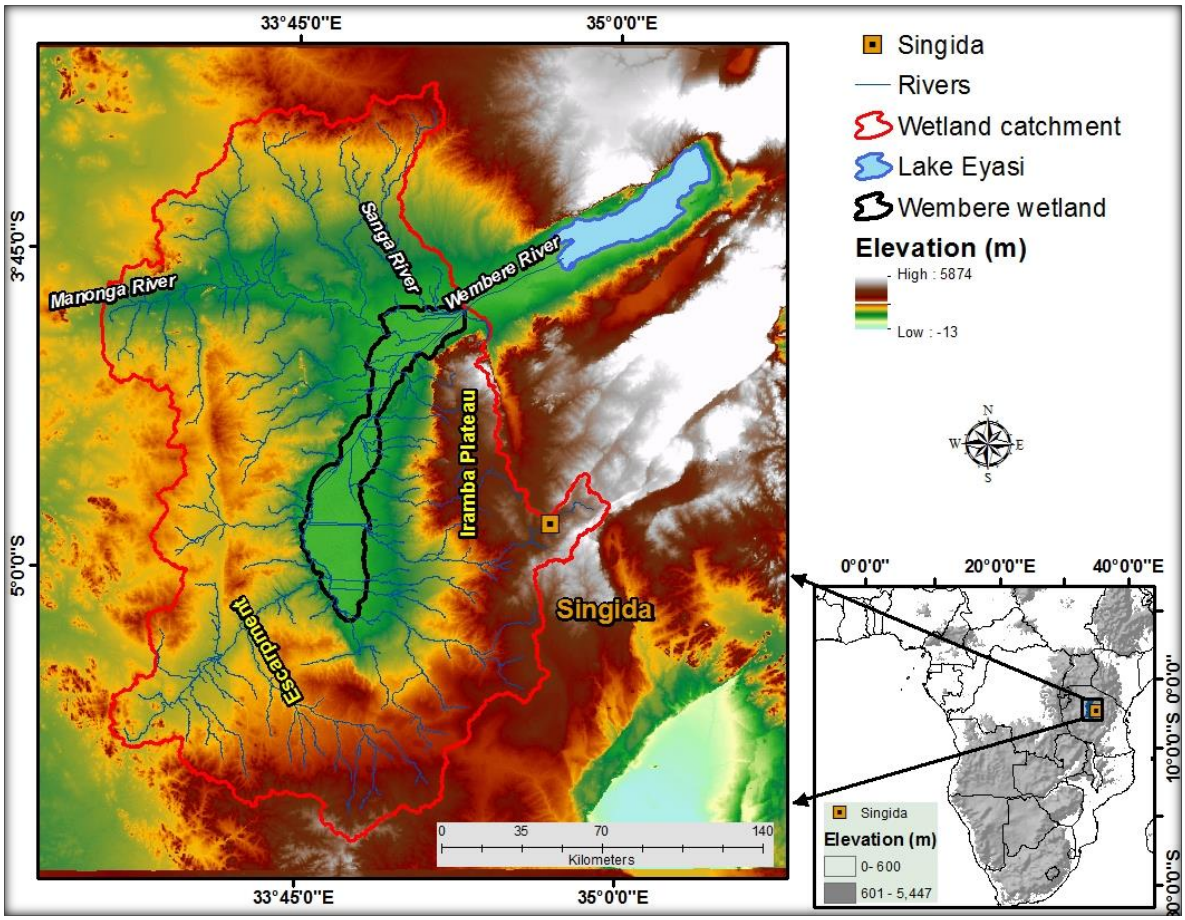

Figure 8.2.1: The location of the Wembere wetland in relation to the topographic setting of the wetland catchment and major rivers.

8.2.1 Hydrological conditions of Wembere wetland

From the wetland and catchment sizes, it appears that the 2 714 km^2 wetland covers 6% of its 42 678 km^2 catchment (Figure 8.2.2a). The cross-sectional profiles show that within the middle (Figure 8.2.2e) and upper reaches of the wetland, steep escarpments bound the wetland (Figure 8.2.2g and f).

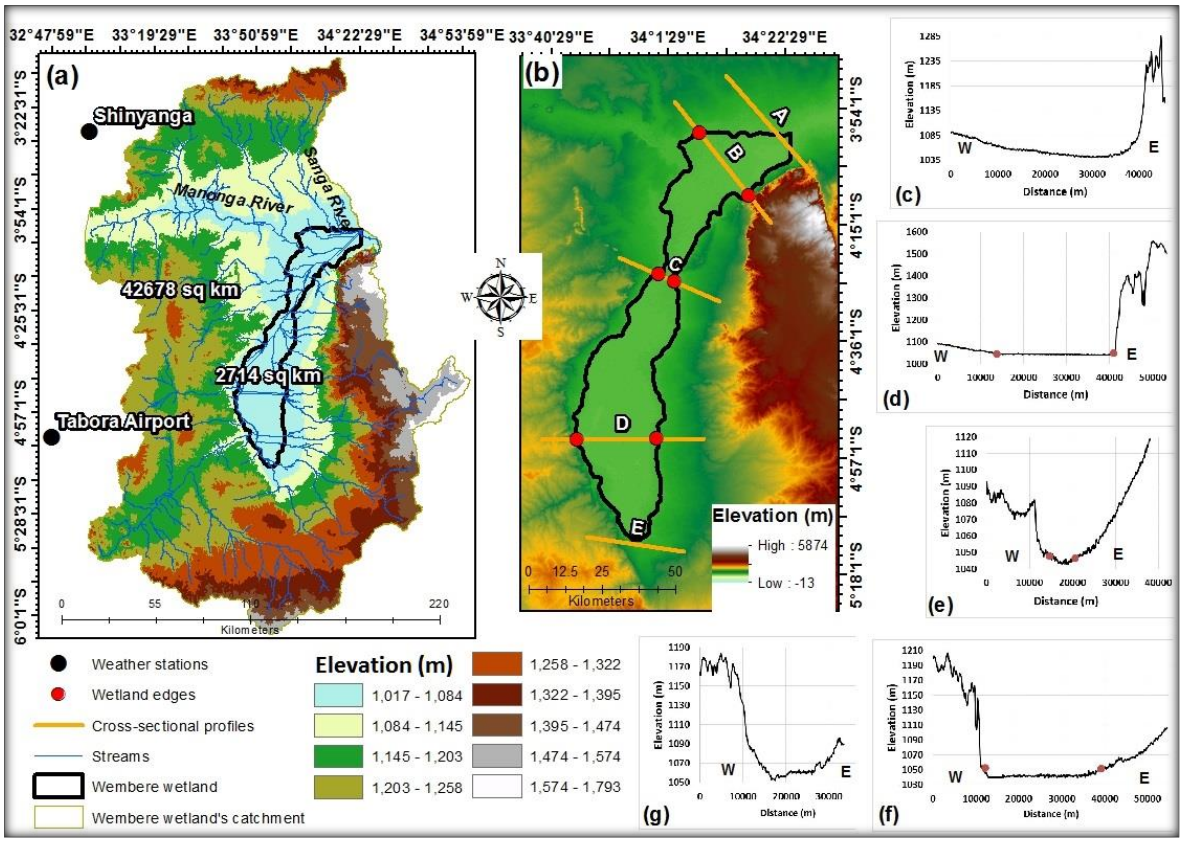

Figure 8.2.2: The location of weather stations and topographic characteristics of the Wembere catchment area (a) and valley (b). Graphs (c)-(g) show cross-sectional profiles at location A to E. W and E in the graphs indicate their West to East orientation.

Potential evapotranspiration greatly exceeds precipitation for 8 months of the year within the northern section of the Wembere wetland catchment (Figure 8.2.3a) and exceeds precipitation throughout the year within the southern section (Figure 8.2.3b). This means that there is a negative surface water balance for 8 months within the northern section and throughout the year within the southern section. The average monthly rainfall for the three months period from October to December is 120 mm for the northern section of the wetland and 60 mm for the southern section. The rainy season starts around September to October, peaks in December to March, and subsides from April to May (Figure 8.2.3a and b).

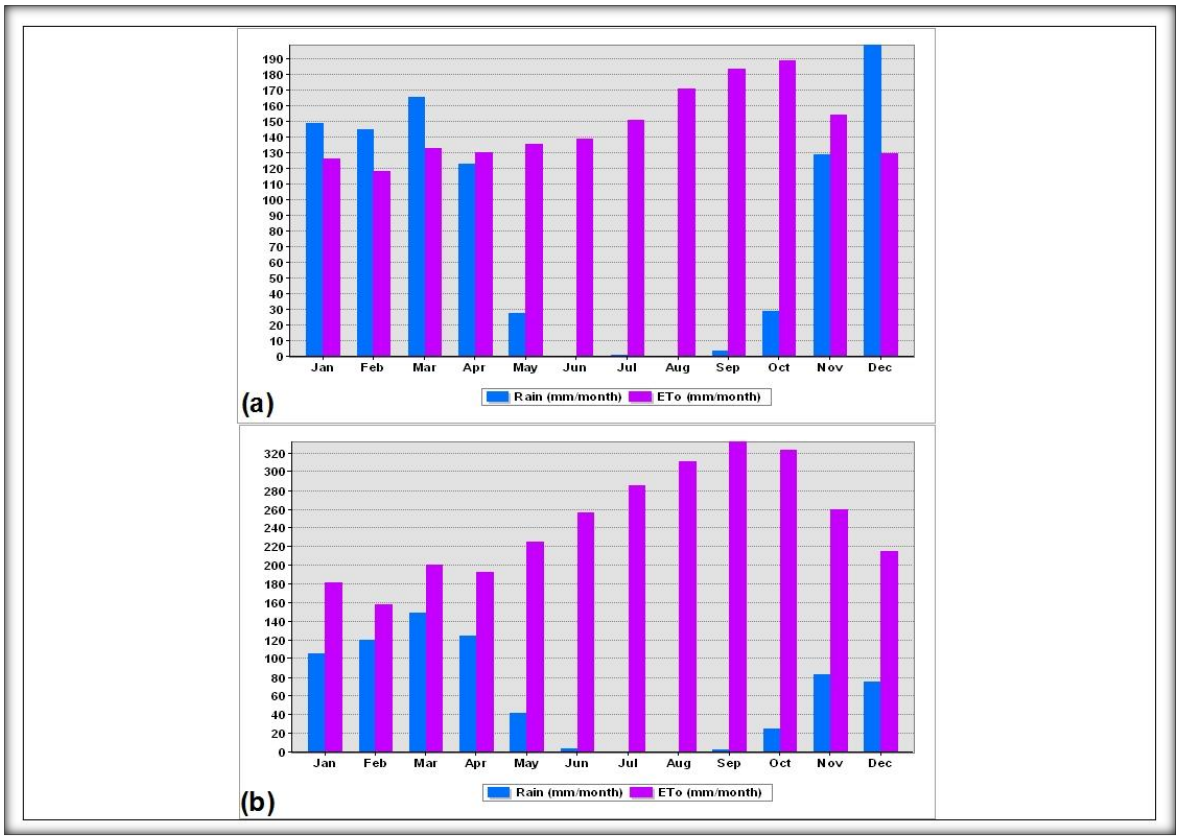

Figure 8.2.3: Monthly average rainfall and potential evapotranspiration for Tabora Airport (a) and Shinyanga (b) weather stations within the Wembere wetland catchment.

Visual interpretations of the LandsatLook images in Figure 8.2.4 show that the timing of peak flooding varies down the length of the wetland. The wetland is dry in September (Figure 8.2.4a). Flooding within the northern section of the wetland peaks in December when limited inundation is observed within the southern section (Figure 8.2.4b). Flooding within the southern section appears to peak in April, at which time the northern section of the wetland is drying (Figure 8.2.4). The flooding characteristics observed might be a reflection of climatic characteristics of the catchment since the northern section of the catchment shows high average rainfall from October to December compared to the southern section.

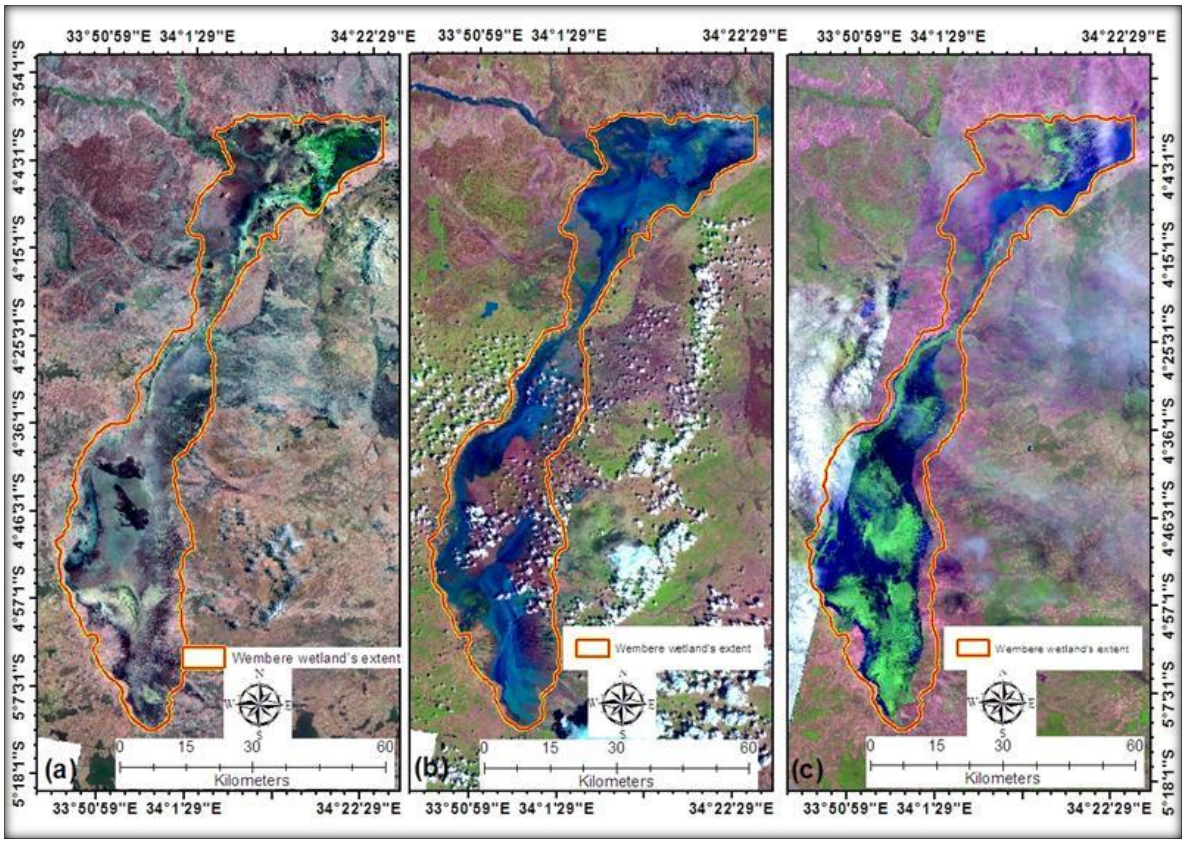

Figure 8.2.4: The map shows mosaics of LandsatLook images showing the saturation condition of Wembere wetland. With (a)-(c) showing the wetlands saturation conditions on 16 and 23 September 2006, 05 and 12 December 2006, and 03 and 28 April 2006 respectively.

8.2.2 Geomorphology and hydrological functioning of the Wembere wetland

The elevation profiles of lines A and B in Figure 8.2.5 show that the escarpments that bound the wetland depression to the west, north and south of the wetland coincide with fault lines. In addition there are a number of short streams, which enter the wetland from high-lying areas adjacent to the Wembere graben (Figure 8.2.5a).

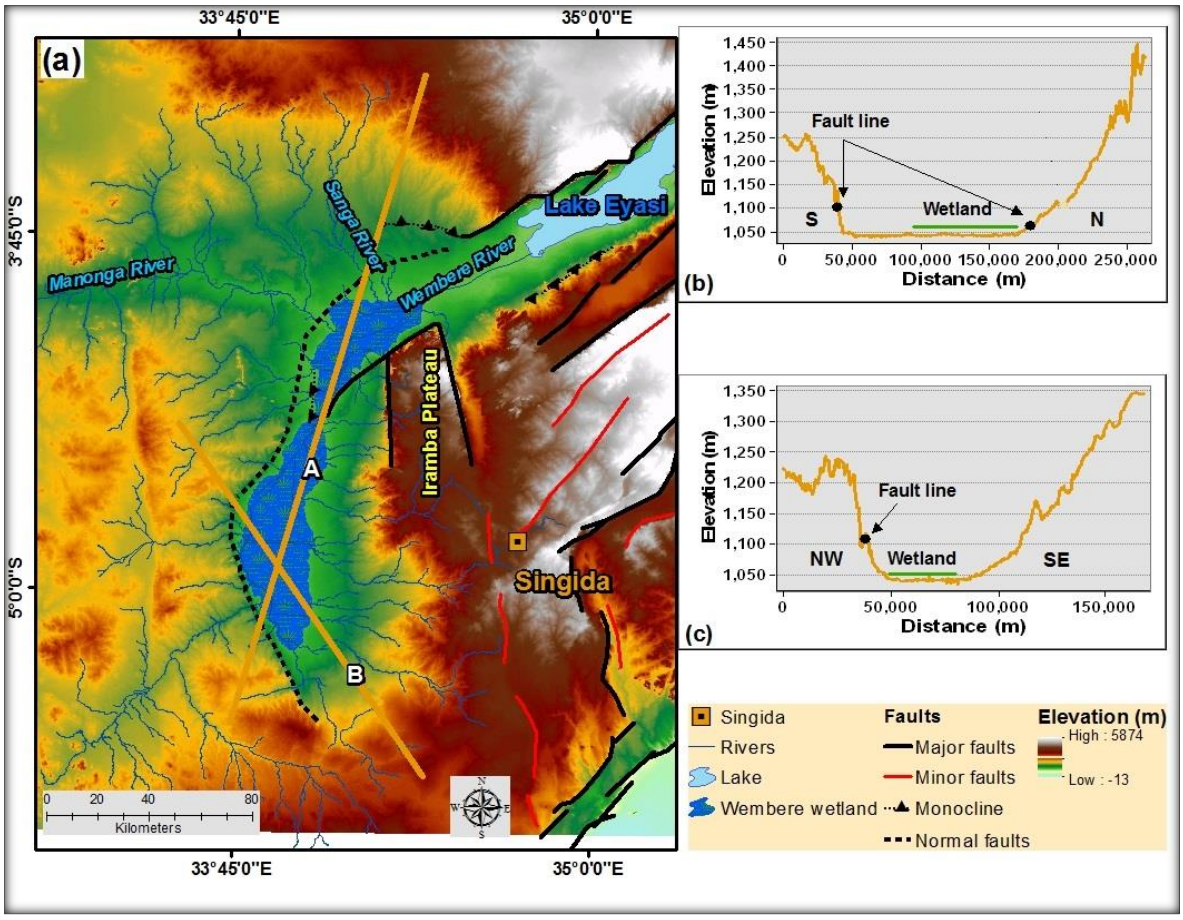

Figure 8.2.5: The topographic and geological characteristics of the Wembere wetland (a) with graphs (b) and (c) showing elevation profiles of lines A and B.

Cross-sectional profiles (b to f) in Figure 8.2.6 show alluvial fans occurring where tributary streams enter the southern section of the Wembere wetland.

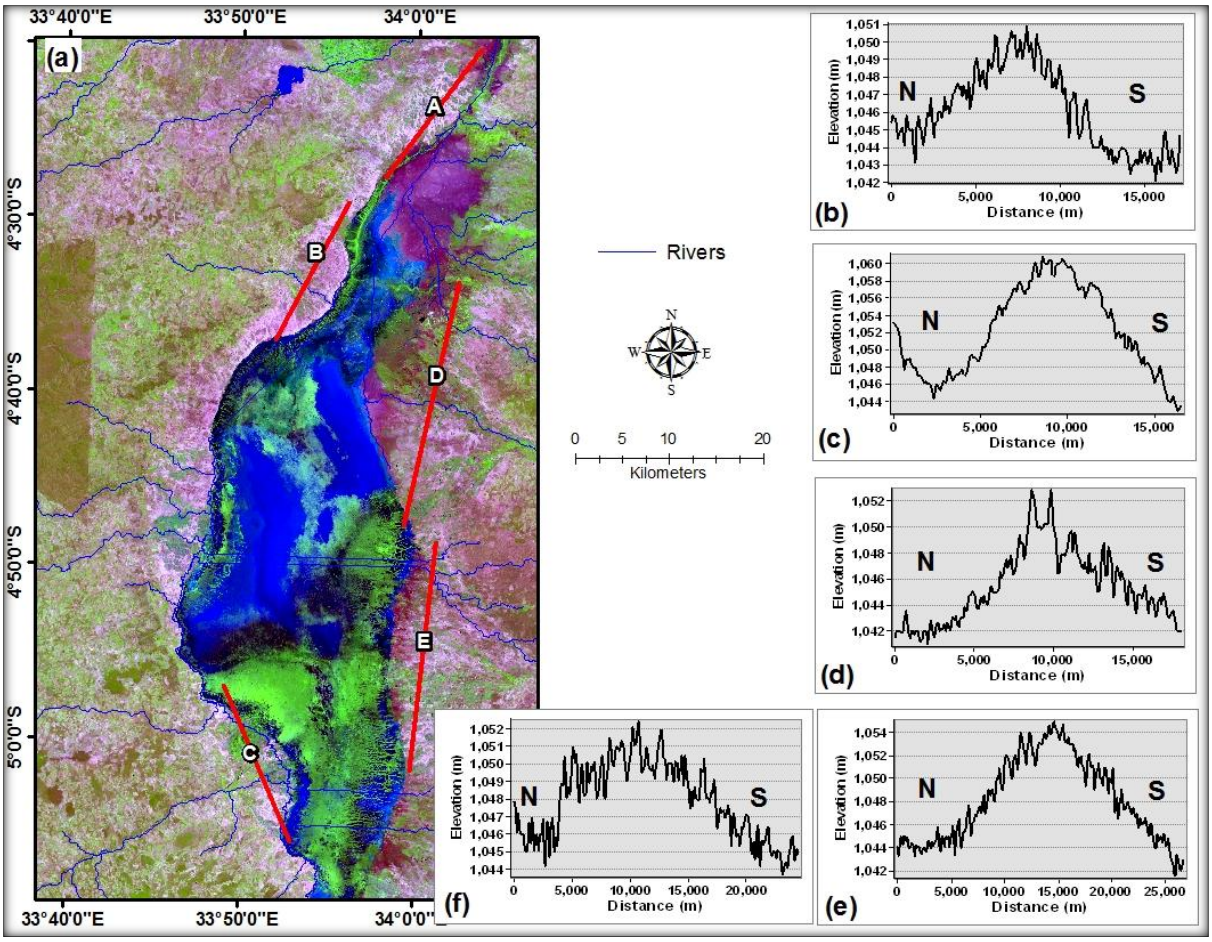

Figure 8.2.6: May 2016 LandsatLook image showing the southern section of the Wembere wetland (a). Graphs (b)-(f) show the elevation profile of lines A-E that cross the areas where tributary fans enter the depression in which the Wembere wetland is situated.

The geology of the catchment is largely composed of Seoka Adamellite (A_4Sg) volcanic rocks, Cenozoic Continental and Lacustrine Sedimentary Rock (Ncl), and Nyanzanian Supergroup (A_4PT) of a combination of volcanic (i.e. metalava) and metamorphic (chlorite schist) rocks (Figure 8.2.7). The wetland area comprises unconsolidated Quaternary sediments (Qa) of sand and gravel.

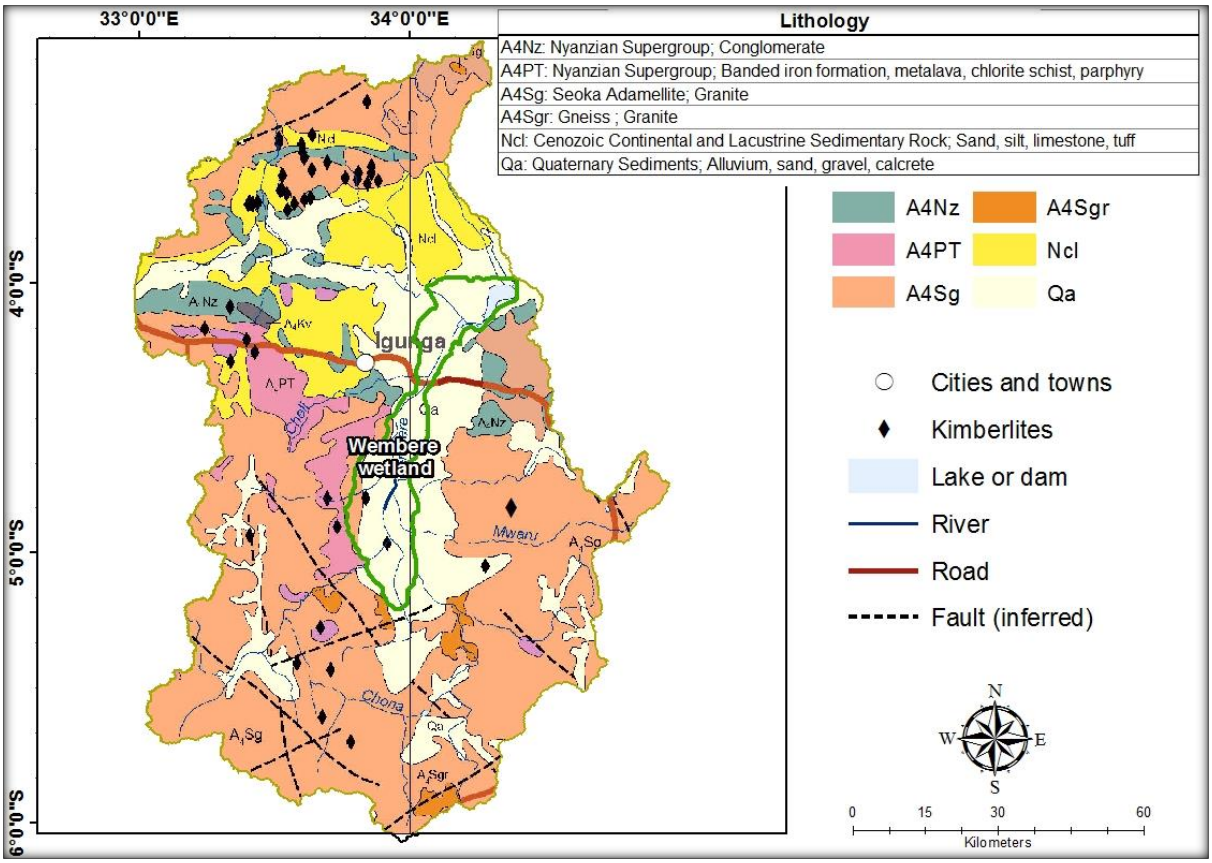

Figure 8.2.7: The geology of the Wembere wetland catchment and the colour-coded areas showing different lithology.

8.3 Bahi wetland

Bahi wetland is a shallow seasonal lake located between latitude 05°50'S and 06°15'S and longitude 35°02'E and 35°19'E, about 90 km west of the city of Dodoma in Tanzania (Figure 8.3.1). The endorheic wetland is fed mainly by the Bubu River and its tributaries that originate to the north-east of the wetland. However, the wetland also receives water from short streams that originate in the surrounding uplands.

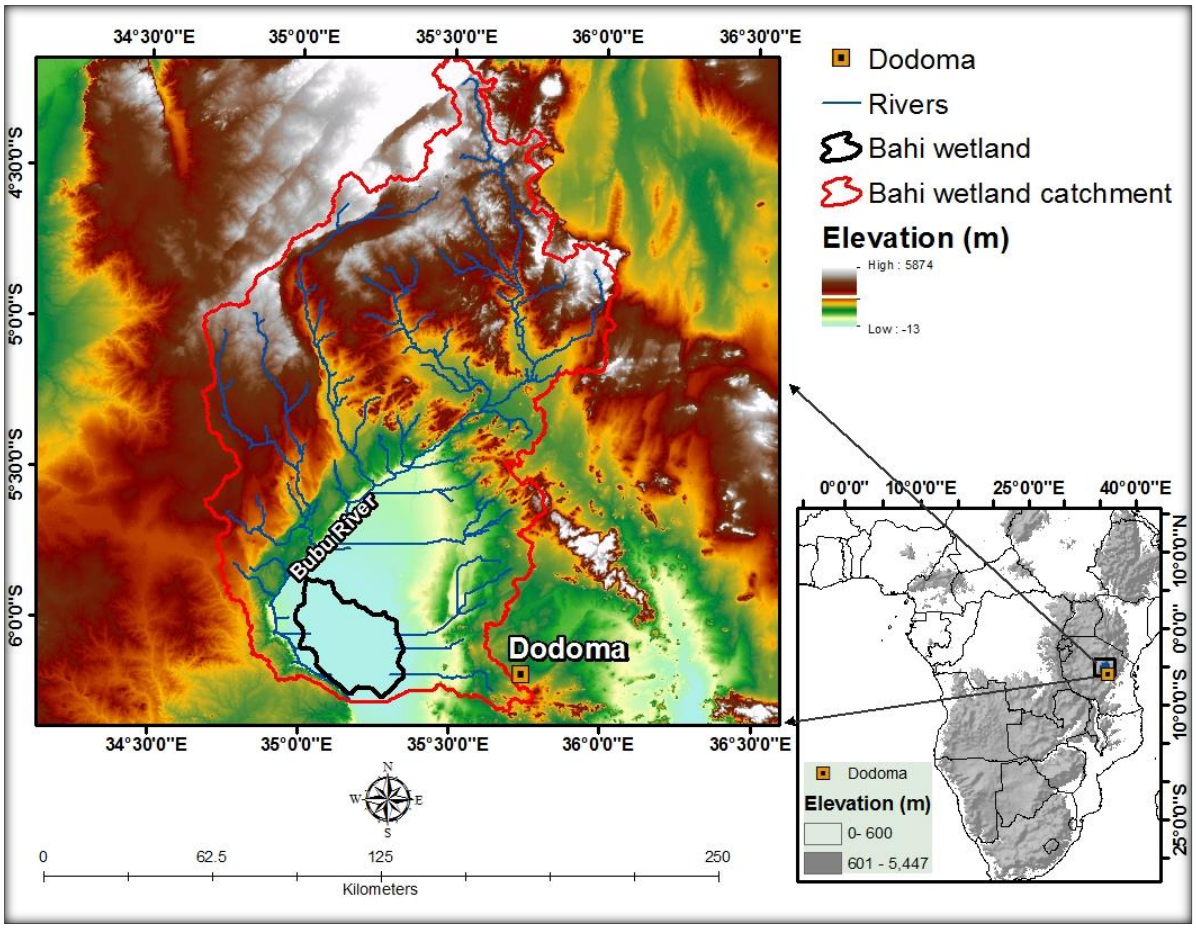

Figure 8.3.1: The location of the Bahi wetland in relation to the topographic settings of the wetland catchment and major rivers.

8.3.1 Hydrological conditions of Bahi wetland

The topographic characteristics of the wetland show that the wetland occupies a broad and relatively flat valley (Figure 8.3.2a and b). The 1 086 km^2 wetland occupies 4.98% of its 21 816 km^2 catchment. The valley appears to be broadly V-shaped upstream of the wetland (Figure 8.3.2c) and near-horizontal to horizontal along its length (Figure 8.3.2d to f).

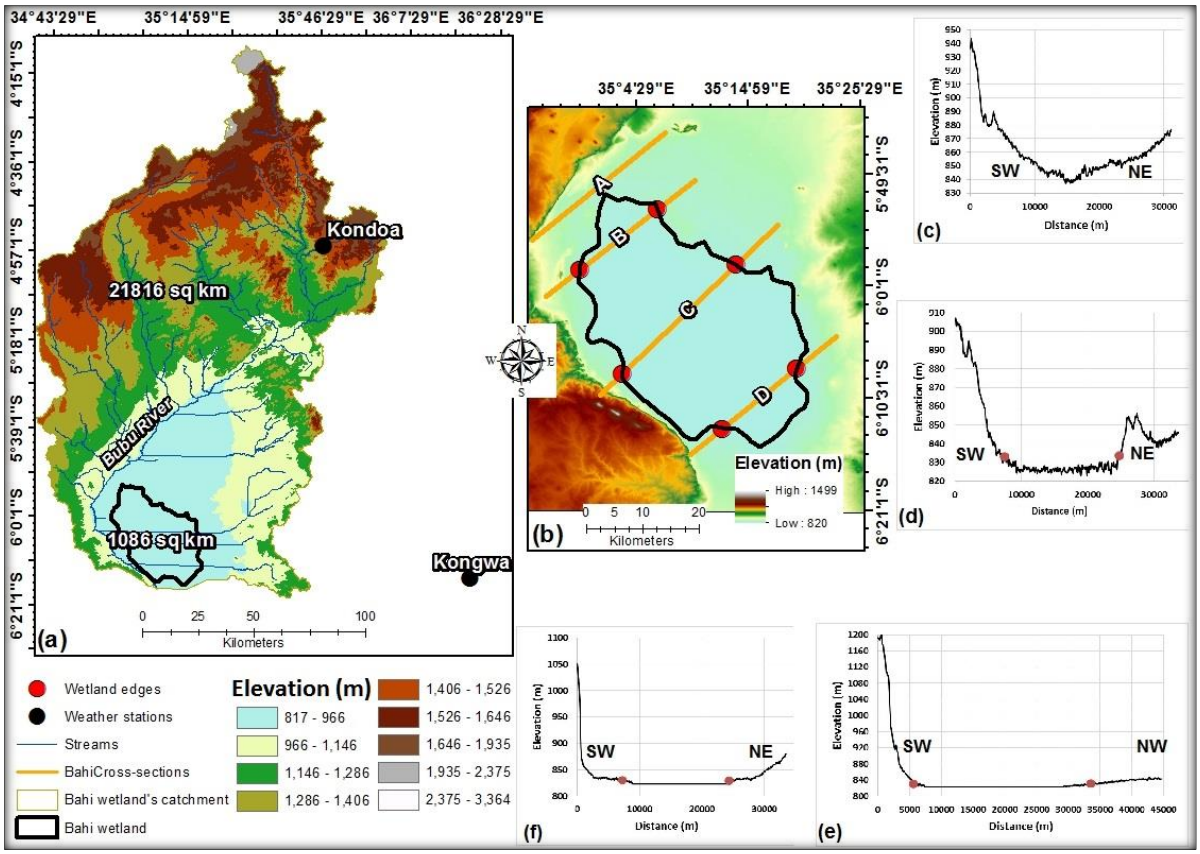

Figure 8.3.2: The location of weather station, topographic characteristics of the Bahi wetland catchment (a) and valley (b). Graphs (c)-(f) show cross-sectional profile at location A-D in the map. SW and NE in the graphs indicate their South-west to North-east orientation.

The two weather stations within and close to the Bahi catchment show that potential evapotranspiration greatly exceeds precipitation for at least 8 months of the year (Figure 8.3.3). This indicates a negative surface water balance within the catchment. Rainfall within and around the Bahi wetland catchment starts in November, peaks around January to March, and ends in May.

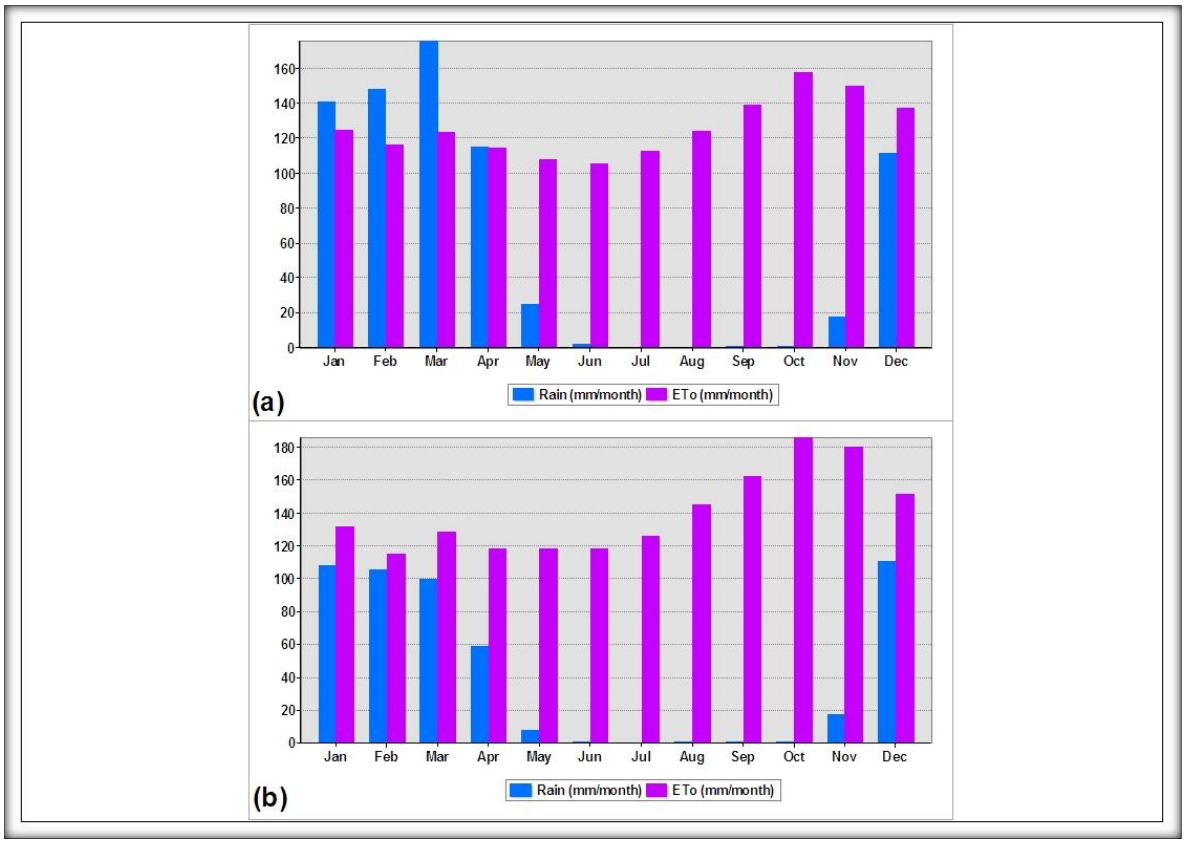

Figure 8.3.3: Monthly rainfall and potential evapotranspiration for Kondoa (a) and Kongwa (b) weather stations.

The LandsatLook images show that the wetland is dry in November at the onset of the rainy season (Figure 8.3.4a) and inundates to peak floods in April in the waning stage of the rainfall season (Figure 8.3.4b). Flooding of the wetland in April reflects the lag between peak precipitation, peak stream flows and wetland flooding.

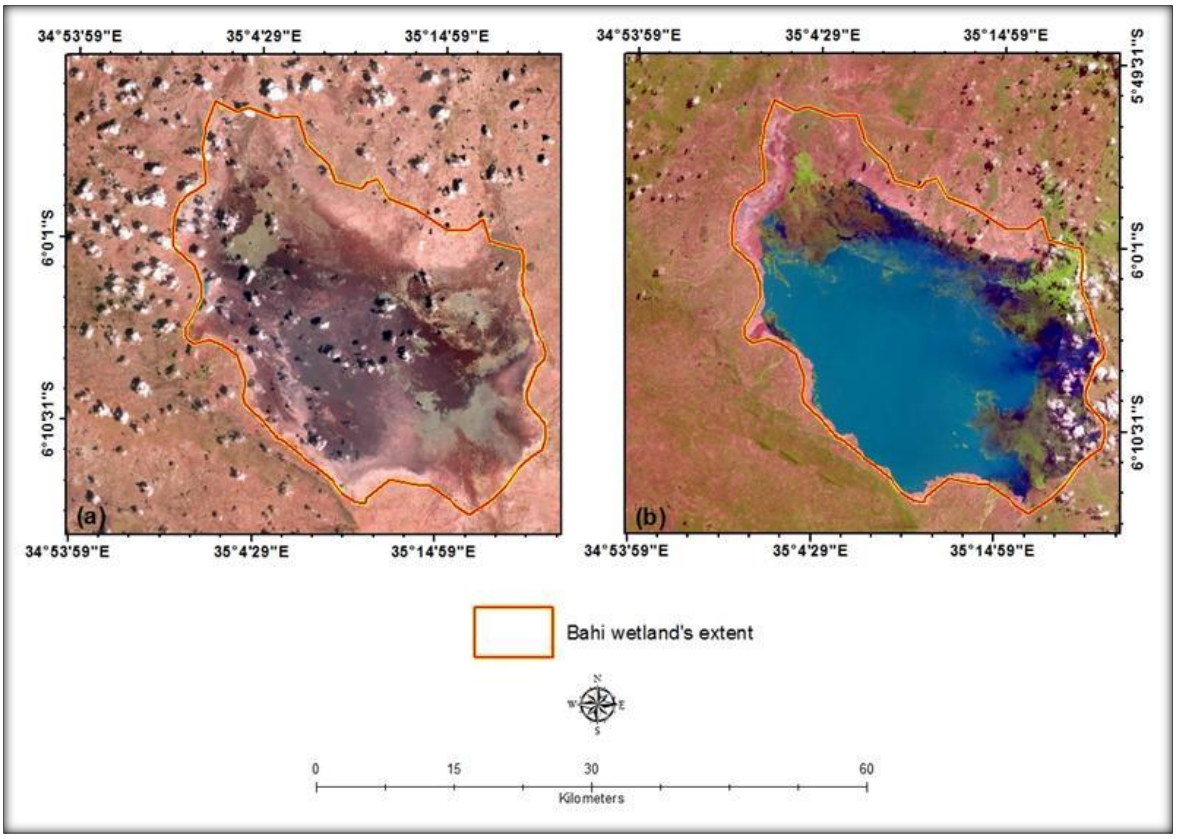

Figure 8.3.4: LandsatLook images showing the saturation condition of Bahi wetland on 02 and 19 November 2006 (a), and 05 and 28 April 2007 (b).

8.3.2 The geology and hydrology of the Bahi wetland

The geology of the Bahi wetland catchment is largely composed of volcanic rocks of the Seoka Adamellite (A_4Sg) and Undifferentiated Granitoid (A_4Sgn), as well as Migmatitic rocks of the Rusizian Complex (A_4Sc) and Migmatitic Gneiss (P_3Cm), while the wetland overlies unconsolidated Quaternary sediments (Qa; Figure 8.3.5).

The wetland appears to occupy a tectonically controlled depression (Figure 8.3.6a). The south-west to north-east and north-west to south-east elevation profile elevation profiles (Figure 8.3.6a and b) show that steep escarpments that bound the wetland valley to the south-west, north-east, north-west and south-east coincide with fault lines.

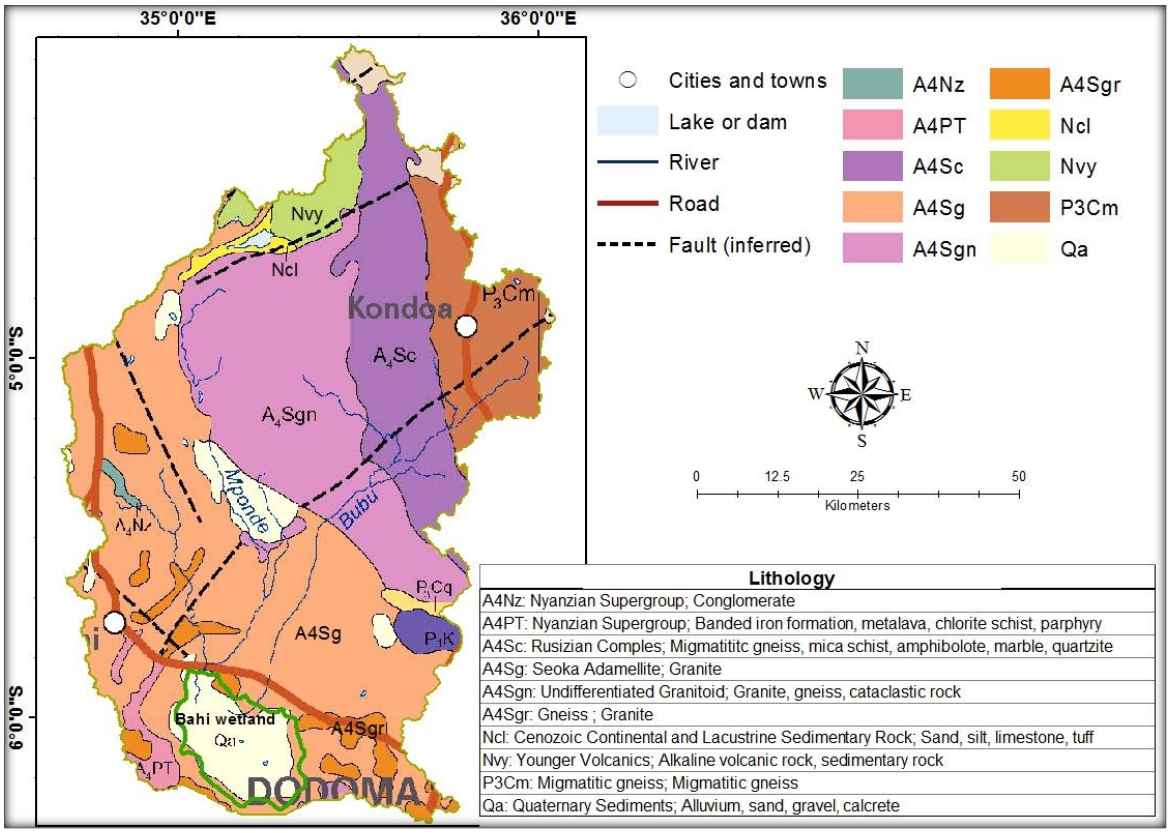

Figure 8.3.5: The geology of the Bahi wetland catchment.

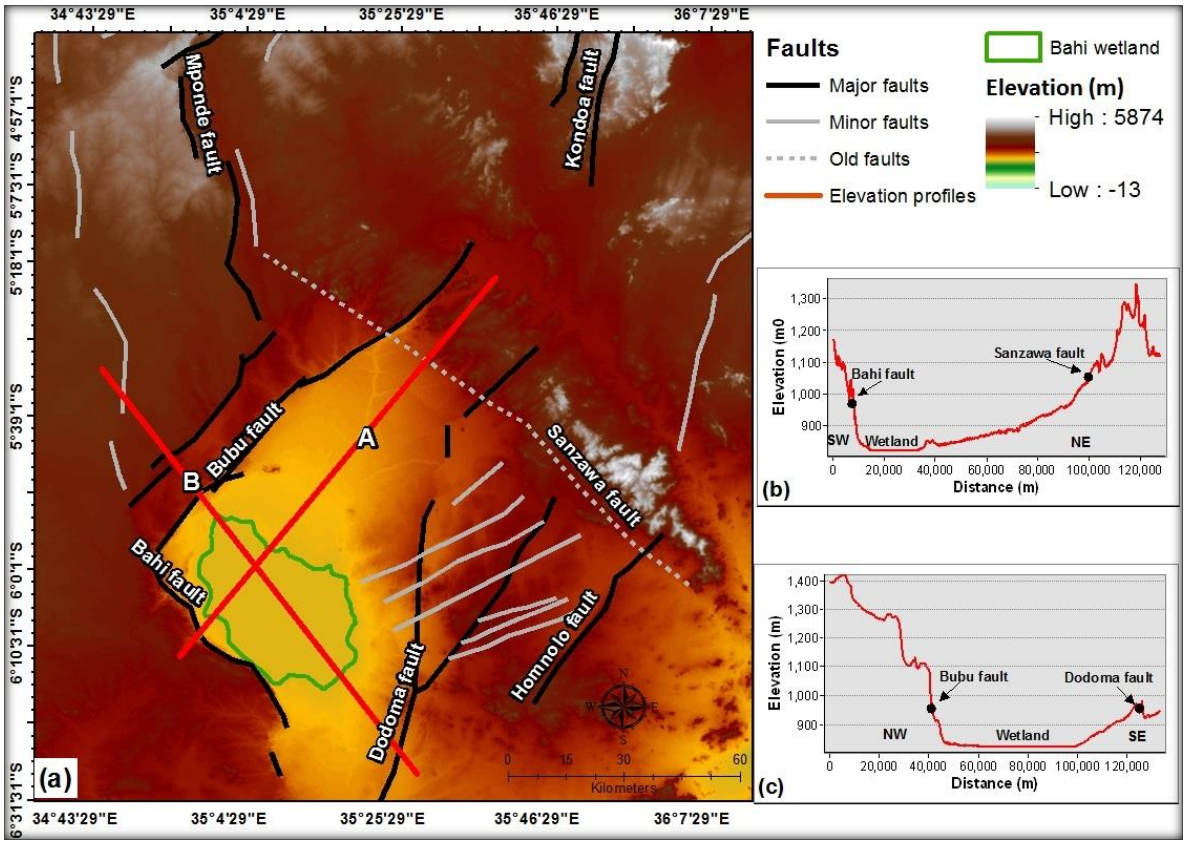

Figure 8.3.6: The topography and associated faults characteristics of the Bahi wetland (a), with graphs (b) and (c) showing the elevation profiles of lines A and B.

8.4 The Usangu wetland

The Usangu wetland in Tanzania lies between latitude 08°31'S and 08°14'S and longitude 33°52'E and 34°35'E (Figure 8.4.1), a distance of approximately 90 km north-east of the city of Mbeya. The NE-SW orientated wetland receives discharge from streams that emanate from the surrounding uplands. The majority of the discharge entering the Usangu plains is generated from the Chunya escarpment to the north, the Kipengere and the Poroto Mountains in the south-west and south-east respectively. These streams unite within the wetland and become the Great Ruaha River, which flows to the north-east.

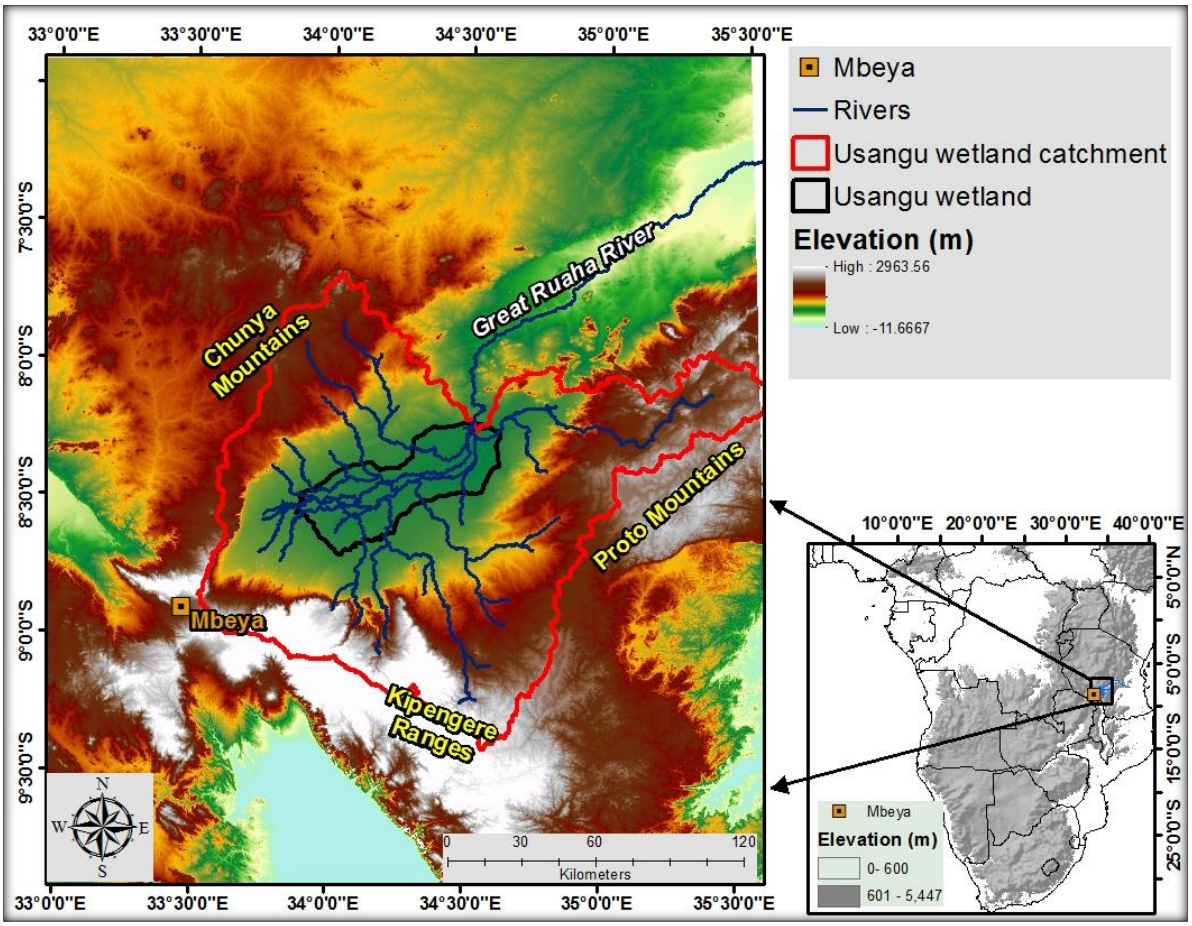

Figure 8.4.1: The location of Usangu wetland in relation to the topographic settings of the wetland catchment, and major streams.

8.4.1 Hydrological conditions of Usangu wetland

The 2 054 km^2 wetland occupies 9.73% of its 21 115 km^2 catchment (Figure 8.4.2a and b). The analyses of cross-sectional profiles show that the wetland occurs within a deep and broad valley (Figure 8.4.2c to g). Below the toe of the wetland (Figure 8.4.2c) the valley is narrow and broadens within the eastern section of the wetland (Figure 8.4.2d). The valley narrows again in the middle of the wetland (Figure 8.4.2e) and it broadens within the western section (Figure 8.4.2f). The valley is narrow above the head of the wetland (Figure 8.4.2g). In addition, the valley within the eastern section of the wetland is broadly U-shaped with a flat valley floor while it tends to be V-shaped in the middle reach, and broadly U-shaped within the western region of the wetland.

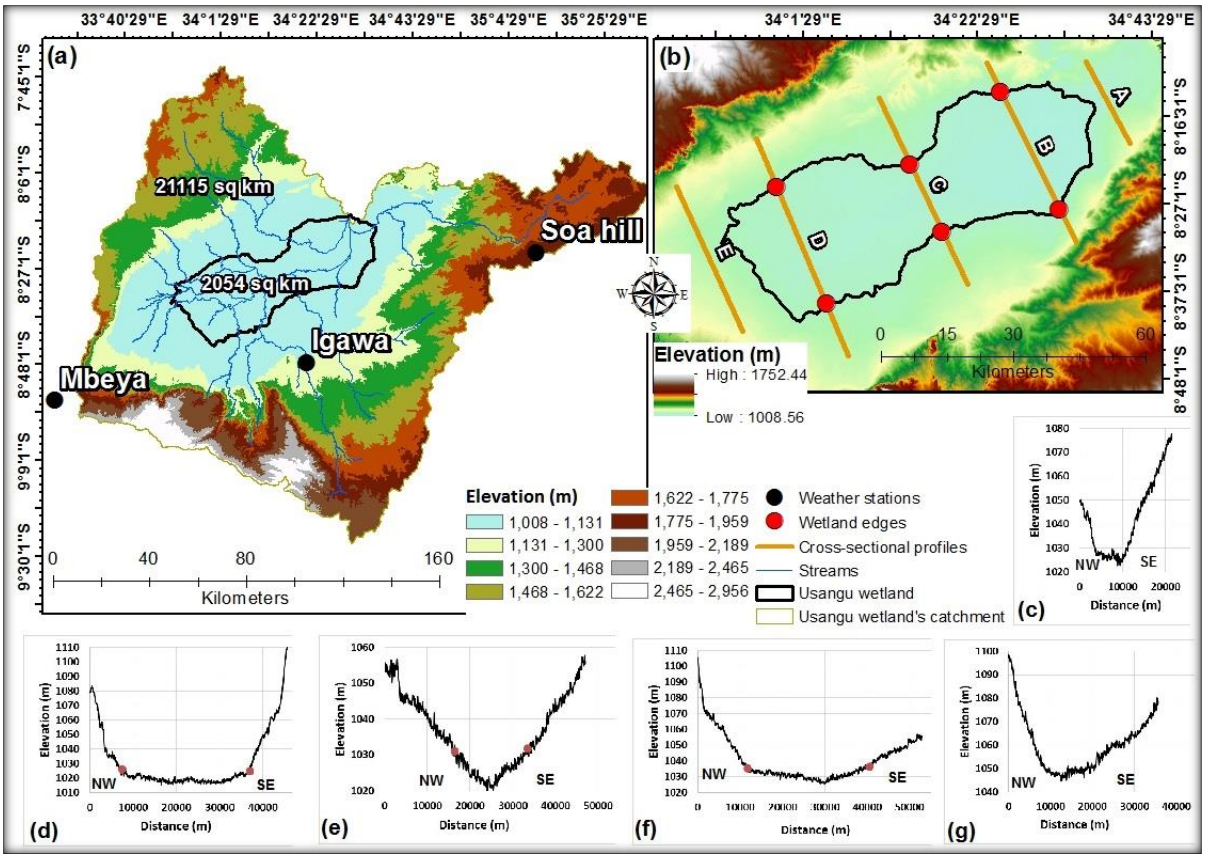

Figure 8.4.2: The location of weather stations and topographic characteristics of the Usangu wetland catchment (a) including the topography of the valley (b). Graphs (c) to (g) show cross-sectional profiles of transects A to E in (b).

The analysis of potential evapotranspiration and precipitation shows the catchment is characterised by high potential evapotranspiration relative to precipitation for 8 months of the year for all weather stations (Figure 8.4.3). This shows that the catchment is characterised by a negative surface water balance. Rainfall within the catchment generally starts around October, peaks in December to March, and ends around April to May.

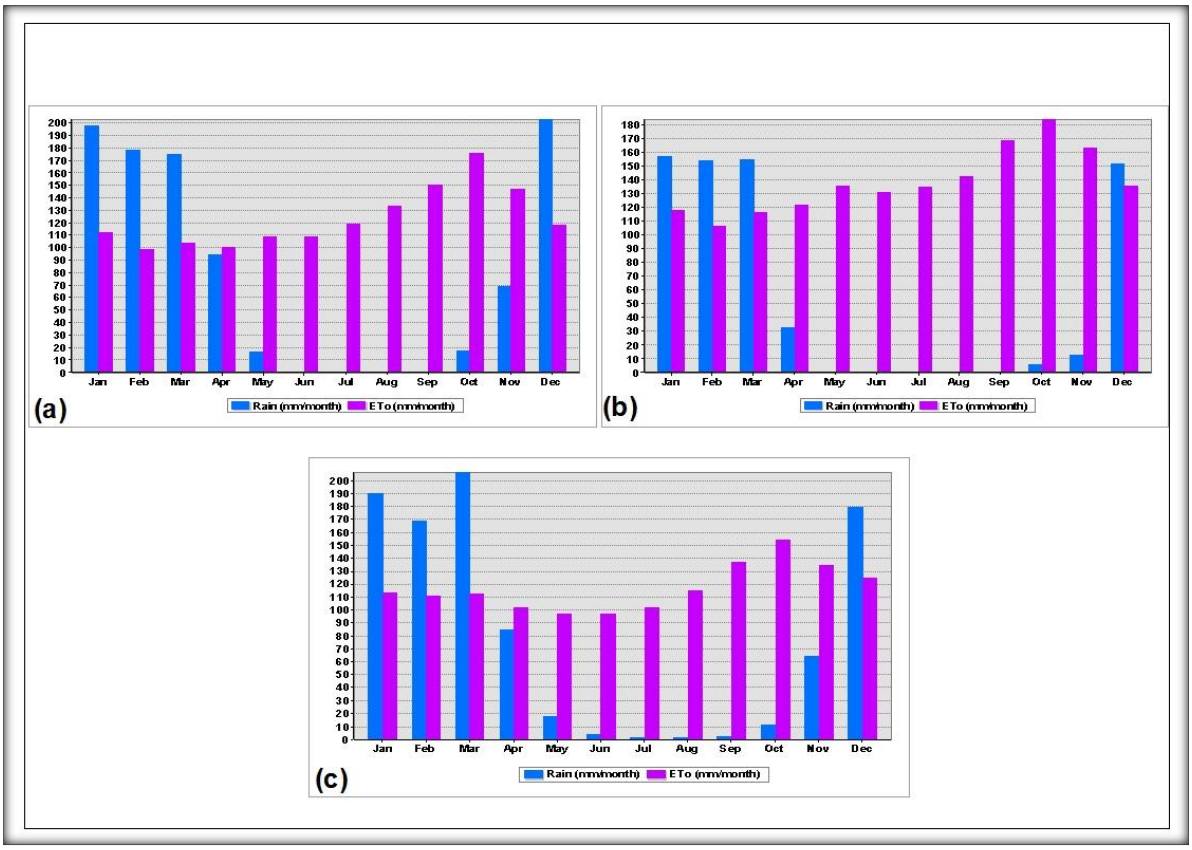

Figure 8.4.3: Monthly rainfall and potential evapotranspiration for Mbeya (a), Igawa (b), and Soa Hill (c) weather stations within and in close proximity to the Usangu wetland catchment.

Visual interpretation of the LandsatLook images shows that the wetland is dry in November at the onset of the rainy season (Figure 8.4.4a) and that flooding peaks at the end of the rainy season in April (Figure 8.4.4b). The western section of the wetland inundates from numerous streams that emanate from the surrounding uplands. These streams appear to join together within the wetland, which is where the most extensive flooding seems to occur (Figure 8.4.4a1 and b1). All streams merge within the eastern section of the wetland such that the eastern parts of the wetland support relatively permanently flooded zones.

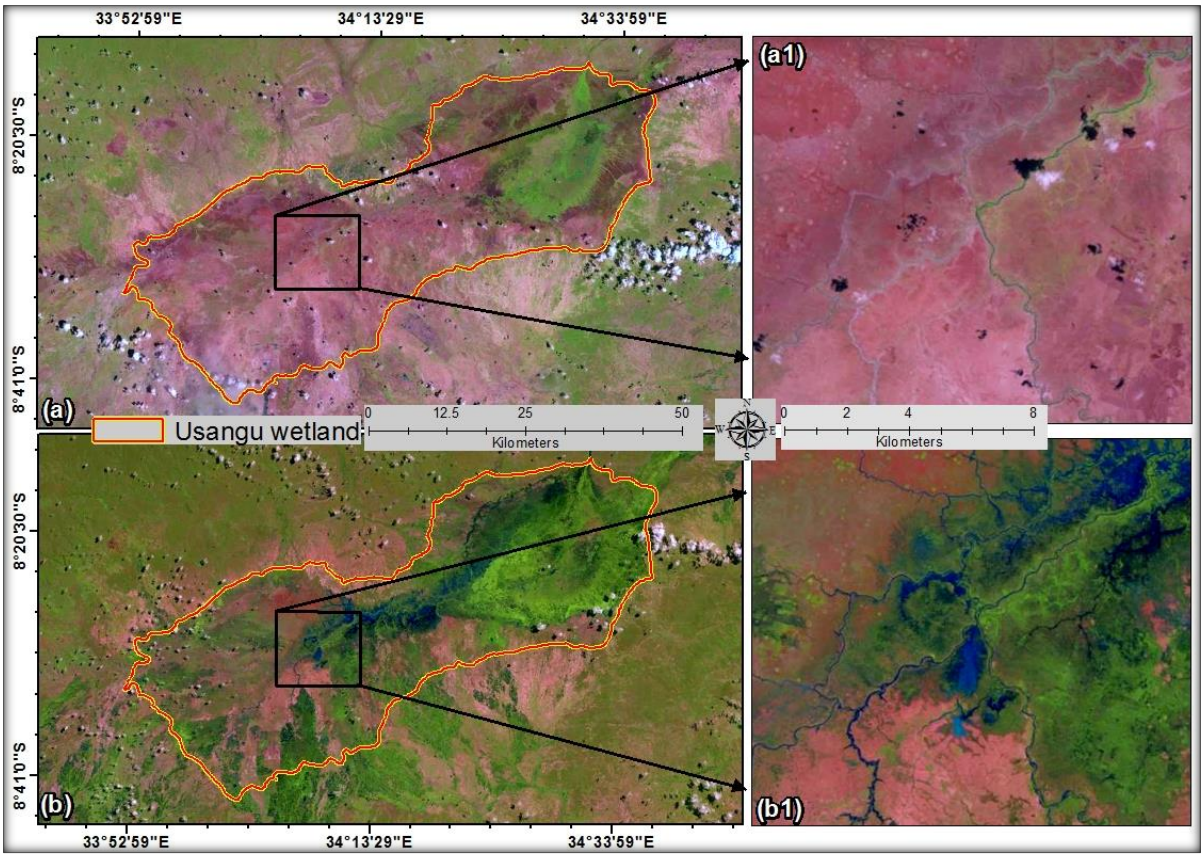

Figure 8.4.4: LandsatLook images depicting the saturation condition of Usangu wetland on 27 November 2009 (a) and 17 April 2009 (b). The insets show the saturation in the vicinity of the confluence of different streams on 27 November 2009 (a1) and 17 April 2009 (b1).

8.4.2 Geology and hydrological functioning of the Usangu wetland

The wetland outlet and the Great Ruaha River are located at the north-eastern end of the wetland (Figure 8.4.5a). The south-west to north-east elevation profile shows that the wetland depression is bounded by a steep escarpment to the south-west while a series of lower-lying ridges occur to the north-east (Figure 8.4.5a). The north-west to south-east orientated elevation profile shows that the wetland depression is bounded by steep escarpments to the north-west and south-east (Figure 8.4.5b). The steep slope from the wetland towards the north-western escarpment coincides with a fault line.

The Seoka Adamellite (A_4Sg) volcanic rocks cover most parts of the catchment to the north and east of the wetland while the wetland area is characterised by unconsolidated Quaternary sediments (Qa; Figure 8.4.6). Baunji Group (P_3Bj) of a combination of sedimentary and metamorphic rocks, Younger Volcanic (Nvy) of a combination of volcanic and sedimentary rocks, and the Seoka Adamellite and granite (A_4Sg) dominate in the northern and south-eastern parts of the catchment. The area downstream of the toe of the wetland is

characterised by a change in lithology from the easily erodible Quaternary sediments (Qa) to the more resistant granite rock of the Seoka Adamellite and the migmatite gneiss of the Usugaran Complex (Figure 8.4.6b).

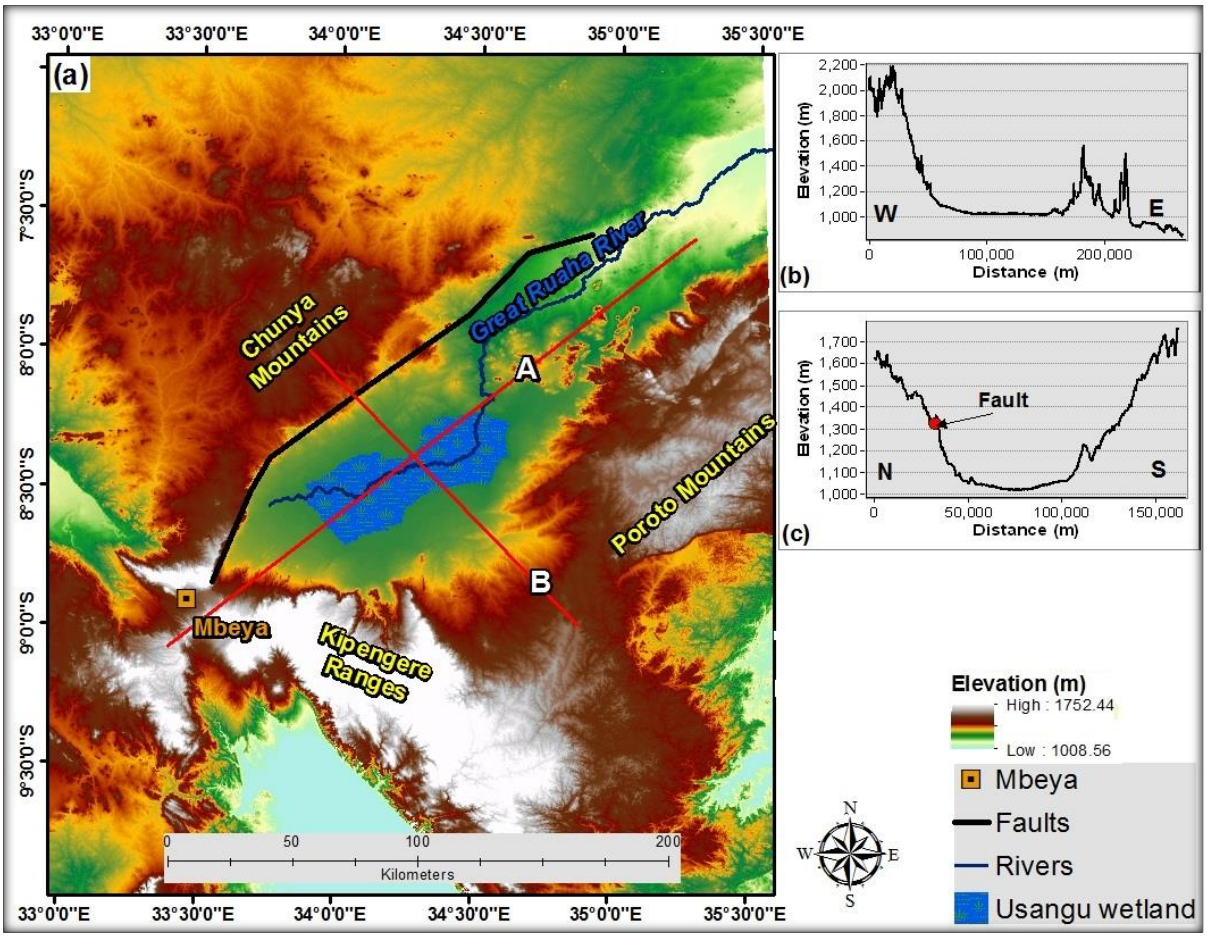

Figure 8.4.5: The geological and topographic settings of the Usangu wetland (a) with graphs (b) and (c) showing the elevation profiles of lines A and B respectively.

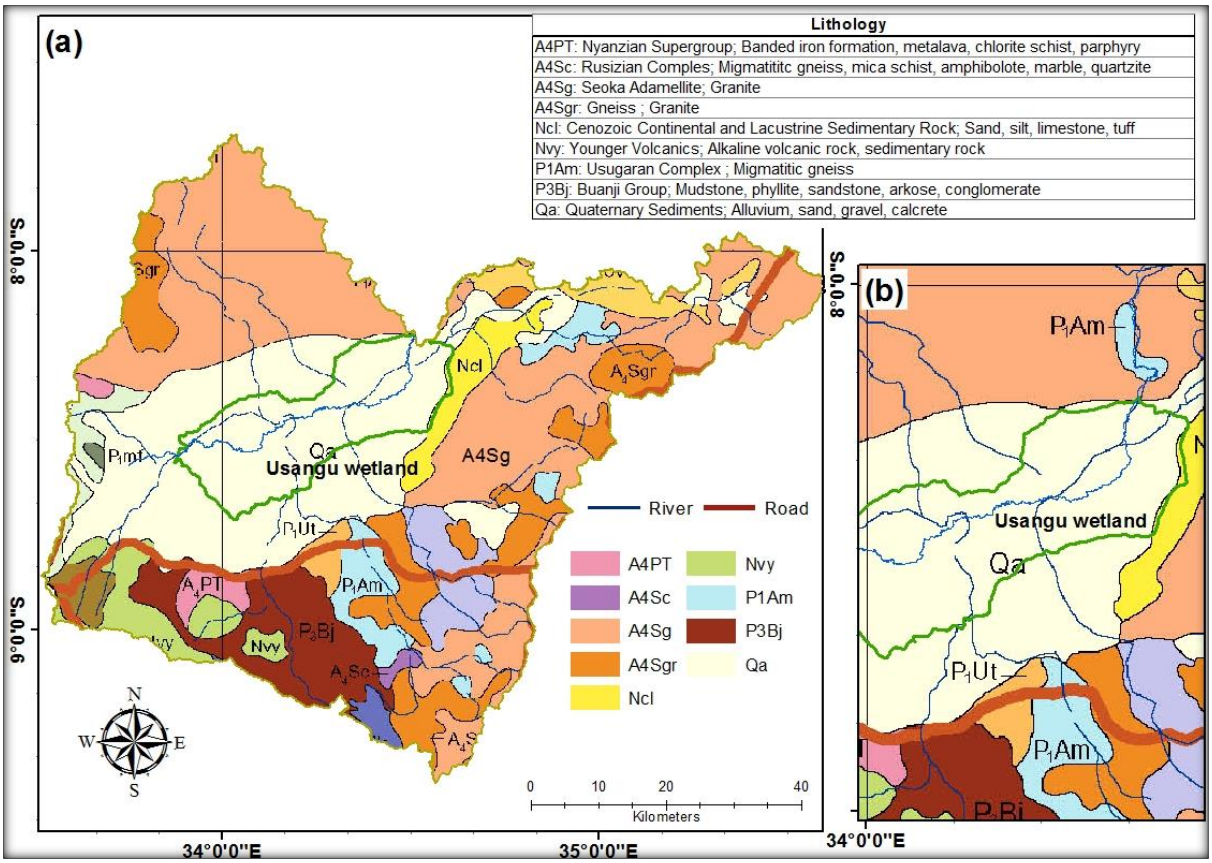

Figure 8.4.6: The geology of the Usangu wetland catchment (a) and the area in the vicinity of the toe of the wetland (b).

8.4.3 The structure and hydrological functioning of the Usangu wetland

The topographic characteristics within the lower reaches of the Usangu wetland and its outlet show the wetland's outlet occurs within a narrow and deep valley (Figure 8.4.7). The topographic profiles of lines A and C in Figure 8.4.7 show that steep escarpments bound the wetland to the north-east and south-west. However, the profile graph of line B shows that the north-eastern escarpment has been incised at the wetland outlet by the Great Ruaha River (line D and Figure 8.4.7e).

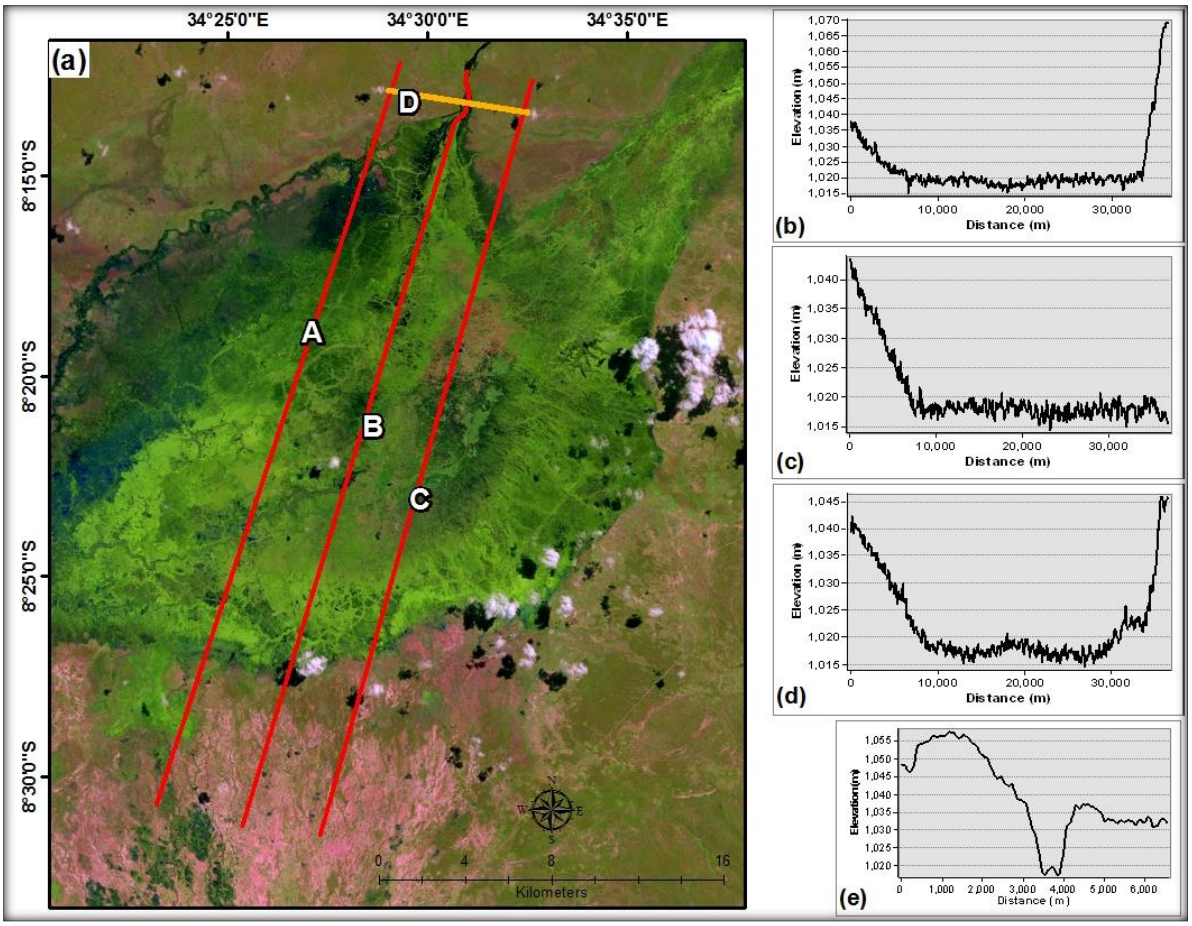

Figure 8.4.7: The 17 April 2009 LandsatLook image showing topographic characteristics of the Usangu wetland (a). The profile graphs (b), (c), and (d) show the profiles of diagonal lines A, B, and C while profile (e) shows the cross-sectional profile of line D.

Within the middle and lower reaches of the Great Ruaha catchment, drainage is directed towards the trunk stream that flows north-eastwards, while within the Usangu wetland's catchment, the drainage is directed radially towards the wetland (Figure 8.4.8). These contrasting drainage patterns suggest that the Usangu may have been an endorheic depression and that the Great Ruaha River captured drainage towards the north-east. This suggests that the wetland might be a remnant of an endorheic lake.

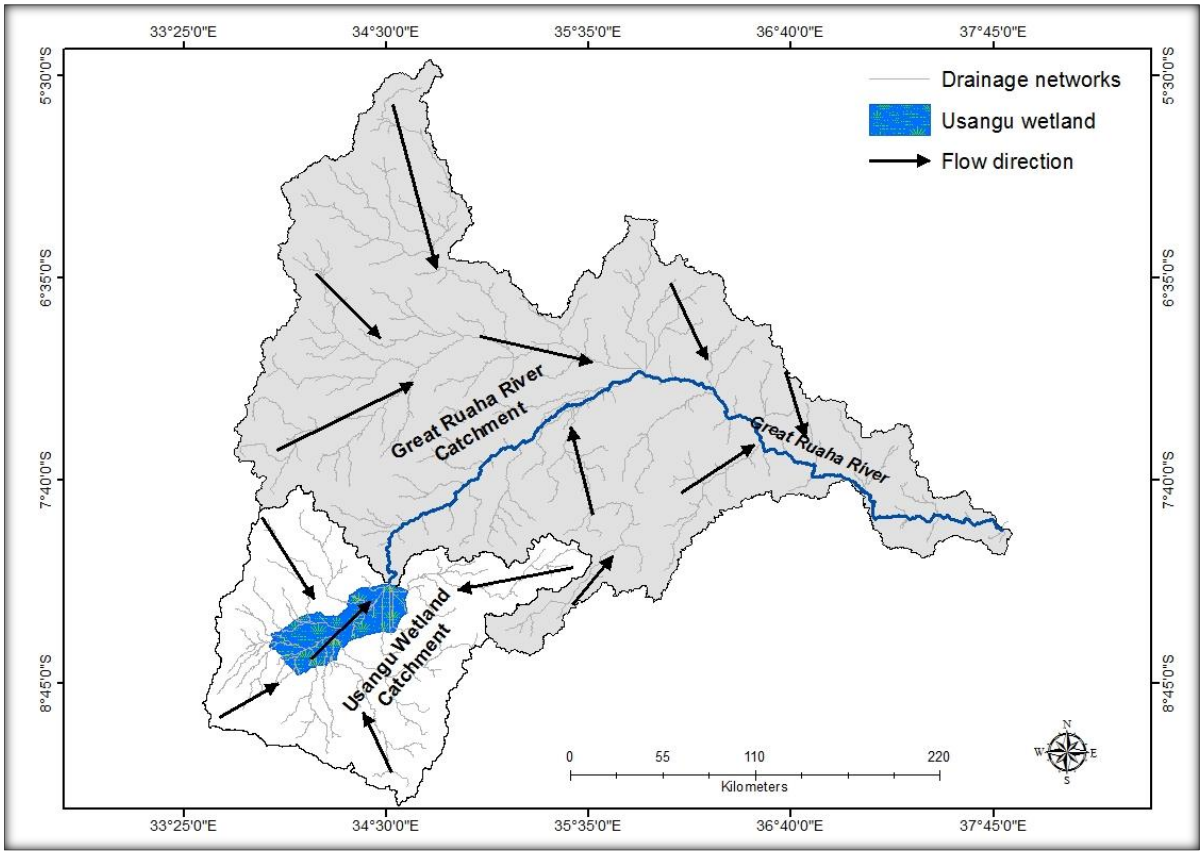

Figure 8.4.8: Drainage into the Usangu wetland and the Great Ruaha River Catchment.

Comparison of the average depth of inundation between the western and eastern sections of the Usangu wetland shows limited depth of inundation below channel water level (Figure 8.4.9) for all sections. Throughout the wetland the average depth of flooding is lower than channel stage heights, suggesting an absence of an alluvial ridge down the length of the wetland. This can be attributed to the lack of a single major influent stream draining into the wetland, and also the absence of a single trunk stream within the wetland. A number of channels exist within the wetland but they lose prominence towards the lower reaches.

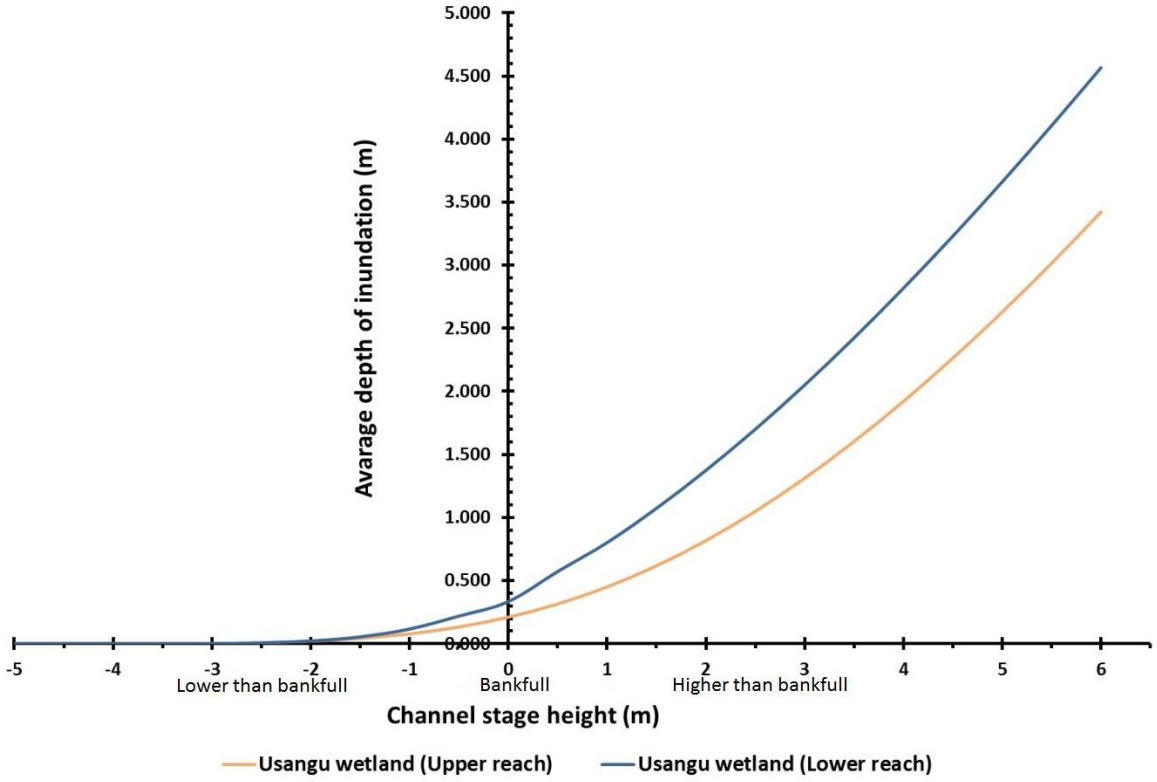

Figure 8.4.9: Comparison of the average depth of inundation within the western and eastern sections of Usangu wetland.

8.5 The Lukanga wetland

The Lukanga wetland is located approximately 100 km north-west of the city of Lusaka and 50 km west of Kabwe in Zambia (Figure 8.5.1), between latitude 13° 45'S and 14° 45'S and longitude 27°00'E and 28° 04'E. The Kafue River flows along the north-western margin of the wetland, which seems to be associated more with westward draining seasonal and perennial tributaries of the Kafue River, the main one being the Lukanga River.

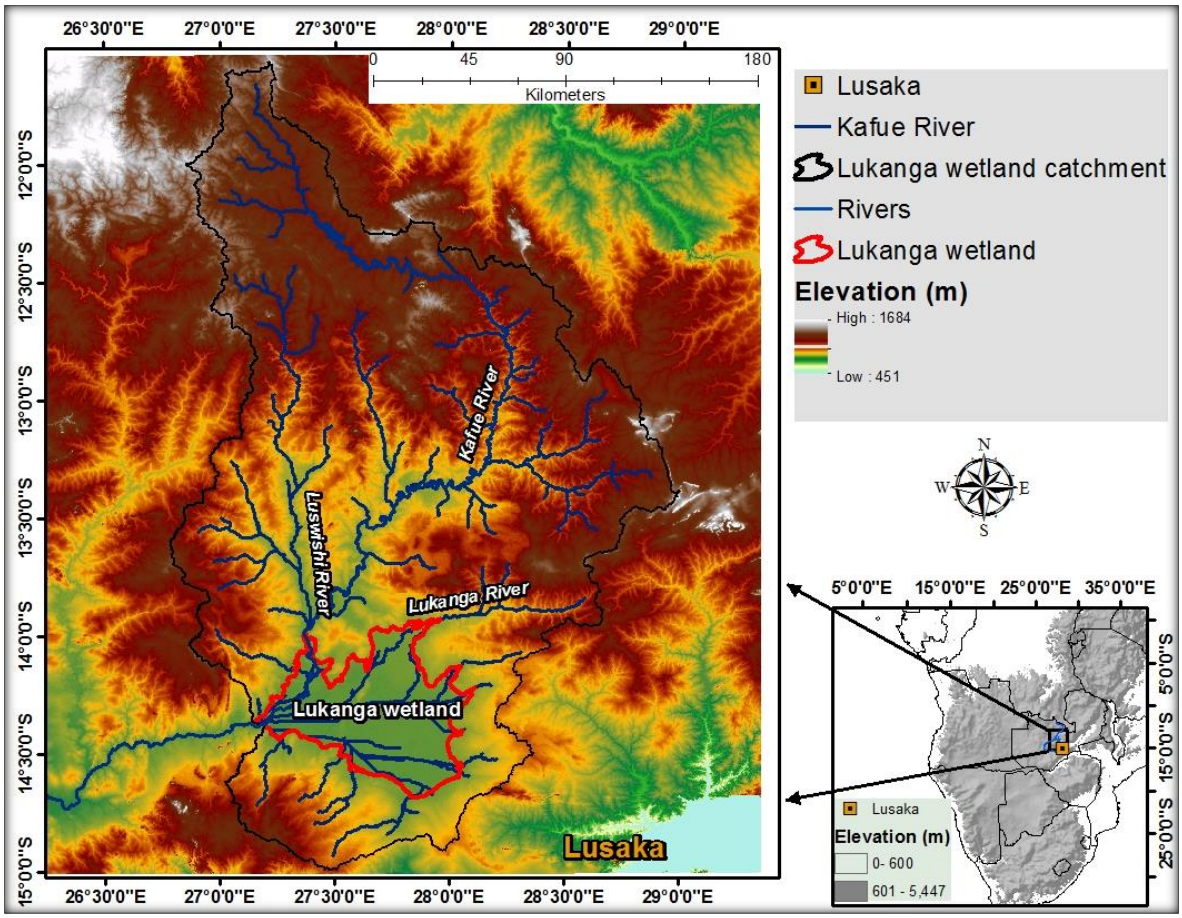

Figure 8.5.1: The location of Lukanga wetland in Zambia.

8.5.1 Hydrological conditions of the Lukanga wetland

The wetland is 4 313 km^2 and occupies 8.5% of its 50 553 km^2 catchment (Figure 8.5.2). The wetland is surrounded by high-lying escarpments and south-to-north oriented cross-sectional profiles show that the valley widens to a width of about 60 km in the central section with total relief over this distance approximating 20 m (Figure 8.5.2b to f). This suggests that short ephemeral streams from the surrounding uplands have the potential to saturate the wetland during the wet season.

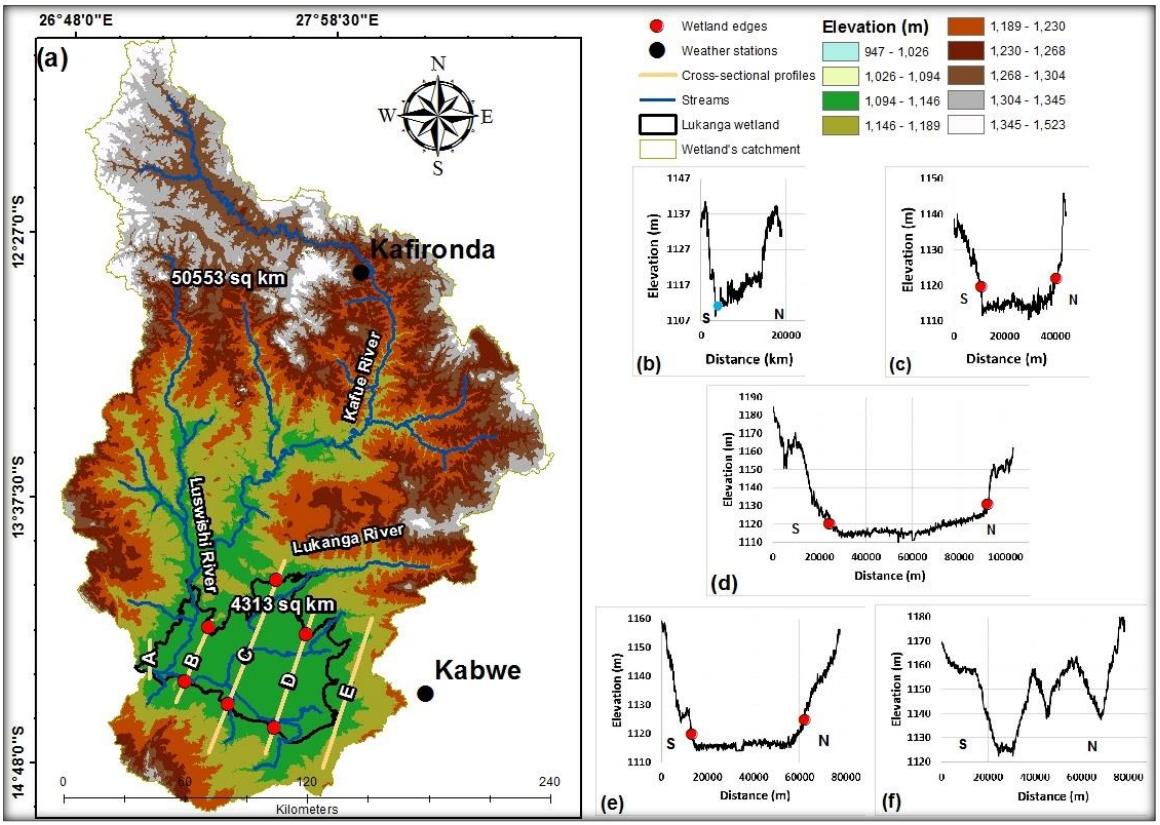

Figure 8.5.2: Topographic characteristics of the Lukanga wetland, its catchment area, and the location of weather stations (a). Graphs (b)-(f) show the cross-sectional profiles of lines A-E. The blue marker in (b) shows the location of the Kafue River and red markers show the wetland boundary.

From the analysis of potential evapotranspiration and precipitation of Kafironda and Kabwe weather stations, it appears that the Lukanga wetland and its catchment are characterised by high potential evapotranspiration rates throughout the year (Figure 8.5.3a and b). Rainfall is in summer (October to March). Given the seasonality of rainfall and high potential evapotranspiration there is a negative surface water balance within the catchment for about 7 months of the year.

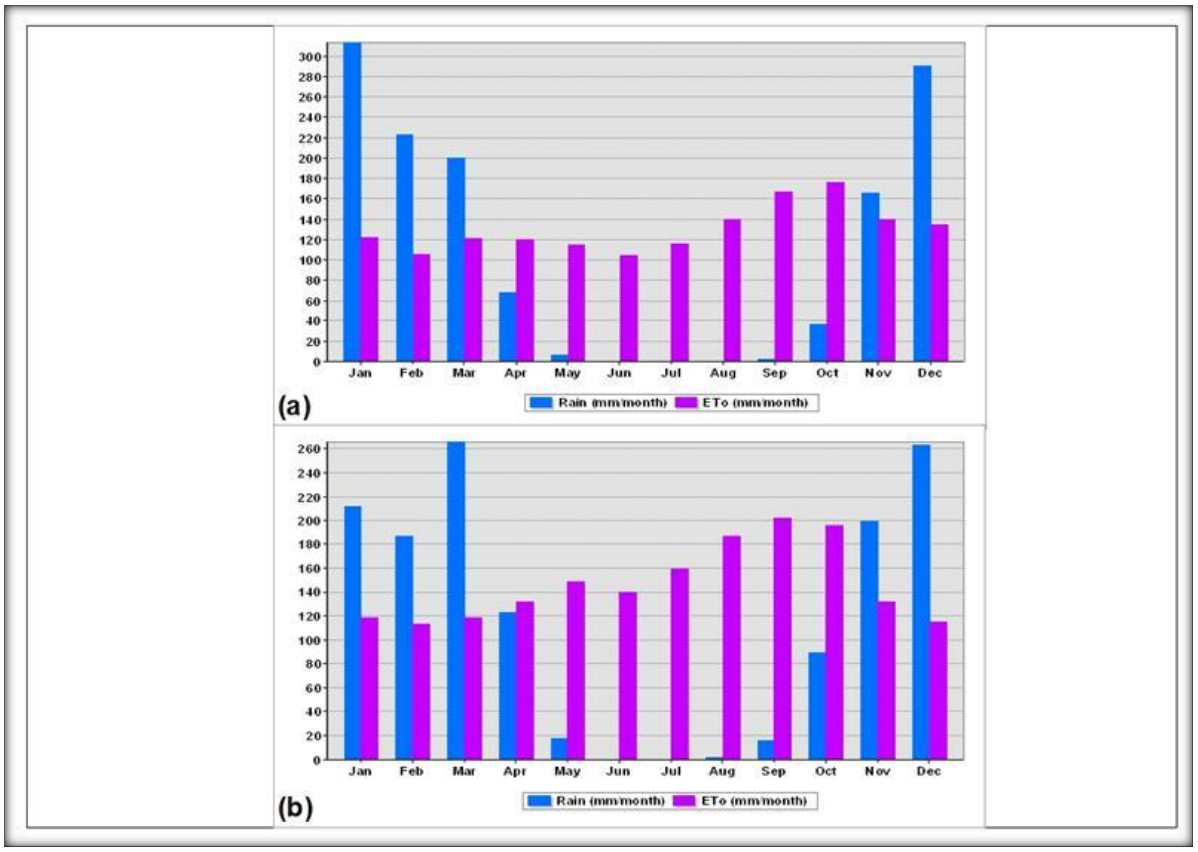

Figure 8.5.3: Monthly rainfall and potential evapotranspiration (ET_0) rates for two weather stations within and in close proximity of the Lukanga wetland's catchment area for the Kafironda (a) Kabwe (b) weather stations.

LandsatLook images show the flooding patterns and major sources of water for the wetland (Figure 8.5.4). Except for the semi-permanently flooded depression in the eastern part of the wetland, the Lukanga wetland is dry in November at the beginning of the rainy season while inundation peaks in April towards the end of the rainy season (Figure 8.5.4a and b).

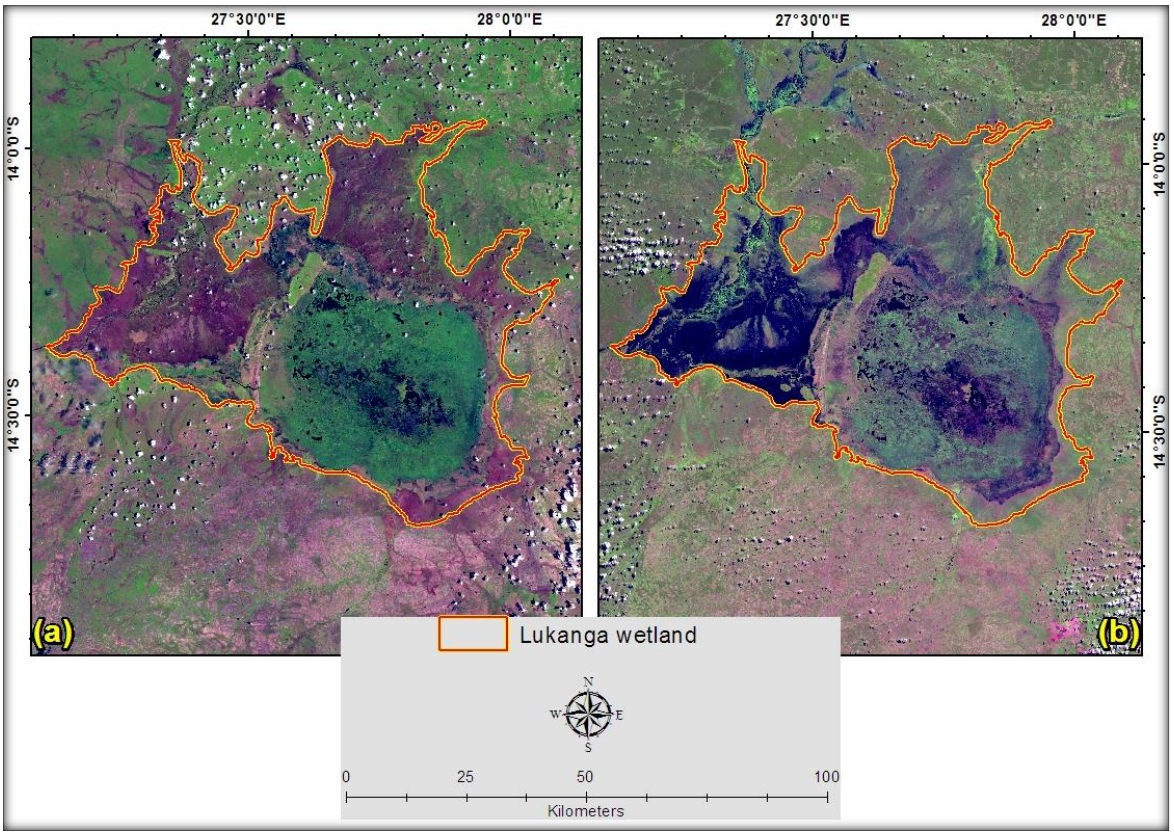

Figure 8.5.4: Mosaicked LandsatLook images showing the saturation condition of Lukanga wetland on 19 and 27 November 2013 (a) and 20 and 27 April 2014 (b).

8.5.2 Geomorphology and hydrological functioning of Lukanga wetland

The topographic characteristics of the Lukanga wetland suggest that it is composed of a number of HGM units (Figure 8.5.5). A shallow depression occupies the south-eastern part of the wetland while a number of valley-bottom wetlands occupy areas where tributaries (particularly the Lukanga River) enter the depression from the north. Figure 8.5.2(d) suggests that where the Lukanga River enters the Lukanga wetland, an alluvial fan has created a gentle slope from the point where the Lukanga River loses confinement and enters the wetland. A floodplain associated with the Kafue River occupies the western part of the Lukanga wetland.

Figure 8.5.5a shows the arrangement of fault lines around the Lukanga wetland complex. The shallow flooded depression occupies the lowest-lying part of the basin. The valley bottom associated with the Lukanga River is at a slightly higher elevation than the depression (Figure 8.5.5b), while the floodplain and the depression are at similar elevation (Figure 8.5.5c). Furthermore, the cross-sectional profile of line C shows that the Kafue River sits on an alluvial ridge that is at least 3 m higher than the outflow channel.

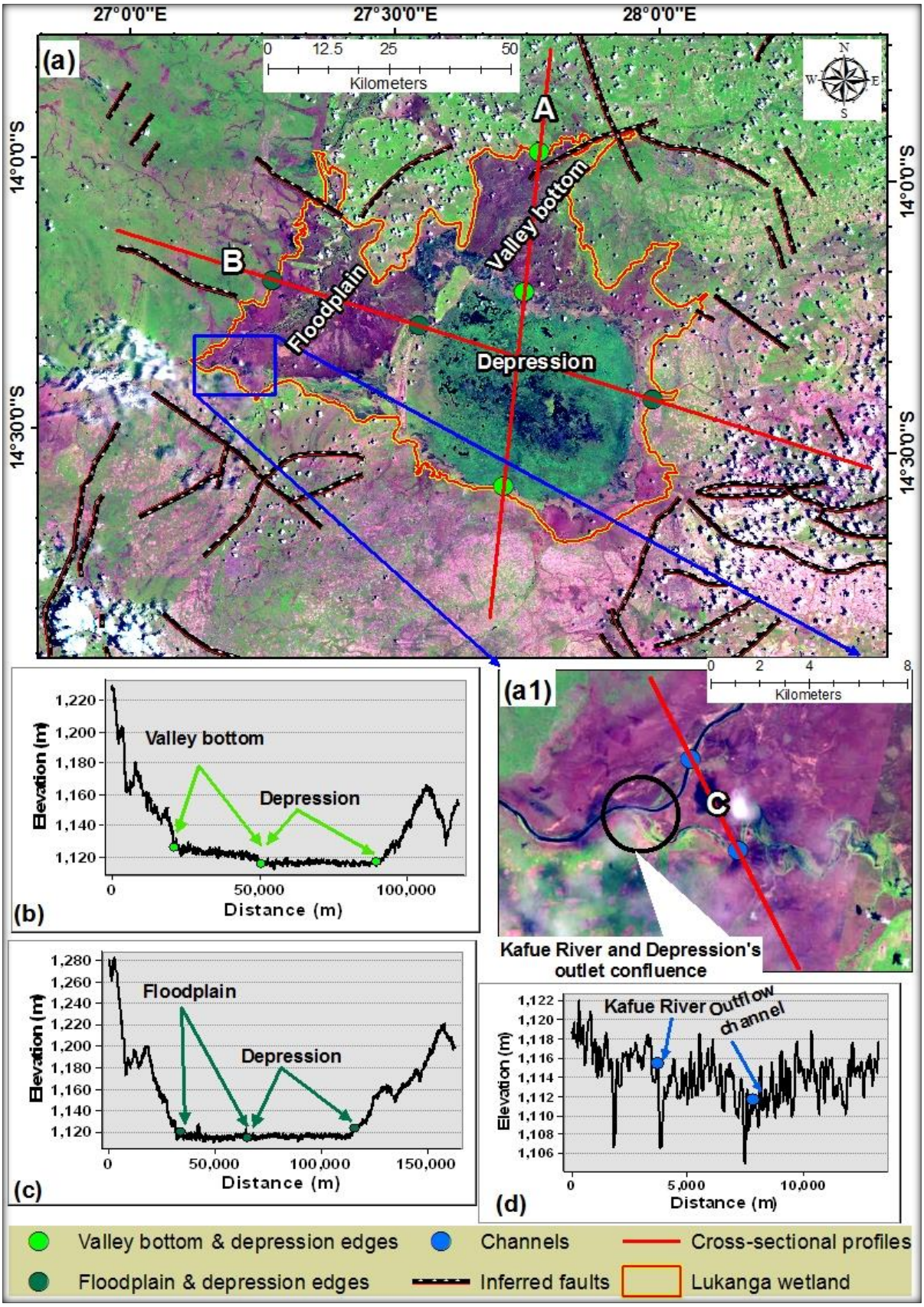

Figure 8.5.5: The November 2013 LandsatLook image showing the different wetland units, fault lines within the Lukanga wetland system (a) and the confluence of the Kafue and Lukanga Rivers (a1). Graphs (b) to (d) represent elevation profiles of lines A, B and C respectively.

The valley cross-sections within the lower reaches and areas below the toe of the floodplain unit on the western edge of the Lukanga wetland (Figure 8.5.6a) show that there is a decrease in valley width from the lower reaches to areas below the toe of the floodplain unit (Figure 8.5.6b to g). There is also a noticeable decrease in channel sinuosity from the lower floodplain to areas below the wetland.

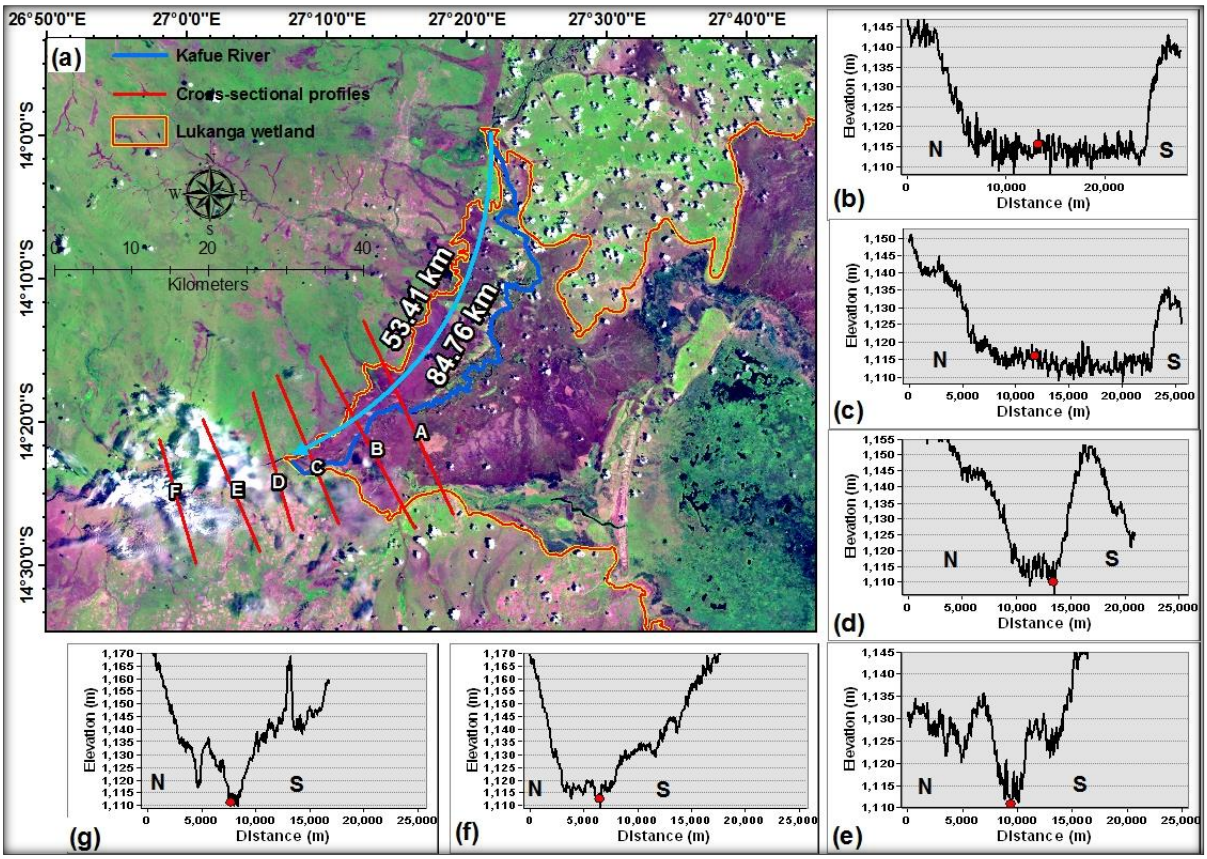

Figure 8.5.6: November 2013 LandsatLook image showing length of the floodplain unit valley and length of the Kafue River within the floodplain unit (blue line; (a)). The graphs (b)-(g) show the cross-sectional profiles of lines A-F.

Figure 8.5.7 shows that the floodplain unit is characterised by floodplain features such as oxbow lakes, meander scars and sinuous channel.

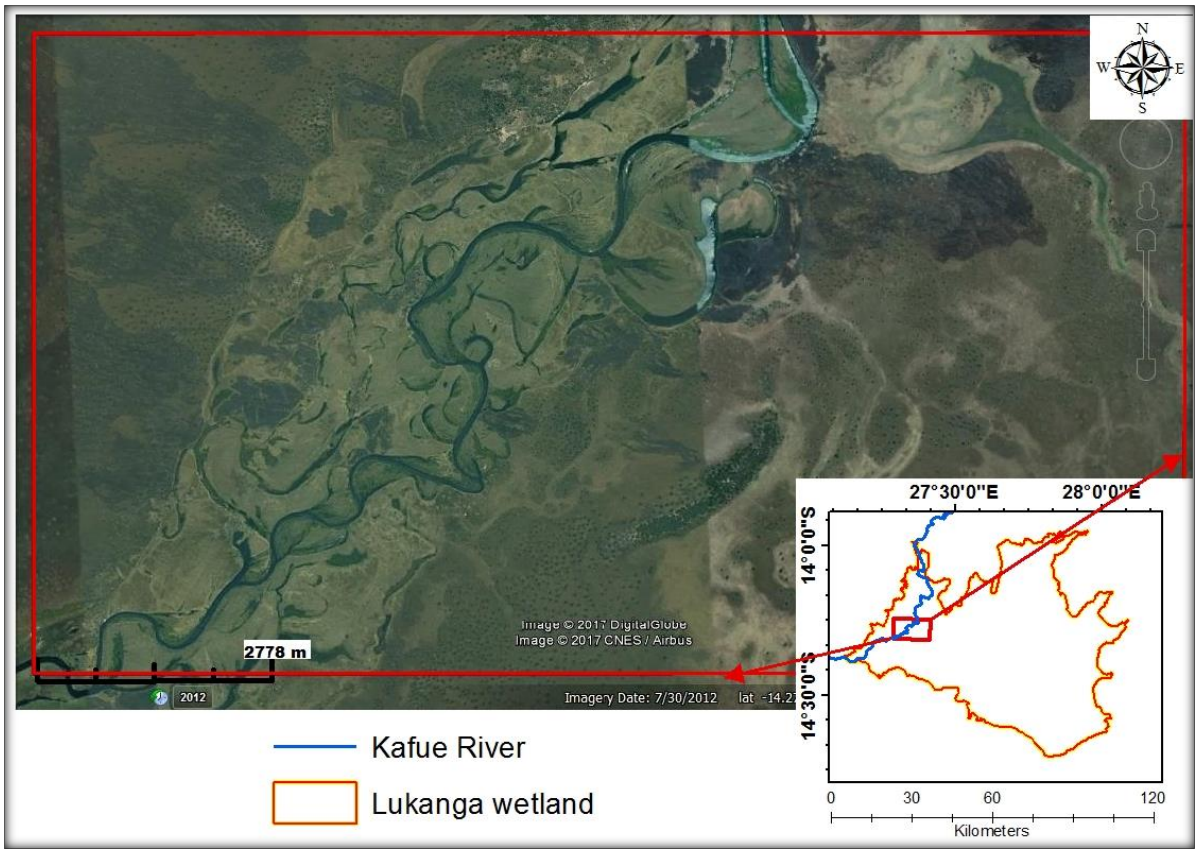

Figure 8.5.7: Google Earth (Image data: DigitalGlobe and CNES/Airbus) image showing floodplain features within the Lukanga floodplain unit.

The geology of the Lukanga wetland catchment is mainly characterised by consolidated Undifferentiated Kundelungu Group (P_3Kk) sedimentary rocks, Lower Roan Group (P_3Krl) metamorphic and sedimentary rocks, Mkushi Gneiss (P_1Mh) of volcanic origin, and Gneiss (P_1Mg) of volcanic origin (Figure 8.5.8a). The Lukanga wetland complex is underlain by unconsolidated Quaternary sediments (Qa) of alluvium, sand, gravel, and calcrete (Figure 8.5.8b). Within the regions with a cover of unconsolidated Quaternary sediments are areas of exposed Kalahari Group (Nk) sediments of unconsolidated aeolian sand and sedimentary rocks such as sandstone and limestone. The area to the west and south-west of the floodplain is characterised by the Undifferentiated Kundelungu Group (P_3Kk), which are composed of sedimentary and metamorphic rocks such as carbonate rock, shale, psammite, and rudite. There are further changes in lithology along the course of the Kafue River to the south-west of the floodplain unit. The change in lithology from the Undifferentiated Kundelungu Group sediments to the volcanic rocks of the Hook Granite (Egh) appears to coincide with the observed increase in channel slope (Figure 8.5.8c). The Hook Granite appears more resistant to channel incision than sedimentary rocks of the Undifferentiated

Kundelungu Group. The observed decline in valley width from the lower reaches of the floodplain wetland unit towards the areas just below the toe of the wetland corresponds with the observed change in lithology. From the longitudinal profile of the Kafue River, it is clear that there is a lithologically controlled topographic step below the toe of the floodplain unit.

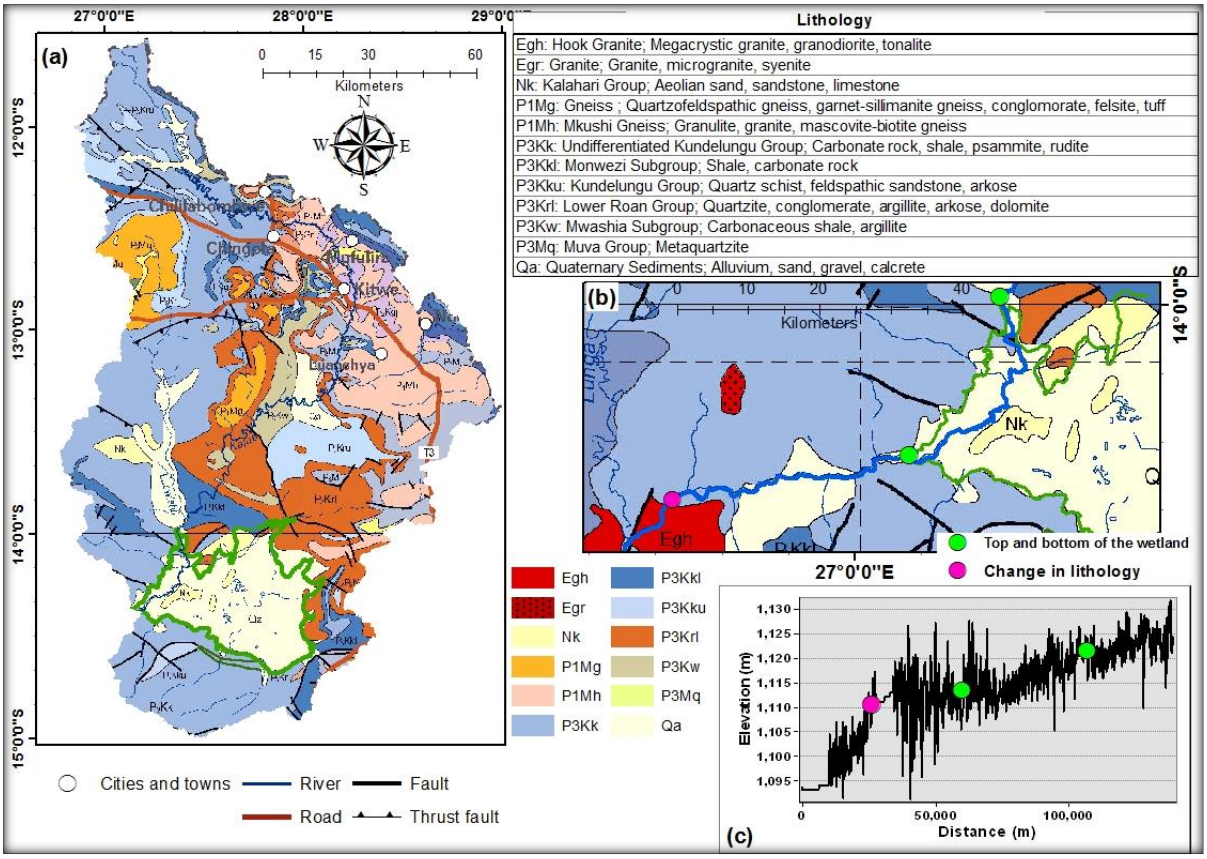

Figure 8.5.8: The geology of Lukanga wetland catchment (a) and area in the vicinity of the toe of the wetland (b). Graph (c) shows the longitudinal profile of the Kafue River from upstream of the wetland to downstream of the toe of the wetland.

The topographic characteristics in the region of the Lukanga wetland show that it is flanked by steep escarpments to the east and west (Figure 8.5.9). To the west there is an elevated ridge that acts as divide between the Lukanga wetland catchment and the Busanga wetland catchment as well as the down warped Kalahari Basin (Figure 8.5.9a, b and c). To the west of the Lukanga wetland there is another elevated ridge that separates the Lukanga wetland catchment and the Luangwa River valley (Figure 8.5.9b).

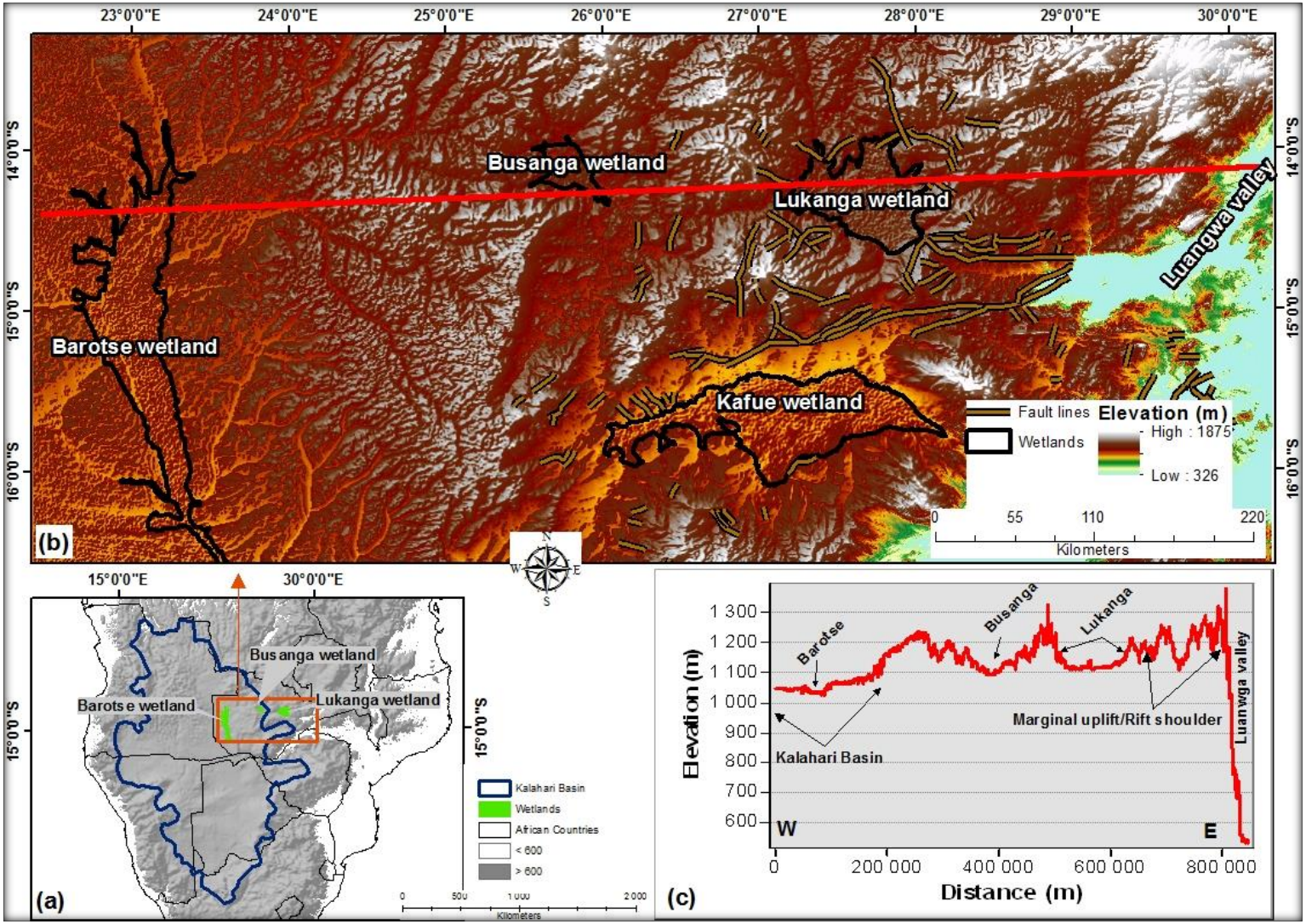

Figure 8.5.9: The location of the Lukanga wetland in relations to the boundary of the Kalahari Basin (a), topographic characteristics in the region of the Lukanga wetland (b), and a profile graph (c) showing elevation profiles of the red lines in (b).

8.6 Discussion

The Wembere, Bahi, Usangu, and Lukanga wetlands occupy between 4.98 and 9.73% of their catchment and typically show a month long lag between peak local rainfall and peak wetland inundation. This could be attributed to the nature of streams which maintain the wetlands hydrologically. Most of these streams are short since they originate from the surrounding uplands and terminate within wetland depressions.

The formation of the Wembere, Bahi, and Usangu wetlands appear to be tectonically controlled as the wetlands are bounded by fault lines and occur within the East African Rift System. According to Foster et al. (1997), within the Wembere area, volcanism and sedimentation could have begun about 5 Ma. Major fault escarpments could have formed about 3 Ma and the present-day rift escarpments could have developed about 1.2 Ma. Judging from the short length and orientation of streams that flow into each of these wetlands, the formation of the Wembere, Bahi, and Usangu graben structures could have diverted the drainage into the depressions, with subsequent flooding leading to wetland formation.

The observed conical shape of elevation profiles across areas where tributary streams enter the southern section of the Wembere wetland suggests that each tributary is associated with an alluvial fan as it leaves the adjacent uplands and enters the Wembere wetland basin, which is relatively flat. The observed sedimentation may ultimately lead to the evolution of the wetland into a complex wetland system that is controlled in fundamental ways by these impinging alluvial fans.

According to Macheyeki et al. (2008), the Bahi wetland occupies a half graben that is an extension of the eastern branch of the East African Rift System. Macheyeki et al. (2008) also highlighted that the fault lines that bound the wetland could be related to rifting associated with the East African Rift System in the Quaternary, with the exception of the northern Sanzane fault. This suggests that faulting within the Bahi depression could have been triggered by the second uplift event that occurred about 5 Ma. Since water enters the wetland through short streams that originate from the tilted blocks within the rift valley (Kamukala and Crafter, 1993), the formation of the depression from tectonic activities could have diverted the drainage networks towards the depression, leading to inundation.

Judging from the orientation of the drainage network of the Usangu wetland catchment in comparison to the orientation of the drainage network of the Great Ruaha River catchment, rifting could have diverted the drainage into the wetland forming an endorheic basin. This is

because the wetland is of tectonic origin since it occupies the Ruaha-Usangu depression that is a southward extension of the eastern branch of the East African Rift System (Delvaux and Hanon, 1993). According to SMUWC (2001), the Usangu wetland occurs in a fault-controlled basin that is filled with lake deposits. This substantiates the occurrence of an endorheic lake prior to the formation of the Usangu wetland. Therefore, headward erosion of the Great Ruaha River could have led to partial desiccation of the lake and the formation of the wetland such that the resistant lithology at the toe of the wetland prevents the Great Ruaha River from incising further into the wetland.

Previous studies (Vrána, 1985; Katongo et al., 2002) failed to determine the origin of the Lukanga wetland. The results of reconnaissance geological mapping, an airborne magnetic survey and petrological study of a small set of samples of rocks suggested that the wetland could have formed from a meteorite impact crater Vrána (1985). Vrána (1985) concluded that the Lukanga swamp is probably a remnant of an ancient meteorite-impact structure. However, from field surveys, analysis of rock types and fault lines, Katongo et al. (2002) failed to find any evidence that could link the formation of the wetland to meteorite impact. Judging from the observed change in lithology from the Undifferentiated Kundelungu Group sediments to the volcanic rocks of the Hook Granite below the toe of the floodplain unit, the increase in valley width upstream of the toe of the wetland and the observed meandering features, the floodplain unit could be lithologically controlled. Therefore, the Tooth et al. (2002) model would best explain the origin of the floodplain unit in the western part of the Lukanga wetland. It seems that the Kafue River could have incised until its bed overlay the resistant Hook Granite, which limited further vertical incision. The Kafue River could have responded to the base level effect by increasing channel sinuosity upstream, planing the valley laterally and giving rise to conditions suitable for the formation of a floodplain wetland. However, the Lukanga wetland itself appears to be a blocked tributary valley depression created by slope reduction associated with aggradation of the Kafue floodplain to the west of the wetland, as described for Lake Futululu on the Futululu tributary of the Mfolozi floodplain (Grenfell et al., 2010).

CHAPTER 9: CLASSIFICATION OF LARGE WETLANDS IN AFRICA'S ELEVATED DRYLANDS

9.1 Relationships amongst wetlands based on wetland variables

This chapter attempts to integrate the analyses of large wetlands in southern Africa's elevated drylands presented thus far. In order to do this, wetlands were classified using cluster analysis based on fifteen nominal and ordinal variables related to different wetland features (Table 9.1). Major axes of variation and the variables that were most highly correlated to this variation were explored using principal components analysis. Variables for wetland features such as channel characteristics (unchannelled, poorly channelled, strongly channelled, sinuosity ratio and channel slope), basin type (exorheic or endorheic), valley charateristics (valley slope, presence of an alluvial ridge, presence of backwater depressions) were used. Wetland and catchment sizes, wetland origin (lithological or tectonic origin) as well as catchment geology (unconsolidated Kalahari sediments, consolidated sedimentary rocks and consolidated volcanic rocks) were also used.

Table 9.1: Variables used to identify similarities and differences in wetland structure and hydrological functioning.

Wetland	Poorly channelled	Strongly channelled	Exorheic basin	Channel slope (%)	Valley slope (%)	Sinuosity ratio	Alluvial ridge	Backwater depressions	Wetland size (km^2)	Catchment size (km^2)	Lithological origin	Tectonic origin	Kalahari Catchment[1]	Non Kalahari Catchment (Sedimentary)[2]	Non Kalahari Catchment (Volcanic)[3]
Kafue	1	0	1	0.0008	0.006	1.81	0	1	7926	362972	0	1	0	1	0
Luapula	0	1	1	0.003	0.008	1.07	0	1	5302	174135	0	1	0	1	0
Lufira	0	1	1	0.005	0.013	2.47	1	1	1335	45688	1	0	0	1	0
Upper Zambezi	0	1	1	0.009	0.015	1.41	0	0	3200	499816	0	1	1	0	0
Barotse	0	1	1	0.012	0.020	1.42	0	0	8368	318888	1	0	1	0	0
Bahi	0	0	0	0.0005[4]	0.006	0.0005	0	0	1086	21816	0	1	0	0	1
Wembere	0	0	0	0.0005	0.003	0.0005	0	0	2714	42678	0	1	0	0	1
Usangu	1	0	1	0.0005	0.019	0.0005	0	0	2054	21115	0	1	0	0	1
Lukanga[5]	0	0	1	0.0005	0.0005	0.0005	0	0	4313	50553	0	0	0	1	0

[1] Catchment geology is mostly characterised by Kalahari sediments

[2] Catchment geology is mostly characterised by sedimentary and metamorphic material without prevalence of Kalahari sediments

[3] Catchment geology is mostly characterised by Volcanic and sedimentary material without prevalence of Kalahari sediments

[4] Unchannelled and poorly channelled wetlands don't have quantitative variables for wetland features such as channel slope, and sinuosity ratio, as a result, a nominal value "0.0005" were assigned

[5] Lukanga wetland is composed of different HGM units and variables for wetland features (such as channel characteristics, wetland origin and valley slope) differ according to the HGM unit, as a result, a nominal value "0" was assigned

9.1.1 Classification of wetlands

The cluster analysis shows that at a height of 15 (Figure 9.1), the wetlands (Group A) were divided into two groups (Group B and Group C). Group B comprisie the Upper Zambezi, Barotse, Lufira, Lukanga, Kafue, and Luapula wetlands which are weakly to strongly channelled, while wetlands in Group C comprising the Usangu, Wembere, and Bahi wetlands, are tectonically controlled and showing limited evidence of channel development. At the second level of division and a height of 8.0, the wetlands in Group B were divided into two groups, with Group E comprising the Upper Zambezi and Barotse wetlands which occupy catchments dominated by Kalahari sediments, while wetlands in Group D, comprising the Lufira, Lukanga, Kafue and Luapula wetlands, are characterised by meandering fluvial features. At the same level of division, the tectonic depression wetlands in Group C were divided into two groups, but at at a height of 7.5, with Group F comprising the Usangu wetland that is exorheic and Group G (the Bahi and Wembere wetlands), which are endorheic. At the third level of division, the only meaningful division was of Group D, such that at a height of 7.3 the Lufira wetland (Group H), which is characterised by an alluvial ridge, was separated from the Lukanga, Kafue and Luapula wetlands (Group I), which lack an alluvial ridge. At the fourth level of division, wetlands in Group I were subdivided into two groups, such that at a height of 5, the Lukanga wetland (Group J), which is a composite of different HGM wetland units, was separated from the Kafue and Luapula wetlands (Group K), which have low valley slopes.

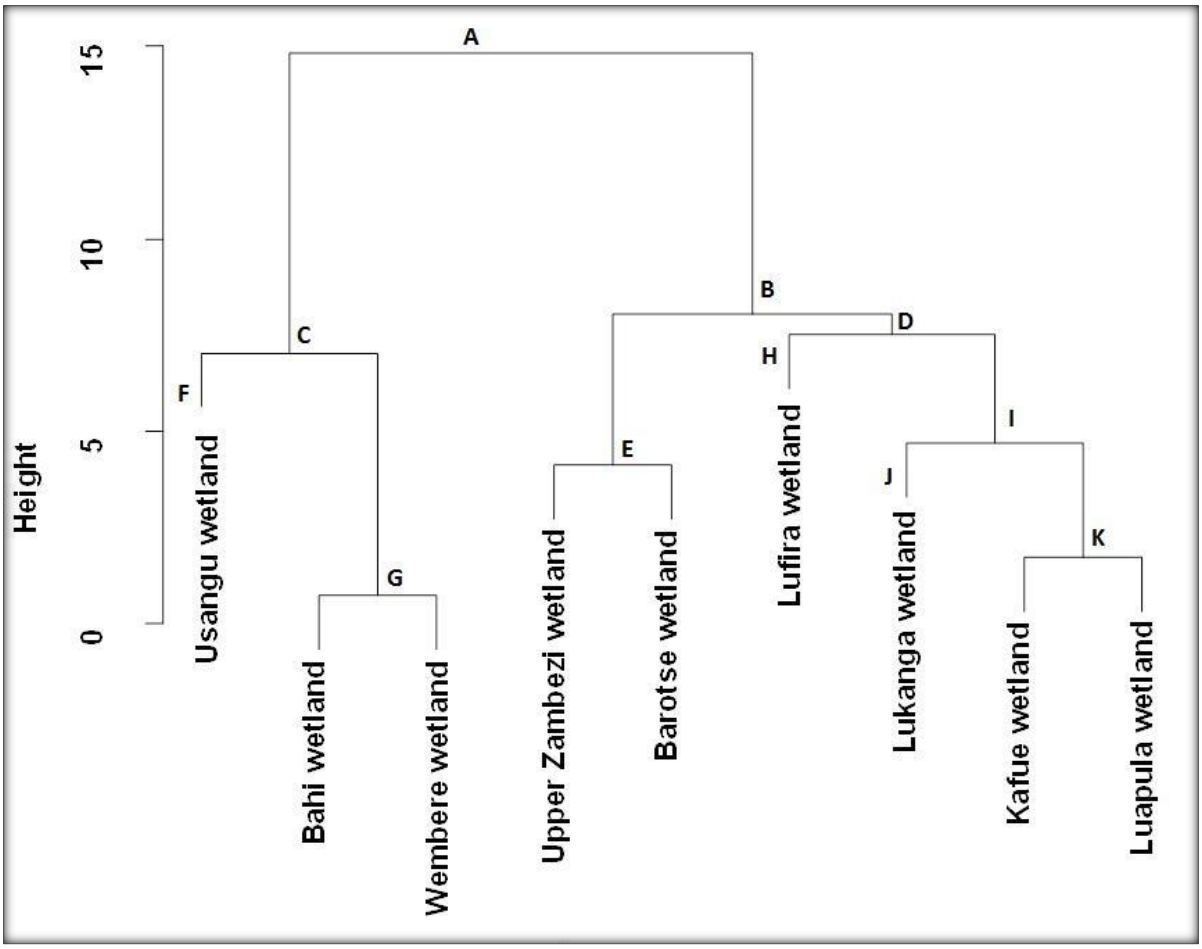

Figure 9.1: Dendrogram showing the classification of wetlands considered in this study.

9.1.2 Principal Component Analysis (PCA)

A total of eight principal components or Factors were considered in the analysis of wetland heterogeneity (Table 9.2). The first two factors accounted for about 61% of the heterogeneity, with a further 16% contributed by Factor 3. The remaining five Factors contributed less than 10% each. Since the first two Factors accounted for over 60% of the variance, the remaining six Factors will be ignored in further analyses.

Table 9.2: The percentages of each Factor's contributions to wetland heterogeneity.

Factor	Total Contribution (%)	Cumulative Total (%)
1	39.36	39.36
2	21.70	61.06
3	15.98	77.03
4	9.44	86.47
5	7.19	93.67
6	3.94	97.60
7	2.33	99.93
8	0.07	100.00

Table 9.3 shows that out of fifteen variables, the presence of strongly channelled streams, the channel being highly sinuous, channel slope, the predominance of volcanic rock in the catchment, the presence of a resistant lithology at the toe of the wetland (lithological origin), the drainage basin being exorheic, the predominance of Kalahari sediment in the catchment, and catchment size, contributed about 79% of the variance for Factor 1. Strongly channelled (Sc), sinuosity ratio (Sr), channel slope (Cs), and non-Kalahari catchment volcanic variables (Cvol) made the highest contribution (about 12% each) to variation in Factor 1, while the remaining nine variables accounted for less than 9% of the variance each.

The predominance of consolidated sedimentary rocks in the catchment (Csed), backwater depressions (Bd), the predominance of unconsolidated Kalahari sediments in the catchment (Ckal), and the presence of a distinct alluvial ridge in the wetland (Ar), contributed about 71% of variance in Factor 2. Consolidated sedimentary rocks in the catchment contributed 25.1%, while backwater depressions and Kalahari sediments in the catchment contributed 19.1 and 17.4% respectively of the variation in Factor 2. This suggests that there is a strong correlation between characteristics of the wetland's catchment geology and wetland characteristics that relate to the formation of backwater depressions.

Table 9.3: The percentages of variables contribution to wetland heterogeneity in Factor 1 and Factor 2. Variables are abbreviated as follows: Poorly channelled (Pc), Strongly channelled (Sc), Exorheic basin (Eb), Channel slope (Cs), Valley slope (Vs), Sinuosity ratio (Sr), Alluvial ridge (Ar), Backwater depressions (Bd), Wetland size (Ws), Catchment size (Cas), Lithological origin (Lo), Tectonic origin (To), Kalahari Catchment (Ckal), Non Kalahari catchment sedimentary (Csed), and Non Kalahari catchment volcanic (Cvol).

Factor 1			**Factor 2**		
Variable	**Total%**	**Cumulative%**	**Variable**	**Total%**	**Cumulative%**
Sc	12.4	12.4	**Csed**	25.12	25.12
Sr	12.23	24.63	**Bd**	19.08	44.2
Cs	12.02	36.65	**Ckal**	17.4	61.6
Cvol	11.85	48.5	**Ar**	9.21	70.81
Lo	8.9	57.4	**Cs**	8.24	79.05
Eb	8.39	65.79	**Vs**	7.06	86.11
Ckal	6.77	72.56	**Cas**	4.41	90.52
Cas	6.32	78.88	**Sr**	3.05	93.57
To	4.98	83.86	**Cvol**	2.58	96.15
Vs	4.95	88.81	**Eb**	1.36	97.51
Ws	3.99	92.8	**To**	1.24	98.75
Ar	2.88	95.68	**Pc**	0.74	99.49
Bd	2.39	98.07	**Sc**	0.37	99.86
Csed	1.19	99.26	**Ws**	0.1	99.96
Pc	0.74	100	**Lo**	0.05	100

The PCA biplot (Figure 9.2) shows that the Bahi, Wembere and Usangu wetlands, with high scores on Factor 1 and low scores on Factor 2, form a clear grouping that is positively correlated with a predominance of volcanic rocks in the catchment (Cvol) and that have a tectonic origin (To). These tectonically controlled depression wetlands are associated with the East African Rift Valley. The Barotse and Upper Zambezi wetlands have negative Factor 1 and Factor 2 scores (approximately -2 to -3.5 for Factor 1 and -2.5 for Factor 2). These wetlands are associated with unconsolidated Kalahari sediments in the catchment (Ckal), large catchments (Cs) and high valley slopes (Vs). The Kafue, Luapula and Lufira wetlands have negative Factor 1 scores and positive Factor 2 scores and are associated with catchments primarily on consolidated sedimentary lithologies (Csed), the presence of alluvial ridges (Ar)

and backwater depressions (Bd). Wetlands with low Factor 1 scores tend to be lithologically controlled (Lo), strongly channelled (Sc) and have sinuous channels (Sr). They are associated with exorheic fluvial systems integrated with the fluvial network. The Lukanga wetland is poorly channelled (Pc).

Although the PCA biplot described above clearly separated the tectonically controlled wetlands (Bahi, Wembere and Usangu) from those wetlands integrated with fluvial systems (Barotse, Upper Zambezi, Kafue, Luapula, Lufira and Lukanga), it provides little insight into factors that govern the distribution of wetlands integrated with the fluvial system. Factors governing the distribution of the Barotse, Upper Zambezi, Kafue, Luapula, Lufira and Lukanga wetlands can be clearly identified by analysing these wetlands on their own. These wetlands are exorheic and their catchments are dominated by lithologies other than volcanic rocks. Given this, the exorheic basin and non-Kalahari catchment volcanic variables become redundant and were therefore excluded from further analyses.

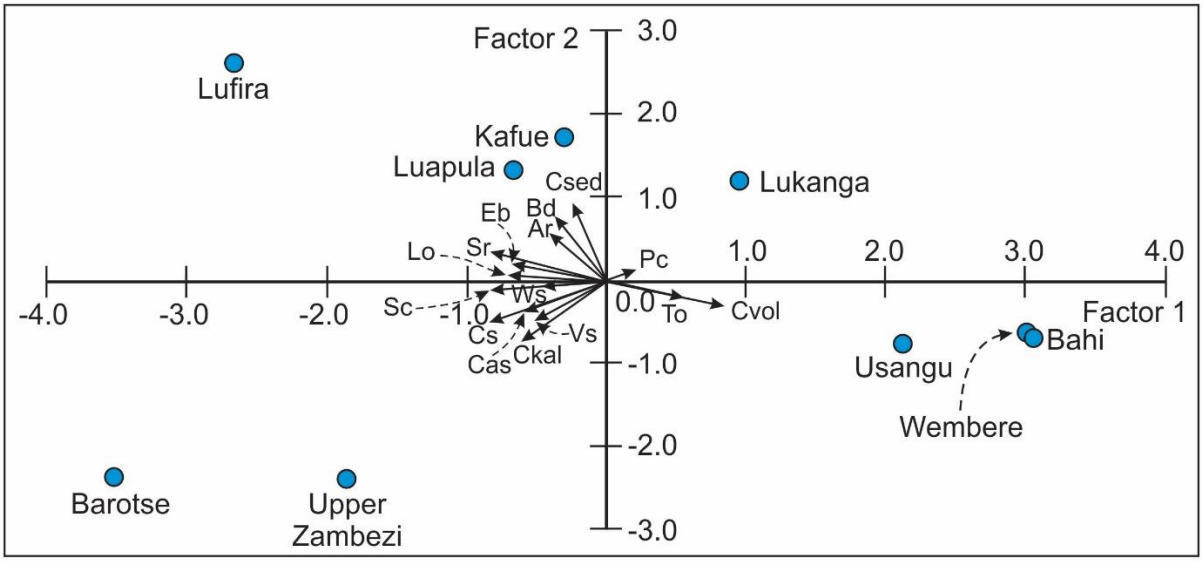

Figure 9.2: Ordination biplot showing the correlation between all 9 wetlands (shown as blue dots) and wetland variables (shown as arrows) in relation to Factor 1 and 2.

The PCA biplot of the Barotse, Upper Zambezi, Kafue, Luapula, Lufira and Lukanga wetlands shows three distinct wetland groupings (Figure 9.3). The Barotse and Upper Zambezi wetlands with negative Factor 1 and Factor 2 scores form a distinct cluster that occur within catchments dominated by Kalahari group sediments (Ckal) and negatively correlated with backwater depressions (Bd). Because Kalahari sediments weather to produce sandy material, streams flowing into and through these wetlands predominately transport sediment as bedload. The Luapula, Lukanga and Kafue wetlands with positive Factor 1

scores and negative Factor 2 scores form a distinct grouping of wetlands which are poorly channelled (Pc) and have a tectonic origin (To). The Lufira wetland with a low Factor 1 score and a positive Factor 2 score has a clearly developed meandering channel and with a clearly developed alluvial ridge (Ar). This wetland has a resistant lithology at its toe (Lo) and the alluvial ridge has developed in response to channel meandering reflected in a high sinuosity ratio (Sr) associated with valley widening.

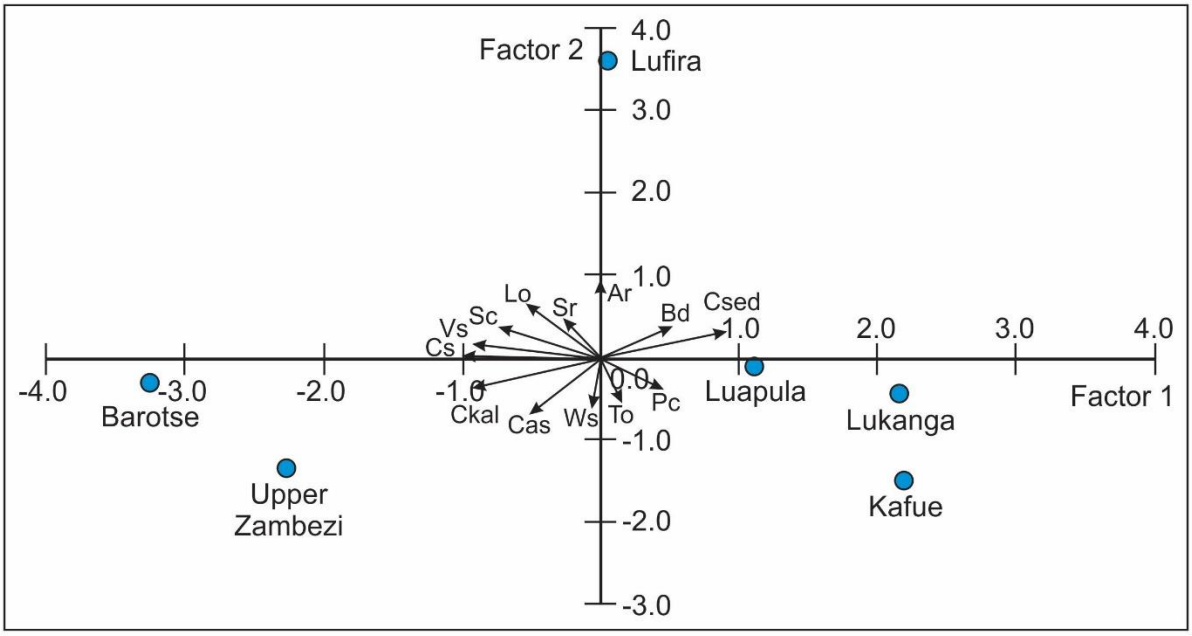

Figure 9.3: Ordination biplot showing the correlation between 6 wetlands (shown as blue dots) and 13 wetland variables (shown as arrows) in relation to Factor 1 and 2.

9.2 Discussion

9.2.1 A conceptual model of factors influencing wetland formation, structure and functioning

A key feature of wetland landforms is that they have broad cross-sections and very gentle longitudinal slopes. Valleys examined in this study are near-horizontal in cross-section with a width (calculated for the purposes of this illustration as area / valley length) that varies from slightly more than 10 km (Lufira) to almost 50 km (Lukanga; Figure 9.4a), and an average valley longitudinal slope that varies between 0.001 % (Lukanga) to 0.02 % (Barotse; Figure 9.4b). The wetlands with the lowest longitudinal valley slopes (<=0.06%) were the Lukanga, Wembere, Bahi and Kafue wetlands. Broad, near-horizontal valleys with gentle longitudinal slopes are landforms suited to the development of wetlands because they

promote flooding of the land surface to a shallow depth (Ellery et al., 2009). This study has aimed to examine the origins of these sorts of landforms.

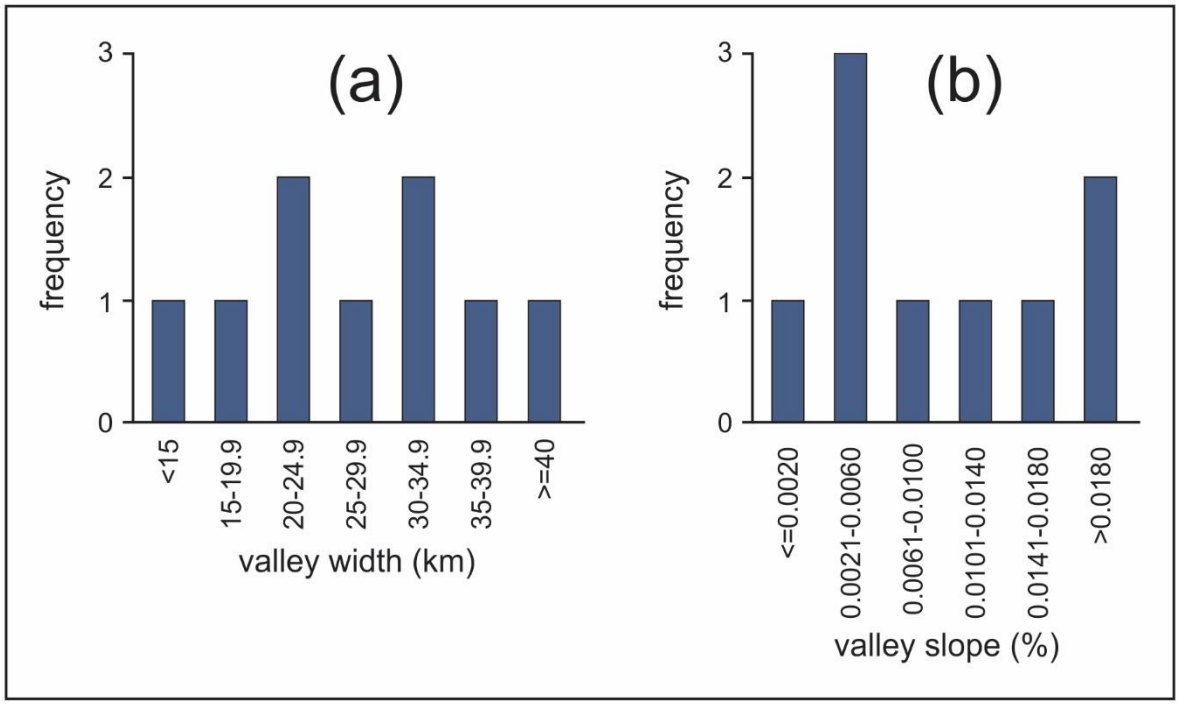

Figure 9.4: Comparison of wetlands based valley width (a) and valley slope (b).

The intention of the development of the conceptual model presented in this chapter is to draw out key factors underpinning the origin and structure of large wetlands in southern African drylands. This study demonstrates a wide range of processes that contribute to wetland formation, structure and functioning. At one extreme it is clear that tectonic processes may be primarily responsible for the creation of basins that host wetlands, such as the Wembere and Bahi wetlands (Figure 9.5). These two wetlands occupy sagging tectonic basins that form part of the East African Rift Valley. These basins have a slope that is very low and their form is irregular-linear to oval, generally with short streams entering the valley all the way along the length of the wetland. They have been influenced to a very limited extent by fluvial processes. The key issue for these landforms is the lowering of the base levels of fluvial systems by crustal sagging and the formation of basins into which water flows. Modification of these basins by sedimentation has not led to restructuring of landforms to the extent that fluvial processes can be considered to control their structure. However, if fluvial input of sediment was greater, as in cases like the Okavango Delta where the size of the catchment of a single inflowing stream is considerable, fluvial processes might overwhelm the effect of tectonic sagging on landscape form. In landscapes that are sagging, fluvial control of

landform development may therefore be limited, depending on factors such as the number of influent streams, catchment size and sediment availability.

At another extreme, wetlands may be structured primarily by fluvial processes. As mentioned previously, this can occur in settings where there is sagging of the crust due to tectonic processes, or it may occur in settings with a stable land surface and base level. The Lufira and Barotse wetlands seem to illustrate such wetland landforms. In both cases these valleys have been widened and the longitudinal slope lowered by fluvial processes upstream of a resistant lithology, to create an environment suited to wetland formation. These wetlands seem to conform to the model of wetland formation described by Tooth et al. (2002) of geological controls in the form of a resistant lithology at the toe of the wetland. The Upper Zambezi wetland may also be lithologically controlled in a similar manner, although there is evidence of tectonic factors involved in its formation.

If these three wetlands (Lufira, Barotse and Upper Zambezi) are controlled primarily by fluvial processes, it is evident that the geology of the catchment and the grade of sediment produced through weathering play a further secondary role in structuring the wetland. Those wetlands that occur in catchments dominated by the production of sediment transported as bedload (Barotse and Upper Zambezi) do not construct significant levees and alluvial ridges, such that these features tend to be absent, with important implications for wetland structure and function. However, where mixed-load sediment transported via the trunk stream is deposited in the wetland, significant alluvial ridges are constructed such that the wetlands have strongly meandering streams that shape valley morphology and wetland functioning.

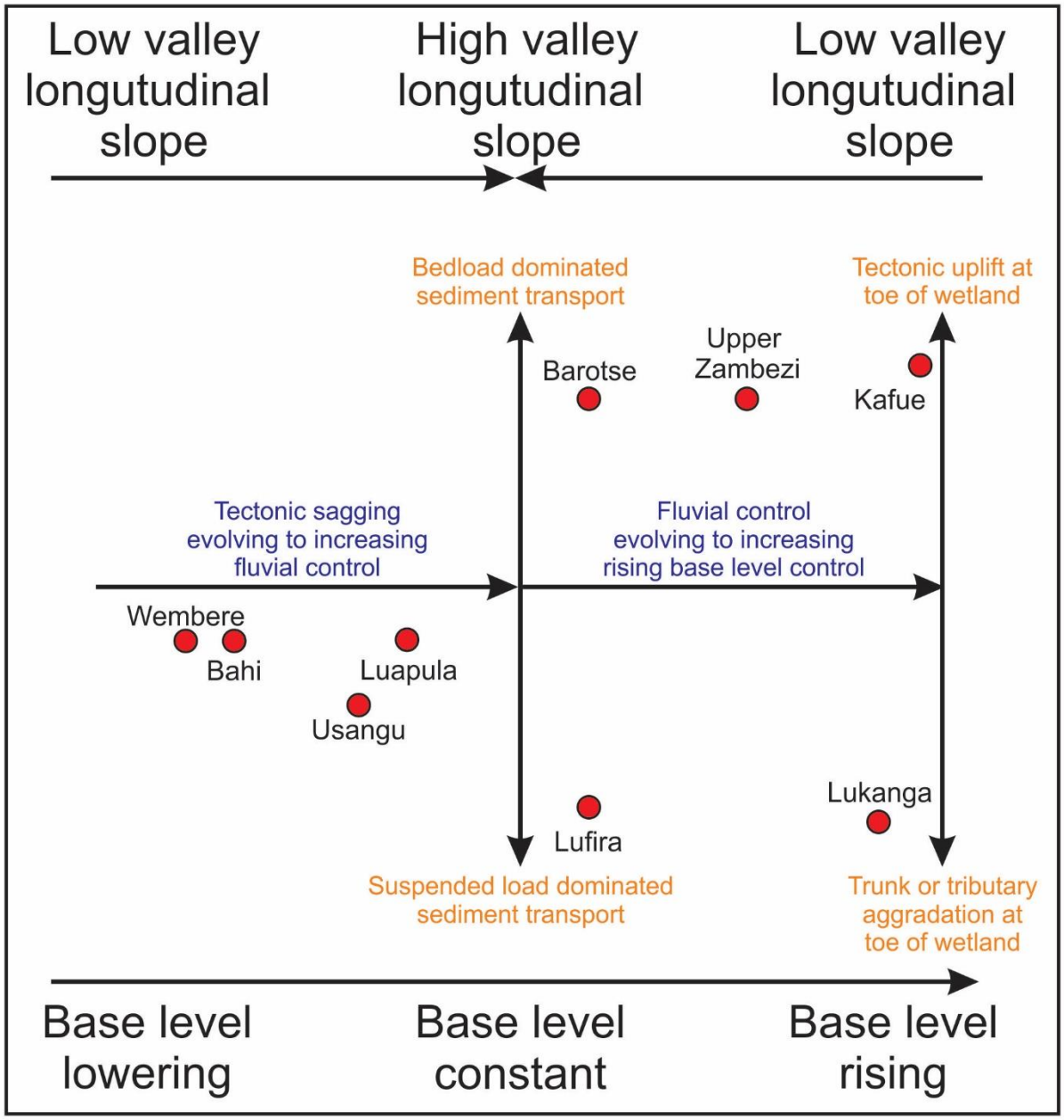

Figure 9.5: A conceptual model of primary factors responsible for shaping wetland structure, evolution and hydrological functioning.

At a third extreme are wetlands that superficially appear to be structured by fluvial processes, but which have their structures modified by gradual rising of the base level at their distal ends, either through marginal uplift adjacent to rift valleys (Kafue and possibly Upper Zambezi), or through aggradation of a floodplain that blocks a tributary valley (Lukanga). An important indicator of this aggradation at the toe of the wetland is a very low longitudinal valley slope, with the Kafue and Lukanga wetlands having the lowest longitudinal slopes of all of the fluvially integrated wetlands examined in this study. There is also evidence that the streams flowing through these wetlands are far smaller than the fluvial system that

fundamentally structured the wetland prior to the gradual elevation of the base level at the toe of the wetland over time.

Wetland formation is clearly more complex than this in that tectonic and fluvial processes may interact to produce landscape features that host wetlands. A very good example of how tectonic and fluvial processes interact to produce a large southern African wetland in a dryland environment is the Okavango Delta in northern Botswana. The Okavango occupies a tectonic depression that is an extension of the East African Rift Valley, but its structure and functioning are primarily a result of fluvial processes associated with the formation of a large alluvial fan in association with rifting (McCarthy et al., 2002); Gumbricht et al., 2001; Goudie, 2005; Stankiewicz and de Wit, 2006). Subsequent to the formation of the half graben that hosts the Okavango Delta, the unconsolidated Kalahari sediment transported from the catchment by the Okavango River has built a conical alluvial fan (McCarthy, 1992) with a remarkably uniform longitudinal slope from the apex to the toe of the wetland (McCarthy and Ellery, 1998; Gumbricht et al., 2001). This uniformity of slope reflects the fact that despite occupying a rift valley the present structure of the Okavango is shaped by fluvial processes (McCarthy et al., 1997). It is therefore possible that during the early phase of rifting the Okavango may have started in a similar position to the Wembere and Bahi wetlands in Figure 9.5, but as sedimentation took place the wetland became increasingly structured by fluvial processes such that at present it occupies a position in Figure 9.5 that is close to that of the Barotse wetland.

It also needs to be recognised that wetlands that are close to the y-axis in Figure 9.5 need not have been subjected to tectonic rifting. Uplift and erosion such that the toe of the wetland is controlled by a local base level and with a downward slope towards the local base level that is appropriate for the discharge, will be positioned close to the y-axis. The Lufira and Barotse are examples of such wetlands.

The conceptual model presented in Figure 9.5 is a plane that considers a gradient along the x-axis from tectonically controlled basins or basins inherited from palaeo-lakes into which streams flow, to valleys structured primarily by fluvial processes, to wetlands that are originally structured by fluvial processes that are experiencing uplift at the distal end of the wetland, leading to longitudinal slope reduction. The y-axis applies firstly to wetlands that are structured by fluvial processes, representing a gradient from bedload (high axis 2 scores) to mixed-load (low axis 2 scores) as the dominant sediment transported by the stream

entering and flowing through the wetland. In the case of wetlands experiencing uplift or sedimentation at the toe of the wetland, the gradient on the y-axis is from tectonic processes (high axis 2 scores) to fluvial aggradation at the toe of the wetland (low axis 2 scores).

Overall, the classification of wetlands considered in this study can be summarised into four distinct groupings with two of these divided further into two groupings each:

1. Tectonic basins with little or no indication of fluvial development (Bahi and Wembere wetlands),
2. Tectonic basins evolving towards a wetland with a structure increasingly shaped by fluvial characteristics (Usangu wetland),
3. Fluvially modified valleys with a local base level at the toe of the wetland such as a resistant lithology, or a tectonic control that limits the rate of incision of easily weathered and eroded lithologies, leading to valley widening and longitudinal slope reduction, which are of two distinct types:
    a. With a catchment on Kalahari Group sediment that is transported fluvially as bedload, and therefore with no prominent alluvial ridge or backwater depressions (Upper Zambezi and Barotse wetlands),
    b. With a catchment that produces abundant fine sediment that is deposited as overbank sediments, leading to channel migration via meandering and to the construction of an elevated alluvial ridge (Lufira wetland)
4. Fluvially modified basins with evidence of gradual elevation of the base level at the toe of the wetland, which are of two types:
    a. Tectonic marginal rift valley uplift such that they behave more as depression wetlands than as wetlands shaped by fluvial processes (Kafue and Luapula wetlands),
    b. Tributary valley wetlands blocked by aggradation of the trunk valley (Lukanga wetland).

9.2.2 Integrating wetland origin with hydrological functioning

The Bahi and Wembere wetlands are tectonic basins which are poorly modified by sedimentological processes since they are poorly channelled. These wetlands lack features associated with fluvial processes such that they are structured more like seasonal lakes. Although the alluvial fans impinging the Wembere wetland act as buffers for lateral connectivity by impeding the transfer of water and sediment from surrounding uplands to the wetland (Brierley and Fryirs, 1999), it is likely that over time both the Wembere and Bahi

will be increasingly modified by streams bringing sediment onto the basin floor such that they will increasingly become structured by fluvial processes. The occurrence of these wetlands within endorheic basins means that they do not have flood attenuation functioning for downstream flooding.

The Usangu, Luapula and Kafue wetlands are poorly channelled wetlands whose origins are influenced largely by tectonic processes, with fluvial processes having a limited influence on their structure and functioning (Figure 9.5). The Usangu wetland is a tectonically controlled depression that is connected to the drainage network downstream via the Great Ruaha River. Given the broadly V-shaped cross-section of the wetland, it seems likely that the streams in the wetland collect water flowing into the valley floor such that the streams are unlikely to carry high sediment loads. The streams are therefore unable to aggrade and the wetland is hardly shaped by fluvial processes. As such it is characterised by a high degree of lateral connectivity between the floodplain and the channel, with limited storage potential such that its average depth of inundation is below channel stage height over the modelled water profile depths (Figure 9.6). The Luapula wetland formed from changes in base level subsequent to the partial draining of Lake Mweru by the Luvua River that eroded headward subsequent to quaternary faulting, which could have lowered the channel base level (Dixey, 1944). The Kafue wetland occupies a depression to the north-west of the uplifted margin of the Luangwa-Kariba rift. However, both wetlands show similar structures and occur within catchments dominated by sedimentary materials that weather to give rise to streams dominated by mixed sediment load. As a result, the two wetlands are characterised by floodplain features such as backwater depressions, meander scars and cut banks that appear to be associated with large palaeo-meandering streams, but lack evidence of a prominent alluvial ridge associated with current channels. Because of the lack of a prominent alluvial ridge down the length of the Kafue and Luapula wetlands, the average depth of inundation for the two wetlands is below channel stage height over the range of modelled water levels (Figure 9.6). This suggests that the wetlands are characterised by effective lateral connectivity, such that they have limited potential to attenuate downstream flooding since floodwater can be easily transferred from the wetland to channel areas in the waning stages of a flood event.

The Barotse wetland is a lithologically controlled wetland that formed in a similar fashion to the Klip River wetland as described by Tooth et al. (2002), while the formation of Upper Zambezi wetland basin appears to have been primarily influenced by the marginal uplift of

the shoulder of the Luangwa-Kariba rift that could have reduced local slopes to the north-west. However, because of similar catchment geological materials (unconsolidated Kalahari group sediments), these two wetlands show similar structures and hydrological functionality. Sediment that enters this wetland is fluvially transported as bedload. Because of the dominance of unconsolidated bedload sediment and the associated depositional characteristics, bed aggradation exceeds bank aggradation, resulting in the occurrence of avulsions such that the wetlands maintain a near-horizontal valley cross-sectional topography. Figure 9.6 shows that the Barotse wetland has the lowest average depth of inundation, which is likely to be due to limited valley cross-sectional topography, resulting in a high degree of lateral connectivity between the channel and the wetland, such that the wetland has limited flood attenuation potential.

The Lufira wetland is a meandering floodplain formed from channel processes in response to lithological variations similar to the Klip River wetland described by Tooth et al. (2002). Because of an adequate supply of fine-grained sediment, overbank deposits have resulted in the development of an alluvial ridge down the length of the wetland. The alluvial ridge acts to limit return flows from the wetland areas to river channels during the waning stage of flood events, resulting in prolonged retention of floodwaters due to extensive inundation of backwater depressions.

The Lukanga is a composite of different HGM wetland units that interact to create a feature that is channelled on the western wetland margin (Kafue River) while the eastern part of the wetland occupies a basin fed by an unchannelled valley bottom tributary wetland. Although the average depth of inundation is lower than channel stage height at water profile depths greater than 0.5 m, Figure 9.6 shows that the wetland has the second highest average depth of inundation. The flood attenuation ability of the wetland is complex and can be attributed to the interactions between the Kafue River along the floodplain HGM unit and the tributary channel and its outflow channel from the depression HGM unit into the floodplain HGM unit. Aggradation along the floodplain valley has resulted in the impoundment of the outflow channel and serves to impede the rate and magnitude of water exchange from the depression and valley-bottom wetlands to the Kafue River.

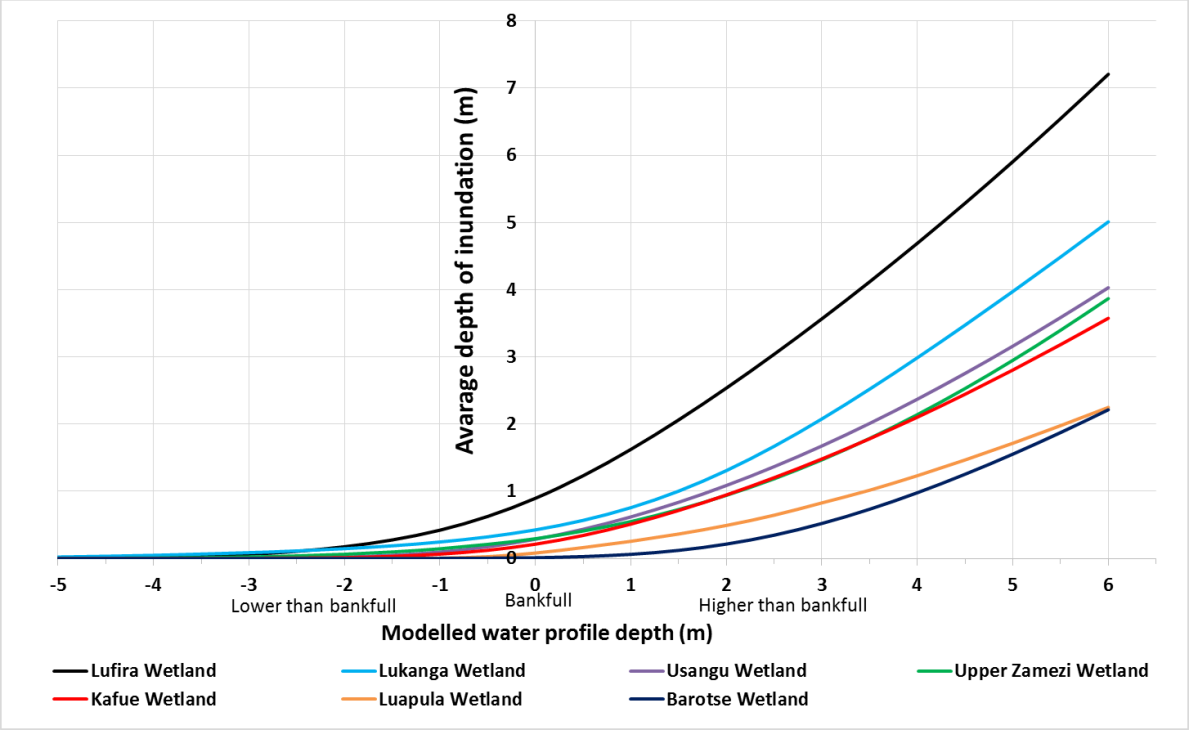

Figure 9.6: Comparison of the average depth of inundation for different wetlands.

CHAPTER 10: DISCUSSION

10.1 Tectonic history and wetland formation

Tectonic activities have played a major role in the formation of depressions that accommodate wetlands through their influence on basin form and hydrology. The two major uplift events that occurred about 30 Ma and 5 Ma initiated faulting and rifting (Partridge and Maud, 1987; Broadley and Cotterill, 2004; Cotterill, 2004; Stankiewicz and de Wit, 2006; Burke and Gunnell, 2008). The first uplift event severed connections between palaeo-drainage networks, including possibly the formation of inland drainage basins such as the Kalahari Basin (Goudie, 2005; Stankiewicz and de Wit, 2006) and the formation of palaeo-lakes such as Palaeo-Lake Makgadikgadi (Moore et al., 2007), Palaeo-Lake Lufira (Broadley and Cotterill, 2004; Cotterill, 2004), and Palaeo-Lake Patrick (Moore et al., 2007; Simms, 2000). The subsequent formation of tectonic depressions diverted drainage into them. The second uplift event that occurred about 5 Ma could have initiated faulting, which led to the formation of southern African lakes such as Lake Mweru, Lake Upemba and East African half grabens that host wetlands such as the Wembere and Bahi wetlands (Broadley and Cotterill, 2004; Cotterill, 2004; Foster et al., 1997; Macheyeki et al., 2008). The second uplift event and subsequent faulting could also have lowered stream base levels and activated channel erosion, such as the Lufira, Upper Zambezi, Luapula, and Usangu basins.

As a result of uplift events, most streams in southern Africa are in a long-term state of incision (Schumm, 1993; Tooth et al., 2004; Goudie, 2005). Headward erosion associated with uplift events could have resulted in the capture of drainage networks, palaeo-lakes and even the desiccation of palaeo-lakes (Simms, 2000; Broadley and Cotterill, 2004; Cotterill, 2004; Moore et al., 2007). The orientation of the drainage networks within the Usangu wetland's catchment relative to the drainage networks within the Great Ruaha basin suggest that the Usangu wetland could be a remnant of an inland basin that was captured by the Great Ruaha River.

Tectonic processes may lead to the formation of rifted depressions such as Lake Malawi or Lake Mweru, or to the formation of shallow depressions between rift valleys. For example, Lake Victoria is believed to be a tectonic sag between the uplifted shoulders of the eastern and western branches of the East African Rift Systems (Scholz et al., 1990; Johnson et al., 1996, 2000). The uplifted rift shoulders are believed to have diverted drainage into the

shallow depression that hosts Lake Victoria. Lake Bangwelu and the associated wetlands may be of similar origin between the Luangwa-Kariba and Mweru-Tshangalele Rifts.

The current study has shown that wetlands such as the Usangu, Wembere, and Bahi wetlands appear to have formed from flooding within rift valleys. Other tectonically controlled wetlands include the Okavango wetland in northern Botswana, which is an alluvial fan that has formed in a half-graben related to the East African Rift system (McCarthy et al., 2002; McCarthy and Ellery, 1998; Gumbricht et al., 2001; Tooth et al., 2015). Increased longitudinal sedimentological connectivity into the depression resulted in the modification of the depression through the formation of an alluvial fan at the point where the trunk stream flows from a relatively confined valley in the region known as the "Panhandle" onto the graben floor.

10.2 Fluvial processes and geological/structural controls on wetland formation

The current study has shown that fluvial processes may play an important role in the formation and modification of broad valleys with near-horizontal cross-sections and gentle longitudinal slopes. The Klip River wetland on the Highveld of South Africa is characterised by a very gentle longitudinal slope (0.1%) over a length of nearly 30 km and a near-horizontal cross-section over a width of up to 1 500 m. Bedrock is typically 2 to 3 m below the floodplain surface and the wetland (especially the lower reaches) comprises intensively meandering reaches. The wetland overlays easily erodible lithologies of the Karoo Supergroup such as shales and sandstones and the toe of the wetland is co-incident with a resistant dolerite dyke (Tooth et al., 2002). Such wetlands are believed to form as a result of a resistant lithology at the toe of the wetland impeding longitudinal connectivity, resulting in increased lateral connectivity as a channel responds to the base level imposed by the resistant lithology. Upstream of the resistant lithology the stream increases its sinuosity through meandering, and widens the valley due to meander migration. The current study has shown that wetlands such as the Barotse, Lufira, Upper Zambezi and Lukanga (floodplain HGM unit) wetlands occupy reaches which overlay easily eroded lithologies upstream of a resistant lithology. Common to all these wetlands, the resistant lithology at the toe of the wetland serves to establish and sustain a local base level for the stream, thus preventing rapid channel incision in an upstream direction. However, for the Barotse, Lufira and Lukanga (floodplain HGM unit) wetlands, it appears that increased lateral channel migration and avulsions upstream of a resistant lithology have led to the formation of broad and gently sloping valleys with wetlands.

10.3 Geomorphological factors related to wetland structure and dynamics

The current study has shown that fluvial processes modify valley morphology through erosion and deposition in order to build a slope down the length of the valley that is appropriate for the discharge. In settings where the slope is too high for the discharge, erosion will occur and lead to a reduction in slope (Ellery et al., 2009). Conversely, where the slope is too low for the discharge, deposition will occur and lead to an increase in the slope (Ellery et al., 2009). Discharge along any reach of a stream is given such that the stream can do one of three things to accommodate the available discharge: 1) vary the width of the channel, 2) vary the depth of the channel, and 3) lower or steepen the slope (Leopold and Maddock, 1953; Ellery et al., 2009). These processes work together such that streams construct a longitudinal slope that is appropriate for the available discharge all the way down the stream course. Given that tributaries add to the discharge of the trunk stream, streams typically build longitudinal slopes that are logarithmic (stream gradient systematically declines downstream). Barriers such as a tributary stream alluvial fan that impinges on the trunk stream or a resistant bedrock lithology may interrupt the idealised logarithmic slope by impeding longitudinal connectivity. Such features may lower longitudinal slope in an upstream direction and steepen slope in a downstream direction thus affecting geomorphological processes such as increasing lateral erosion (causing valley widening), and enhancing sedimentation upstream.

The current study has shown that catchment geology and the consequent sedimentological characteristics play an important role in shaping wetland structure and consequent hydrological functioning. Sedimentation processes modify the morphology of valleys and tectonic depressions through aggradation processes that determine the morphology of the wetland system. This is well illustrated by comparison of two large southern African wetlands, the Okavango wetland in northern Botswana (Tooth et al., 2015) and the Bahi wetland in Tanzania (this study), both of which occur within endorheic depressions that formed from tectonic activity. However, the structure of the two wetlands differs considerably as a result of sedimentological processes related to catchment characteristics. The Okavango wetland is an alluvial fan with a conical shaped cross-sectional profile (Gumbricht et al., 2001) while the Bahi wetland is seasonally flooded with a near-horizontal cross-sectional profile. The Okavango wetland has a high supply of unconsolidated sediments which are mainly transported as bedload (McCarthy and Ellery, 1998). The wetland is maintained hydrologically from the Okavango River that drains a catchment of 708 600 km^2

that is primarily on unconsolidated Kalahari sands. In contrast, the Bahi wetland appears to have a low supply of unconsolidated bedload sediments since it is fed mainly by the Bubu River that drains a 21 816 km^2 catchment that is mainly on granite of the Seoka Adamellite Undifferentiated Granitoid Complex. In simple terms the Bahi wetland's catchment weathers to produce sediment of variable grain size that is transported as bedload (sand) and suspended load (silt and clay). Furthermore, the Okavango wetland is fed by a single influent stream from its very large catchment, whereas, despite the presence of a dominant influent stream, there are multiple influent streams to the Bahi wetland. The difference in wetland structure between the Okavango and Bahi wetlands could be related to the age of the basins, the size of the catchments and therefore the amount of sediment supplied to each of the systems, and the nature of the sediment load entering the wetland. The Okavango could have formed in the Miocene after the first uplift event (Goudie, 2005; Stankiewicz and de Wit, 2006) and the Bahi wetland could have formed subsequent to the second uplift event that occurred about 5 Ma (Macheyeki et al., 2008). Therefore, the longer-term sedimentation processes within the Okavango Delta relative to that of the Bahi wetland could also explain the different wetland structures of the two wetlands.

The comparison of meandering and anastomosing floodplains as illustrated in the current study provides further illustration of the effect of catchment geology and sedimentological regime on wetland structure. Along meandering wetland reaches, spatial variation in rates of sedimentation within a wetland give rise to a diverse range of geomorphic features such as levees, alluvial ridges, oxbow lakes and backwater depressions (Makaske et al., 2001; Tooth et al., 2002; McCarthy et al., 2010; Ashworth and Lewin, 2012; Lewin and Ashworth, 2014; Larkin et al., 2017a), which influence wetland structure and hydrological functioning. On floodplains with anastomosing streams, bed aggradation and avulsions result in the formation of near-horizontal valley cross-sections characterised by multiple channels, vegetated bars and the absence of an alluvial ridge (Makaske et al., 2009; Liu and Wang, 2017; Larkin et al., 2017b; Wohl et al., 2017). The current study has shown that the formation of an alluvial ridge appears to be influenced by the quantity and nature of sediment supplied to the wetland. For instance, both the Lufira and Barotse wetland appear to have formed from lithological controls as described by Tooth et al. (2002). However, these wetlands differ in terms of their structure and hydrological functioning. The Lufira wetland catchment is mainly composed of consolidated metamorphic (i.e. Kundelungu Group) and sedimentary rocks (i.e. Monwezi Group) that weather to give rise to a range of particle sizes from sand to silt and clay.

However, the catchment of the Barotse wetland is mainly composed of unconsolidated Kalahari sands such that streams transport mainly bedload sediment. Overbank deposits of fine material have resulted in the construction of an alluvial ridge down the length of the Lufira wetland while bedload deposits of unconsolidated Kalahari sands within the Barotse wetland have resulted in the formation of a multi-channelled valley with a near-horizontal cross-section. As a result of sedimentation characteristics and fluvial processes the Lufira wetland has a lower longitudinal channel slope (0.005%), a prominent alluvial ridge and backwater depressions, while the Barotse wetland, which is more than twice the size of the Lufira wetland, has a higher channel slope (0.012%) and lacks a prominent alluvial ridge and backwater depressions.

10.4 Climatic controls on wetland formation

In arid and semi-arid regions where climatic conditions yield a negative surface water balance, large catchment sizes play an important role in maintaining wetlands hydrologically (Ellery et al., 2009; Tooth and McCarthy, 2007). The current study has shown that wetlands in Africa's elevated drylands form within catchments that are characterised by a negative surface water balance since evapotranspiration in the region greatly exceeds precipitation for about 7 to 9 months of the year. Wetlands considered in the current study occupy between 2% and 10% of their catchment areas and are maintained hydrologically from streams that drain their catchments. This is a common characteristic of wetlands in drylands where wetlands usually occupy less than 15% of their catchments and require water inputs from the catchment via streams inflows (Ellery et al., 2009; Mumba and Thompson, 2005).

For wetlands considered in this study, peak wetland inundation typically occurs at the end of the rainy season, which suggests that direct precipitation partially influences peak wetland inundation. Although the resolution of the timing of peak flows is not particularly accurate as it could only be resolved to the nearest month based on available satellite imagery and climatic data, there is evidence that wetlands that occupy a small percentage of their catchment area show a longer lag between peak local rainfall and peak wetland inundation relative to wetlands that occupy a large percentage of their catchment area (Figure 10.1). Wetland size relative to catchment size is clearly an important factor in determining the timing of peak wetland flooding. However, there are other important factors that may influence this. Firstly, the presence of wetlands in the catchment upstream of the wetland being considered would attenuate peak flows within the catchment and therefore delay the maximum extent of flooding. For example, the Barotse and Chobe wetlands are located

upstream of the Upper Zambezi wetland while the Kafue wetland is located downstream of the Lukanga wetland complex. Secondly, the shape of the catchment as well as that of the wetland will affect the timing of inundation: semi-circular catchments are likely to have tributaries contributing flow to the wetland at approximately the same time (e.g. the catchments of the Wembere, Bahi and Usangu wetlands) whereas linear catchments should have a longer delay in the arrival of the peak flood (e.g. the catchments of the Lufira and Barotse wetlands). Thirdly, timing of inundation will be affected by the proportion of flow that is via tributaries entering the wetland down its length versus the contribution of a single influent stream entering at the head of the wetland. In the case of a single influent stream the wetland itself will slow water flow and therefore delay the floodwaters to a greater extent than will occur if tributaries enter all the way down its length. For example, the Wembere and Bahi wetlands are not channelled and receive much of their inflow from tributary streams, while overbank flows from a single influent stream play a major role in the hydrological regime of the Lufira and Kafue wetlands. Fourthly, the nature and topography of the catchment is likely to affect runoff characteristics, as sandy Kalahari sediments in a gently-sloping catchment are likely to attenuate runoff to a greater degree than mature quartzites with shallow and skeletal soils in steep catchments. The amount and timing of rainfall in the catchment can contribute to variation in runoff characteristics, as higher rainfall would likely lead to more immediate runoff than a semi-arid catchment. For example, the catchment of the Luapula wetland is mostly humid while those of the Upper Zambezi and Kafue wetlands are mostly semi-arid (Figure 10.2). All these wetlands occur downstream of large wetland systems but the Luapula wetland shows a relatively short time lag between peak local rainfall and peak wetland inundation.

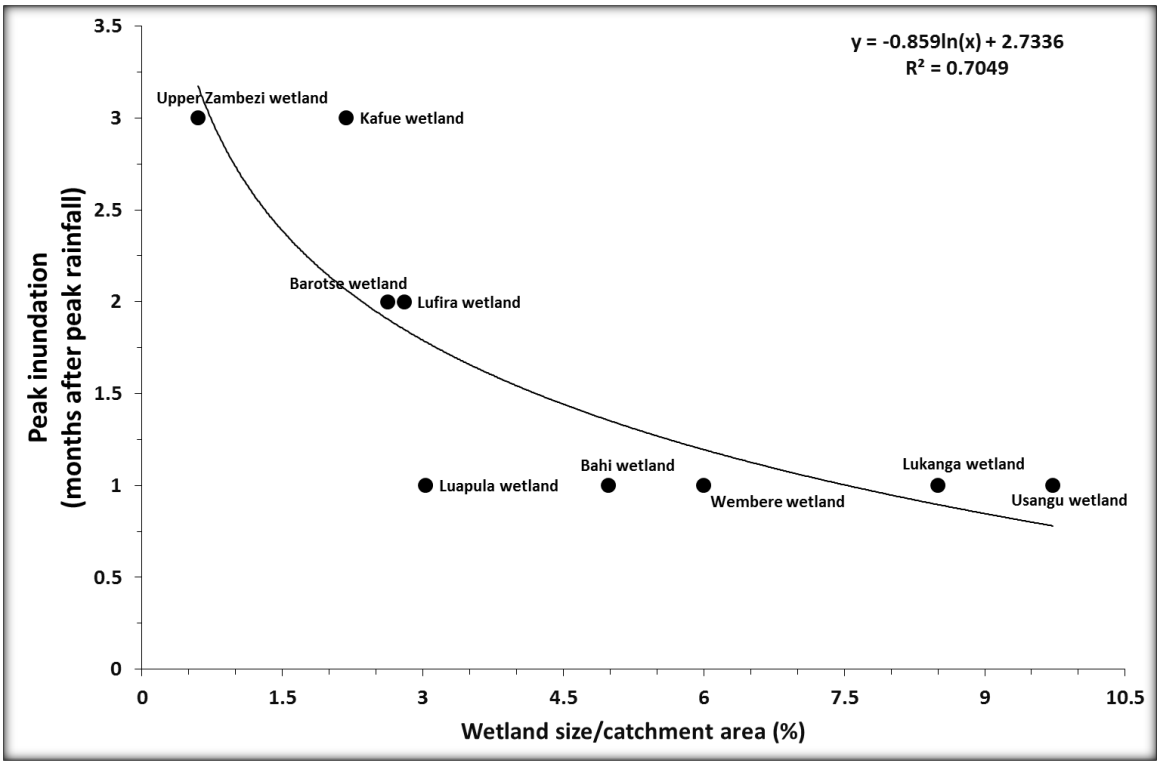

Figure 10.1: The lag between peak wetland inundation and peak local rainfall for wetlands which occupy small and large percentages of their catchment areas.

There is a general decline in both wetland and catchment sizes from southern Africa to East Africa (Figure 10.2). Wetlands which occupy less than 4% of their catchments were mainly southern African floodplains, namely the Upper Zambezi, Barotse, Kafue, Luapula, and Lufira wetlands, while those that occupy more than 4% of their catchment areas tended to occur in East African depressions, namely the Usangu, Wembere, and Bahi wetlands. The exception to this pattern was the Lukanga wetland, which occupied about 8% of its catchment. The small catchment sizes in East Africa may be attributed to the prevalence of clearly defined and steep sided rift valleys in the region. The tectonic processes that created the East African Rift Valley exert important controls on the drainage networks, leading to short tributaries flowing into the rift axis (Wembere and Bahi wetlands), and occasionally to longer rivers that flow along the rift axis (Scholz et al. 1990).

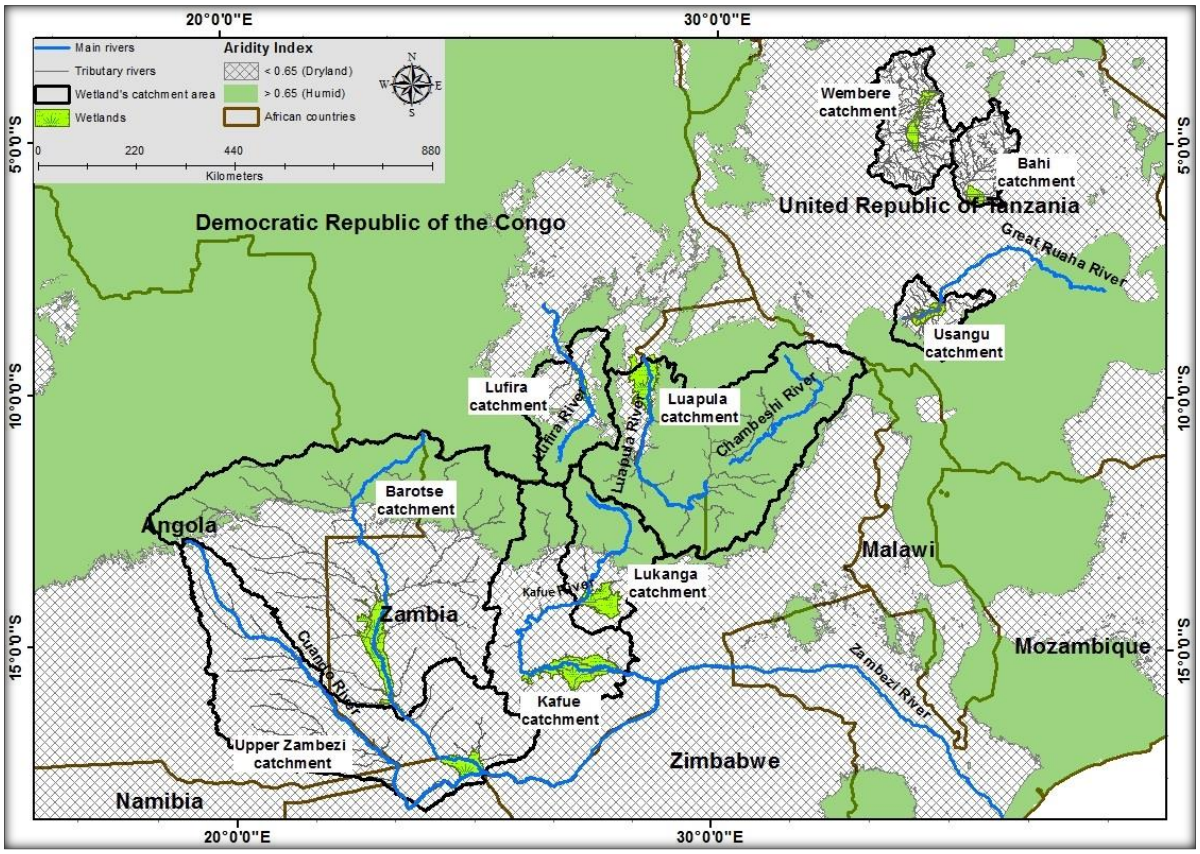

Figure 10.2: The distribution of wetlands and their catchment areas in relation to the distribution of dryland. Note that where two or more wetlands occur in the same catchment, the lower wetland catchment extent includes the extent of the upper catchment.

10.5 The contribution of this study to wetland science

Since the realisation of the importance of wetlands for waterfowl habitats more than 5 decades ago, there has been considerable interest in wetland research focussing on ecological understanding and the hydrological and socio-economic benefits of wetlands. Recognition of the importance of wetlands to human well-being led to the realisation of knowledge gaps that needed further research in order to inform management decisions. Before 1950, wetlands were regarded as of limited value and their artificial drainage for farming, grazing and development were promoted (McCormick, 1978). Between 1950 and 1970, wetlands were primarily valued based on their importance as waterfowl habitats such that research focused primarily on wetland ecology (Cowardin et al., 1977; McCormick, 1978; Stearns, 1978). After Gosselink and Turner (1978) highlighted the hydrological regime as the primary factor determining wetland formation and structure, wetland science started to focus mostly on understanding the wetland hydrological regime and its influence on the physiochemical environment and consequently on wetland biota.

Currently, the hydrological regime is still regarded as the primary determinant of wetland structure and functioning (e.g. Mitsch and Gosselink, 2015; House et al., 2016; Halabisky et al., 2016; Campbell et al., 2016). According to Gosselink and Turner (1978) and Mitsch and Gosselink (2015), prolonged flooding directly modifies soil chemical and physical properties, particularly through reduction in oxygen availability in the root zone. However, flooding should be sufficiently shallow to allow the establishment of macrophytes that are adapted to tolerate anaerobic conditions in the root zone. Flooding of soils to a shallow depth leads to biogeochemical changes in the soil associated with anaerobic conditions, which typically lead to increased solubility of metals and reduced rates of organic matter decomposition (Vepraskas, 2016). These biogeochemical changes in the soil mean that only plants adapted to these conditions are able to establish, such that wetlands are characterised by biotic communities adapted to survive in soils dominated by anaerobic conditions (Gosselink and Turner, 1978; Mitsch and Gosselink, 2015). These characteristics are summarised in Figure 10.3, which illustrates the relationship between basin physiography and climate, which are viewed as given externalities, the hydrological regime (depth, duration and frequency of inundation), edaphic characteristics, and the biotic response.

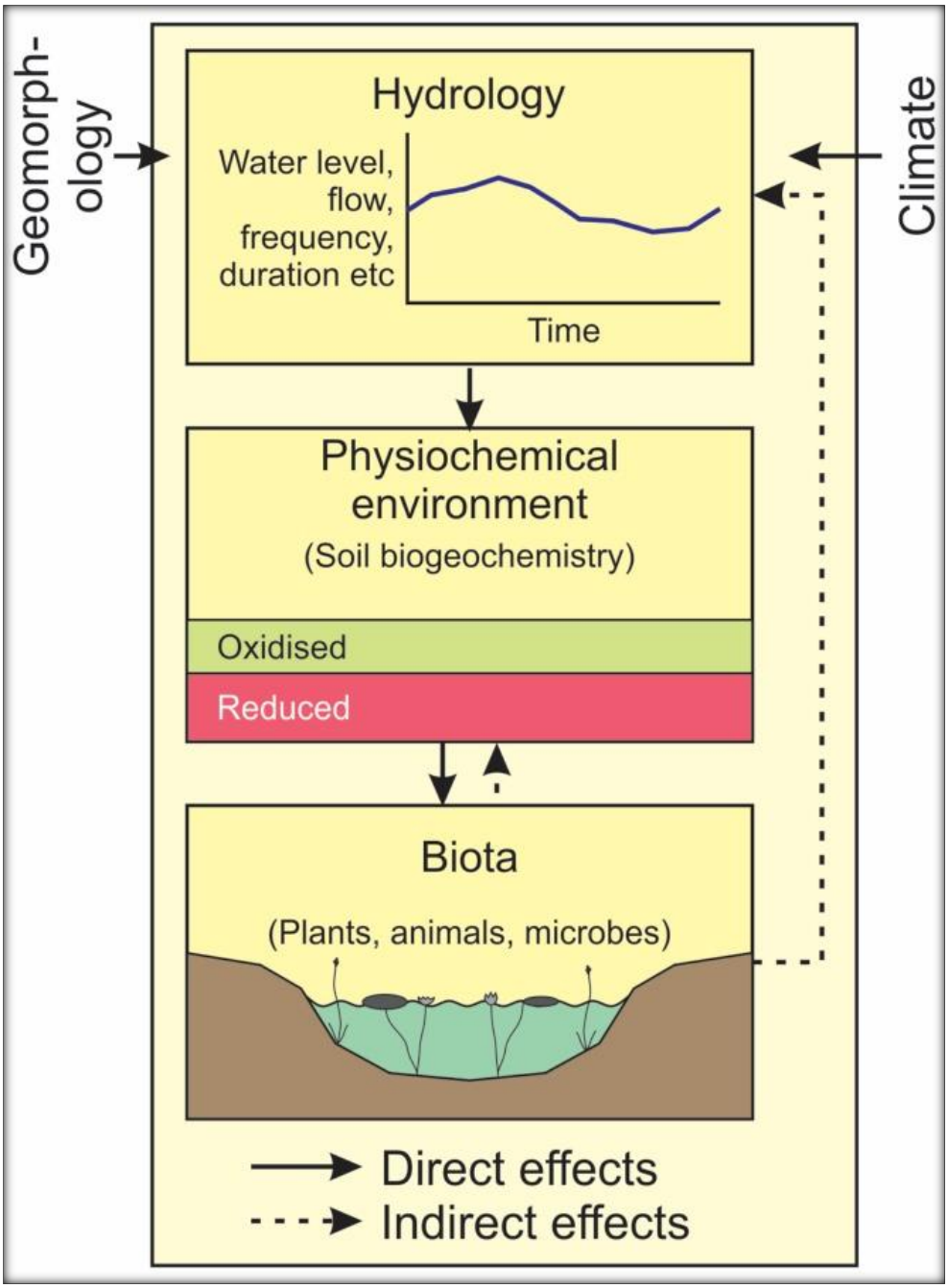

Figure 10.3: The relationship between hydrology and edaphic and biotic characteristics of wetlands (modified after Gosselink and Turner, 1978).

When more diverse ecological benefits of wetlands were realised in the early 1990's, wetland classification systems evolved to incorporate the role of the hydrological regime in influencing ecological functions of wetlands (e.g. Brinson, 1993). The hydrological regime, particularly the source of water and its pattern of flow through the wetland, as well as the biotic response to the hydrological regime, became the primary interests for wetland scientists and managers (e.g. Faulkner, 2004; House et al., 2016; Halabisky et al., 2016; Campbell et al., 2016). In the late 20th and early 21st century, southern African

geomorphologists worked on the Okavango Delta and smaller floodplain wetlands in South Africa. This work started to reveal important knowledge gaps related to wetland origin and dynamics (e.g. McCarthy et al., 1993a; McCarthy et al., 1997; McCarthy and Hancox, 2000; Gumbricht et al., 2001). For example, while working within the Okavango Delta in Botswana, McCarthy et al. (1997) realised that streams have other functions than just the transfer of water. In support of McCarthy et al.'s (1997) work in the Okavango Delta, McCarthy and Hancox (2000) highlighted the role of geological and fluvial geomorphological processes in wetland origin and their medium-term dynamics and long-term evolution.

Tooth et al. (2002), Grenfell et al. (2008), and Grenfell et al. (2010) provided more detailed conceptualisations on how geological and fluvial geomorphological processes shape the landscape and determine the origin and evolution of different types of wetland. However, no attempts have been made to examine the applicability of these conceptual models in providing a better understanding of the origin and dynamics of large wetland systems. As a result, no attempts have been made to consolidate existing geomorphological knowledge into a conceptual model that places appropriate emphasis on geomorphological processes as a primary determinant of wetland origin, structure and dynamics. In simple terms, the geological and geomorphological processes that govern the formation of wetlands as they relate to the creation of broad (near-horizontal in cross-section) and gently sloping valleys (longitudinally), have been overlooked (McCarthy and Hancox, 2000). This is evident from the Tooth et al.'s (2015) modification of the Gosselink and Turner (1978) conceptual model that places the hydrological regime within the broader framework of climate, geomorphology, and human activities as they relate to wetland origin, structure and hydrological functioning (Figure 10.4). Nonetheless, the Tooth et al. (2015) model does reveal that the influence of the hydrological regime on wetland formation and dynamics is a result of the interactions between geomorphology, climate and human activities. However, current and previous studies (e.g. Tooth et al., 2002; Grenfell et al., 2008; Grenfell et al., 2010) provided enough information on the geomorphic origin of wetlands to consolidate existing knowledge into a conceptual model that places appropriate emphasis on geomorphological processes as a primary determinant of wetland origin, structure and dynamics. In order to increase our understanding of wetland processes it is therefore necessary to more explicitly integrate knowledge of geological and geomorphological processes within existing conceptual models.

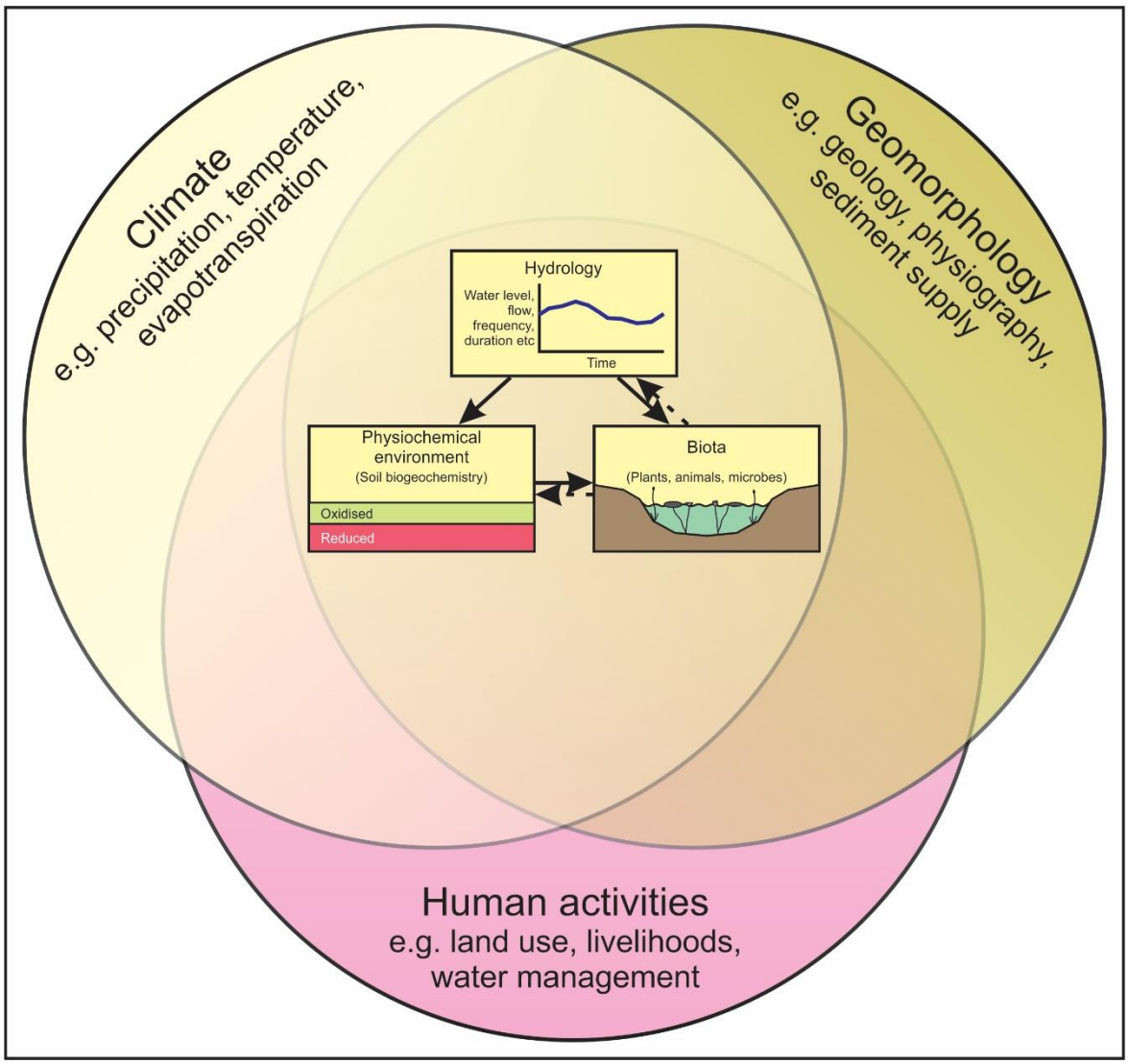

Figure 10.4: The influence of hydrology on wetland structure and function, and the biotic feedbacks that affect wetland hydrology as a result of the interaction between geomorphology, climate and human activities. (Modified from Tooth et al., 2015).

10.6 Incorporation of geological and geomorphological processes in a model of wetland formation and dynamics

Lithological characteristics together with structural and tectonic processes, exert long-term effects on physiographic characteristics at a continental to sub-continental scale. In combination with climate, physiography is modified through weathering, transport and deposition, to produce a landscape form that includes features shaped primarily by the fluvial system (Figure 10.5). Climate produces runoff that leads to flooding of parts of the Earth's surface, such that water may simply drain into shallow basins, or it may modify basin form through erosion and deposition that lead to the formation of broad valleys with a gentle

longitudinal slope, which are ideally suited to wetland formation. The morphology and dynamics of some wetlands are therefore as much a product of how flowing water interacts with and modifies a landscape to produce a landform that floods to a shallow depth for prolonged periods, as they are about the water itself. Once a wetland landform has been created through processes of erosion and deposition, it is then appropriate to consider the effect of the hydrological regime on soil biogeochemistry and biota, as discussed by Gosselink and Turner (1978). However, the lack of attention paid to how a wetland landform is created in existing models of wetland structure and function, is a conceptual gap that limits the ability of managers to effectively make decisions in the interests of maintaining dynamic functioning wetland ecosystems.

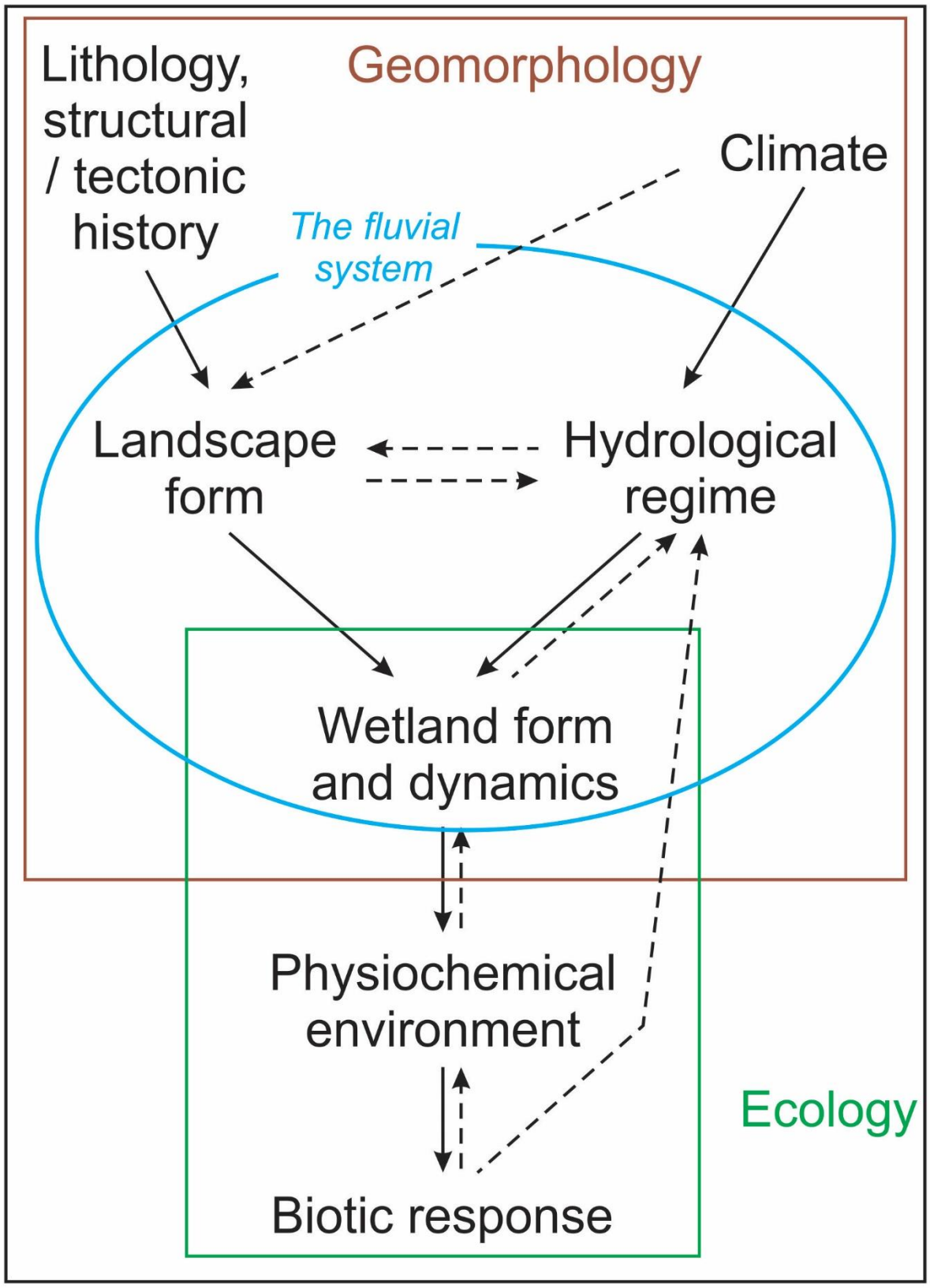

Figure 10.5: Conceptual illustration of the role of geomorphological processes on the formation of wetlands that incorporates the influence of hydrology (i.e. prolonged flooding) on the physiochemical and biotic characteristics of a wetland. The solid arrows show direct effects while the hashed arrows show feedbacks.

Although the conceptual model presented above is applicable to all wetlands, it is likely that for individual wetlands different components of the model may be more applicable than others. For example, rifting associated with the extension of the East African Rift Valley into southern Africa has created graben structures that host wetlands such as the Wembere and Bahi wetlands. In such cases water is viewed as draining relatively passively into the basin and flooding it, such that the structure and functioning of the wetland that is created can be described by the Gosselink and Turner (1978) model, where the hydrological regime is the primary driver of the wetland system (Figure 10.6a). In the case of landforms resulting from scouring of the land surface by ice and the deposition of terminal moraines in northern Europe, northern Asia and northern North America during the last ice age that ended about 10 000 y BP, passive flooding of the basin to a shallow depth would similarly be explained by the Gosselink and Turner (1978) model.

In the case of the Usangu wetland, which formed within a depression caused by crustal sagging in the East African Rift Valley, the basin has been altered by deposition associated with fluvial processes, such that it is increasingly being structured by fluvial processes that interact with regional drainage. Despite its tectonic origin, the Usangu wetland is therefore transitional to a wetland that is driven primarily by fluvial processes. In many cases structural and tectonic basins are not filled passively by water draining a catchment, particularly where streams originate from large catchments. The graben structure that hosts the Okavango Delta illustrates this very clearly. Given that the Okavango River drains a catchment of 708 600 km^2, much of which is unconsolidated Kalahari Group sediments, a large amount of clastic sediment is deposited within the ecosystem annually (approximately 200 000 tonnes; McCarthy and Ellery, 1998). The deposition of sediment within the original half-graben has created an alluvial fan that hosts the wetland with a structure that is a product of fluvial processes. Therefore, despite a tectonic origin, the morphology of the wetland is a product of fluvial processes such that in respect of the model depicted in Figure 10.6, the Okavango would be positioned close to the Barotse floodplain in Figure 10.6(b).

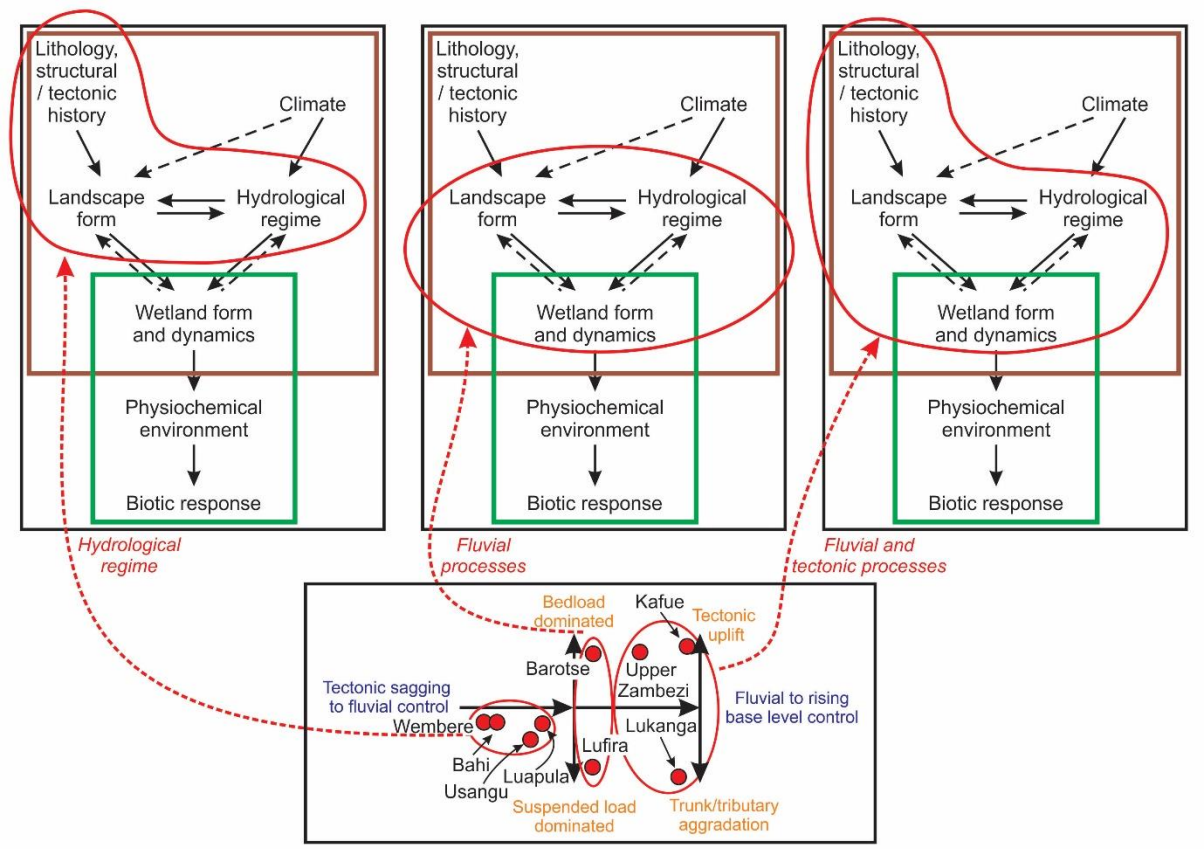

Figure 10.6: An illustration of the utility of the conceptual model developed in this study highlighting factors that are most likely to be responsible for influencing the structure, evolution and hydrological functioning of the wetlands considered in this study.

Given uplift events in southern and eastern Africa during the Pleistocene, and the associated lowering of base levels, streams have incised in order to lower their beds and reduce their longitudinal slopes. This erosion has propagated headwards, initially creating deeply incised valleys that gradually widened due to lateral erosion. However, as stream incision takes place, variation in the resistance of different lithologies to weathering and erosion creates a stepped stream longitudinal profile, with slope steepening at and downstream of resistant lithologies and slope reduction in an upstream direction of these lithologies. Once an appropriate stream grade has been achieved upstream of a resistant lithology, the stream course becomes increasingly sinuous, leading eventually to a meandering or anastomosing stream. Meander migration and avulsion associated with anastomosing streams likely lead to valley widening. These processes seem to characterise the Barotse (anastomosing stream) and Lufira (meandering stream) wetlands (Figure 10.6b), both of which are characterised by broad valleys with a near-horizontal cross-section and very gentle longitudinal slopes. In

these cases, the wetland that is formed is entirely a product of fluvial processes interacting with lithological variation.

Wetlands that are clearly fluvial but that occur on the margins of rift valleys experience slope reduction due to crustal uplift at the margins of rift valleys, such as the Kafue and Upper Zambezi wetlands in this study (Figure 10.6c). Lake Victoria and its marginal wetlands formed between the Eastern and Western East African Rift Valleys, due to uplift along the margins of the rift valleys. Lake Bangweulu between the Mweru-Tshangalele and Luangwa-Kariba rift valleys, may have a similar origin. Although the Kafue and Upper Zanbezi wetlands have a fluvial origin they are increasingly structured by marginal uplift and therefore the passive inundation of their respective basins as described by Gosselink and Turner (1978). A second mechanism of longitudinal slope reduction is by aggradation of a trunk stream that reduces the longitudinal slope of a tributary, leading to prolonged inundation, as is the case for the Futululu tributary of the Mfolozi floodplain in South Africa (Grenfell et al., 2010), and the Lukanga wetland in this study.

This study has highlighted the need for expansion of our understanding of wetlands beyond considering the hydrological regime as the primary determinant of wetland structure and functioning. The notion that the hydrological regime of a wetland is a product of basin morphology needs to be reconsidered. Water both responds to basin morphology, but it is also a powerful agent that shapes basins through erosion and deposition, creating wetland landforms.

The importance of this for catchment and wetland management is not trivial. For example, Ellery and McCarthy (1994) allude to the importance of clastic sediment input to the Okavango Delta in order to prevent salinisation of this ecosystem. The introduction of bedload sediments to the ecosystem promotes channel switching over timescales of centuries. Salinisation over similar timescales threatens this freshwater ecosystem in a setting where dissolved sediment dominates the sediment budget (clastic sediment amounts to approximately 200 000 tonnes per annum and dissolved sediment to about 500 000 tonnes per annum) and where the water loss component of the water balance is driven by evapotranspiration. Channel switching allows renewal of locally salinized soils by leaching of toxic salts (mainly sodium carbonate), into deep groundwater, such that over extended periods the ecosystem retains its freshwater character. These authors argue that interruption of sediment supply to this ecosystem reduces the likelihood of channel switching, which

would limit renewal of salinized soils and thus increase the risk of salinization of the ecosystem.

Construction of large dams in the catchments of wetlands described in this study has taken place and is taking place rapidly. The treatment of dams as though their sole function is to enable water management, will lead to erosion downstream, with potentially disastrous consequences for wetland ecosystems. Wetland science needs to engage to a greater extent with geomorphic processes if wetlands are to be protected, conserved and managed appropriately. This study is an initial attempt to develop a framework to stimulate this understanding.

10.7 Classification of wetlands based on their geomorphic origin and hydrological functioning

There are numerous wetland classification systems such as the Cowardin et al. (1977) classification system and the HGM classification system (Brinson, 1993; Brooks et al., 2013), which has been modified for South Africa by Ollis et al. (2013). Although the HGM classification system attempts to classify wetlands on the basis of their hydrological characteristics (the way that water enters, flows through and leaves a wetland) and the geomorphic setting of the wetland, it lacks consideration of the geomorphological processes giving rise to a particular wetland structure and suite of dynamics. These classification systems, therefore, provide limited insight into the relationship between wetland origin, dynamics and hydrological functioning (McCarthy and Hancox, 2000). The current study has shown that geomorphological processes determine wetland origin, shape wetland structure and influence dynamics, and therefore influence their hydrological functioning. Wetlands considered in this study were differentiated into three major types: (1) depression wetlands such as the Usangu, Bahi and Wembere wetlands, which occur within depressions formed from tectonic activities; (2) high gradient floodplain wetlands such as the Lufira and Barotse wetlands that formed as a result of fluvial processes interacting with lithological controls, and (3) low gradient floodplain wetlands such as the Upper Zambezi, Kafue and Lukanga wetlands that have elevated base levels due to aggradation of trunk stream floodplains (Lukanga) or tectonic uplift along rift valley margins (Upper Zambezi and Kafue).

In respect of the significance of this study for inferring flood attenuation functionality, a single feature formed the focus of this study: the degree of connectivity between the wetland and the primary stream flowing through the wetland. Where connectivity had been reduced

by trunk stream aggradation through the development of an alluvial ridge, flood attenuation functionality was viewed as having been enhanced. This functionality was assessed semi-quantitatively by comparing bankfull elevation of the trunk stream with elevation of the adjacent wetland surface. However, it is clear that there are likely to be other factors that have been highlighted in this study that are likely to strongly affect flood attenuation functionality, with a key factor being the longitudinal slope. As wetland longitudinal slope is reduced, for example, by uplift along rift valley margins as is the case for the Kafue wetland, or by trunk aggradation along the Kafue floodplain unit for the Lukanga tributary wetland, flood attenuation functionality must increase. For this reason flood attenuation functionality in the case of these two factors is likely to increase along the x-axis of Figure 10.7 from the centre where wetlands typically have a high slope towards the left and right edges due to longitudinal slope reduction. Furthermore, in the centre of the x-axis, flood attenuation functionality would increase from the top of the y-axis because of decreased trunk stream – wetland connectivity.

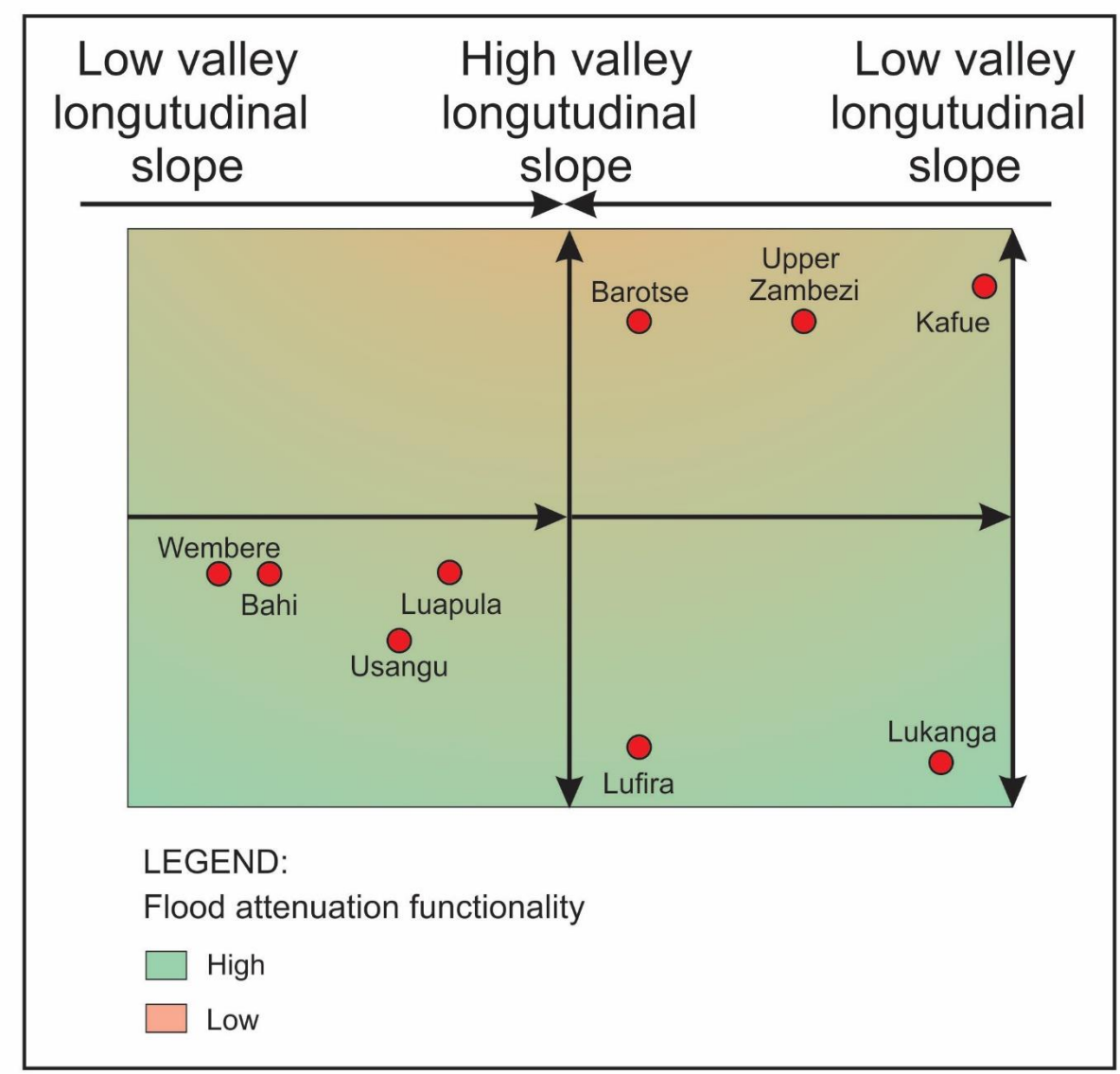

Figure 10.7: Comparison of wetland flood attenuation functionality based on valley longitudinal slope.

This study has attempted to understand factors contributing to the formation of large wetlands in dryland environments, and to consider how these factors contribute to flood attenuation functionality. It is perhaps naively simplistic but represents the beginning of the development of such understanding, and much more needs to be done.

10.8 The need for rapid assessment of wetland geomorphological processes

Wetland systems continue to be degraded and lost through anthropogenic activities such as agriculture, catchment degradation, and drainage for agricultural, urban, mining, as well as industrial developments (Maltby, 1991; Turner, 1991; Finlayson et al., 1999; Gürlük and Rehber, 2006; Ellery et al., 2009; Beuel et al., 2016). The rate of wetland loss and degradation has increased greatly in the 20th and early 21st centuries (Davidson, 2014).

However, the growth of wetland science, particularly of large wetlands in developing countries, is limited (McCarthy and Hancox, 2000; Tooth and McCarthy, 2007; Hughes et al., 2014). As a result, poor understanding of wetland processes is one of the contributing factors to increased wetland degradation and loss (Ellery et al., 2009; Tooth et al., 2009). This is because the lack of understanding of wetland processes often results in poor wetland management (Ellery and McCarthy, 1994; Ellery et al., 2003; 2009; McCarthy et al., 1997). For example, McCarthy et al. (2010) have shown that more than a century of human interventions without proper understanding of wetland processes has altered wetland processes in the Seekoeivlei wetland in South Africa, such that there is little chance of restoring the wetland to a near-natural state.

At the rate at which wetlands continue to be degraded and lost (Davidson, 2014) there is an urgent need to undertake studies that contribute to effective wetland management (Turner, 1991). However, there are limitations to improving process-based knowledge of wetlands, including limited expertise and the labour and technology intensive nature of the kinds of studies that are needed (Stein et al., 2009). This kind of work is also very costly. Gaining access to many wetlands is difficult and many natural hazards limit the willingness of scientists to undertake studies in these systems, including life-threatening diseases and wild animals (Ellery et al., 2003). As a result there is growing interest in rapid wetland assessments (e.g. Fennessy et al., 2007; Kotze et al., 2012; Beuel et al., 2016; Mclnnes and Everard, 2017; Behn et al., 2018) that are less costly than comprehensive field survey based studies such as conducted by Tooth et al. (2002), Grenfell et al. (2008), Joubert and Ellery (2013), Edwards et al. (2016) and Larkin et al. (2017a). This is because decision makers require simple, user friendly and cost effective tools that enhance sound decision making (De Leo and Levin, 1997).

There is also a need for understanding wetland geomorphological processes that emphasise factors that underpin their structure and dynamics (McCarthy and Hancox, 2000; Tooth and McCarthy, 2007; Ellery et al., 2009). Understanding wetlands from a geomorphic perspective allows management efforts to work to a greater extent with (rather than against) natural processes, which will lead to more sustainable outcomes. Therefore, in order to inform wetland management there is a need for carrying out rapid assessments of geomorphological processes that shape wetland structure, functioning and dynamics. The current study has demonstrated that Earth Observation (EO) data and GIS technology offer practical means for carrying out rapid assessments of wetland geomorphological processes and dynamics.

10.9 The use of GIS and remote sensing in wetland studies

GIS and remote sensing have proven to be useful tools for acquiring information about wetland systems that are difficult to access. There are a number of reviews on the use of remote sensing data and techniques for generating information about wetland systems (e.g. Rundquist et al., 2001; Ozesmi and Bauer, 2002; Ritchie and Das, 2015). Rundquist et al. (2001) have shown that remote sensing can be widely used for wetland inventory and mapping, wetland classification, wetland ecological change detection, and estimating wetland plant biomass. Aerial photographs, multispectral-satellite images, radar data, and ancillary data such as edaphic and elevation data are the most widely used datasets. Image classification techniques are the most widely used methods for wetland mapping (Ozesmi and Bauer, 2002), including visual image analysis, digital image classifications (supervised classifications, unsupervised classifications, and hybrid classifications), and rule-based classifications that involve the use of satellite images and ancillary data (Ozesmi and Bauer, 2002). Techniques such as indices for detecting and delineating waterbodies from satellite images (McFeeters, 1996; Xu, 2006) are less commonly used and do not feature in many reviews of wetland remote sensing.

From satellite images, wetlands can be delineated based on spectral radiance, yet most wetlands occur in broad and gently sloping valleys that are topographically distinct from surrounding uplands. Given the topographic settings of most wetlands, it seems appropriate to develop and use methods that distinguish wetlands from the surrounding uplands using topographic datasets such as digital elevation models (DEM's). The advantages of topography-based methods over the most commonly used image classification methods for delineating wetlands relates to the nature of the datasets used. Compared to satellite images, DEM datasets minimise the effects of spectral confusion and cloud cover on the accuracy of the method. Yet, the use of topography-based methods for delineating wetland areas is very limited. The most used and documented topographic-based methods are complex topographic algorithms and indices (e.g. Ndayisaba et al., 2017), which are mostly combined with image classification techniques (e.g. Wright and Gallant, 2007; Kulawardhana et al., 2007; Li and Chen, 2005). A simple topographically-based method like the cut-and-fill method developed in this study has been successfully applied to delineate wetland areas from DEM's.

GIS and remote sensing have rarely been used to identify the geomorphological processes relating to wetland origin and dynamics. Most wetland geomorphological studies rely on field survey methods to acquire geomorphological information related to wetland origin and

dynamics; Table 10.1 illustrates the possible use of GIS and remote sensing in acquiring and analysing such information. The table also provides a relatively comprehensive list of some of the studies where such information was obtained from conventional survey methods. The analysis of the influence of catchment geology, local and regional tectonics on wetland origin and structure has rarely been utilised in previous studies, although several studies have included these aspects, such as Ellery and McCarthy (1994), McCarthy and Ellery (1998), Gumbricht et al. (2001) and McCarthy (2013).

Often, wetland geomorphic features are visually identified and measured in-situ (Table 10.1). Wetland boundaries are delineated from the analysis of soil chroma, valley cross-sectional profiles are computed from conventional surveying and channel longitudinal profiles are plotted from contour maps of approximately 1:10 000 scale (e.g. Tooth et al., 2002; Tooth et al., 2004; Tooth et al., 2009; Ellery et al., 2012), from conventional surveying (e.g. McCarthy et al., 1997; Marren et al., 2006; Ellery et al., 2009; Grenfell et al., 2010) and a combination of conventional surveying and contour maps (e.g. Tooth and McCarthy, 2007; Grenfell et al., 2008). Lithological variations can be identified in-situ from exposed bedrock or from geological maps (e.g. Tooth et al., 2002; Johnson et al., 2001; Longmore, 2001; Ellery et al., 2012; Edwards et al., 2016). From the current study, wetland geomorphic features such as backwater depressions, meander scars and oxbow lakes, were easily identified from LandsatLook images. Valley cross-sectional profiles and channel longitudinal profiles were plotted from DEM's using Geographic Information Systems methods. Wetland boundaries, catchment areas, and tributary stream lines were automated from the DEM, while trunk streams were digitised from Google Earth. Channels, wetland and catchment areas were overlaid on geological maps to identify lithological and tectonic influences on wetland formation and dynamics. Precipitation and evapotranspiration estimates were obtained from meteorological datasets while flooding extent was obtained from visual analysis of LandsatLook images. Such analyses provided adequate information to assess the hydrological characteristics of wetlands.

Table 10.1: The information required in studies of geomorphological origin and dynamics of wetlands as well as the usefulness of remote sensing and GIS in obtaining such information.

Information required	**List of some of the studies where such information has been used**	**How each of these studies attained the required information**	**How GIS and remote sensing successfully obtain such information**
Channel longitudinal profile (i.e. Relations between valley and stream longitudinal characteristics)	McCarthy et al., 1997; Tooth et al., 2002; Tooth et al., 2004; Marren et al., 2006; Tooth and McCarthy, 2007; Ellery et al., 2009; Tooth et al., 2009; Grenfell et al., 2008; Grenfell et al., 2010; McCarthy et al., 2010; Ellery et al., 2012; Joubert and Ellery, 2013; Edwards et al., 2016; Larkin et al., 2017b	**Topographic survey** McCarthy et al., 1997; Marren et al., 2006; Ellery et al., 2009; Grenfell et al., 2010; McCarthy et al., 2010; Joubert and Ellery, 2013; Edwards et al., 2016 **Topographic maps** Tooth et al., 2002; Tooth et al., 2004; Tooth et al., 2009; Ellery et al., 2012; Larkin et al., 2017b **Combination of topographic survey and maps** Tooth and McCarthy, 2007; Grenfell et al., 2008	The current study has shown that GIS and Digital Elevation Model (DEM) can be used to successfully plot channel longitudinal profiles
Valley cross-sectional profile	McCarthy and Ellery, 1994; McCarthy et al., 1997; Smith, 1997; Gumbricht et al., 2001; Longmore, 2001; Tooth et al., 2002; Ellery et al., 2003; Tooth et al., 2004; Marren et al., 2006; Tooth and McCarthy, 2007; McCarthy et al., 1997; Grenfell et al., 2008; Ellery et al., 2009;Tooth et al., 2009; Grenfell et al., 2010; McCarthy et al., 2010; Humphries et al., 2010; Humphries et al., 2011; Ellery et al., 2012; McCarthy, 2013; Joubert and Ellery, 2013; Edwards et al., 2016; Larkin et al., 2017a	**Topographic survey** McCarthy and Ellery, 1994; McCarthy et al., 1997; Smith, 1997; Longmore, 2001; Gumbricht et al., 2001; Tooth et al., 2002; Tooth et al., 2004; Ellery et al., 2003; McCarthy et al., 1997; Tooth and McCarthy, 2007; Grenfell et al., 2008; Ellery et al., 2009; Tooth et al., 2009; Grenfell et al., 2010; McCarthy et al., 2010; Humphries et al., 2010; Humphries et al., 2011; Ellery et al., 2012; McCarthy, 2013; Joubert and Ellery, 2013; Edwards et al., 2016 **Topographic maps** Larkin et al., 2017a **Combination of topographic survey and maps** Marren et al., 2006	The current study has shown that GIS and Digital Elevation Model (DEM) can be used to plot valley cross-sections

Information required	List of some of the studies where such information has been used	How each of these studies attained the required information	How GIS and remote sensing successfully obtain such information
Depth to bedrock	Longmore, 2001; Tooth et al., 2002; Tooth et al., 2004; Marren et al., 2006; McCarthy et al., 1997; Tooth and McCarthy, 2007; Grenfell et al., 2008; Ellery et al., 2009; Grenfell et al., 2010; Humphries et al., 2011; Ellery et al., 2012; Joubert and Ellery, 2013; Edwards et al., 2016	**Sediment cores** Longmore, 2001; Tooth et al., 2004; Marren et al., 2006; Tooth and McCarthy, 2007; Grenfell et al., 2008; Grenfell et al., 2010; Humphries et al., 2011; Ellery et al., 2012; Joubert and Ellery, 2013; Edwards et al., 2016 **Exposed lithology** McCarthy et al., 1997 **Combination of exposed lithology and sediment cores** Tooth et al., 2002; Ellery et al., 2009	GIS and remote sensing cannot be used since the elevations of exposed lithology or sediment cores depths can only be taken in-situ. As a result the depth to bedrock were not analysed in the current study
Stratigraphy of valley fill	McCarthy and Ellery, 1994; McCarthy and Hancox, 2000; Tooth et al., 2002; Tooth et al., 2004; Marren et al., 2006; Tooth and McCarthy, 2007; Grenfell et al., 2008; Ellery et al., 2009; Tooth et al., 2009; Grenfell et al., 2010; McCarthy et al., 2010; Humphries et al., 2010; Humphries et al., 2011; Ellery et al., 2012; McCarthy, 2013; Joubert and Ellery, 2013; Edwards et al., 2016; Larkin et al., 2017a	**Sediment cores** McCarthy and Ellery, 1994; McCarthy and Hancox, 2000; Tooth et al., 2002; Tooth et al., 2004; Marren et al., 2006; Tooth and McCarthy, 2007; Grenfell et al., 2008; Ellery et al., 2009; Tooth et al., 2009; Grenfell et al., 2010; McCarthy et al., 2010; Humphries et al., 2010; Humphries et al., 2011; Ellery et al., 2012; McCarthy, 2013; Joubert and Ellery, 2013; Edwards et al., 2016; Larkin et al., 2017a	GIS and remote sensing cannot be used since sediment cores can only be taken in-situ. As a result stratigraphy of valley fill were not analysed in the current study

Information required	List of some of the studies where such information has been used	How each of these studies attained the required information	How GIS and remote sensing successfully obtain such information
Variation in lithological characteristics	Tooth et al., 2002; Tooth et al., 2004; Tooth and McCarthy, 2007; Grenfell et al., 2008; Ellery et al., 2009; Tooth et al., 2009; McCarthy et al., 2010; Grenfell et al., 2010; Ellery et al., 2012; Joubert and Ellery, 2013; Edwards et al., 2016; Larkin et al., 2017b	**Superimposing wetland boundary and geological maps** Tooth et al., 2002; Tooth et al., 2004; Tooth and McCarthy, 2007; Grenfell et al., 2008; Ellery et al., 2009; Tooth et al., 2009; McCarthy et al., 2010; Grenfell et al., 2010; Ellery et al., 2012; Joubert and Ellery, 2013; Edwards et al., 2016; ; Larkin et al., 2017b	The current study has shown that wetland boundaries and geological spatial datasets can easily be overlaid in a GIS environment. Wetlands can be easily delineated from DEM
Identification of landforms and wetland features including channels, channel pattern, backwater depressions, meander scars, oxbow lakes, as well as other depositional and erosional features	McCarthy 1992; McCarthy et al., 1993b; McCarthy and Ellery, 1994; McCarthy et al., 1997; McCarthy and Ellery, 1998; McCarthy and Hancox, 2000; Longmore, 2001; Gumbricht et al., 2001; Tooth et al., 2002; Ellery et al., 2003; Tooth et al., 2004; Marren et al., 2006; Tooth and McCarthy, 2007; McCarthy et al., 1997; Grenfell et al., 2008; Ellery et al., 2009; Tooth et al., 2009; Grenfell et al., 2010; McCarthy et al., 2010; Humphries et al., 2010; Humphries et al., 2011; Ellery et al., 2012; McCarthy, 2013; Joubert and Ellery, 2013; Tooth et al., 2015; Edwards et al., 2016; Larkin et al., 2017a; ; Larkin et al., 2017b	**Site visits** McCarthy and Ellery, 1998; McCarthy and Hancox, 2000; Gumbricht et al., 2001; Longmore, 2001; Ellery et al., 2003; Humphries et al., 2010; Ellery et al., 2012 **Aerial photography or satellite imagery** McCarthy, 1992; McCarthy et al, 1993b; Marren et al., 2006; Humphries et al., 2011 **Combination of aerial photography and site visits** McCarthy and Ellery, 1994; Tooth et al., 2002; Tooth et al., 2004; McCarthy et al., 1997; McCarthy et al., 1997; Tooth and McCarthy, 2007; Grenfell et al., 2008; Tooth et al., 2009; Ellery et al., 2009; Grenfell et al., 2010; McCarthy et al., 2010; McCarthy, 2013; Joubert and Ellery, 2013; Tooth et al., 2015; Edwards et al., 2016; Larkin et al., 2017a; ; Larkin et al., 2017b	Wetland features, channel characteristics as well as depositional and erosional landforms can be confidently identified and analysed from satellite images, Google Earth and aerial photography

Information required	List of some of the studies where such information has been used	How each of these studies attained the required information	How GIS and remote sensing successfully obtain such information
Relations between trunk and tributary streams such as tributary alluvial fans in relation to trunk valley connectivity or relations between trunk stream and blocked tributary lakes	Ellery et al., 2003; Marren et al., 2006; Tooth and McCarthy, 2007; McCarthy et al., 2010; Grenfell et al., 2008; Grenfell et al., 2010; Humphries et al., 2011; Ellery et al., 2012; Joubert and Ellery, 2013; Edwards et al., 2016; Larkin et al., 2017a; ; Larkin et al., 2017b	**Site visits** Ellery et al., 2003; Ellery et al., 2012 **Aerial photography** McCarthy et al., 2010; Humphries et al., 2011 Combination of site visits and aerial photography Marren et al., 2006; Tooth and McCarthy, 2007; Grenfell et al., 2008; Grenfell et al., 2010; Joubert and Ellery, 2013; Edwards et al., 2016; Larkin et al., 2017a; ; Larkin et al., 2017b	Trunk stream, tributary streams, alluvial fans, and blocked lakes can be easily identified from satellite images and aerial photography. Stream lines can be automated from the DEM or digitised from Google Earth. Once these features are identified their relationships can be analysed
Relations between wetland valley and local fault lines	McCarthy, 1992; McCarthy, 1993; Ellery et al., 1993; McCarthy et al., 1993a; Ellery and McCarthy, 1994; McCarthy and Ellery, 1994; McCarthy et al., 1997; Smith, 1997; McCarthy and Ellery, 1998; McCarthy and Hancox, 2000; Gumbricht et al., 2001; McCarthy et al., 2002; Tooth and McCarthy, 2007; McCarthy, 2013	**Superimposing wetland boundary and local fault lines** McCarthy, 1992; McCarthy, 1993; Ellery et al., 1993; McCarthy et al., 1993a; Ellery and McCarthy, 1994; McCarthy and Ellery, 1994; McCarthy et al., 1997; Smith, 1997; McCarthy and Ellery, 1998; McCarthy and Hancox, 2000; Gumbricht et al., 2001; McCarthy et al., 2002; Tooth and McCarthy, 2007; McCarthy, 2013	The current study has shown that fault lines or geological maps in spatial data formats can be overlaid with wetland boundaries and their relations can be analysed in a GIS environment

Information required	List of some of the studies where such information has been used	How each of these studies attained the required information	How GIS and remote sensing successfully obtain such information
Relations between wetland valley and regional tectonics	Ellery and McCarthy, 1994; McCarthy and Ellery, 1998; Gumbricht et al., 2001; McCarthy, 2013	**Superimposing wetland boundary and regional fault lines or rift valleys** Ellery and McCarthy, 1994; McCarthy and Ellery, 1998; Gumbricht et al., 2001; McCarthy, 2013	In a GIS environment, wetland boundaries can be overlaid with fault lines and rift valleys while regional elevation profiles depicting rift shoulders can be plotted from DEM and the location of wetlands can be identified along the elevation profiles
Catchment geology	McCarthy and Ellery, 1998; McCarthy and Hancox, 2000; Grenfell et al., 2008; Edwards et al., 2016	**Superimposing wetland boundary and geological maps** McCarthy and Ellery, 1998; McCarthy and Hancox, 2000; Grenfell et al., 2008; Edwards et al., 2016	The current study has shown that catchment geology can be analysed from geological maps in spatial data format while catchment areas can be delineated from DEM

CHAPTER 11: CONCLUSION AND RECOMMENDATIONS FOR FURTHER STUDIES

11.1 Introduction

The current study defined large African wetlands as wetlands larger than 1 000 km^2 in extent while elevated drylands were successfully mapped as areas at an elevation above 600 m above mean sea level and with an Aridity Index < 0.65. The definition of large wetlands and elevated drylands from the GLWD, global aridity map and DEM spatial datasets, enabled the identification of twenty large wetlands from which nine were identified as study sites. As a result objective 1 of the study, which aimed to identify and map large wetlands in southern Africa's elevated drylands using GIS techniques, was achieved.

In general the distribution of wetlands considered in this study shows some relationship with seismic activity associated with rifting. Geomorphological factors such as channel response to sustained base levels either as a result of a resistant lithology at the toe of the wetland, sedimentary fill within the trunk valley impeding tributary flows, or fluctuations in lake water level were identified as important factors responsible for the formation of wetlands such as the Lufira, Lukanga and Luapula wetlands respectively. As a result objective 2, which was to identify the likely geological and geomorphological factors that influence wetland formation, was achieved.

The current study has shown that wetland structure, which is influenced by geomorphological factors which determine wetland origin and evolution, influence wetland hydrological functioning. For example, both the Barotse and Lufira wetlands formed from lithological controls but their structure and hydrological function differs as a result of sedimentological characteristics. Mixed load sediment within the Lufira wetland resulted in the formation of an alluvial ridge such that the wetland is characterised by a high average depth of inundation and impaired lateral connectivity. On the other hand, bedload sediment planed the Barotse wetland laterally such that the wetland lacks an alluvial ridge. As a result the wetland is characterised by low average depth of inundation and high lateral connectivity. This shows that the current study related wetland formation and structure to hydrological functioning, thus achieving objective 3. It is recognised that this analysis was somewhat simplistic and could be refined by considering additional factors, such as wetland longitudinal slope.

The current study has shown that wetlands formed and shaped from different processes showed different wetland features, while those shaped from similar processes show similar features. For example, the Barotse and Upper Zambezi wetlands were shaped from deposition of Kalahari sediments, mainly as bedload, such that the wetlands were characterised by anastomosing channels and lacked backwater depressions. Since wetland features were successfully related to wetland origin and evolution the main aim of the study was achieved.

Although many geomorphologists are sceptical of theory since they assign innate virtue to fieldwork (Rhoads and Thorn, 1993), the current study successfully achieved its aim and objectives using spatial data analysis without any field verification. However, it should be noted that for studies such as this, the use of spatial data cannot proceed without a deep appreciation of theoretical background and the use of strands of evidence or inference to the best explanation in order to support the interpretation of spatial data. This was very well illustrated in this study were abductive reasoning with inference to conceptual models of wetland origion and theoretical background on wetland processes was used to aid the interepretation of spatial datasets. Abductive reasoning is a common practice in the earth science dormain (Oh, 2019) were many scientists generate possible explanations of earth processes based on inference to the most logical explanation (Rhoads and Thorn, 1993). This is because earth science phenomena are often inaccessible and make it very difficult for scientists to collect data (Kim, 2002) and processes are too slow to subject to experimentation. As a result, earth scientists frequently rely on inference to the most logical explanation. Therefore, in order to generating an understanding of inaccessible and hard to traverse wetland systems the current study has illustrated that the future may be the analysis of spatial data through abductive reasoning.

11.2 Limitations of the study and recommendation for future studies

Wetlands can be classified based on their geomorphic origin and such classification schemes can provide greater understanding of how natural processes occurring within distinct wetland systems can shape wetland structure and hydrological functioning. However, the material presented in this study is a first step at presenting a classification system of wetlands based on their origin, and on its own it not a comprehensive classification. Furthermore, it was clear from the comparison of wetland types from the current study and those from the commonly used classification of Ollis et al. (2013) for small wetlands in South Africa, that the

classification of Ollis et al. (2013) could not be easily adopted for large wetlands. Therefore, it is recommended that the development of a comprehensive classification system should not only take into consideration the geomorphic processes of wetland origin but its scope should be comprehensive enough to cater for wetlands of different sizes which occur in various climatic and landscape settings. However, to achieve this there is still a need for further studies similar to the current study, in order to generate enough information on different wetland systems in order to enhance our understanding of the origin of wetland systems.

The current study was conducted solely from a desktop perspective with the use of spatial datasets and satellite imageries. The most widely available and utilised topographic datasets are Digital Elevation Model products such as the SRTM and ASTER products. These are radar and optical remote sensing products respectively that cannot penetrate water bodies and other surface features such as vegetation. As such, the elevations of such surface features are represented within the constraints of these datasets. The effects of vegetation cover were evident in the valley cross-sectional and channel longitudinal profiles. Furthermore, the SRTM DEM data were collected in February 2000, and as such the topographic conditions of wetlands presented in the current study reflect wetland conditions nearly two decades ago. .These datasets were used in this study since there is a lack of up-to-date topographic datasets that are not affected by vegetation cover. However, the findings of the current study can be verified through high resolution spatial datasets. For instance, high resolution topographic datasets that do not include vegetation, such as bare earth LiDAR derived datasets, can be used when they become more widely and easily accessible.

Since the current study only used spatial datasets, it is important to put in context the spatial resolution and scale of the datasets used. The GTOPO30 DEM with a spatial resoultution of 1 km was used at a continental scale to map the topography of the study area while SRTM DEM with a 30 m spatial resolution was used to plot channel longitudinal profiles and valley cross-sections at a wetland or basin scale. The SRTM DEM has the highest spatial resolution in terms of the DEM that are freely available. The LandsatLook images used are of the same spatial resolution with the SRTM DEM and these two are the core datasets for the current study and their spatial resolution is suitable for mapping at a wetland scale since the current study is dealing with large wetlands covering a minimum area of 32 by 32 km. The implication of the 30 m spatial resolution is that the smallest feature that might be mirepresented with respect to the current study is the channel width and channel water elevation if the width of the channel is less than the 30 m spatial resolution of the DEM and

LandsatLook images. However, the current study is dealing with large wetlands that are maintained by large rivers whose width can stretch from 50 m to over 200 m within the wetland. With regard to the issue of scale, only the geological map of the SADC region at scale of 1:2 500 000, has to be placed in the context of the current study. The implication of the scale of the geological map is that a geology that is less than 25 km in size might be misrepresented on the map. However, since the smallest wetland considered in the current study covers and area that is above 32 by 32 km, the wetland and catchment geology has been faily represented although a geological map with a finer spatial resolution could adequately depict lithological variations.

The global lakes and wetlands database (GLWD) used in this study were also found to represent wetland boundaries that differed from those mapped in this study. Some wetlands are actually larger while others are smaller in extent in than they were mapped in the GLWD. Therefore, some large wetlands could have been missed from the selection criteria. Therefore, while the database is suitable for identifying and mapping wetlands at their geographic locations, there needs to be revision of these maps. Therefore, studies that aim to analyse wetland sizes may use the dataset to identify a wetland and then correct or update wetland boundaries through appropriate wetland delineation methods. This again shows that there is a need to update wetland boundaries and the GLWD if and when necessary.

The novel use of the cut-and-fill method in different topographic settings has shown that, in confined valley settings, wetland delineation can be achieved by setting the planar surface at the assumed elevation of the wetland edges. This can be achieved simply by digitising points at the wetland edges and extracting the elevations from the DEM to interpolate a planar surface rather than digitising points along the channel. However, if elevation values are taken along the channel, the interpolated surface can be raised and lowered to the elevation of the assumed wetland edges by editing the original elevation values. However, in delineating alluvial fans such as the Okavango Delta that is comprised of both confined and unconfined topographic settings, the method cannot be easily applied. Delineation of such wetlands requires the use of two planar surfaces to separately delineate the confined and unconfined wetland reaches and then superimpose the two cut-and-fill results. Given that the geomorphological processes governing the formation of small and large wetlands such as tectonic depressions and floodplains may be similar, it is envisaged that the cut-and-fill method can be applicable for small wetlands in similar topographic settings provided that high spatial resolution DEMs with high vertical accuracy are used. However, the method is a

supplement and not a substitute for satellite image classification methods as it is more useful for delineating wetlands in confined valley settings and is suitable for delineating a single wetland at a time. This is because the method relies on the interpolation and precise placement of the planar surface at a longitudinal slope approximating that of the wetland down the valley length and at an elevation above the wetland area. As a result small wetlands along tributary streams are delineated as part of the surrounding upland since tributaries are usually at higher elevations than the elevation of the main wetland.

LITERATURE CITED

Acharya, G., and Barbier, E.B. (2000). Valuing groundwater recharge through agricultural production in the Hedejia-Nguru wetlands in northern Nigeria. *Agricultural Economics*, *22*(3), 247–259.

Acreman, M., and Holden, J. (2013). How wetlands affect floods. *Wetlands*, 33(5), 773–786.

Airbus Defence and Space, (2013). *Airbus Defence and Space to provide new satellite imagery for Google Maps and Google Earth*. Retrieved 2016/02/18 from http://www.space-airbusds.com/en/press_centre/airbus-defence-and-space-to-provide-new-satellite-imagery-for-google-maps-and-google-earth.html

Ariza-Villaverde, A.B., Jiménez-Hornero, F.J., and Gutiérrez de Ravé, E. (2013). Multifractal analysis applied to the study of the accuracy of DEM-based stream derivation. *Geomorphology*, 197, 85–95.

Ashley, G.M., Maitima Mworia, J., Muasya, A.M., Owen, R.B., Driese, S.G., Hover, V.C., Renult, R.W., Goman, M.F., Mathai, S., and Blatt, S.H. (2004). Sedimentation and recent history of a freshwater wetland in a semi-arid environment: Loboi Swamp, Kenya, East Africa. *Sedimentology*, 51(6), 1301–1321.

Ashworth, P.J., and Lewin, J. (2012). How do big rivers come to be different? *Earth-Science Reviews*, 114(1–2), 84–107.

Aster Validation Team. (2009). *ASTER Global DEM Validation - Summary Report* (Prepared by ASTER GDEM METI/ERSDAC NASA/LPDAAC USGS/EROS), (June 2009), 28.

Banko, G. (1998). *A review of assessing the accuracy of and methods including remote sensing data in forest inventory*. International Institute for Applied Systems Analysis, Interim Report IT-98-081, Laxenburg, Austria.

Behn, K., Becker, M., Burghof, S., Möseler, B.M., Willy, D.K., and Alvarez, M. (2018). Using vegetation attributes to rapidly assess degradation of East African wetlands. *Ecological Indicators*, 89, 250–259.

Beuel, S., Alvarez, M., Amler, E., Behn, K., Kotze, D., Kreye, C., Leemhuisc, C., Wagnere, K., Willyf, K.D., Ziegler, S., and Becker, M. (2016). A rapid assessment of anthropogenic disturbances in East African wetlands. *Ecological Indicators*, 67, 684–692.

Bhowmik, A.K., Metz, M., and Schäfer, R.B. (2015). An automated, objective and open source tool for stream threshold selection and upstream riparian corridor delineation. *Environmental Modelling & Software*, 63, 240–250.

Bodini, A., Ricci, A., and Viaroli, P. (2000). A multimethodological approach for the sustainable management of perifluvial wetlands of the Po River (Italy). *Environmental Management*, 26(1), 59–72.

Brierley, G., Fryirs, K., and Jain, V. (2006). Landscape connectivity: The geographic basis of geomorphic applications. *Area*, 38(2), 165–174.

Brierley, G.J., and Fryirs, K. (1999). Tributary-trunk stream relations in a cut-and-fill landscape: a case study from Wolumla catchment, New South Wales, Australia. *Geomorphology*, 28(1–2), 61–73.

Brinson, M.M. (1993). *A Hydrogeomorphic Classification for Wetlands.* Wetland research program technical report WRP-DE-4, Washington, DC.

Broadley, D.G., and Cotterill, F.P.D. (2004). The reptiles of southeast Katanga, an overlooked "hot spot." *African Journal of Herpetology*, 53(1), 35–61.

Brooks, R.P., Brinson, M.M., Wardrop, D.H., and Bishop, J.A. (2013). Hydrogeomorphic (HGM) Classification, Inventory, and Reference. *Wetlands*, 39–60.

Bullock, A., and Acreman, M. (2003). The role of wetlands in the hydrological cycle. *Hydrology and Earth System Sciences*, 7(3), 358–389.

Burke, K., and Gunnell, Y. (2008). *The African erosion surface: a continental-scale synthesis of geomorphology, tectonics and environmental change over the past 180 million years*. Geological Society of America Memoir, 201.

Cai, X., Chilonda, P., and Matete, M. (2012). *Doubling irrigation for southern Africa—do we have enough water and where is the hope?* IWMI: 141, Cresswell Street: Weavind Park, Pretoria, South Africa.

Campbell, D., Keddy, P.A., Broussard, M., and McFalls-Smith, T.B. (2016). Small changes in flooding have large consequences: experimental data from ten wetland plants. *Wetlands*, 36(3), 457–466.

Carabajal, C.C., and Harding, D.J. (2005). ICESat validation of SRTM C-band digital elevation models. *Geophysical Research Letters*, 32(22), L22S01.

Cardoso, G.F., Souza, C., and Souza-Filho, P.W.M. (2014). Using spectral analysis of Landsat-5 TM images to map coastal wetlands in the Amazon River mouth, Brazil. *Wetlands Ecology and Management*, 22(1), 79–92.

Chen, A., Leptoukh, G., and Kempler, S. (2009). Visualization of NASA campaign mission vertical profiles using Google Earth. 2009 17th International Conference on Geoinformatics, *Geoinformatics 2009*, 35, 419–427.

Chen, L., Jin, Z., Michishita, R., Cai, J., Yue, T., Chen, B., and Xu, B. (2014). Dynamic monitoring of wetland cover changes using time-series remote sensing imagery. *Ecological Informatics*, 24, 17–26.

Chomba, M. (2014). *Property rights and benefit sharing: a case study of the Barotse floodplains*, Zambia. School of social science, Monash South Africa, MSc. Monash South Africa.

Chorowicz, J. (2005). The East African rift system. *Journal of African Earth Sciences*, 43(1–3), 379–410.

Congalton, R.G. (1991). A review of assessing the accuracy of classifications of remotely sensed data. *Remote Sensing of Environment*, 37(1), 35–46.

Cottterill, F.P.D. (2004). Drainage evolution in south-central Africa and vicariant speciation in swamp-dwelling weaver birds and swamp flycatchers. *The Honeyguide*, 50(1), 7–25.

Cowardin, L.M., Carter, V., Golet, F.C., and LaRoe, E.T. (1977*). Classification of wetlands and deep-water habitats of the United States (an operational draft).* Alaska Resources Library and Information Services, Anchorage, Alaska.

Davidson, N.C. (2014). How much wetland has the world lost? Long-term and recent trends in global wetland area. *Marine and Freshwater Research*, 65(10), 934–941.

De Leo, G.A., and Levin, S. (1997). The multifaceted aspects of ecosystem integrity. *Conservation Ecology*, 1(1), 3.

Delvaux, D.F., and Hanon, M. (1993). Neotectonics of the Mbeya Area, SW Tanzania. *Royal Museum for Central Africa*, 87–97.

Deshpande, S.S. (2013). Improved floodplain delineation method using high-density LiDAR Data. *Computer-Aided Civil and Infrastructure Engineering*, 28(1), 68–79.

DeVantier, B.A., and Feldman, A.D. (1993). Review of GIS applications in hydrologic modelling. *Journal of Water Resources Planning and Management*, 119(2), 246-261.

Dixey, F. (1944). The geomorphology of Northern Rhodesia. *Trans. Proc. Geol. Sec. S. Africa*, 47, 9–45.

Dong, Z., Wang, Z., Liu, D., Song, K., Li, L., Jia, M., and Ding, Z. (2014). Mapping wetland areas using Landsat-derived NDVI and LSWI: A Case Study of West Songnen Plain, Northeast China. *Journal of the Indian Society of Remote Sensing*, 42(September), 1–8.

Dronova, I., Gong, P., Wang, L., and Zhong, L. (2015). Mapping dynamic cover types in a large seasonally flooded wetland using extended principal component analysis and object-based classification. *Remote Sensing of Environment*, 158, 193–206.

Dutta, D., Teng, J., Vaze, J., Lerat, J., Hughes, J., and Marvanek, S. (2013). Storage-based approaches to build floodplain inundation modelling capability in river system models for water resources planning and accounting. *Journal of Hydrology*, 504, 12–28.

Edwards, R. (2009). *The origin and evolution of Dartmoor Vlei in the Kwazulu-Natal Midlands, South Africa*. (MSc Thesis). University of KwaZulu-Natal, South Africa.

Edwards, R.J., Ellery, W.N., and Dunlevey, J. (2016). The role of the in situ weathering of dolerite on the formation of a peatland: The origin and evolution of Dartmoor Vlei in the KwaZulu-Natal Midlands, South Africa. *Catena*, 143, 232–243.

Ellery, W.N., and McCarthy, T.S. (1994). Principles for the sustainable utilization of the Okavango Delta ecosystem, Botswana. *Biological Conservation*, 70(2), 159–168.

Ellery, W.N., Ellery, K., and McCarthy, T.S. (1993). Plant distribution in islands of the Okavango Delta, Botswana: determinants and feedback interactions. *African Journal of Ecology*, 31, 118–134.

Ellery, W.N., Grenfell, M., Grenfell, S., Kotze, D.C, McCarthy, T.S., Tooth, S., Grundling, P.L., Beckedahl, H., Le Maitre, D., and Ramsay, L. (2009). *WET-Origins: Controls on the distribution and dynamics of wetlands in South Africa*. WRC Report No TT 334/09, Water Research Commission, Pretoria.

Ellery, W.N., Grenfell, S.E., Grenfell, M.C., Humphries, M.S., Barnes, K., Dahlberg, A., and Kindness, A. (2012). Peat formation in the context of the development of the Mkuze floodplain on the coastal plain of Maputaland, South Africa. *Geomorphology*, 141-142, 11–20.

Ellery, W.N., McCarthy, T.S., and Smith N.D. (2003). Vegetation, hydrology, and sedimentation patterns on the major distributary system of the Okavango Fan, Botswana. *Wetlands*, 23, 357–375.

ESRI, (2013). *ArcGIS Resources*. Retrieved 2015/03/19 from http://resources.arcgis.com/en/help/main/10.1/index.html#//

ESRI, (n.d). *Floodplain delineation from LIDAR points*. Retrieved 2016/09/21 from http://desktop.arcgis.com/en/arcmap/10.3/manage-data/las-dataset/floodplain-modeling-using-lidar-in-arcgis.htm

Evans, T.L., Costa, M., Tomas, W.M., and Camilo, A.R. (2014). Large-scale habitat mapping of the Brazilian Pantanal wetland: A synthetic aperture radar approach. *Remote Sensing of Environment*, 155, 89–108.

Faulkner, S., and Gov, S. (2004). Urbanization impacts on the structure and function of forested wetlands. *Urban Ecosystems*, 7, 89–106.

Fennessy, M.S., Jacobs, A.D., and Kentula, M.E. (2007). An evaluation of rapid methods for assessing the ecological condition of wetlands and evaluation of rapid methods for assessing the ecological. *Wetlands*, 27(3), 543–560.

Finlayson, C.M., Davidson, N.C., Spiers, A.G., and N.J. Stevenson. (1999). Global wetland inventory – current status and future priorities. *Marine and Freshwater Research*, 50, 717–727.

Flügel, T.J. (2014). *The evolution of the Congo-Kalahari watershed: African mega–geomorphology*. (PhD Thesis). University of Cape Town. South Africa.

Food and Agriculture Organization of the United Nations (FAO) Water, (2013). *CLIMWAT 2.0 for CROPWAT*. Retrieved 2015/03/11 from http://www.fao.org/nr/water/infores_databases_climwat.html

Foster, A., Ebinger, C., Mbede, E., and Rex, D. (1997). Tectonic development of the northern Tanzanian sector of the East African Rift System. *Journal of the Geological Society*, 154, 689–700.

Fraser, L.H., and Keddy P.A. (2005). *The world's largest wetlands: ecology and conservation*. Cambridge University press. Cambridge.

Fryirs, K.A., and Brierley, G.J. (2013). *Geomorphic analysis of river systems: An approach to reading the landscape*. Chichester: Blackwell publishing.

Fryirs, K.A., Brierley, G.J., Preston, N.J., and Kasai, M. (2007b). Buffers, barriers and blankets: The (dis)connectivity of catchment-scale sediment cascades. *Catena*, 70(1), 49–67.

Fryirs, K.A., Brierley, G.J., Preston, N.J., and Spencer, J. (2007a). Catchment-scale (dis)connectivity in sediment flux in the upper Hunter catchment, New South Wales, Australia. *Geomorphology*, 84(3–4), 297–316.

Funkenberg, T., Binh, T.T., Moder, F., and Dech, S. (2014). The Ha Tien Plain – wetland monitoring using remote-sensing techniques. *International Journal of Remote Sensing*, 35(8), 2893–2909.

Furman, T., Nelson, W.R., and Elkins-Tanton, L.T. (2016). Evolution of the East African Rift : Drip Magmatism, Lithospheric Thinning and Mafic Volcanism. *Geochimica Et Cosmochimica Acta*, 185 (2016), 418-434.

Furtado, L.F.A., Silva, T.S.F., Fernandes, P.J.F., and Novo, E.M.L.M. (2015). Land cover classification of Lago Grande de Curuai floodplain (Amazon, Brazil) using multi-sensor and image fusion techniques. *Acta Amazonica*, 45(2), 195–202.

Gallant, J. (2011). Adaptive Smoothing for Noisy DEMs. *Geomorphometry*, 37–40.

Gibbs, M.S., Clarke, K., and Taylor, B. (2016). Linking spatial inundation indicators and hydrological modelling to improve assessment of inundation extent. *Ecological Indicators*, 60, 1298–1308.

Girvetz, E.H., and Zganjar, C. (2014). Dissecting indices of aridity for assessing the impacts of global climate change. *Climatic Change*, 126(3-4), 469–483.

Gong, P., Niu, Z., Cheng, X., Zhao, K., Zhou, D., Guo, J., Liang, L., Wang, X., Li, D., Huang, H., Wang, Y., Wang, K., Li, W., Wang, X., Ying, Q., Yang, Z., Ye, Y., Li, Z., Zhuang, D., Chi, Y., Zhou, H., and Yan, J. (2010). China's wetland change (1990-2000) determined by remote sensing. *Science China Earth Sciences*, 53(7), 1036–1042.

Google Earth Blog, (2014). *Digital Globe releases first images from WorldView-3*. Retrieved 2016/02/22 from http://www.gearthblog.com/blog/archives/2014/08/digital-globe-releases-first-images-worldview-3.html

Google Inc., (n.d). *Attribution guidelines for google maps and google earth*. Retrieved 2016/02/22 from http://www.google.co.za/permissions/geoguidelines/attr-guide.html

Gosselink, J.G., and Turner, R.E. (1978). The role of hydrology in freshwater wetland ecosystems. In: Good, R.E., Whigham, D.F., and Simpson, R.L. (Eds). *Freshwater wetlands: Ecological processes and management potential.* Academic Press, New York.

Goudie, A.S. (2005). The drainage of Africa since the Cretaceous. *Geomorphology*, 67(3–4), 437–456.

Grenfell, M.C., Ellery, W., and Grenfell, S.E. (2008). Tributary valley impoundment by trunk river floodplain development: A case study from the KwaZulu-Natal Drakensberg toe hills, Eastern South Africa. *Earth Surface Processes and Landforms*, 2044(33), 2029–2044.

Grenfell, S.E., Ellery, W.N., Grenfell, M.C., Ramsay, L.F., and Flögel, T.J. (2010). Sedimentary facies and geomorphic evolution of a blocked-valley lake: Lake Futululu, northern Kwazulu-Natal, South Africa. *International Association of Sedimentologists*, 1-16.

Guiraud, R., and Bosworth, W. (1997). Senonian basin inversion and rejuvenation of rifting in Africa and Arabia: synthesis and implications to plate-scale tectonics. In Burke, K., and Gunnell, Y. (2008). *The African erosion surface: a continental-scale synthesis of geomorphology, tectonics and environmental change over the past 180 million years*. Geological Society of America Memoir, 201.

Gumbricht T., McCarthy, T.S., and Merry, C.L. (2001). The Topography of the Okavango Delta, Botswana, and its tectonic and sedimentological implications. *South African Journal of Geology*, 104, 243-264.

Gürlük, S., and Rehber, E. (2006). Evaluation of an integrated wetland management plan: case of Uluabat (Apollonia) Lake, Turkey. *Wetlands*, 26(1), 258–264.

Haack, B. (1996). Monitoring wetland changes with remote sensing: An east African example. *Environmental Management*, 20(3), 411–419.

Haddon, I.G. (2005). *The Sub-Kalahari Geology and Tectonic Evolution of the Kalahari Basin. Southern Africa.* (PhD Thesis). University of the Witwatersrand, South Africa.

Haddon, I.G., and McCarthy, T.S. (2005). The Mesozoic-Cenozoic interior sag basins of Central Africa: The Late-Cretaceous-Cenozoic Kalahari and Okavango basins. *Journal of African Earth Sciences*, 43(1–3), 316–333.

Halabisky, M., Moskal, L.M., Gillespie, A., and Hannam, M. (2016). Reconstructing semi-arid wetland surface water dynamics through spectral mixture analysis of a time series of Landsat satellite images (1984-2011). *Remote Sensing of Environment*, 177, 171–183.

Hirt, C., Filmer, M.S., and Featherstone, W.E. (2010). Comparison and validation of recent freely-available ASTER-GDEM ver1, SRTM ver4.1 and GEODATA DEM-9S ver3 digital elevation models over Australia. *Australian Journal of Earth Sciences*, 57(3), 337-347.

Holmes, P., and Meadows, M. (2012). *Southern African Geomorphology: Recent Trends and New Directions*. Bloemfontein: SUN MeDIA.

House, A.R., Thompson, J.R., and Acreman, M.C. (2016). Projecting impacts of climate change on hydrological conditions and biotic responses in a chalk valley riparian wetland. *Journal of Hydrology*, 534, 178–192.

Hughes, D.A., Tshimanga, R.M., Tirivarombo, S., and Tanner, J. (2014). Simulating wetland impacts on stream flow in southern Africa using a monthly hydrological model. *Hydrological Processes*, 28, 1775–1786.

Hughes, R.H., and Hughes, J.S. (1992). *A directory of African wetlands*. Gland, Switzerland and Cambrige, UK: IUCN.

Humphries, M.S., Kindness, A., Ellery, W.N., and Hughes, J.C. (2011). Water chemistry and effect of evapotranspiration on chemical sedimentation on the Mkuze River floodplain, South Africa. *Journal of Arid Environments*, 75(6), 555–565.

Humphries, M.S., Kindness, A., Ellery, W.N., and Hughes, J.C. (2010). Sediment geochemistry, mineral precipitation and clay neoformation on the Mkuze River floodplain, South Africa. *Geoderma*, 157, 15-26.

International Mire Conservation Group (IMCG). (2004). *Zambia*. Retrieved 2016/0701 from Http://www.imcg.net/media/download_gallery/gpd/africa/zambia.pdf

International Seismological Centre. (2012). *On-line Bulletin*. Retrieved 2016/02/02 from http://www.isc.ac.uk.

Iriondo, M. (2004). Large wetlands of South America: a model for Quaternary humid environments. *Quaternary International*, 114(1), 3–9.

Islam, M.A., Thenkabail, P.S., Kulawardhana, R.W., Alankara, R., Gunasinghe, S., Edussriya, C., and Gunawardana, A. (2008). Semi-automated methods for mapping wetlands using Landsat ETM+ and SRTM data. *International Journal of Remote Sensing*, 29(24), 7077–7106.

Jensen, T.R. (2008). *Introductory digital image processing: A remote sensing perspective*. Pearson Educational Inc. Pearson Prentice Hall.

Jin, H., Huang, C., Lang, M.W., Yeo, I.Y., and Stehman, S. V. (2017). Monitoring of wetland inundation dynamics in the Delmarva Peninsula using Landsat time-series imagery from 1985 to 2011. *Remote Sensing of Environment*, 190, 26–41.

Johnson, T.C., Kelts, K., and Odada, E. (2000). The Holocene history of Lake Victoria. *Ambio: A Journal of the Human Environment*, 29(1), 2–11.

Johnson, T.C., Scholz, C.A., Talbot, M.R., Kelts, K., Ricketts, R.D., Ngobi, G., Beuning, K., Ssemmanda, I., and McGill, J.W. (1996). Late Pleistocene desiccation of Lake Victoria and rapid evolution of cichlid fishes. *Science*, 273, 1091–1093.

Johnston, C.A., Bridgham, S.D., and Schubauer-Berigan, J.P. (2001). Nutrient dynamics in relation to geomorphology of riverine wetlands. *Soil Science Society of America Journal*, 65(2), 557–577.

Joubert, R., and Ellery, W.N. (2013). Controls on the formation of Wakkerstroom Vlei, Mpumalanga province, South Africa. *African Journal of Aquatic Science*, 38(2), 135-151.

Junk, W.J., Bayley, P.B., and Sparks, R.E. (1989). The flood pulse concept in river-floodplain systems. In Dodge, D.P. (Ed.) Proceedings of the International Large River Symposium. *Canadian Special Publication of Fisheries and Aquatic Sciences.* 106, 110-127.

Kadykalo, A.N., and Findlay, C.S. (2016). The flow regulation services of wetlands. *Ecosystem Services*, 20, 91–103.

Kamukala, G.L., and Crafter, S.A. (Eds). (1993). *Wetlands of Tanzania*. Proceedings of a Seminar on the Wetlands of Tanzania, Morogoro, Tanzania, 27-29 November, 1991.

Katongo, C., Koeberl, C., Reimold, W.U., and Mubu, S. (2002). Remote sensing, field studies, petrography, and geochemistry of rocks in central Zambia: No evidence of a meteoritic impact in the area of the Lukanga Swamp. *Journal of African Earth Sciences*, 35(3), 365–384.

Keddy, P.A. (2000). *Wetland ecology: principles and conservation*. Cambridge university press. Cambridge.

Kennedy, D., and Bishop, M.C. (2011). Google earth and the archaeology of Saudi Arabia. A case study from the Jeddah area. *Journal of Archaeological Science*, 38(6), 1284–1293.

Kiamehr, R., and Sjöberg, L.E. (2005). Effect of the SRTM global DEM on the determination of a high-resolution geoid model: a case study in Iran. *Journal of Geodesy*, 79(9), 540–551.

Kim, C.J. (2002). Inferences frequently used in earth science. *Journal of Korean earth science society*, 23(2), 188-193.

Kotze, D.C., Ellery, W.N., Macfarlane, D.M., and Jewitt, G.P.W. (2012). A rapid assessment method for coupling anthropogenic stressors and wetland ecological condition. *Ecological Indicators*, 13(1), 284–293.

Kotze, D.C., Marneweck, G.C., Batchelor, A.L., Lindley, D.S., and Collins, N.B. (2007). *WET-EcoServices: A technique for rapidly assessing ecosystem services supplied by wetlands.* WRC Report No TT 339/09, Water Research Commission, Pretoria.

Kulawardhana, R.W., Thenkabail, P.S., Vithanage, J., Biradar, C., Islam M.A., Gunasinghe, S., and Alankara, R. (2007). Evaluation of the wetland mapping methods using Landsat ETM+ and SRTM Data. *Journal of Spatial Hydrology*, 7(2), 62–96.

Kumar, L., Sinha, P., and Taylor, S. (2014). Improving image classification in a complex wetland ecosystem through image fusion techniques. *Journal of Applied Remote Sensing*, 8(1), 083616.

Lane, C.R., Anenkhonov, O., Liu, H., Autrey, B.C., and Chepinoga, V. (2014). Classification and inventory of freshwater wetlands and aquatic habitats in the Selenga River Delta of Lake Baikal, Russia, using high-resolution satellite imagery. *Wetlands Ecology and Management*, 23(2), 195–214.

Larkin, Z.T., Ralph, T.J., Tooth, S., and McCarthy T.S. (2017b). The interplay between extrinsic and intrinsic controls in determining floodplain wetland characteristics in the South African drylands. *Earth Surface Processes and Landforms*, 42, 1092-1109.

Larkin, Z.T., Tooth, S., Ralph, T.J., Duller, G.A.T., McCarthy, T., Keen-Zebert, A., and Humphries, M.S. (2017a). Timescales, mechanisms, and controls of incisional avulsions in floodplain wetlands: Insights from the Tshwane River, semiarid South Africa. *Geomorphology*, 283, 158–172.

Lê, S., Josse, J., and Husson, F. (2008). FactoMineR: An R package for multivariate analysis. *Journal of Statistical Software*, 25(1), 1–18.

Lehner, B., and Döll, P. (2004). Development and validation of a global database of lakes, reservoirs and wetlands. *Journal of Hydrology*, 296(1-4), 1–22.

Leopold, L.B., and T. Maddock. (1953). *The Hydraulic Geometry of Stream Channels and Some Physiographic Implications*, Professional Paper 252, U.S. Geological Survey, Washington, DC.

Lewin, J., and Ashworth, P.J. (2014). Defining large river channel patterns: Alluvial exchange and plurality. *Geomorphology*, 215, 83–98.

Li, J., and Chen, W. (2005). A rule-based method for mapping Canada's wetlands using optical, radar and DEM data. *International Journal of Remote Sensing*, 26(22), 5051–5069.

Li, Z., Xu, J., Shilpakar, R.L., and Ma, X. (2014). Mapping wetland cover in the greater Himalayan region: a hybrid method combining multispectral and ecological characteristics. *Environmental Earth Sciences*, 71(3), 1083–1094.

Lidzhegu, Z., and Palamuleni, L.G. (2012). Land use and land cover change as a consequence of the South African land reform program: A remote sensing approach. *Journal of Food, Agriculture and Environment*, 10 (3 and 4), 1441–1447.

Lillesand, T.M., Kiefer, R.W., and Chipman, J.W. (2004). *Remote sensing and image interpretation (5th Edition)*, Wiley, New York.

Liu, B., and Wang, S. (2017). Planform characteristics and development of interchannel wetlands in a gravel-bed anastomosing river, Maqu Reach of the Upper Yellow River. *Journal of Geographical Sciences*, 27(11), 1376–1388.

Longmore, J.L. (2001). *The geomorphology of wetlands in the upper Mooi River catchment KwaZulu-Natal*. (MSc Thesis). University of Natal, South Africa.

Lyon, J.G., and McCarthy, J. (1995). *Wetland and environmental applications of GIS*. Lewis publishers, London.

Mabhaudhi, T., Mpandeli, S., Madhlopa, A., Modi, A.T., Backeberg, G., and Nhamo, L. (2016). Southern Africa's water-energy nexus: Towards regional integration and development. *Water*, 8, 235

Macheyeki, A.S., Delvaux, D., De Batist, M., and Mruma, A. (2008). Fault kinematics and tectonic stress in the seismically active Manyara–Dodoma Rift segment in Central Tanzania – Implications for the East African Rift. *Journal of African Earth Sciences*, 51(4), 163–188.

Makaske, B. (2001). Anastomosing rivers: A review of their classification, origin and sedimentary products. *Earth Science Reviews*, 53(3-4), 149–196.

Makaske, B., Smith, D.G., Berendsen, H.J.A., de Boer, A.G., van Nielen-Kiezebrink, M.F., and Locking, T. (2009). Hydraulic and sedimentary processes causing anastomosing morphology of the upper Columbia River, British Columbia, Canada. *Geomorphology*, 111(3–4), 194–205.

Malan, H. (2010). The status of research on wetland ecology, management and conservation in South Africa. McInnes, R., Mackay, H., Zavagli, M. and Mkambule, V. (Eds.). *Ramsar workshop of the STRP National Focal Points of Africa and other wetland experts*, Johannesburg, South Africa, 30 November - 2 December 2010. WRC Report Number SP 9/11.

Maltby, E. (1991). Wetland management goals: Wise use and conservation. *Landscape and Urban Planning*, 20(1–3), 9–18.

Marren, P.M., McCarthy, T.S., Tooth, S., Brandt, D., Stacey, G.C., Leong, A. and Spottiswoode, B. **(**2006). A comparison of mud- and sand-dominated meanders in a downstream coarsening reach of the mixed bedrock-alluvial Klip River, eastern Free State, South Africa. *Sedimentary Geology*, 190, 213-26.

McCarthy T.S., and Ellery W.N. (1994). The effect of vegetation on soil and ground water chemistry and hydrology of islands in the seasonal swamps of the Okavango Fan, Botswana. *Journal of Hydrology*, 154(1-4), 169–193.

McCarthy, T.S. (1992). Physical and biological processes controlling the Okavango Delta – A review of recent research. *Botswana Notes and Records*, 24(1992), 57–86.

McCarthy, T.S. (1993). The great inland deltas of Africa. *Journal of African Earth Science*, 17(3), 275–291.

McCarthy, T.S. (2013). The Okavango Delta and its place in the geomorphological evolution of southern Africa. *South African Journal of Geology*, 116, 1-54.

McCarthy, T.S., and Ellery, W.N. (1998). The Okavango Delta. *Transactions of the Royal Society of South Africa*, 53(2), 157–182.

McCarthy, T.S., and Hancox, P.J. (2000). Wetlands. In: Patridge, T.C., and Maud, R.R. (Eds). *The Cenozoic of Southern Africa*. Oxford University Press, New York.

McCarthy, T.S., Barry, M., Bloem, A., Ellery, W.N., Heister, H., Merry, C.L., and Sternberg, H. (1997). The gradient of the Okavango fan, Botswana, and its sedimentological and tectonic implications. *Journal of African Earth Sciences*, 24(1–2), 65–78.

McCarthy, T.S., Ellery, W.N., and Ellery, K. (1993a). Vegetation-induced, subsurface precipitation of carbonate as an aggradational process in the permanent swamps of the Okavango (delta) fan, Botswana. *Chemical Geology*, 107(1-2), 111–131.

McCarthy, T.S., Franey, N.J., Ellery, W.N., and Ellery, K. (1993b). The use of SPOT imagery in the study of environmental processes of the Okavango Delta, Botswana. *South African Journal of Science*, 89(9), 432–436.

McCarthy, T.S., Smith, N.D., Ellery, W.N., and Gumbricht, T. (2002): The Okavango Delta – semiarid alluvial-fan sedimentation related to incipient rifting. In Renaut, R.W., and Ashley, G.M. (Eds). *Sedimentation in continental rifts*. SEPM (Society for Sedimentary Geology), Special Publication, 73, 179–93.

McCarthy, T.S., Tooth, S., Kotze, D.C., Collins, N.B., Wandrag, G., and Pike, T. (2010). The role of geomorphology in evaluating remediation options for floodplain wetlands: The case of Ramsar-listed Seekoeivlei, eastern South Africa. *Wetlands Ecology and Management*, 18(2), 119–134.

McCartney, M., Rebelo, L., Mapedza, E., Silva, D., and Finlayson, C.M. (2011). The Lukanga Swamps: use, conflicts, and management. *Journal of International Wildlife Law and Policy*, 37–41.

McCauley, L.A, and Anteau, M.J. (2014). Generating nested wetland catchments with readily-available digital elevation data may improve evaluations of land-use change on wetlands. *Wetlands*, 1–10.

McCormick, J. (1978). Ecology and the regulation of freshwater wetlands. In: Good, R.E., Whigham, D.F., and Simpson, R.L. (Eds). *Freshwater wetlands: Ecological processes and management potential.* Academic Press, New York.

McFeeters, S.K. (1996). The use of the Normalized Difference Water Index (NDWI) in the delineation of open water features. *International Journal of Remote Sensing*, 17(7), 1425-1432.

McInnes, R.J., and Everard, M. (2017). Rapid Assessment of Wetland Ecosystem Services (RAWES): An example from Colombo, Sri Lanka. *Ecosystem Services*, 25, 89–105.

McMillan, H.K., and Brasington, J. (2007). Reduced complexity strategies for modelling urban floodplain inundation. *Geomorphology*, 90(3-4), 226–243.

McNutt, M. (1998). Supperswells. *Reviews of Geophysics*, 36(2), 211–244.

Miliaresis, G.C., and Argialas, D.P. (1999). Segmentation of physiographic features from the global digital elevation model/GTOPO30. *Computers and Geosciences*, 25, 715–728.

Mitsch, W.J., and Gosselink, J.G. (2015). *Wetlands*. John Wiley and Sons, Inc. Hoboken, New Jersey.

Moore, A.E., Cotterill, F.P.D., Main, M.P.L., and Williams, H.B. (2007). The Zambezi River. In Gupta, A. (Ed). *Large Rivers: Geomorphology and Management*. Chichester: John Wiley and Sons.

Mumba, M., and Thompson, J.R. (2005). Hydrological and ecological impacts of dams on the Kafue Flats floodplain system, southern Zambia. *Physics and Chemistry of the Earth, Parts A/B/C*, 30(6–7), 442–447.

National Aeronautics and Space Administration (NASA). (n.d). *Landsat data enriches Google Earth*. Retrieved 2016/02/02 from https://spinoff.nasa.gov/Spinoff2015/ee_1.html

Ndayisaba, F., Nahayo, L., Guo, H., Bao, A., Kayiranga, A., Karamage, F., and Nyesheja, E. M. (2017). Mapping and monitoring the Akagera wetland in Rwanda. *Sustainability (Switzerland)*, 9(2), 1–13.

Niu, Z., Zhang, H., Wang, X., Yao, W., Zhou, D., Zhao, K., Zhao, H., Li, N., Huang, H., Li, C., Yang, J., Liu, C., Liu, S., Wang, L., Li, Z., Yang, Z., Qiao, F., Zheng, Y., Chen, Y., Sheng, Y., Gao, X., Zhu, W., Wang, W., Wang, H., Weng, Y., Zhuang, D., Liu, J., Luo, Z., Cheng, X., Guo, Z., and Gong, Peng. (2012). Mapping wetland changes in China between 1978 and 2008. *Chinese Science Bulletin*, 57(22), 2813–2823.

Nugent, C. (1990). The Zambezi River: tectonism, climatic change and drainage evolution. *Palaeogeography, Palaeoclimatology, Palaeoecology*, 78(1-2), 55–69.

Oh, P.S. (2019). Features of modeling-based abductive reasoning as a disciplinary practice of inquiry in earth science cases of novice students solving a geological problem. *Science & Education*, 28, 731–757.

Ollis, D.J., Snaddon, C.D., Job, N.M., and Mbona, N. (2013). *Classification system for wetlands and other aquatic ecosystems in South Africa. User Manual: Inland Systems*. SANBI Biodiversity, Series 22. South African National Biodiversity Institute, Pretoria.

Olofsson, P., Foody, G.M., Herold, M., Stehman, S.V., Woodcock, C.E., and Wulder, M.A. (2014). Good practices for estimating area and assessing accuracy of land change. *Remote Sensing of Environment*, 148, 42–57.

Olsen, K.H., and Morgan, P. (1995). Introduction: progress in understanding continental rifts. In: K.H. Olsen (Ed.), Continental rifts: evolution, structure, and tectonics. *Developments in Geotectonics*, (25), 3–26.

Overton, I.C. (2005). Modelling floodplain inundation on a regulated river: integrating GIS, remote sensing and hydrological models. *River Research and Applications*, 21(9), 991–1001.

Ozesmi, S.L., and Bauer, M.E. (2002). Satellite remote sensing of wetlands. *Wetlands Ecology and Management*, 10, 381–402.

Partridge, T., and Maud, R. (1987). Geomorphic evolution of Southern Africa since the Mesozoic. *South African Journal of Geology*, 90, 179–208.

Pik, R., Marty, B., and Hilton, D.R. (2006). How many mantle plumes in Africa? The geochemical point of view. *Chemical Geology*, 226(3-4), 100–114.

Powell, S.J., Letcher, R.A., and Croke, B.F.W. (2008). Modelling floodplain inundation for environmental flows: Gwydir wetlands, Australia. *Ecological Modelling*, 211(3–4), 350–362.

Qi, S., Brown, D.G., Tian, Q., Jiang, L., Zhao, T., and Bergen, K.M. (2009). Inundation extent and flood frequency mapping using LANDSAT imagery and digital elevation models. *GIScience & Remote Sensing*, 46(1), 101–127.

Ramachandra, T.V., and Kumar, U. (2008). Wetlands of Greater Bangalore, India: Automatic Delineation through Pattern Classifiers. *Electronic Green Journal*, 1(26), 1–26.

Rebelo, L.M., McCartney, M.P., and Finlayson, C.M. (2010). Wetlands of Sub-Saharan Africa: distribution and contribution of agriculture to livelihoods. *Wetlands Ecology and Management*, 18(5), 557–572.

Reschke, J., and Hüttich, C. (2014). Continuous field mapping of Mediterranean wetlands using sub-pixel spectral signatures and multi-temporal Landsat data. *International Journal of Applied Earth Observation and Geoinformation*, 28(1), 220–229.

Rhoads, B.L., and Thorn, C.E. (1993). Geomorphology as science: the role of theory. *Geomorphology*, 6, 287-307.

Ritchie, M., and Das, S. (2015). *A brief review of remote sensing data and techniques for wetlands identification*. Extended abstracts of 14th SAGA biennial technical meeting and exhibition, 1–5.

Romshoo, S.A., and Rashid, I. (2014). Assessing the impacts of changing land cover and climate on Hokersar wetland in Indian Himalayas. *Arabian Journal of Geosciences*, 7(1), 143–160.

Rundquist, D.C., Narumalani, S., and Narayanan, R.M. (2001). A review of wetlands remote sensing and defining new considerations. *Remote Sensing Reviews*, 20(3), 207–226.

Schael, D.M., Gama, P.T., and Melly, B.L. (2015). *Ephemeral Wetlands of the Nelson Mandela Bay Metropolitan Area: Classification, Biodiversity and Management Implications*. Report Number: 2181/1/15. Water Research Commission, Gezina.

Schelle, P., and Pittock, J. (2006). Restoring the Kafue Flats: A partnership approach to environmental flows in Zambia. *Water Management*, 1–10.

Scholz, C.A., Rosendahl, B.R., Versfelt, J.W., and Rach, N. (1990). Results of high-resolution echo-sounding of Lake Victoria. *Journal of African Earth Sciences*, 11(1-2), 25–32.

Schumm, S.A. (1993). River response to base level change: implications for sequence stratigraphy. *The Journal of Geology*, 101(2), 279–294.

Schumm, S.A., Dumont, J.F., and Holbrook, J.M. (2000). *Active tectonics and alluvial rivers*. Cambridge: Cambridge university press.

Sharma, A., and Tiwari, K.N. (2014). A comparative appraisal of hydrological behaviour of SRTM DEM at catchment level. *Journal of Hydrology*, 519, 1394–1404.

Simms, M.F. (2000). Appendix A. Preliminary report on Lake Patrick. In Gupta, A. (Ed). *Large Rivers: Geomorphology and Management*. Chichester: John Wiley & Sons.

Smith, L.C. (1997). Satellite remote sensing of river inundation area, stage, and discharge: A review. *Hydrological Processes*, 11(10), 1427–1439.

SMUWC. (2001). *Sustainable management of the Usangu Wetland and its catchment*. Final Report, United republic of Tanzania, 2001

Soille, P., Vogt, J., and Colombo, R. (2003). Carving and adaptive drainage enforcement of grid digital elevation models, *Water Resources Research*, 39(12), 1366.

Stankiewicz, J., and de Wit, M.J. (2006). A proposed drainage evolution model for Central Africa - Did the Congo flow east? *Journal of African Earth Sciences*, 44(1), 75–84.

Stearns, F. (1978). Management potential: Summary and recommendations. In: Good, R.E., Whigham, D.F., and Simpson, R.L. (Eds). *Freshwater wetlands: Ecological processes and management potential.* Academic Press, New York.

Stein, E.D., Fetscher, A.E., Clark, R.P., Wiskind, A., Grenier, J.L., Sutula, M., Collins J.N., and Grosso, C. (2009). Validation of a wetland rapid assessment method: use of EPA's level 1-2-3 framework for method testing and refinement. *Wetlands*, 29(2), 648–665.

Steinfeld, C.M.M., Kingsford, R.T., and Laffan, S.W. (2013). Semi-automated GIS techniques for detecting floodplain earthworks. *Hydrological processes*, 27(4), 579-591.

Stokes, S.J. (1994). The limit of government's regulatory authority over non-adjacent wetlands: hoffman homes, inc. V. Epa. *Energy law journal*, 1, 137–152.

Taylor, J.R., and Lovell, S.T. (2012). Mapping public and private spaces of urban agriculture in Chicago through the analysis of high-resolution aerial images in Google Earth. *Landscape and Urban Planning*, 108(1), 57–70.

Tempfli, K., Huurneman, G., Bakker, W., and Janssen, L. (Eds). (2009). *Principles of Remote Sensing: An Introductory Textbook*. The International Institute for Geo-Information Science and Earth Observation (ITC), Enschede.

Thomas, D.S.G., and Shaw, P.A. (1988). Late Cainozoic drainage evolution in the Zambezi Basin: Geomorphological evidence from the Kalahari Rim. *Journal of African Earth Sciences*, 7(4), 611–518.

Thomas, D.S.G., O'Connor, P.W., Bateman, M.D., Shaw, P.A, Stokes, S., and Nash, D.J. (2000). Dune activity as a record of late Quaternary aridity in the Northern Kalahari: new evidence from northern Namibia interpreted in the context of regional arid and humid chronologies. *Palaeogeography, Palaeoclimatology, Palaeoecology*, 156(3-4), 243–259.

Thomas, R.F., Kingsford, R.T., Lu, Y., Cox, S.J., Sims, N.C., and Hunter, S.J. (2015). Mapping inundation in a heterogeneous floodplain wetland, the Macquarie Marshes, using Landsat Thematic Mapper. *Journal of Hydrology*, 524, 194–213.

Timberlake, J.R. (1998). *Biodiversity of the Zambezi Basin wetlands: review and preliminary assessment of available information-Phase 1*. Consultancy report for IUCN ROSA, Harare. Occasional Publications in Biodiversity No. 3. The Zambezi Society/Biodiversity Foundation for Africa, Harare/Bulawayo

Tomlinson, C.J., Chapman, L., Thornes, J.E., and Baker, C. (2011). Remote sensing land surface temperature for meteorology and climatology: A review. *Meteorological Applications*, 18(3), 296–306.

Tooth, S., and McCarthy, T.S. (2007). Wetlands in drylands: geomorphological and sedimentological characteristics, with emphasis on examples from southern Africa. *Progress in Physical Geography*, 31(1), 3–41.

Tooth, S., Brandt, D., Hancox, P.J. and McCarthy, T.S. (2004). Geological controls on alluvial river behaviour: A comparative study of three rivers on the South African Highveld. *Journal of African Earth Sciences*, 38(1), 79–97.

Tooth, S., Ellery, W.N., Grenfell, M.C., Thomas, A., Kotze, D.C., and Ralph, T. (2015). *10 reasons why the geomorphology of wetlands is important*. Retrieved 2017/03/07 from http://wetlandsindrylands.net/wp-content/uploads/2015/10/10-Reasons-Geomorphology-of-Wetlands-NEAR-FINAL-FULL-COLOUR.pdf

Tooth, S., McCarthy, T.S., Brandt, D., Hancox, P.J., and Morris, R. (2002). Geological controls on the formation of alluvial meanders and floodplain wetlands: the example of the Klip River, eastern Free State, South Africa. *Earth Surface Processes and Landforms*, 27(8), 797–815.

Tooth, S., Rodnight, H., McCarthy, T.S., Duller, G.A.T. and Grundling, A.T. (2009). Late quaternary dynamics of a South African floodplain wetland and the implications for assessing recent human impacts. *Geomorphology*, 106(3–4), 278–291.

Townsend, P., and Walsh, S. (2001). Remote sensing of forested wetlands: application of multitemporal and multispectral satellite imagery to determine plant community composition and structure. *Plant Ecology*, 129–149.

Townsend, P.A., and Walsh, S.J. (1998). Modelling floodplain inundation using an integrated GIS with radar and optical remote sensing. *Geomorphology*, 21(3-4), 295–312.

Trigg, M.A., Michaelides, K., Neal, J.C. and Bates, P.D. (2013). Surface water connectivity dynamics of a large scale extreme flood. *Journal of Hydrology*, 505, 138–149.

Turner, K. (1991). Economics and wetland management. *Ambio*, 20(2), 59–63.

Turpie, J., Smith, B., Emerton. L., and Barnes, J. (1999). *Economic value of the Zambezi basin wetlands*. IUCN Regional Office for Southern Africa.

United States Geological Survey (USGS). (1999). *GTOPO30 documentation*. Retrieved 2014/11/13 from http://webgis.wr.usgs.gov/globalgis/gtopo30/gtopo30.htm

United States Geological Survey (USGS). (2015). *LandsatLook images*. Retrieved 20 March 2015 from http://landsat.usgs.gov/LandsatLookImages.php

United States Geological Survey (USGS). (n.d). *Shuttle Radar Topography Mission (SRTM) 1 Arc-Second Global*. Retrieved 2014/12/04 from https://lta.cr.usgs.gov/SRTM1Arc

Valimba, P. (2004). *Rainfall variability in southern Africa, its influences on streamflow variations and its relationships with climatic variations*. (PhD Thesis). Rhodes University, South Africa.

van der Waal, B., and Rowntree, K. (2015). *Assessing Sediment Connectivity At the Hillslope, Channel and Catchment Scale*. WRC Report No 2260/1/15.

van Deventer, H., Nel, J., Maherry, A., and Mbona, N. (2014). Using the landform tool to calculate landforms for hydrogeomorphic wetland classification at a country-wide scale. *South African Geographical Journal*, 1–16.

van Steenbergen, F., Kool, M., Vuik, R., and van den Pol, B. (2015). *Floodplains in Zambia: The Scope for shallow well development*. Spate Irrigation Network Foundation. Retrieved 2017/05/26 from http://spate-irrigation.org/wp-content/uploads/2015/03/OP16_Flood-Wells-Zambia_SF.pdf

Vepraskas, M.J. (2016). History of the concept of hydric soil. In: Vepraskas, M.J. and Craft, C.B. (Eds). *Wetland Soils: Genesis, Hydrology, Landscapes and Classification (Second Edition)*. CRC Press, Taylor & Francis Group, Boca Raton, Florida.

Verhoeven, J.T.A., Arheimer, B., Yin, C., and Hefting, M.M. (2006). Regional and global concerns over wetlands and water quality. *Trends in Ecology and Evolution*, 21(2), 96-103.

Vrána, S. (1985). Lukanga Swamp: Probably astrobleme. *Meteoritics*, 20, 125–139.

Ward, D.P., Petty, A., Setterfield, S.A., Douglas, M.M., Ferdinands, K., Hamilton, S.K., and Phinn, S. (2014). Floodplain inundation and vegetation dynamics in the Alligator Rivers region (Kakadu) of northern Australia assessed using optical and radar remote sensing. *Remote Sensing of Environment*, 147, 43–55.

Wellington, J.H. (1949). Zambezi-Okovango development projects. *Geographical Review*, 39(4), 552–567.

Williams, L., Harrison, S., and O'Hagan, A.M. (2012). *The use of wetlands for flood attenuation*. Report for an Taisce by Aquatic Services Unit, University College Cork.

Wohl, E., Lininger, K.B., and Scott, D.N. (2017). River beads as a conceptual framework for building carbon storage and resilience to extreme climate events into river management. *Biogeochemistry*, 1–19.

Wright, C., and Gallant, A. (2007). Improved wetland remote sensing in Yellowstone National Park using classification trees to combine TM imagery and ancillary environmental data. *Remote Sensing of Environment*, 107(4), 582–605.

WWF Tanzania Country Office (WWF-TCO). (2010). *Assessing environmental flows for the Great Ruaha River, and Usangu wetland*, Tanzania. Retrieved 2016/07/04 from http://www.waterandnature.org/sites/default/files/grr_flow_assessmentfinal_reportwwf2010.pdf

Xu, H. (2006). Modification of normalised difference water index (NDWI) to enhance open water features in remotely sensed imagery. *International Journal of Remote Sensing,* 27(14), 3025–3033.

Yeh, E.T. (2009)."From Wasteland to Wetland? Nature and Nation in China's Tibet". *Environmental History*, 14 (January): 103-137.

Zervakou, A.D., and Tsombos, P.I. (2010). *GIS in urban geology: the case study of Nafplio, Argolis prefecture, Greece*. Bulletin of the Geological Society of Greece, Proceedings of the 12th International Congress.

Zhao, M., Langston, C.A., Nyblade, A.A., and Owens, T.J. (1999). Upper mantle velocity structure beneath southern Africa from modelling regional seismic data. *Journal of Geophysical Research*, 104(B3), 4783–4794.

Zomer, R.J., Trabucco, A., van Straaten, O., and Bossio, D.A. (2006). *Carbon, land and water: A global analysis of the hydrologic dimensions of climate change mitigation through afforestation/reforestation.* Colombo, Sri Lanka: International Water Management Institute.